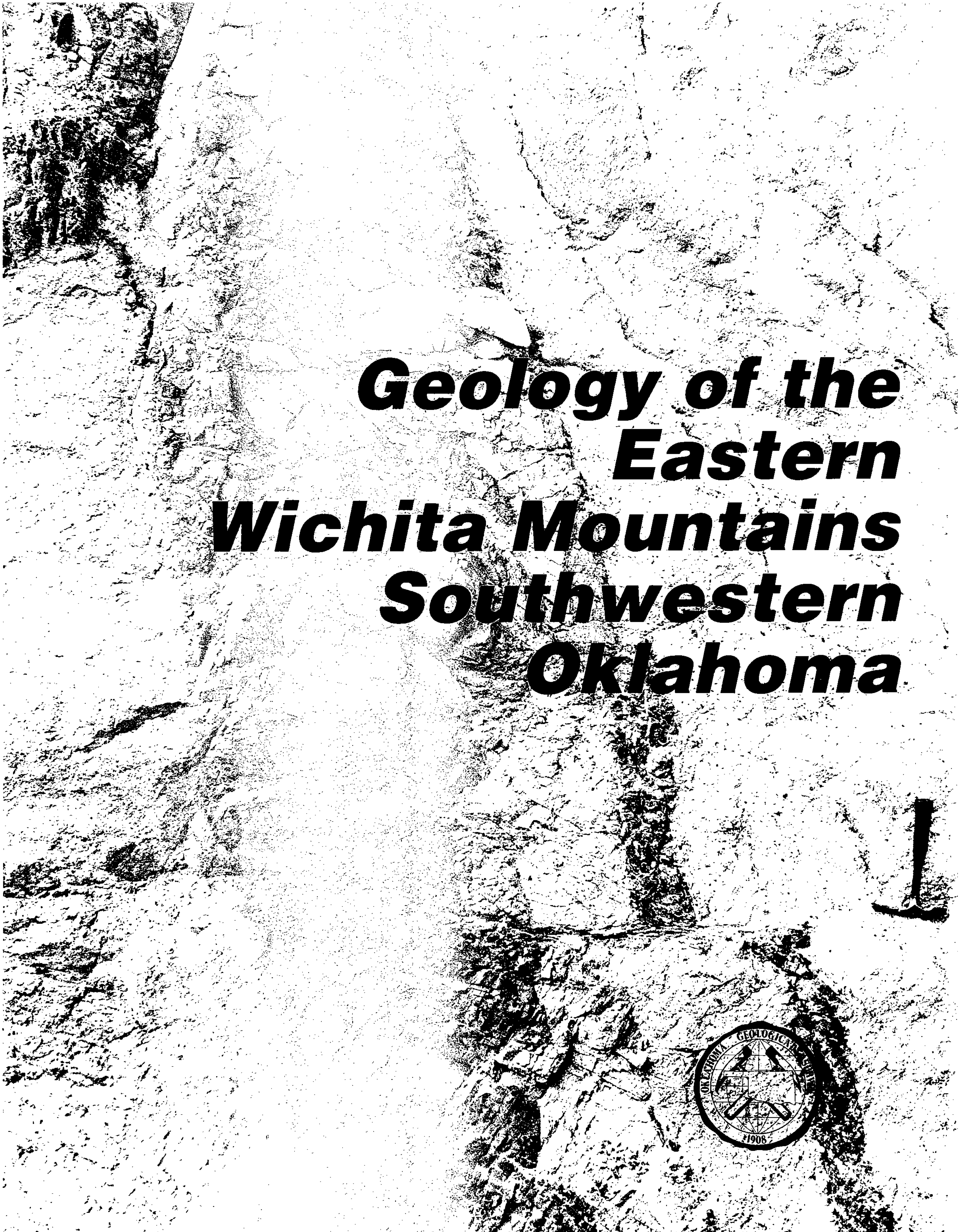

Geology of the Eastern Wichita Mountains Southwestern Oklahoma

Oklahoma Geological Survey 1982 GUIDEBOOK 21

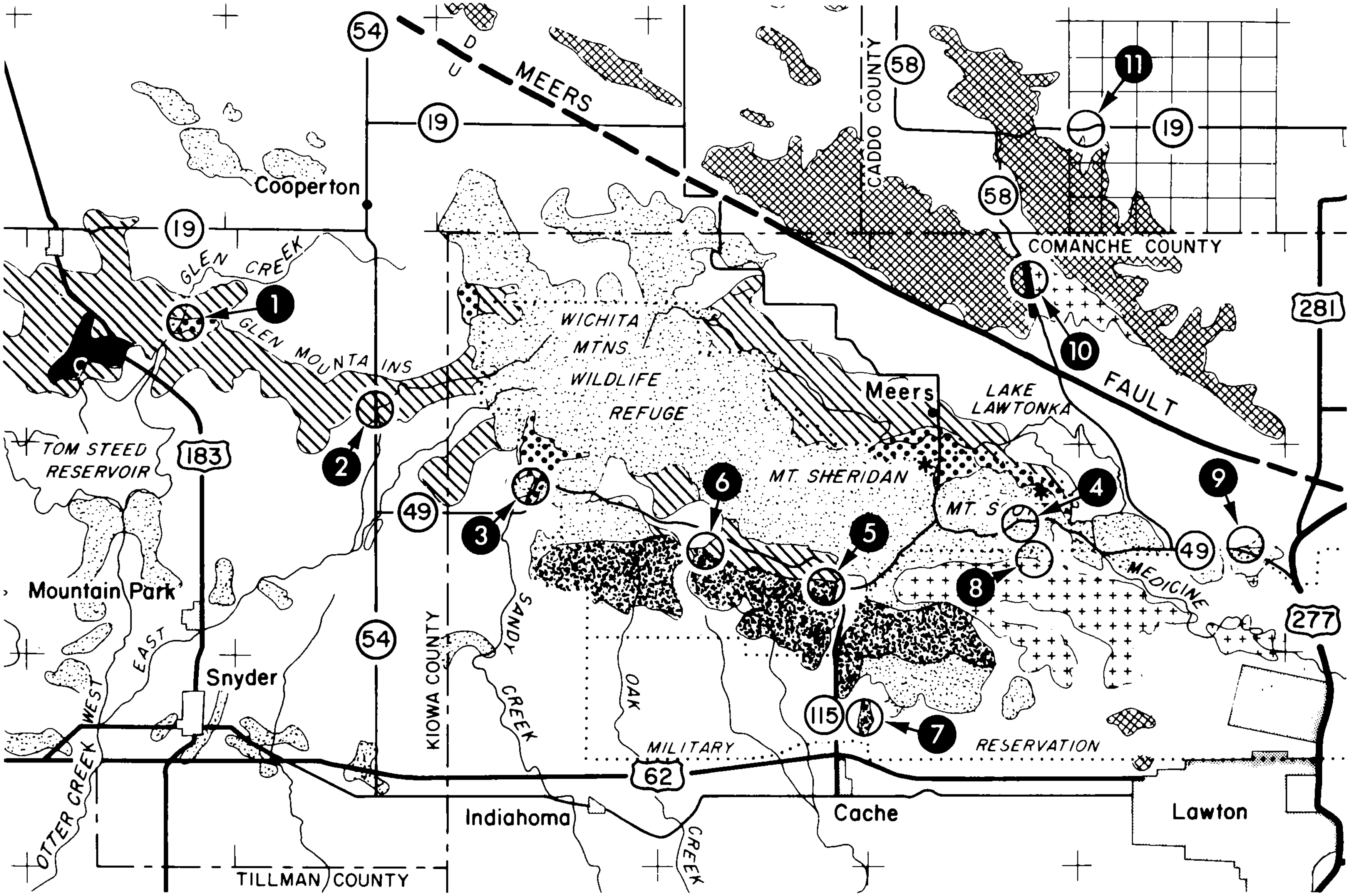

Field-Trip Stops

(Adapted from fig. 2)

OKLAHOMA GEOLOGICAL SURVEY
Charles J. Mankin, *Director*
GUIDEBOOK 21

ISSN 0078-4400

GEOLOGY OF THE EASTERN WICHITA MOUNTAINS SOUTHWESTERN OKLAHOMA

M. Charles Gilbert and **R. Nowell Donovan**, *Editors*

Department of Geological Sciences
Virginia Polytechnic Institute & State University
Oklahoma Geological Survey
The University of Oklahoma

Department of Geology
Oklahoma State University

Authors and Stop Leaders:

A. Babaei, Oklahoma State University
Samuel A. Bowring, University of Kansas
J. A. Brewer, Cornell University (now at Cambridge University, England)
R. Nowell Donovan, Oklahoma State University
Joe D. Giddens III, University of Texas, Arlington
M. Charles Gilbert, Virginia Polytechnic Institute & State University
Oklahoma Geological Survey
Wendel J. Hoppe, University of Kansas
James R. Miller, University of Texas, Arlington
Benjamin N. Powell, Phillips Petroleum Company
D. J. Sanderson, Queen's University, Belfast, Northern Ireland
Nancy Scofield, South Dakota School of Mines & Technology
J. Ronald Sides, University of Texas, Arlington
Marjorie L. Stockton, University of Texas, Arlington

Guidebook for Field Trip 1, March 26–28, 1982, preceding annual meeting of Geological Society of America, South-Central Section

The University of Oklahoma
Norman
1982

Front Cover

Dike of Cold Springs Breccia cutting Glen Mountains Layered Complex in the NW¼SE¼SW¼NE¼ sec. 14, T. 4 N., R. 17 W. (see Stop 1, lower E–14 section). Note that the dike "T's" in the upper part of the photo. In the lower part of the photo, near the hammer, an offset with some horizontal component can be seen.

Back Cover

Folds in rocks of the Arbuckle Group (Upper Cambrian–Lower Ordovician) in the Slick (or Limestone) Hills, on the north flank of the Wichita Uplift.

This publication, printed by The University of Oklahoma Printing Services, Norman, Oklahoma, is issued by the Oklahoma Geological Survey as authorized by Title 70, Oklahoma Statutes, 1971, Section 3310, and Title 74, Oklahoma Statutes, 1971, Sections 231–238. 1,000 copies have been prepared for distribution at a cost to the taxpayers of the State of Oklahoma of $11,638.

PREFACE

This guidebook follows in the tradition of several earlier guidebooks on the Wichita Mountains area, published by the Oklahoma Geological Survey. Particularly useful are those by Stone (1967), Johnson and Denison (1973), and Powell and Fischer (1976). These guidebooks not only provide discussions and data on areas and units not covered in the present effort, but also supplement areas covered here. This new book is warranted because much work has been initiated since 1976. Presentation of some of this newer work in a guidebook format allows early discussion and pinpoints outcrops critical to interpretation of the region.

All the stops are new in the sense that none has been listed in a published guidebook before. Stops are concentrated in the eastern Wichitas, where the largest outcrops occur and where the most complete section of the Wichita Uplift block is exposed. We are pleased to have a series of stops covering not only all major aspects of the igneous stratigraphy and key lower Paleozoic sedimentary units, but some of the important structural features as well. An important part of the guidebook is the series of 1:12,000-scale geologic maps on topographic bases accompanying the stop descriptions. Some of these have been supplemented with structure sections to amplify the field relations. An additional useful feature is the series of topical discussions in the first part of the book. These discussions provide background for the stops, describe the regional setting of the Wichita Mountains crustal block, and give contexts for the field relations.

The guidebook contributes to a larger effort by the Oklahoma Geological Survey to make available a new, detailed geologic map of the Wichita Mountains, with Gilbert responsible for the igneous units and Donovan for the lower Paleozoic sedimentary outcrops. This guidebook and the forthcoming map should help the geologic community gain a better understanding of the evolution of the Southern Oklahoma Aulacogen. The nature of the basement and the specific features of the Wichita Uplift are obviously important in following development of the Anadarko and Hollis–Hardeman Basins.

A number of individuals and organizations must be acknowledged for their contributions. Some are recognized in the articles that follow. Specifically for their willingness to permit and aid access to the field stops, we thank T. O. Materials Co., and the Nelson Davis family [now operated as Blue Rock Pit by Robert Spillers] (Stop 1); Jerry Treadwell (Willis Ranch), James Raasch, and James and Nick Callen (Stop 2); Jim Snell, and Robert and John Phelon (Stop 3); the Wichita Mountains Wildlife Refuge, Robert Karges, manager, and Tom Westmoreland, chief public use specialist (Stops 3–6); the Commanding General, Fort Sill, through Anne Powell, Public Affairs Office (Stops 7 and 8); Jim Wright and Woody Wolverton (Stop 9); and Mr. and Mrs. Oliver, of Kimball Ranch (Stop 10).

The staff of the Oklahoma Geological Survey worked hard to bring this guidebook to fruition; special thanks are due William D. Rose, editor, and T. Wayne Furr, manager of cartography.

M. CHARLES GILBERT
R. NOWELL DONOVAN
January 1982

CONTENTS

GEOLOGIC SETTING OF THE EASTERN WICHITA MOUNTAINS WITH A BRIEF DISCUSSION OF UNRESOLVED PROBLEMS

M. Charles Gilbert

INTRODUCTION

Background

Four early publications outlined the surface geologic relations of the eastern Wichita Mountains: Taff (1904) provided the framework by outlining the principal rock groups, igneous and sedimentary; Taylor (1915) described the main granitic units and first identified the Meers Quartzite; Hoffman (1930) mapped in more detail the igneous exposures of the eastern Wichitas, emphasizing the micrographic nature of the granites; and Decker (1939) described the stratigraphy of the lower Paleozoic sedimentary section (Timbered Hills Group and Arbuckle Group), some parts of which have their type sections in the Wichitas. The tectonic setting and geologic relations, as presently understood, are shown in figures 1 and 2. Later, six modifications in interpretation significantly altered our understanding of the geology: (1) Schoonover (1948) recognized the Carlton rocks as extrusive rhyolites, adding a volcanic element not heretofore appreciated; (2) Harlton (1951) noted significant faulting with surface expression in the sedimentary units; (3) H. E. Hunter (Gilbert, 1960; Hiss, 1960; Spencer, 1961) realized that the gabbroic rocks are mostly part of a large, layered, lopolithic complex, entirely similar to other such well-known bodies in the world, an idea also championed by Hamilton (1956, 1959) in somewhat different form; (4) Tilton and others (1962) showed that the granites and rhyolites are Cambrian, thus anomalous for the continental interior; (5) Hoffman and others (1974) popularized the idea that the Wichita Uplift–Anadarko Basin is an aulacogen; and finally (6) Brewer and others (1981, 1982) presented evidence for a deep, large thrust-fault system on the north, representing a strong compressional phase during uplift.

G. W. Chase worked in the Wichita Mountains area for the Oklahoma Geological Survey from 1949 to 1955, producing a number of seminal publications, the most comprehensive of which was Chase and others (1956); the geology of the region as shown on the 1954 state geologic map (Miser, 1954) is due principally to him. Other work by Chase survives only in manuscript form. Finally, three articles should be consulted for their comprehensive presentation and review of available data: Ham and others (1964) laid the groundwork for our modern understanding of the Wichita Mountains–Arbuckle Mountains basement; Powell and others (1980) revised the basement lithostratigraphy, cogently discussing uncertainties of ages and correlations; and Myers and others (1981) discussed the geochemistry of the Wichita Granite Group. Many other individual sources of data or ideas would need to be cited for a complete review of the geology. However, all these may be found in the reference lists of the publications just noted, and to some degree in the list accompanying this guidebook. Only a brief outline of the geologic history is given here. Powell and others (1980), Powell and Fischer (1976), and Johnson and Denison (1973) gave helpful and more detailed reviews.

Geologic Setting

The Wichita Mountains are a series of Cambrian to possibly Proterozoic igneous knobs, and Cambrian to Ordovician sedimentary hills, protruding through the Permian shaly plains of southwestern Oklahoma (fig. 2). The mountains have a maximum relief of about 1,100–1,200 ft on the southeastern end, near Lawton, Oklahoma, but this dwindles along the 120-km length of the range to about 700–800 ft on the northwestern end, near Granite. The primary reason for this difference is the rise in local base level from 1,100–1,300 ft to 1,600 ft (fig. 3). The range is of much greater geologic significance than its topographic aspect might seem to warrant. Only the Wichitas, and Arbuckles of southern Oklahoma, contain useful exposures of basement for the southern Mid-continent. To the west, basement is not exposed until reaching central New Mexico; to the south, not until the Llano region, to the north and east, not until the Saint Francois Mountains of southeastern Missouri or the Black Hills of South Dakota. Furthermore, the basement character in the Wichitas is different from each of these other areas, both in age (the others are Proterozoic, 1.2–1.5 b.y.) and in distribution of rock types. The Wichita axis is also markedly different in tectonic setting in comparison with these other areas of exposed basement. It is part of a regional system called an aulacogen (Burke and Dewey, 1973; Hoffman and others, 1974), which serves to emphasize the role of faulting and extensional strains during an early part of the history. Arguments for significant left-lateral, strike-slip faulting have also been advanced for later in the history, during the uplift phase, specifically for the Arbuckles (for example, Wickham, 1978). By implication, such a style of activity would apply also to the Wichitas. The picture is further complicated by the recent COCORP results for a deep seismic-reflection line from the Hardeman Basin across the Wichita Uplift and Anadarko Basin, as described in this guidebook by Brewer. These results show a hitherto unsuspected deep, large Proterozoic basin beneath the Hollis–Hardeman Basin to the south, and thrust faulting 20–24 km deep on the north, reflecting a strong compressional phase during uplift.

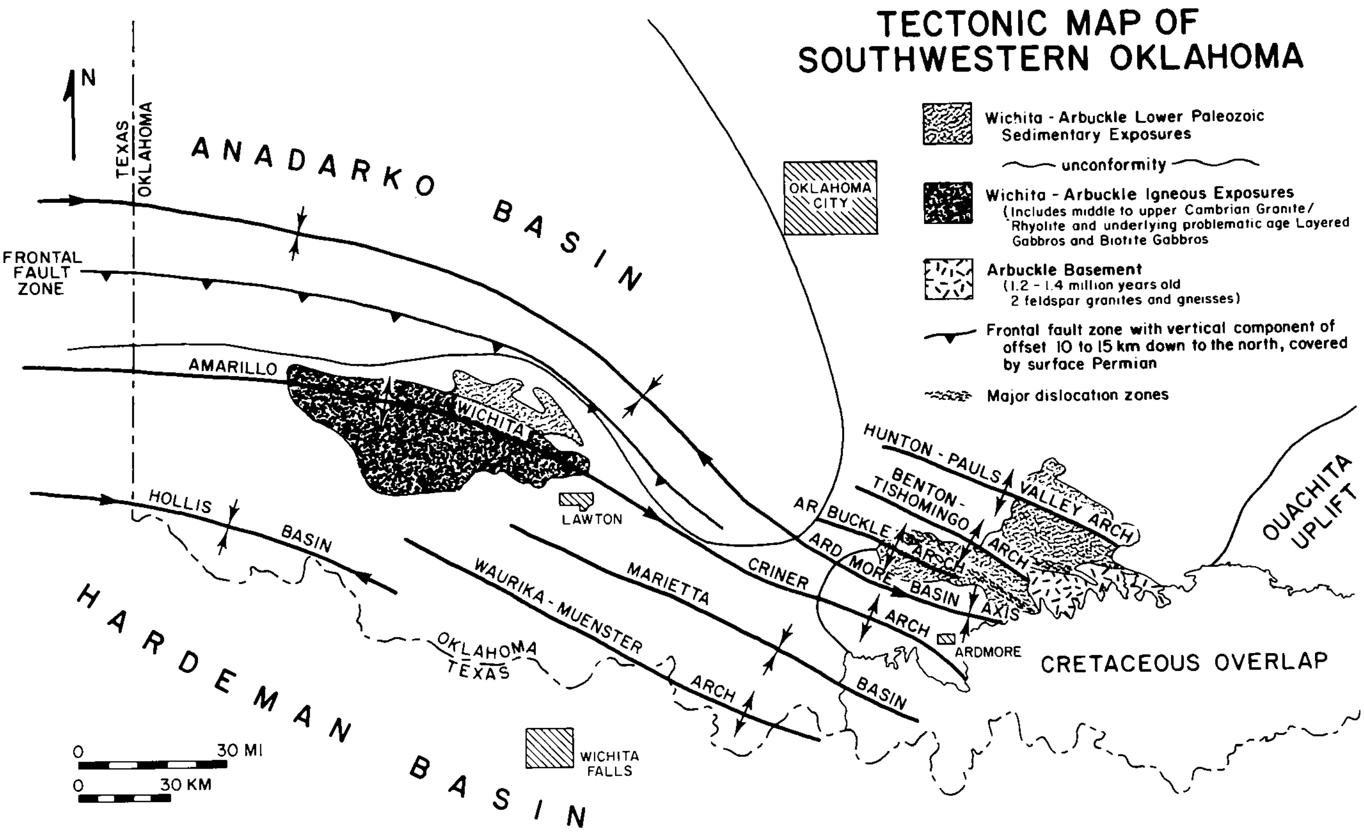

Figure 1. Tectonic map of southwestern Oklahoma. From Powell and others (1980, Part II, fig. 1).

Interestingly, the surface topography of the Wichita Mountains also is unusual because it is a fossil Permian surface just now being uncovered (fig. 3). No really substantial modifications by recent weathering or erosion have altered the fundamental forms developed 200 m.y. ago. Whereas this fact has been known, in part, for some time (for example, Evans, 1929), the extent of the preservation has only now begun to be appreciated. Gilbert (1979) recognized the topography as a classic example of the tor type. Implications for the tectonic history and surrounding Permian sediments are now being explored.

Figure 4 is a simplified version of the basement of Oklahoma and nearby Texas. The oldest basement in the immediate region appears to be in the Eastern Arbuckle province (Bickford and Lewis, 1979; Denison, 1978), where ages as old as about 1.4 b.y. are now accepted. A number of apparently younger provinces were delineated by Denison (1966) in Oklahoma and by Muehlberger and others (1967) in Texas. The relations between and among these younger terranes are unknown. Commonly, however, rhyolites and shallow-seated granites dominate, implying only modest amounts of erosion before Cambrian time. Of special note are two provinces, the Tillman Metasedimentary Group and the Wichita Mountains igneous assemblage. The Tillman is the only terrane where low-rank metasediments are important. The work of Brewer and others (1981, 1982), as described later in this guidebook (Brewer), now indicates that these rocks may only be the top portion of a huge Proterozoic basin whose size (depth) may rival that of the Paleozoic Anadarko. Ham and others (1964) first erected the Tillman Group and assigned to it the limited outcrop of Meers Quartzite in the Wichita Mountains. This assignment is discussed by me later in this article, and by Sides and Miller in a following article.

The igneous rocks of the Wichita Uplift are a bimodal suite of (1) substrate exposed gabbros (Raggedy Mountain Gabbro Group) and buried basalts (Navajoe Mountain Basalt–Spilite Group), and (2) overlying rhyolites (Carlton Rhyolite Group) and granites (Wichita Granite Group). No other exposed province in the Midcontinent, nor other identified nearby basement, has layered gabbros similar to those in the Wichitas (Glen Mountains Layered Complex). Furthermore, the younger units of the group (Roosevelt Gabbros) intrusive into the complex, are of a distinctive, biotite-bearing, hydrous tholeiitic character (Powell, this guidebook), not found in other nearby parts of the basin. Bowring and Hoppe (this guidebook) are able to show convincingly that at least some of these younger gabbros are 550 m.y. in age, limiting the erosional interval that preceded the major rhyolite–granitic period. The felsic rocks are similar in petrographic character to many others of the Midcontinent basement, for example the Saint Francois Mountains of southeastern Missouri, but are only ~525 m.y. in age in comparison with ~1,500 m.y. in Missouri.

Figure 5 (Gilbert, 1981b) is a summary description

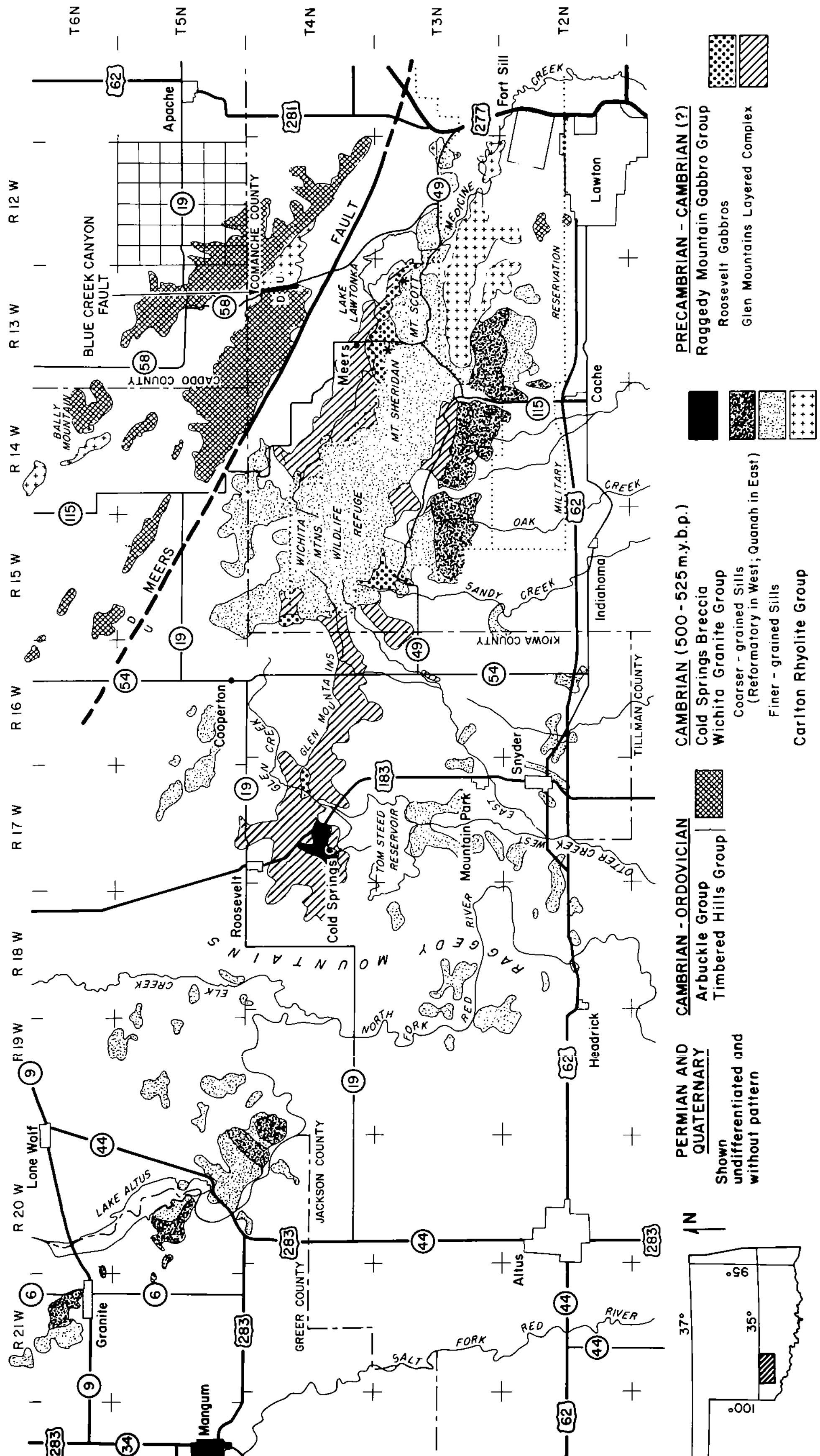

Figure 2. Geologic map of Wichita Mountains, Oklahoma. Modified from Powell and others (1980, Part I, fig. 1, and Part II, fig. 2).

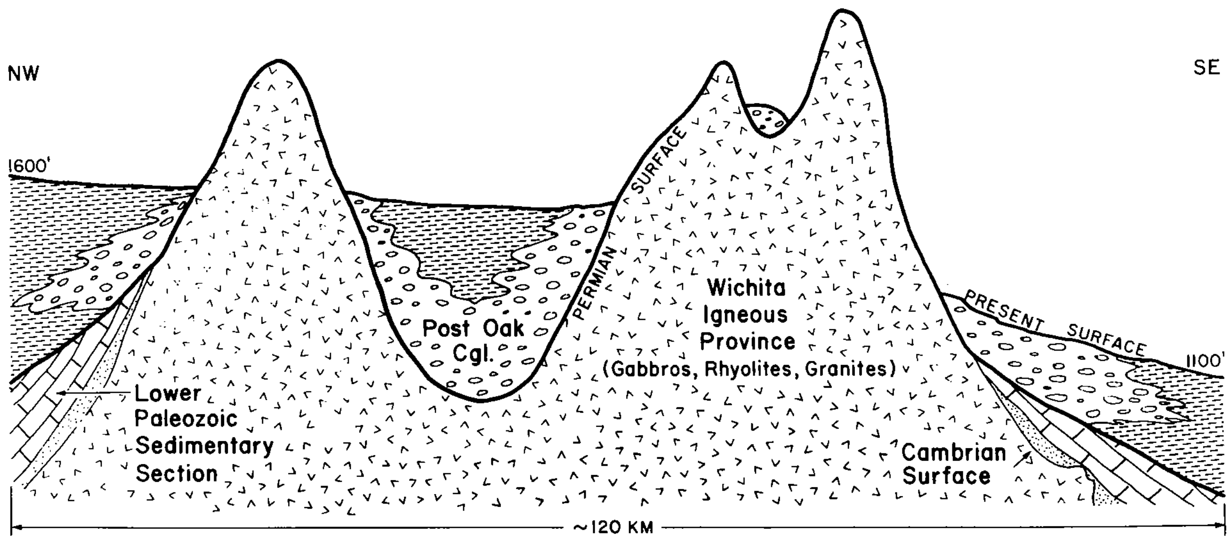

Figure 3. Diagrammatic structural and topographic profile along axis of Wichita Mountains, emphasizing Permian unconformity and overlying units.

of the geologic development of the Wichita Uplift region, and table 1 is an abbreviated listing of the stratigraphic units. The figure shows five stages in the development, from the mid-Proterozoic to the Permian. Stage 1 includes the earlier generation and emplacement of granitoids, perhaps equivalent to the Eastern Arbuckle province (for example, Tishomingo Granite); uplift to strip away the cover rocks of which we have no obvious record; and then profound subsidence during which the Tillman Group accumulated to thicknesses of more than 10 km, with an apparent depositional axis somewhere south of the present mountains. These sediments appear to thin to the north, as Brewer discusses later.

Stage 2 encompasses three events wherein massive amounts of basaltic liquid rose into the upper crust. The oldest of these (as yet undated) is the intrusion of a large, layered, gabbroic lopolith whose characteristics are like the Stillwater and Bushveld and similar bodies (Powell and others, 1980). Whether other events preceded this one, to arrive at stage 2, is unclear. We do not know what the host rock was for this intrusion, although most have assumed that it was the Tillman, and the Meers Quartzite has been so interpreted as inclusions of the Tillman Group (Ham and others, 1964; Powell and others, 1980). Several alternative views are worth considering and will be discussed later. In any case, the drawing shows the Tillman as host. Brewer and others (1981) argued that the Pennsylvanian Burch Fault had an earlier (Proterozoic?) history, and it is shown as having been initiated during this stage with the intrusion of the lopolith. The minimum size of the body was estimated to be 65 km in length, and 4,000 km^3 (Gilbert, 1982). The basalts defined by Ham and others (1964) as the Navajoe Mountain Basalt–Spilite Group were seen by them as the surface expression of the gabbroic intrusions (Raggedy Mountain Gabbro Group) (basaltic 1, 3). However, at that time, the two distinct components of the group were not recognized, so the basaltic pulse to which the extrusives should be related is now unclear. They are shown as related to the Glen Mountains Layered Complex. Powell and Phelps (1977) and Powell and others (1980) emphasized that the phase chemistry of the exposed portions of the complex shows clearly that the analyzed minerals were not at the roof of the body but must have been down inside at some depth. Several kilometers of overlying gabbroic material and its host rock would need to be stripped away before the later rhyolitic extrusions occurred. In any case, before this uplift was fully accomplished, hydrous gabbros rose and intruded the complex, forming a series of plutons (the Roosevelt Gabbros—basaltic 3), themselves internally layered. All of these are biotite (and hornblende) bearing. Four have been recognized at the surface. The largest is the Mount Sheridan, at 8 km in diameter, and the most recently identified is the Mount Baker hornblende gabbro, noted briefly by Stockton and Giddens in this guidebook. Powell and others (1980) noted that biotite-bearing basement samples are common in the descriptions listed in Ham and others (1964), particularly toward the west. Consequently, these units may turn out to be as significant volumetrically as the Glen Mountains Layered Complex. Powell gives an updated description of these gabbros later in this guidebook. During stage 2, both up and down motions seem probable, resulting in net uplift and erosion into the gabbroic units. A significant part of this happened between 550 and 525 m.y. ago, based on the new work reported by Bowring and Hoppe.

Stage 3 begins with a profound erosional unconformity on the substrate gabbros. Ham and others (1964) first presented this argument primarily on the basis of relations determined by study of basement wells. Powell and others (1980) accepted and further amplified the reasoning, using phase chemistry. Some workers have disputed this interpretation, but mapping in the eastern Wichitas by Gilbert and by

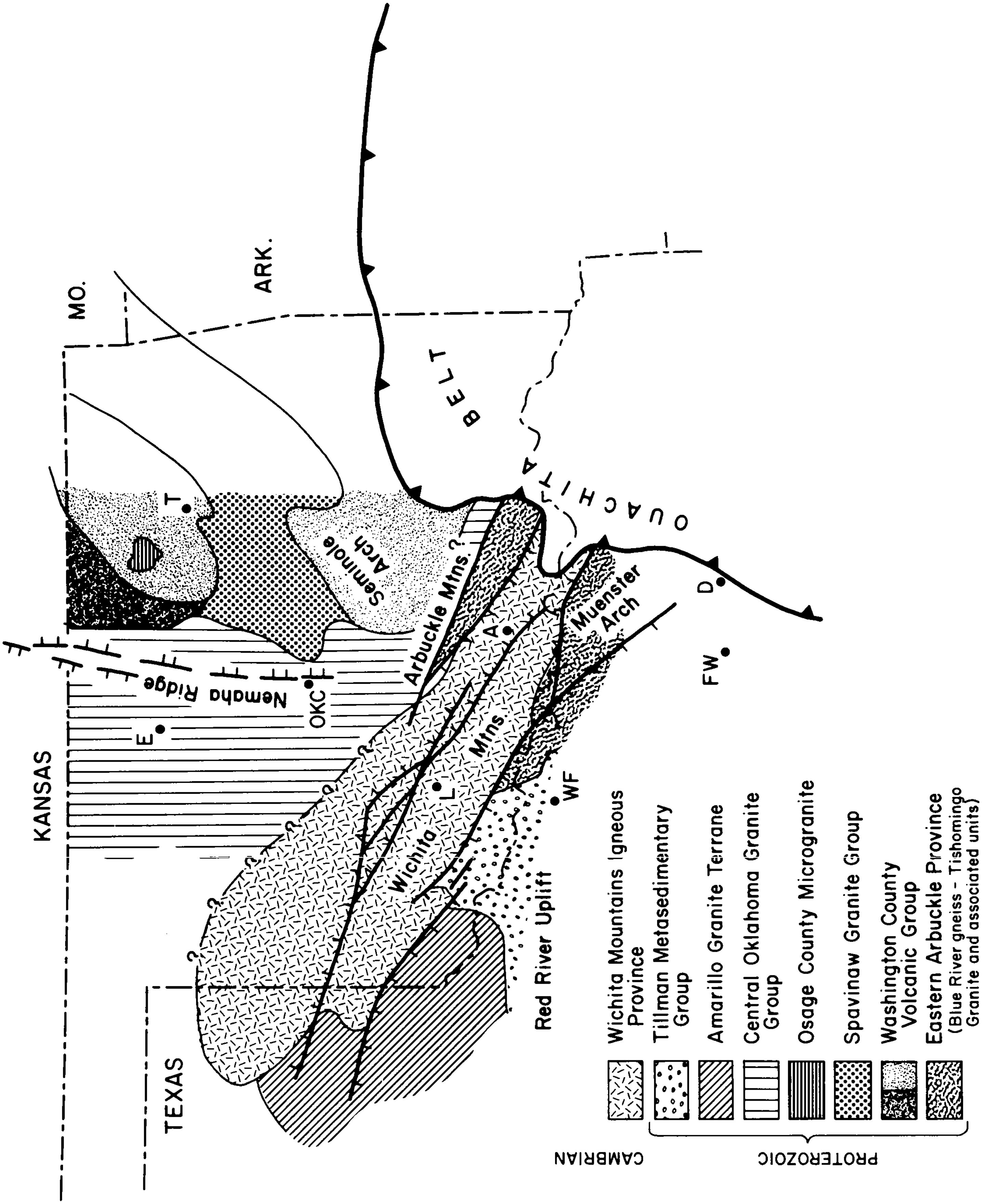

Figure 4. Regional basement map of Southern Oklahoma Aulacogen area. Compiled from Denison (1966), Muehlberger and others (1967), and Luza (1978).

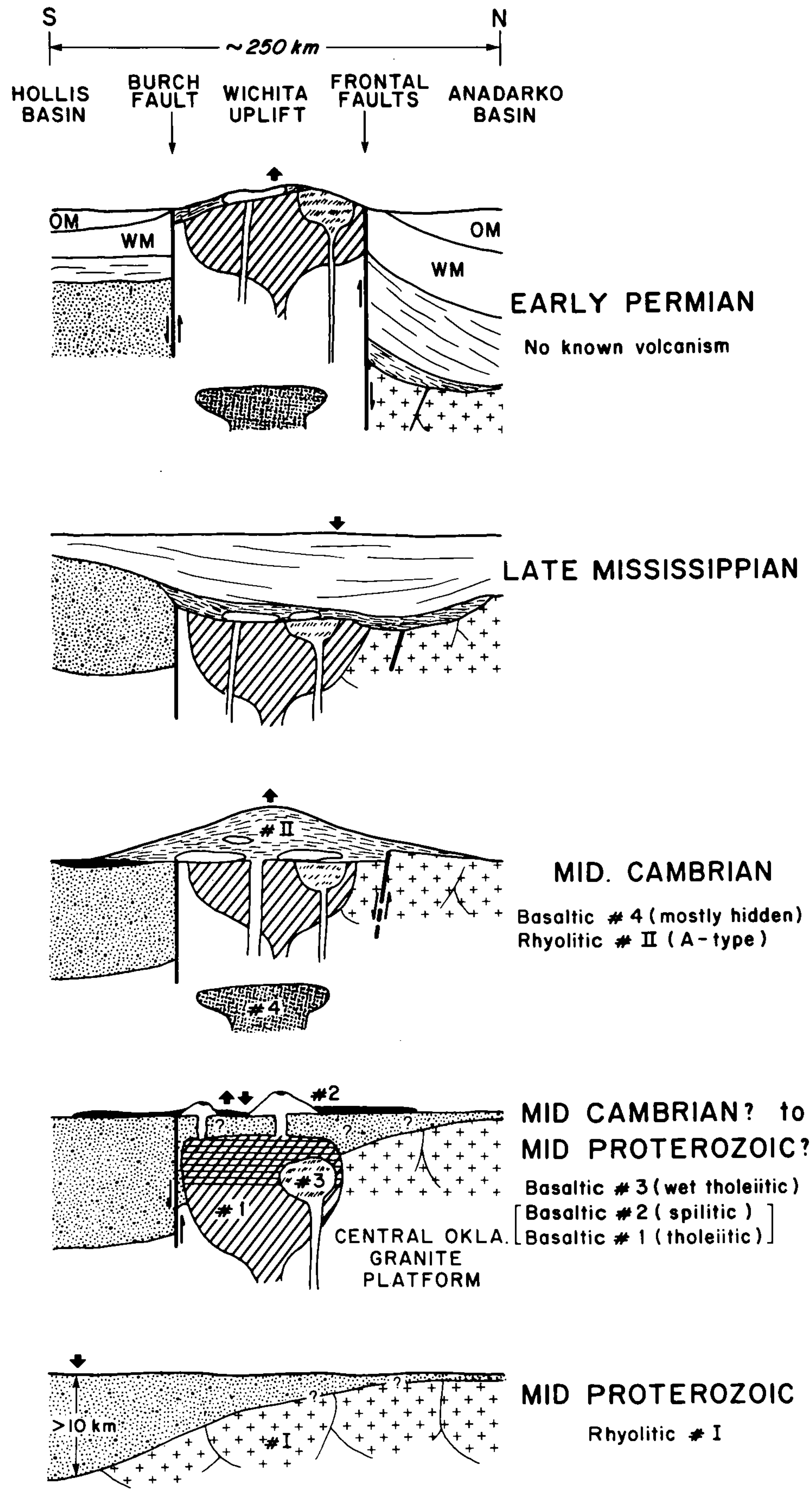

Figure 5. Geological development of Wichita Mountains crustal block, viewed diagrammatically across axis of uplift. Most faults shown at high angle, although the frontal faults are known to dip 30°–40° to south (see Brewer, this guidebook). Strike-slip movement not precluded. Rhyolitic I = shallow older basement granites, perhaps equivalent to eastern Arbuckle province. Basaltic 1 = Glen Mountains Layered Complex. Basaltic 2 = Navajoe Mountain Basalt–Spilite Group. Basaltic 3 = Roosevelt Gabbros. Rhyolitic II = Carlton Rhyolite Group and Wichita Granite Group. Basaltic 4 = late diabase. Short, heavy arrows indicate net motion of land surface, by subsidence, uplift, or erosion.

TABLE 1.—SIMPLIFIED LITHOSTRATIGRAPHIC CHART OF SOUTHERN OKLAHOMA AULACOGEN

STRATIGRAPHY
SOUTHERN OKLAHOMA AULACOGEN - WICHITA MOUNTAINS BLOCK

			Major Units	Age	Exposed
Clastic	Passive (external)		Pontotoc thru Cloud Chief	Permian	Wichita Mtns. - Anadarko Basin
			uuuuuu		
	Active (internal)		Morrow thru Virgil	Pennsylvanian	No
		T	xxxxxx		
			Kinderhook thru Springer	Mississippian	No
			uuuuuu		
	Shelf Type		Woodford	Devonian-Mississippian	No
Carbonate			uuuuuuu		
			Hunton	Silurian-Devonian	No
			uuuuuuu		
	Basin Type		Viola	Upper Ordovician	Wichita Mtns.
			Simpson	Ordovician	No
	Clastic Base		Arbuckle Group	Cambro-Ordovician	Wichita Mtns.
			xxx? (seismic only)		
			Timbered Hills Group	Cambrian	"
			uuuuuuu		
			Late diabase	~0.52by	Wichita Mtns.
			Wichita Granite Group	0.52by	Wichita Mtns.
			Carlton Rhyolite Group	0.52by	Wichita Mtns.
		N	xxxxxxx		
			uuuuuuu		
			Navajoe Mountain Basalt-Spilite Group	.55-1.4by(?)	No
			Raggedy Mountain Gabbro Group		Wichita Mtns.
			Roosevelt Gabbros	0.55by	
			Glen Mountains Layered Complex	0.55-1.4by(?)	
		N?	xxxxxxx		
			Tillman Metasedimentary Group	1.0-1.3by(?)	Wichita Mtns. (?)
			uuuuuuu		
			Older Basement	>1.2by(?)	No

"uuu" represent unconformities; "xxx" = periods of faulting with N = normal; T = thrust

Stockton and Giddens, and chemical studies of the Sandy Creek Gabbro by Powell, all bear out this relation. Some of the data are presented in the field-stop descriptions. This unconformity becomes the surface upon which the 525–500–m.y. Carlton Rhyolite Group extrudes and along which some units of the chemically equivalent Wichita Granite Group intrude. Gilbert (1978d) noted the large preponderance (10:1) of rhyolite to granite, which is also a peculiar feature of the region. Because rhyolites are extremely susceptible to post-emplacement alteration, chemical studies of the granites are expected to provide a better measure of the pristine igneous liquids. Myers and others (1981) used the A-type designation for those liquids. Gilbert (1978d, 1982) pointed out the large amount of Cambrian basaltic liquid necessary somewhere in the crustal column to go with the rhyolite liquid, either as a chemical source or a heat source. This is indicated in figure 5 by basaltic unit 4. Our only measure of this material is probably the late diabasic dikes and plugs which cut all other igneous units. Tensional strains are shown by normal faulting during and preceding volcanism, as argued first by Ham and others (1964) and also by Brewer and others (1982). Whether the aulacogen should be dated as beginning from this mid-Cambrian faulting, or the earlier Burch Fault, is not resolved. A net uplift results, owing to the build-up of the extrusive pile to a thickness of perhaps several kilometers in places.

Stage 4 represents the slow, overall subsidence of the Anadarko Basin region to receive 4 to 6 km of carbonate muds and shelf-type carbonates on the igneous substrate of the Wichita province. This subsidence carried forward from the Late Cambrian to the Mississippian, with the deposition center being within the present Anadarko Basin by Silurian–Devonian Hunton time (Amsden, 1975). Cambrian depocenters are unclear because key strata are eroded from the uplift and the deep Anadarko Basin has not yet been adequately sampled.

Stage 5 represents the uplift and formation of structural features as seen today. The uplift began in latest Mississippian to earliest Pennsylvanian time, with a number of pulses each shedding a new flood of debris out into the adjoining Hollis Basin on the south and Anadarko Basin on the north. A major compressional phase seems to be documented by the COCORP results, with large overthrusting of the core area out over the Anadarko. The Pennsylvanian fill of the Anadarko is partly derived from the Wichita Mountains area, particularly the "granite wash." About 3–6 km of section was added to the basin. Subsequently, tectonism waned in the Wichitas while additional sediments were being added to the Anadarko, seemingly from continued activity in the Ouachita tectonic belt to the southeast. Permian sediments accumulated to 2–4 km in thickness, finally burying the Wichita Mountains area, whose igneous core had been exposed. The record is skimpy for deposition during subsequent periods, although it is assumed by some that Cretaceous units eventually covered this area as well. Recent exhumation has exposed the Permian and two Cambrian unconformities, plus all major igneous units, with the exception of the Navajoe basalts.

Additional discussion of some of the stratigraphic units follows, as well as an outline of problems awaiting resolution.

IGNEOUS RELATIONS

General Statement

Table 2 presents the most recent rationalization of basement lithostratigraphy after Powell and others (1980), with proposed modifications of (1) granite terminology from Myers and others (1981) and (2) gabbro nomenclature from Stockton and Giddens (this guidebook; and 1982). A diagrammatic cross section of the igneous relations, as they existed at the close of Carlton Rhyolite volcanism and late diabase emplacement, and before the start of mid-Cambrian sedimentation (Reagan Sandstone), is shown in figure 6. While this diagram is not drawn to scale, it illustrates many key relations well-displayed in the eastern Wichitas; it is also meant to be representative of the whole province, from the way the *exposed* units are distributed.

From the recent dating of the Mount Sheridan Gabbro (Roosevelt Gabbros) at 550 m.y. by Bowring and Hoppe (this guidebook), the erosional interval during which the gabbroic substrate was planed off can now be estimated at less than 50 m.y., and probably less than 25 m.y. This unconformity appears to have been regionally low and planar, but with local relief of at least 100 m, and perhaps as much as 200 m. A saprolitic zone should have developed. Layering in the individual plutons of the Roosevelt Gabbros is both subparallel and at high angles to layering in the host Glen Mountains Layered Complex. Whereas some of the discordance is presumably due to intrusive flow relations, the suggestion is still clear that some tilting of the earlier layered complex may have preceded emplacement of the later gabbros. No systematic studies have been directed to this question.

Onto this mid-Cambrian surface poured out the Carlton rhyolites. As the volcanic stack accumulated, some of the rhyolitic liquid began to intrude the earlier volcanics and along the unconformity, the latter now also becoming an intrusive contact. The resulting Wichita granites are mainly sill-like sheets. Bulbous, pendant-shaped plutons, the common forms of many epizonal and mesozonal bodies, such as those in the Sierra Nevada Batholith, are not known in the Wichitas. A number of unusual, hybrid "igneous" rocks have been recognized in the Wichitas for some time (Huang, 1955). As these are always found along the gabbro-granite contact, it would appear that the origin of these rocks is tied to interaction between the gabbroic saprolite and rhyolitic liquid. Gilbert (1982) also argued that the dominance of rhyolites over granites (Gilbert, 1978d) is due to the

TABLE 2.—LITHOSTRATIGRAPHIC CLASSIFICATION OF BASEMENT ROCKS OF WICHITA PROVINCE, OKLAHOMA

(Underlined units crop out in Wichita Mountains)

Age (m.y.)	Group	Formation	Member	General Lithology
?		diabase		Fine-grained diabase cutting all older units but not Reagan ss.
514 ± 10?		Cold Springs Breccia		Dark-gray microdiorite blocks in matrix of pink leuco-granite; locally medium-gray quartz monzodiorite blocks in light gray granodiorite matrix
525 ± 25	Wichita Granite Group	*East*: Quanah, Cache, Medicine Park, Saddle Mountain; *West*: Lugert, Cooperton, Long Mountain, Reformatory, Headquarters; Mount Scott		Group typified by medium-to fine-grained alkali feldspar granites; granophyric texture sporadically dis-tributed within the group.
525 ± 25	Carlton Rhyolite Group	Bally Mountain, Blue Creek Canyon, Fort Sill		Rhyolitic lavas interbedded with minor tuffs and agglomerates
?		Otter Creek Microdiorite		Fine-grained diorite and quartz diorite
?	Navajoe Mountain Basalt-Spilite Group			Extrusive basalts variably altered
552±7	Raggedy Mountain Gabbro Group	Roosevelt Gabbros	Mt. Baker hornblende Gabbro	Medium- to fine-grained hornblende-biotite, 2-pyroxene, no olivine, gabbro
			Glen Creek Gabbro	Medium-grained biotite-amphibole-bearing olivine gabbro
			Sandy Creek Gabbro	Medium-grained biotite amphibole-bearing gabbro ± olivine
			Mount Sheridan Gabbro	Medium-grained biotite gabbro locally fractionated to ferrogranodiorite
509-730 1,300-1,500		Glen Mountains Layered Complex	N Zone	anorthositic gabbro with cumulus plagioclase
			M Zone	Anorthosite, anorthositic gabbro, and troctolite with cumulus plagioclase augite, olivine
			L Zone	Anorthositic gabbro with minor troctolite; coarse-ophitic augite; cumulus plagioclase and olivine
			K Zone	Alternating bands of anorthosite and troctolite; cumulus plagioclase, olivine
			G Zone	Troctolite and olivine gabbro; medium grained; cumulus plagioclase olivine
?	Tillman Metasedimentary Group	Meers Quartzite		Metaquartzite and meta-graywacke with andalusite and sillimanite; inclusions in rocks of Raggedy Mountain Gabbro Group and Wichita Granite Group

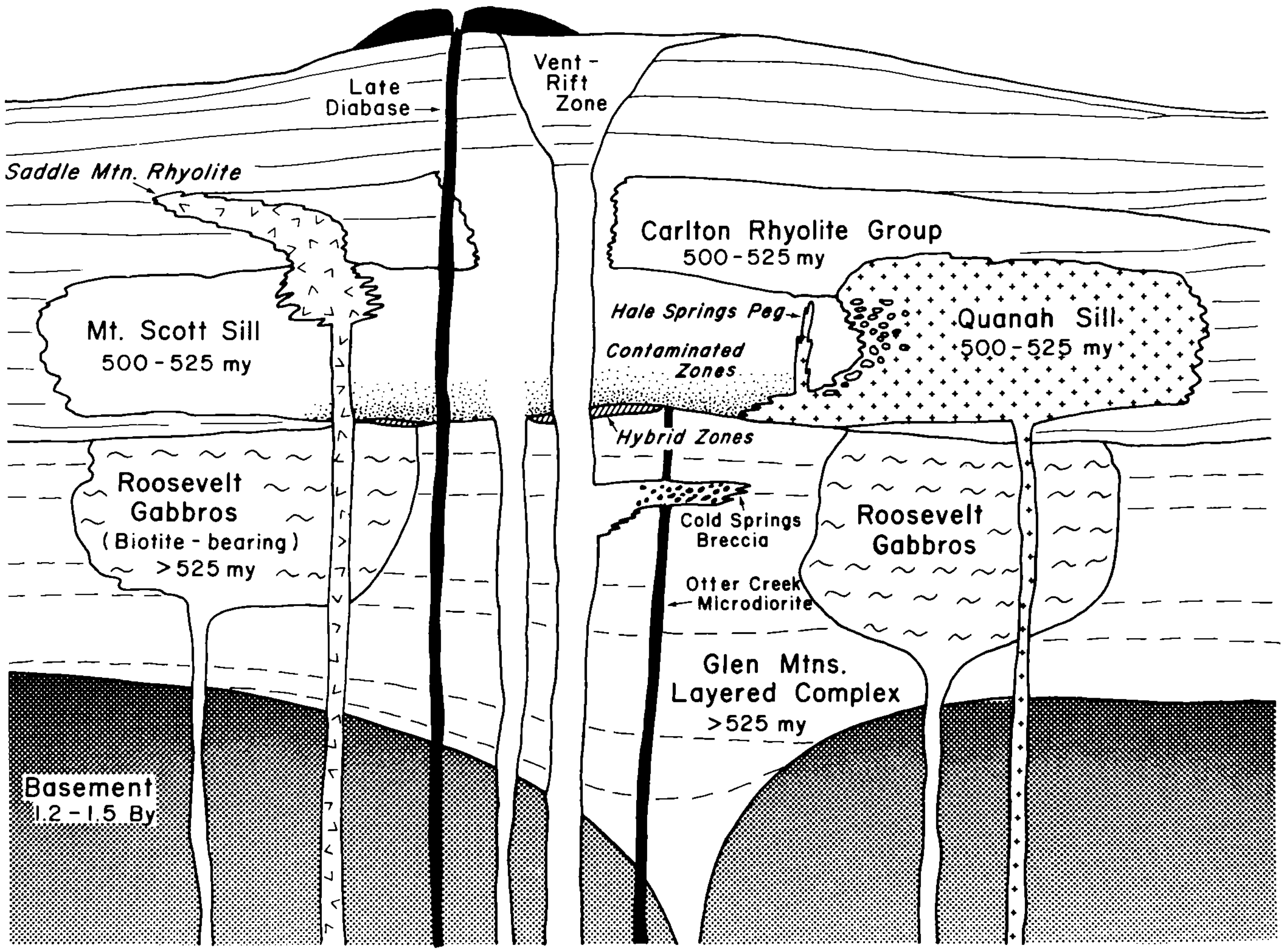

Figure 6. Diagrammatic section of igneous relations exposed in eastern Wichitas as they existed at end of volcanism in Cambrian time and before deposition of Reagan Sandstone. Mid-Cambrian unconformity, now also a surface of intrusion, separates gabbros from rhyolites and granites. From Myers and others (1981, fig. 1).

unusually dense substrate. With gabbroic rocks plating the upper part of the crustal column for 4 or 5 km, buoyancy relations did not permit rhyolitic liquid to stop before reaching the surface. Thus, the granites mostly are thought to be hosted in their own ejecta, rather than gabbro. (Locally, gabbro is intruded by granite, but the argument here is for the regional scale.) This also accounts for the extreme sheet forms of the granites, wherein the Mount Scott Granite, for example, is at least 55 km in one horizontal dimension.

Final igneous activity is represented by a late diabase that cuts all other units (Ham and others, 1964). Although this unit is of small volume, it may in fact represent the largest pulse of basaltic liquid to enter the crustal columns (Gilbert, 1978d, 1982). This is because the estimated 40,000 km^3 of rhyolite liquid must be generated ultimately by basaltic liquid. Because the mass of rhyolite is so large, and extends (or extended) out beyond the immediate boundaries of the gabbroic substrate that can be mapped, there is somewhere in the crustal column additional enormous masses of gabbro. This has two immediate consequences: (1) the geophysical anomalies (magnetic and gravity) represent the combined effect of several different basaltic pulses (1, 3, and 4 of fig. 5) and so the gabbros cannot really be modeled as one lopolithic body, as Pruatt (1975) did; and (2) study of the chemistry of these late diabase bodies will be necessary to constrain petrogenetic models of the rhyolitic liquids.

Table 3 lists chemical data for two of the distinct types of basaltic liquid and for two of the rhyolitic liquid that have been identified. This is another way of noting the strong bimodality of the Wichita province. The Glen Mountains Layered Complex has not yet been characterized as to the original liquid composition. The Roosevelt Gabbros, however, are small enough so that judicious sampling (and averaging) may reasonably yield an equivalent liquid. This is the oldest composition listed. In comparison, the youngest is a newly averaged set of five late diabases, whose chemistry does not differ markedly from the Roosevelt Gabbros. An example of one of the earliest rhyolitic liquids, if not the earliest, is the Mount Scott Granite. It is also the most calcic. One of the youngest

TABLE 3.—CHEMISTRY OF SELECTED IGNEOUS UNITS, WICHITA MOUNTAINS, OKLAHOMA

(All Fe as Fe_2O_3)

Wt.%	(Pre-granite) Roosevelt Gabbros	(Post-granite) Late Diabase	(Early-granite) Mt. Scott Granite	(Late-granite) Quanah Granite
SiO_2	47.3	46.6	72.3	76.2
TiO_2	3.0	3.6	.44	.16
Al_2O_3	15.0	13.5	12.3	11.8
Fe_2O_3	13.5	16.4	3.9	2.4
MnO	.21	.21	.08	.02
MgO	8.2	5.4	.31	.03
CaO	8.8	8.7	1.2	.23
Na_2O	1.99	2.3	3.8	4.0
K_2O	.36	.75	4.3	4.75
P_2O_5	.22	.61	.08	.01
Sr ppm	406	371	91	9
Rb ppm	6	22	127	169

granite types is the Quanah, which all workers agree has alkaline characteristics. Whereas other rocks can be found that range between these extreme mafic and silicic compositions, in most cases they can be shown to be products of hybridization or contamination, and (or) of only local distribution. No compelling data or arguments exist for primary (and large-volume) intermediate igneous rock, at least from the surface exposures.

Raggedy Mountain Gabbro Group

Figure 7 shows the distribution of formations and members of the group. This presentation incorporates results of the latest mapping and revisions in nomenclature. The older part of the group consists of the Glen Mountains Layered Complex, whose age is problematic, with estimates ranging between 0.5 and 1.4 b.y. [see Powell and others (1980) for a complete discussion, and also Roggenthen and others (1981)]. The younger part consists of the Roosevelt Gabbros, one member of which has been definitively dated at 550 m.y. (see Bowring and Hoppe, this guidebook, for data on the Mount Sheridan Gabbro).

Glen Mountains Layered Complex

Useful field and petrographic data are given in Powell and Fischer (1976). The lithostratigraphy is codified in Powell and others (1980). Stockton and Giddens (this guidebook) introduce the new unit, N Zone, as a stratigraphic member above the M Zone in the Cooperton Quadrangle. Provisionally, this nomenclature is extended farther east on the basis of reconnaissance mapping and data compilation. In this way, a somewhat consistent pattern emerges wherein the belts of outcrop trend at lower angles (~ N. 60° W.) than the regional structure and igneous-outcrop distribution (~ N. 70–80° W.).

Members of this formation are designated as zones. The G Zone is anomalous owing to its limited outcrop, somewhat different modal proportions, and phase chemistry (Spencer, 1961; Powell and others, 1980). The K Zone may be taken as the lowest unit of the normally exposed sequence cropping out as a belt along the southern margins of the Glen Mountains. The overlying L Zone is generally distributed about the K Zone belt, but it has a somewhat more extensive outcrop in the area where the northwest-trending fold axis crosses U.S. Highway 183 south of Roosevelt. The unit seems to thin to the east. The M Zone overlies the L Zone and dips consistently to the north-northeast. The newly recognized N Zone has a gradational contact with the underlying M Zone. Eastward, the N Zone passes under the Mount Scott Granite sheet, reemerging in the Central Lowland and west of Meers. Because of limited mapping, data generated on rocks of the layered complex in the east could not readily be correlated with the type sections

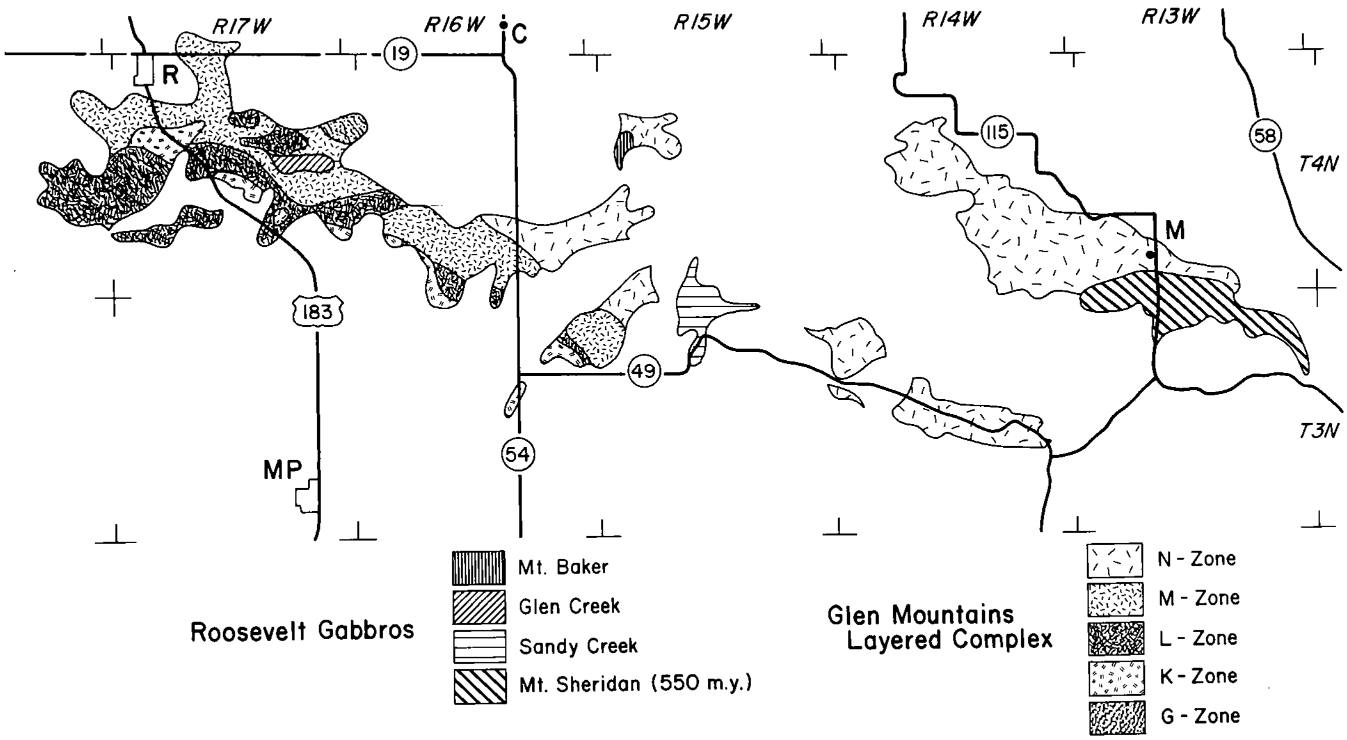

Figure 7. Surface outcrops of Raggedy Mountain Gabbro Group.

in the Glen Mountains. With the recognition of an additional member by Stockton and Giddens, it should be possible to pull this information together. Estes (1980) provided an interesting set of phase-chemistry data from a traverse west of Meers. Rates of change in the cryptic layering are more rapid than in the Glen Mountains area. This section, here taken to be in the N Zone, is probably one of the highest stratigraphically in all the exposures.

Roosevelt Gabbros

Powell discusses this unit in detail in an accompanying article. Stockton and Giddens, also in an accompanying article, recognize a new, fourth member of the unit, the Mount Baker hornblende gabbro. This latter pluton crops out on the western flank of Mount Baker in the Cooperton Quadrangle (secs. 18–19, T . 4 N., R. 15 W.) and is distinctive, in part, owing to cm-size, poikilitic hornblende crystals not otherwise seen in the Wichitas. Bowring and Hoppe present data documenting a 550-m.y. age for the Mount Sheridan Gabbro. The Mount Sheridan is the largest of the exposed members, having a diameter of at least 8 km.

Carlton Rhyolite Group

Ham and others (1964) were the first to show the extent of this group across the southern Oklahoma basement. By surface and subsurface correlation, they pulled together the widespread but limited surface outcrops of rhyolite into the Carlton unit. Four principal areas are now recognized: (1) the East and West Timbered Hills of the Arbuckle Mountains in southern Oklahoma (Colbert porphyry); (2) the Bally Mountain section (T. 6 N., R. 14 W.) on the far northern and eastern sides of the Wichitas, which they took to be a type section; (3) the Blue Creek Canyon section along Stumbling Bear Pass, on State Highway 58 (T. 4 N., R. 12–13 W.); and (4) the Fort Sill section, basis for the designation "Carlton," underlying most of the original military reservation (T. 2–3 N., R. 12–13 W.). This latter section is the largest of the four, and one of the first areas to be recognized as containing extrusive volcanic rocks (Schoonover, 1948). Figure 2 shows the three outcrop areas of the Carlton in the Wichitas.

An erosional interval separates the Carlton from the underlying Raggedy Mountain Gabbro Group and from the overlying sedimentary Timbered Hills Group (basal Reagan Sandstone and Honey Creek Formation; see table 1). However, Ham and others (1964) chose Bally Mountain as a type section because 3,600 ft of an apparently continuous sequence could be measured to the upper unconformity. The Blue Creek Canyon sequence is similar in that the unconformable relationship with the overlying Timbered Hills Group is well displayed; however, the section is truncated on the west by thrusting so that less section is exposed.[1] Thus, these two sections are probably relatively high in the stratigraphic se-

[1] The name of this section needs a brief explanation. Taff (1904) and early workers called the creek-heading in the surrounding hills Blue Creek, and the ravine to the south Blue Creek Canyon. Presumably by an accident of map-making, Blue Creek was omitted, because maps now show this stream as Canyon Creek. Further difficulty arises because the State Highway Department, after improving Oklahoma 58 in the early 1960's, renamed

quence of the group. Presumably, the section of Colbert porphyry in the Arbuckles likewise is high, because it also lies under the upper unconformity. On the other hand, the Fort Sill section is probably very low in the group, because the Mount Scott Granite, which has intruded along the lower unconformity on the gabbros and rests on gabbro on the north side of Mount Scott itself, *overlies* at least part of the rhyolite, as seen on the south side of Mount Scott. Abundant outcrops of Meers Quartzite also occur in the vicinity, and, as amplified below, this unit may have its stratigraphic "home" on this lower unconformity.

Much of this basal sequence generally has a more massive character in comparison with the Bally Mountain section. Hanson (1977) gave the most comprehensive recent discussion of the Carlton Group, reporting a considerable amount of reconnaissance geochemistry. However, problems exist in working with the chemical composition of extrusive rocks because much post-consolidation alteration is common in volcanics. Furthermore, the Carlton Group has been exposed to near-surface weathering and ground-water circulation three different times in its history (see table 1). Consequently, it may be more useful to explore the granite chemistries, which are assumed to be derived from equivalent liquids, as guides to ultimate sources of the liquids. In addition, Hanson's analyses appear to have variable precision, so that arguments based on small differences cannot be built on his data alone. Nevertheless, compilation of data from his thesis yields table 4, from which some interesting observations follow. The Fort Sill section is petrographically different from the other three in that quartz represents about 40 percent of the alkali-feldspar–quartz-phenocryst assemblage. The other sections are also quartz-saturated, but they have less than 10 percent quartz phenocrysts. The groundmass of most reported Carlton samples (all investigators) is between 80 and 90 percent, with most phenocryst percentages clustering around 9 to 15.

These data, taken together, imply that:

1. The bulk-rock system closely approaches the synthetic system SiO_2–$NaAlSi_3O_8$–$KAlSi_3O_8$, which can thus be used as an interpretive guide; the phenocrysts can be plotted as the crystal phases, and the groundmass (balance of rock) treated as quenched liquid.
2. The rhyolite magmas were near-liquidus and thus of high temperature, probably not less than 950°–1,000° C.
3. Because quartz is the phenocrystic phase, rather than tridymite, which is the stable SiO_2 polymorph for the emplacement T and P, the crystallization of the phenocrysts occurred at some depth. Thus, the liquid was not generated near the surface (at low pressure), as might be expected in a meteoritic impact or melting of roof rock by a gabbro.
4. Provided that preferential mechanical segregation of quartz phenocrysts relative to alkali feldspar did not occur, the Fort Sill section was probably emplaced at *lower* temperatures than were the other three sections.
5. The bulk composition of the magma(s), and their source rock(s), lie on the feldspar side of the boundary curve in the system SiO_2–$NaAlSi_3O_8$–$KAlSi_3O_8$ (Qtz–Ab–Or).
6. On a worldwide basis, Carlton rhyolites compare most closely with rhyolites from bimodal mafic–silicic associations, as in southern Queensland (Ewart, 1979). Only such rhyolites have alkali feldspar phenocrysts dominating over plagioclase, and with plagioclase low to absent.

the defile through which the highway and creek pass, once known as Blue Creek Canyon, as Stumbling Bear Pass. Another source of confusion lies in the name of that portion of the Wichitas underlain by carbonate rocks. Geologists have generally referred to these as the Limestone Hills, whereas many local people have called them the Slick Hills. These names are used interchangeably in this guidebook.

If the composition of alkali feldspar phenocrysts were determined, model three-phase triangles in Qtz–Ab–Or could be constructed. None being available as yet, the normative ab–or values can be used as an estimate. Hanson's data (1977) generally show $ab/(ab + or)$ or $(ab + an)/(ab + an + or)$ in the range of 50 to 60 percent, with the exception of the Blue Creek Canyon section. Data from a few individual analyses in Ham and others (1964), and some others generated by Gilbert and Myers (unpublished, 1981), also show this range. Burwell (1956) reported six feldspar analyses from Wichita granites (which should be similar) that yield similar values. This establishes the most Or-rich composition possible for the feldspar portion of the quartz–alkali feldspar tie-line, and the trailing edge of the three-phase triangle, L (liquid)–Qtz–F (alkali feldspar). This line falls on the Ab-Qtz side of the minimum in the higher pressure, dry system. If the system were H_2O-saturated, this line would be on the Or–Qtz side. However, there is no evidence for a wet original condition, but only that the magma became H_2O-saturated during emplacement at very low pressure, necessitating a very low water fugacity and low absolute water content (probably less than 1 to 2 weight percent H_2O). Thus, the L position on the boundary curve must be to the right of this Qtz–F line, and the triangle faces (points) toward Qtz–Or. This means that the source of the magma was probably ultimately plagioclase-saturated. We cannot specifically exclude a composition that was very quartz-poor and K-spar-saturated, because the exact position of the boundary curve, its minimum, and the thermal trough in the feldspar liquidus-phase field are all unknown at elevated pressure in the H_2O-free system. The range of bulk compositions that would permit this phase behavior on extreme fractional crystallization is limited and therefore not considered further at this time.

Plagioclase is rare as a primary phase in the rhyolites. The question arises as to whether such plagioclases are xenocrysts, restites, or parts of a fractional crystallization process. No definitive answer is possible as yet, but the discussion above would be compatible with a model of either partial melting (restites) or crystal fractionation.

If a partial-melt model were assumed, then the Fort Sill section would represent an early liquid, as argued on stratigraphic grounds earlier (see also Hanson, 1977). The phenocryst assemblage of quartz + alkali feldspar in the Fort Sill rhyolites is consistent with derivation on a high-pressure boundary curve, although it is not likely that the observed phenocrysts are left over from the melting. The rhyolites have no exotic inclusions that could be related to lower or middle crustal regimes. Only the less common plagioclase crystals may be a precursor material. The separation of the partial melt from its source appears to have been a high-temperature, mechanically clean, and rather complete event. This melt must have had a bulk composition of about 35 percent SiO_2 in Qtz–Ab–Or. After rising to near the surface, the melt must plot close to the lower pressure boundary curve to generate 40 percent quartz phenocrysts. Tie-line constraints would place the boundary curve on the feldspar side of the bulk-melt composition. A more quantitative model can be constructed when additional data are available on the phenocryst and groundmass feldspars.

The other three outcrop areas, in contrast, have phenocryst assemblages with little quartz. The boundary curve for these rocks must lie on the quartz side of their bulk isopleths. This implies different bulk compositions, or different depths (pressures) of phenocryst crystallization, or different water contents. Study of the granites shows several distinct chemical classes (Myers and Gilbert, 1980; Myers and others, 1981). Because of the presumed intimate chemical relation between granites and rhyolites, distinctions found in the granites should apply equally to the rhyolites. The differences are subtle, however, and many highly precise determinations are necessary to make the comparison. These are not yet available.

In summary, before turning to the granites, table 4 documents a real difference between the Fort Sill section of the Carlton Group and the other three areas. The most obvious of these are (1) phenocryst ratios, (2) normative quartz content, and (3) concentrations of the trace elements Sr, Ba, and Mn. Interestingly, the Mount Scott Granite, an early one, is much less siliceous than the Fort Sill section (normative qtz = 32) but very close in its Sr content of 91 ppm (table 3). Because the Sr content normally falls with increasing SiO_2, and does so in the Wichita granites, the Fort Sill rocks present something of an anomaly for the province. It may be that many of the quartz phenocrysts in this early section are xenocrysts picked up from a quartzitic sedimentary section.

Wichita Granite Group

Hoffman (1930), indirectly Merritt (1958), and Ham and others (1964) and Merritt (1967) provided the lithostratigraphic framework used with this group until recently. Powell and others (1980) accepted that framework in their overall revision of the igneous stratigraphy of the province. Myers and others (1981) provisionally modified the granite nomenclature, partly on the basis of new chemical data and partly on the basis of new mapping by Gilbert. These are incorporated into table 2, amplified in tables 5 and 6, and shown in figure 8. For this review, table 7 is helpful in noting the factors employed in the geological analysis of the granites. Each of these internal and external factors has possible ambiguity, so that the answer sought on primary aspects is not always clear-cut. Nevertheless, all these factors have been utilized individually or as groups. Much of the detailed work is still in progress; therefore, discussion will be limited.

Two factors not employed by earlier workers in the Wichitas are layering and fracture patterns. Layering, defined by alignment of the alkali feldspars, is subtle but surprisingly common where crystal shapes approximate rectangular parallelepipeds. This alignment reflects magmatic flow conditions during intrusion. Whereas many local variations are particularly noticeable near high-angle, intrusive contacts, some regularity prevails at the scale of 10^2–10^3 m. Overall, the layering is taken to be parallel to the margins of the granites, as the flow directions must have been. The granites appear to have been emplaced as subhorizontal sheets. Thus, the attitude of the layering today is a measure of the imposed structure.

The fractures so prominent in the granites can be classified according to age and origin into primary and secondary types (Gilbert, 1982). Primary fractures are Cambrian in age and reflect the physical conditions of emplacement. These primary fractures can be divided into two classes: (1) those subparallel to the layering, with generally shallow dips regionally, and (2) those resulting from contraction on solidification, a kind of cooling column analogous to that commonly seen in surface basalts but much more ill defined, with generally steep dips, and perpendicular to layering fractures. Secondary fractures are Pennsylvanian in age and tectonically induced, reflecting strain in the brittle sheet during uplift. These are high-angle to vertical, some kilometers in length, and dominate the topography. They are discussed with the structure.

Miarolitic cavities are distinctive features of certain exposures of the granites. They represent vapor-phase formation from saturation of volatile constituents in the melt. Presumably, this vapor was mostly H_2O (and CO_2?), and was released as the melt was emplaced at very shallow depths. Pressures are estimated to have been in the 10^1–10^2–bar range, on the basis of the stratigraphy, abundant quench textures, cooling-related fractures, and body shape. Consequently, although a late vapor phase did form, the H_2O content of the melt was probably less than 1 to 2 weight percent, a quite "dry" magma (Burnham and Jahns, 1962). The vapor phase forming the cavities was released during the crystallization of the groundmass but after flow had ceased, because the cavities

TABLE 4.—CHARACTERISTICS OF MAJOR OUTCROP AREAS OF CARLTON RHYOLITE GROUP

From Hanson (1977)

Phenocryst Modal Data	Fort Sill Section	Blue Creek Canyon Section	Bally Mountain Section	Arbuckles Section
Alkali feldspar	8.9 (5)*	7.8 (15)	11.1 (3)	11.7 (3)
Plagioclase	tr "	.1 "	tr "	1.3 "
Quartz	6.0 "	.3 "	.8 "	.8 "
Qtz / (Qtz + Feldspar)	.40	.04	.07	.06
Normative Data				
qtz	39 (6)	34 (19)	32 (14)	35 (7)
or	26 "	32 "	24 "	26 "
ab	25 "	19 "	30 "	27 "
an	6 "	7 "	7 "	5 "
(ab + an) / (ab + an + or)	.54	.45	.61	.55
Trace Elements, ppm				
Sr	99 (6)	51 (19)	68 (15)	79 (7)
Ba	4251 "	2149 "	1659 "	1758 "
Mn	162 (18)	330 (28)	291 (21)	339 (12)
Cu	5 "	12 "	8 "	5 "
Zn	78 "	106 "	100 "	80 "

* Values in ( ) indicate number of samples averaged.

are not generally strung out or aligned. The vapor did not escape the cavities until solidification was complete and the rock mass rigid enough to support the load, because the holes are not deformed. Normally, the cavities are 1 to 5 cm in diameter. Other areas where granophyric texture (taken to indicate quenching) is common, but cavities are not, may have lost their vapor before complete solidification, so that the holes closed and are not now recognizable. More detailed mapping of such features on finer scales possibly would be useful as a guide to extent of overburden during intrusion.

The granites are 90 to 95 percent alkali feldspar and quartz. These granites are classic hypersolvus types, after the usage of Tuttle and Bowen (1958). Plagioclase occurs systematically as a primary phase only in the Mount Scott Granite, and then not uncommonly surrounded by alkali feldspar. Mafic phases are amphibole, biotite, and magnetite, but there is generally an antipathetic relationship between amphibole and biotite. Each of the named granites has a distinctive mafic signature, with amphibole more common in the province as a whole. Amphibole types are mainly arfvedsonite or hastingsite,

TABLE 5.—PROVISIONAL LITHOSTRATIGRAPHIC UNITS OF WICHITA GRANITE GROUP IN EASTERN WICHITAS

(Modified from Myers and others, 1981, table 4)

Formation	Petrography	Type Locality or Reference	Age Relations
Quanah	Facies C - Medium-grained, granophyric biotite-bearing Facies B - Fine-grained aplitic phase of A Facies A - Typical, arfvedsonite-bearing, grain size ∿10mm.	Taylor (1915); Chase (1954) and Gilbert (1977-81) unpub. Quanah Parker Lake Dam to Little Baldy may be used as reference area for "A", SW-23-3N-14W.	Cuts Mt. Scott and Cache; the youngest in the east.
Cache	Granophyric microporphyry, grain size ≤ 1-2mm, magnetite, very low C. I.	Green (1952) and Gilbert (1977-81, unpub.) See analyses W 743, WM-1, E. side of hill 1545' SW SW SW-7-2N-13W.	Cut by Quanah. Relationship to Mt. Scott unclear.
Medicine Park	Granophyric microporphyry, grain size ≤ 1-2mm, magnetite, very low C. I., distinct purplish cast, pyroxene-bearing in places.	Denison (1973; 1977, unpub.); Gilbert (1977-81, unpublished). NE-18-3N-12W.	Appears to cut Mt. Scott. Relationship to Cache & Quanah unclear.
Saddle Mountain	Gradational from spherulitic-porphyritic to granophyric-porphyritic; hornblende + biotite.	Hoffman (1930); Gilbert (1977-81, unpublished) SW-30-5N-14W to NE-7-4N-14W.	A possible differentiate of Mt. Scott. Relations to other units unclear.
Mt. Scott	Facies B - microgranite with C. I. as A but no ovoid feldspar, appears to underlie A Facies A - Typical, variably granophyric porphyry with ovoid feldspar, primary plagioclase, hornblende, ≤ 2-4 mm, C. I. of 4 to 6.	Merritt (1965); Gilbert (1977-81, unpublished). Top of Mt. Scott, SE-11-3N-13W, and Ira Smith Quarry, SE-4-3N-15W are type areas for "A". Typical outcrops for "B" are granites overlying Carlton Group and Meers Quartzite in N half of 15 & 16-3N-13W.	Appears to be oldest in the east.

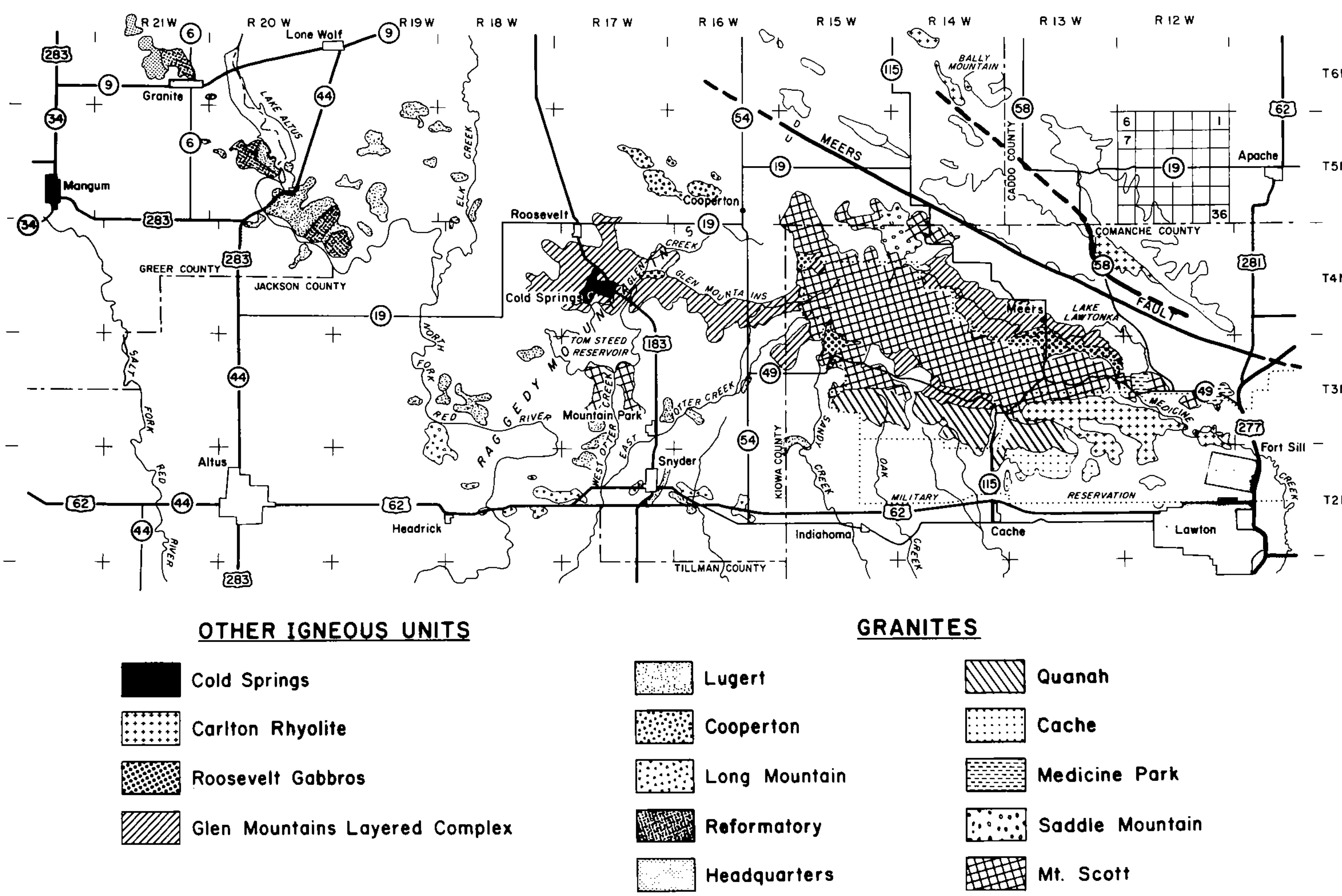

Figure 8. Surface outcrops of Wichita Granite Group (Myers and others, 1981, fig. 2).

TABLE 6.—BULK-ROCK CHEMISTRY OF WICHITA GRANITE UNITS IN EASTERN WICHITA MOUNTAINS
(Modified from Myers and others, 1981, table 5)

Wt %	Mt. Scott(10)# A	Saddle Mountain(2)	Medicine Park(1)	Cache(2)	Quanah(4) A
SiO_2	72.3 (1.3-.6)+	74.2 (.2)	75.5	77.2 (.4)	76.2 (.9-.5)
TiO_2	.44 (.05-.03)	.41 (.02)	.24	.14 (.01)	.16 (.05-.04)
Al_2O_3	12.3 (.4-.3)	12.6 (.25)	11.7	11.7 (.05)	11.8 (.2-.1)
*Fe_2O_3	3.9 (.4-.3)	3.0 (.25)	2.4	1.3 (.4)	2.4 (.6)
MnO	.08 (.02-.08)	.04 (.01)	.00	.01 (.01)	.02 (.01)
MgO	.31 (.22-.31)	.31 (.06)	.05	.03 (.03)	.03 (.06-.03)
CaO	1.2 (.2-.2)	.76 (.17)	.37	.32 (.03)	.23 (.12-.15)
Na_2O	3.8 (.4-.7)	3.7 (.2)	2.9	3.5 (.2)	4.0 (.4-.6)
K_2O	4.3 (.05-.07)	4.43 (.03)	4.6	5.18 (.15)	4.75 (.3-.4)
P_2O_5	.08 (.06-.02)	.07 (.01)	.01	.01 (.01)	.01 (.01)
H_2O/LOI^x	.34 (.3-.2)	.57 (.03)	.28	.34 (.14)	.56 (1.0-.4)
TOTAL	99.06	100.09	98.05	99.73	100.16
Sr ppm	91 (9-7) [6]#	ND	35 [1]	7 [1]	9 (4) [2]
Rb ppm	127 (8-11)	ND	140	231	169 (8)
Partial Norms					
qtz	31.6	33.8	41.0	36.5	34.4
or	25.7	26.2	27.7	30.7	28.0
ab	32.5	31.3	25.0	29.7	33.8
an	3.8	3.3	1.8	0.9	0.2

Number of analyses averaged.

+ Range of values is average; if 2 values, first is positive variation, second is negative.

* Total Fe as Fe_2O_3.

$^x H_2O$ + from the wet chemical analysis has been averaged with "loss on ignition" from the XRF data. These are not strictly comparable.

Analysis List

Mt. Scott: SQ, W78, W738, W7248A, W992, W998, C196, M1, WM9, IMS
Saddle Mtn.: W7125, C246
Medicine Park: W017
Cache: W743, WM1
Quanah: W984, W986, C193, C464

TABLE 7.—FACTORS CONSIDERED IN DEFINITION, MAPPING, AND CORRELATION OF GRANITE UNITS

	Informational Content + = reflects primary feature; - = modifies primary feature
I. Internal to Granite Bodies	
Order of crystallization:	+ bulk composition; PT conditions - flowage differentiation
Mineral assemblage:	+ bulk composition; PT conditions - post-magmatic changes
Texture:	+ cooling rate; volatiles; pressure - complex relations; post-magmatic changes
Layering:	+ original body shape; intrusive style - localized
Fracture patterns:	+ original body shape; intrusive style - later tectonic activity
Geochemistry:	+ original source - same source; late volatile transfer; weathering
II. External to Granite Bodies	
Contacts:	+ order of intrusion - remobilization
Similarity of units:	+ similar physical setting related in time - settings not in time pattern
Volcanic-tectonic setting:	+ style in which units occur - mixed settings; previously unknown setting

although Huang (1958) reported the two together at one locality in the Quanah. Other primary phases noted are ferroaugite (Thornton, 1975), acmite, zircon, monazite, sphene, fluorite, and apatite. Myers and Gilbert have examined feldspars by the electron microprobe and find typical core-to-rim traverses as shown in figure 9. The four data groups in the lower part of the figure represent point determinations across four individual grains in the rock. The determinations are expressed in mole percent on the feldspar ternary diagram. The An component is very low, and therefore only the bottom part of each triangle is shown. The spatial relations of the point determinations in a core-to-rim traverse are shown in the upper part of the figure for the first data-set down. Essentially, the feldspar is completely exsolved to very pure Or- and Ab-rich end members, reflecting a low temperature of equilibration (<350°C). The scale of the exsolution in some cases is, as shown in the lowest data-set, approximately that of the electron beam (~1 um), accounting for the apparent range of intermediate compositions.

The bulk-rock chemistry of the Wichita Granite Group was discussed by Myers and others (1981). Myers and Gilbert (1980) had noted that when careful determinations were plotted on variation diagrams a natural clustering of three groups resulted (fig. 10). One of these clusters, the most SiO_2-poor, came from only Mount Scott Granite samples. This igneous class was named the "Mount Scott." A restricted set of determinations that plotted between 74 and 75 weight percent SiO_2, derived mostly from samples of Reformatory Granite (in the western province), was called the "Reformatory" class. The most silica-rich cluster came from samples from a variety of named granites, and so this class was named "Mountain Park," after the small town near the area of some of the analyzed samples. The range of chemical values appropriate to the three classes, from our present data-set, is given in table 8. The distribution of the three classes is shown in figure 11. The Mount Scott class is typical of the eastern Wichitas; Reformatory is typical of the west; and Mountain Park is scattered all along the length of the exposures. This spatial control is thought to reflect different primary liquids that arrived at the surface from different, but perhaps related, sources. The Mount Scott class appeared early, but the other two classes show no time relation. For example, the Mountain Park class includes the early Headquarters Granite and the late Quanah Granite.

Chappell and White (1974) devised a simple classification of granitoid rocks as I-type and S-type according to source. The I-type granitoids are those from an igneous-rock parentage. That is, the liquids could have been derived by fractional crystallization from basalts or by partial melting of some previously crystallized igneous suite. S-types are those granitoids whose liquids came from partial melting of sedimentary material. Each of these types has distinctive chemical, isotopic, and petrographic indices. Loiselle and Wones (1979) pointed out another suite of granitoids that do not fit readily into the I-type and

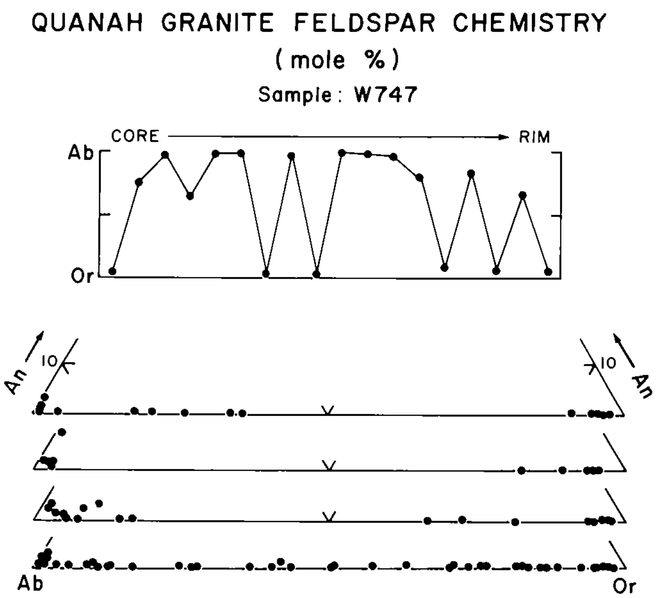

Figure 9. Electron microprobe determinations along traverses across originally homogeneous alkali feldspars from Quanah Granite.

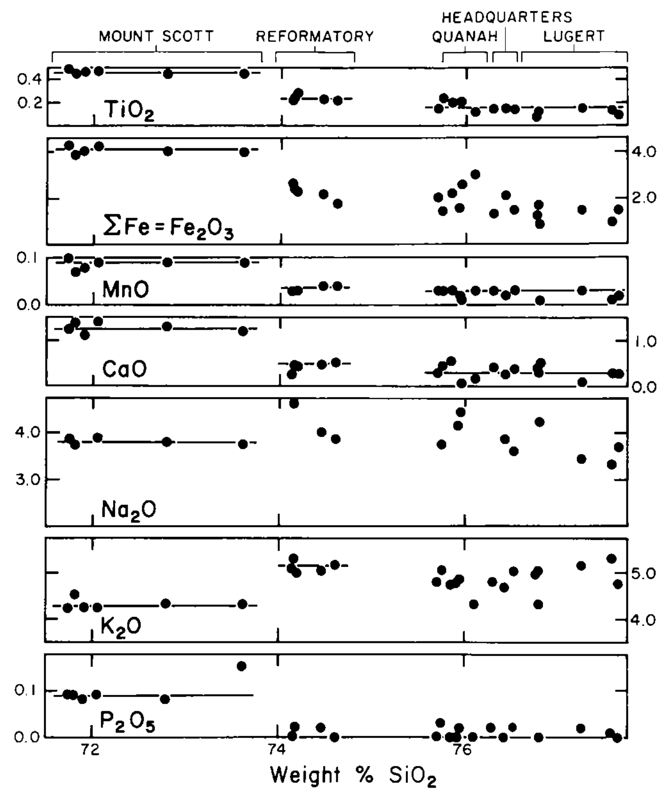

Figure 10. Harker variation diagram for some of available determinations from Wichita Granite Group. Three clusters can be seen which are discussed in text.

TABLE 8.—CHEMICAL SIGNATURE OF GRANITE CLASSES OF WICHITA GRANITE GROUP

Oxide wt%/Class	*Mt. Scott*	*Reformatory*	*Mountain Park*
SiO_2	71.0-73.6	73.8-74.7	75.0-77.6
TiO_2	>0.4	0.2- 0.3	.1-.25
Fe_2O_3 (total Fe)	>3.5	1.8-2.7	1.2-2.6
MnO	>.07	0.02-0.05	0.00-0.04
CaO	1.0-1.5	0.3-0.7	0.1-0.6
K_2O	∿4.3	4.2-5.3	4.1-5.5
P_2O_5	.08	.00-.02	.00-.01
Rb (ppm)	127	127	174
Sr (ppm)	91	41	22

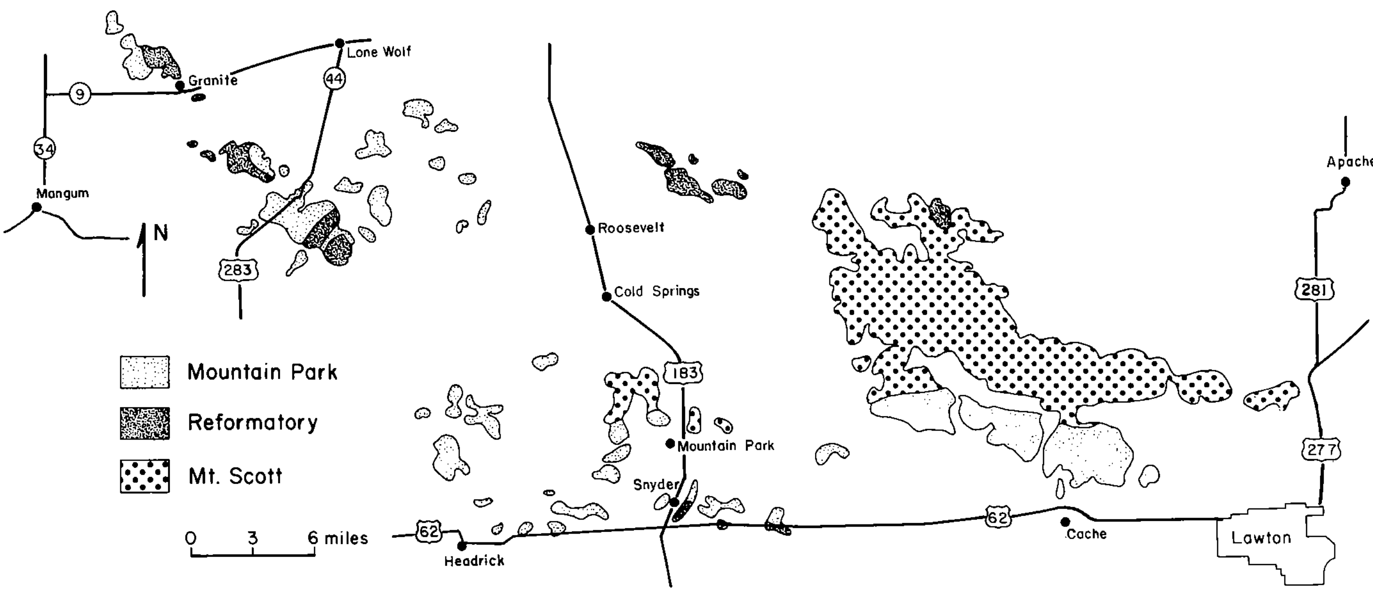

Figure 11. Map showing distribution of Wichita granite outcrops, divided into three geochemically distinct classes.

S-type classification. These are the set known by a variety of names that included anorogenic, alkaline, and anhydrous. The source of these rocks appears to be alkali basalt that interacted with an already depleted and dry, lower crustal section. They proposed that this set be called "A-type," and discussed their indices. Table 9 lists these indices, and their values for the Wichita Granite Group. This designation is more useful, and appears to be based on chemical data of higher precision, than the attempt to label the granites as calc-alkaline, as was done by Hanson and Al-Shaieb (1980).

The modal and chemical data of the three classes of Wichita granites are plotted on appropriate diagrams after Loiselle and Wones (figs. 12, 13). Our granites clearly belong to the A-type. Plotting of their normative chemistry in the system SiO_2–$NaAlSi_3O_8$–$KAlSi_3O_8$ (fig. 14) yields isopleths around which the three-phase triangles discussed with the Carlton Rhyolite may be placed. Gilbert and Myers are developing a specific model for the origins of these liquids. Although the bulk compositions of Wichita granite classes plot most similarly to rhyolites from the bimodal associations noted by Ewart (1979), estimated original alkali feldspar compositions are more like those from Icelandic rhyolites (Ewart, 1979).

Trace-Element Data

A set of limited chemical data for selected samples was generated by INAA methods, arranged through the courtesy of Salman Bloch, of the Oklahoma Geological Survey. No claim to high precision is made for the values, but they are taken to be indicative of the likely range of concentrations to be found with more intensive effort. Figure 15 reports results for Sc, Zn, Hf, U, and Th over the range of SiO_2 occurring in rocks of the Wichita igneous province. The striking SiO_2 bimodality is clear from the figure.

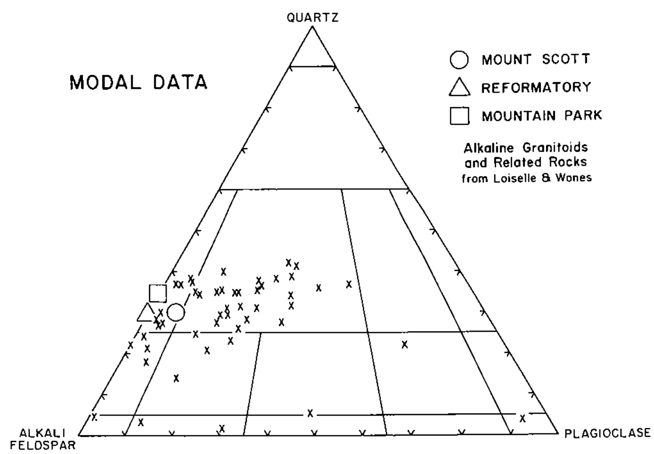

Figure 12. Modal data for the three chemically defined classes of Wichita granites, compared with other A-type granitoids as plotted by Loiselle and Wones (1979; and written communication, 1980).

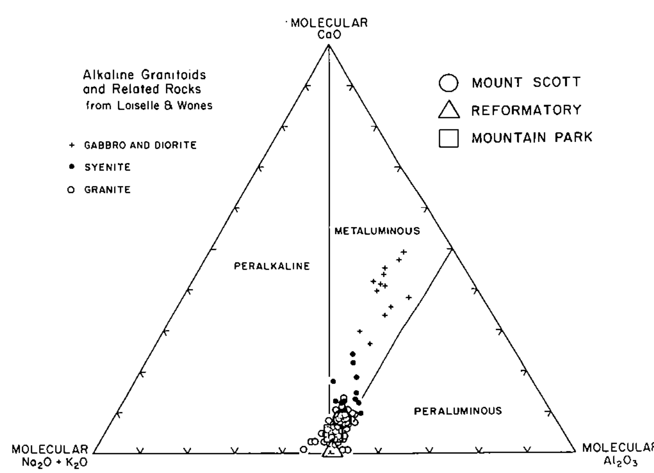

Figure 13. Chemical data for the three Wichita granite classes, compared with other igneous suites with A-type characteristics as compiled by Loiselle and Wones (1979; written communication, 1980).

Regular variation of trace elements with SiO_2 is demonstrated with the exception of Zn, which may well be spurious owing to contamination in the low-silica rocks. Limited data compiled by Ewart (1979) from the bimodal volcanic associations in southern Queensland indicate Zn at 145 ppm and Hf at 10 ppm for the rhyolites at 76 weight percent SiO_2, which is comparable to the Wichitas.

Figure 16 presents chondrite normalized rare-earth data for the Mount Scott Granite and rhyolite dikes which cut Wichita granites. The behavior of the plots, particularly with the heavier rare earths, indicates that some of the values such as Er and Tm may have low precision (G. N. Hanson, 1980). The Mount Scott data are averages of three samples, the dikes, two; but each sample of a type had practically identical patterns. Several significant trends are observed:

1. Mount Scott granite and the dikes have similar overall patterns.
2. A distinct, negative Eu anomaly exists, indicating for the source materials: (a) medium- to low-oxygen fugacities, and (b) abundant plagioclase.
3. The absolute concentration of REE appears to be fairly high.
4. The pattern is relatively enriched in light elements and depleted in heavy rare earths, and resembles those taken from liquids equilibrated with hornblende (G. N. Hanson, 1980).

Finally, Arth (1979) noted that absolute abundance of Yb varies with Al_2O_3 for trondhjemites (a class of low-K tonalites). Only the low-Al_2O_3 group has Yb greater than 1–2 ppm, and these are "oceanic" suites, whereas the granite and rhyolite analyzed here have 7 to 9 ppm. Ewart (1979) listed 5 to 9 ppm Yb for the Queensland rhyolites, a bimodal association. Such comparisons, if nothing else, show the inappropriateness of a calc-alkaline label for the Wichita province silicic rocks (see Hanson and Al-Shaieb, 1980).

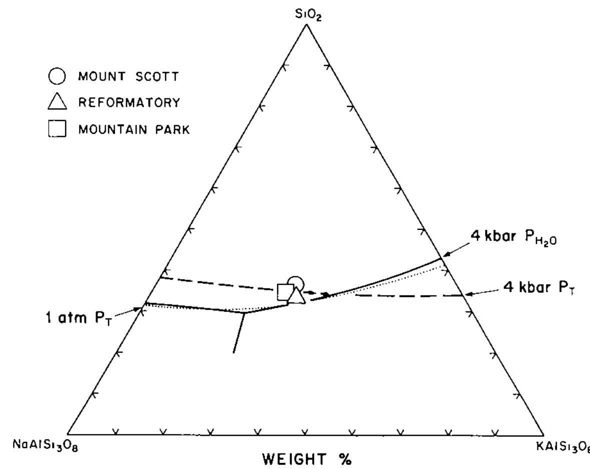

Figure 14. Position of the three chemical classes of Wichita granites in system SiO_2 (Qtz)–$NaAlSi_3O_8$ (Ab)–$KAlSi_3O_8$ (Or), with locations of boundary curves shown from Steiner and others (1975).

TABLE 9.—CHARACTERISTICS OF A-TYPE GRANITES

Index	*Wichita Granite Group*
Low CaO	<0.5; <1.5 wt% (2 sets)
Low Al_2O_3	11.6-13.0 wt%
High Fe/(Fe + Mg)	.92 - .98 (by wt.)
High K_2O/Na_2O	1.1-1.5 (by wt.)
High K_2O	4.2-5.3 wt%
Generally low f_{H_2O}	estimated $\leq$ 1 wt% H_2O in magma
High HF/H_2O	F-bearing alkali amphiboles
Enriched incompatible trace elements (REE, except Eu; Zr, Nb, Ta)	negative Eu-anomaly: Zircon-rich pegmatites; Zr, .03 wt%
Low in mafic trace elements (Co; Sc; Cr; Ni)	Co, Sc: <.0005 wt%
Low in "feldspar" trace elements (Ba, Sr, Eu)	Sr: 22-91 ppm
Initial $^{87}Sr/^{86}Sr$ 0.703-0.712	0.707 ± .001 (Johnson and Denison, 1973)

Gilbert and Myers (1981; Myers and others, 1981) measured Rb and Sr concentrations in 81 samples of Wichita igneous rocks, with emphasis on the granites. Figure 17 shows Rb/Sr plotted against SiO_2 for the granites. A general increase in Rb and decrease in Sr occur with increasing SiO_2, yielding the ratio increase plotted. The three granite classes, which were defined on the basis of major-element chemistry, can be discerned (see table 8). Note especially the tight clustering of Mount Scott data at the low-silica end. This would seem to argue for an especially homogeneous magma, particularly where the extreme spatial difference between the points is about 55 km. Figure 18 shows the averages for the three granite classes in comparison with other but more limited data from the Wichita province for the rhyolite dikes and Carlton Group. Also shown are data from another A-type granitoid province, the 1.5–b.y. Wolf River Batholith of Wisconsin (Anderson and Cullers, 1978). The Wolf River symbol represents the main granitoid body, and the Belongia Coarse, which is one of the bodies differentiated from it. Bonin and others (1978) reported Rb–Sr data for an anorogenic, hypersolus complex from Evisa (Corsica), similar to those in Nigeria and New Hampshire, and their average is also plotted for reference. The Evisa rocks are thought to be derived by fractional crystallization from mantle sources without important crustal contamination. One could argue for trends in the Wichita data that are compatible with differentiation processes.

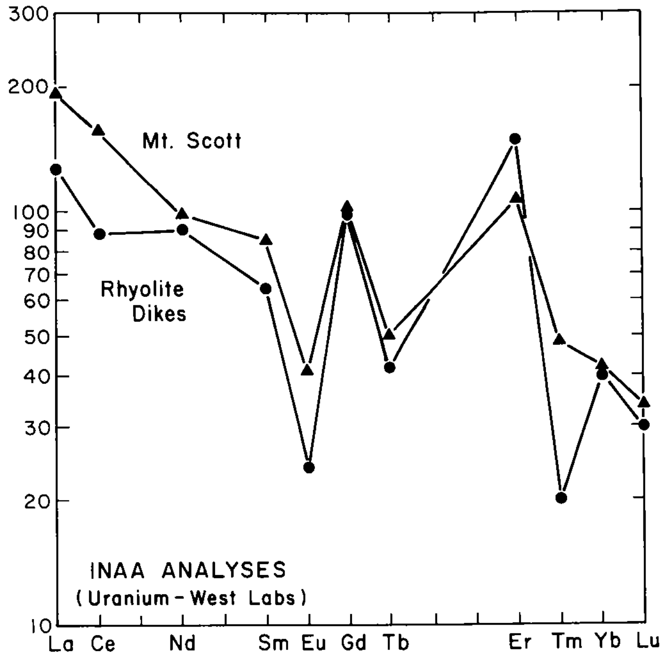

Figure 16. Rare-earth data averaged for three samples of Mount Scott Granite and two samples of rhyolite dikes cutting Wichita granites. These are chondrite-normalized values (Hanson, 1980).

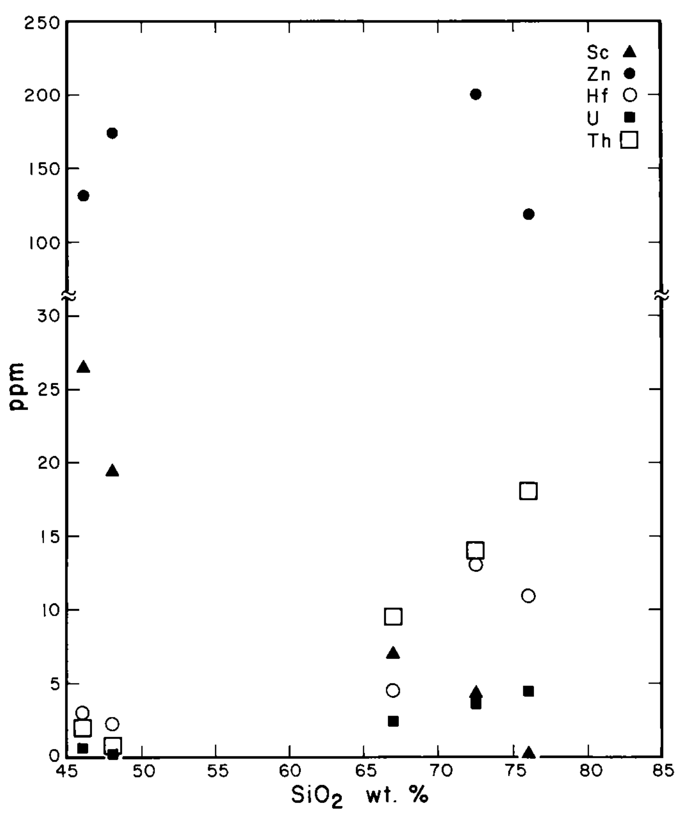

Figure 15. Variation of trace elements with SiO_2 content for rocks of Wichita igneous province.

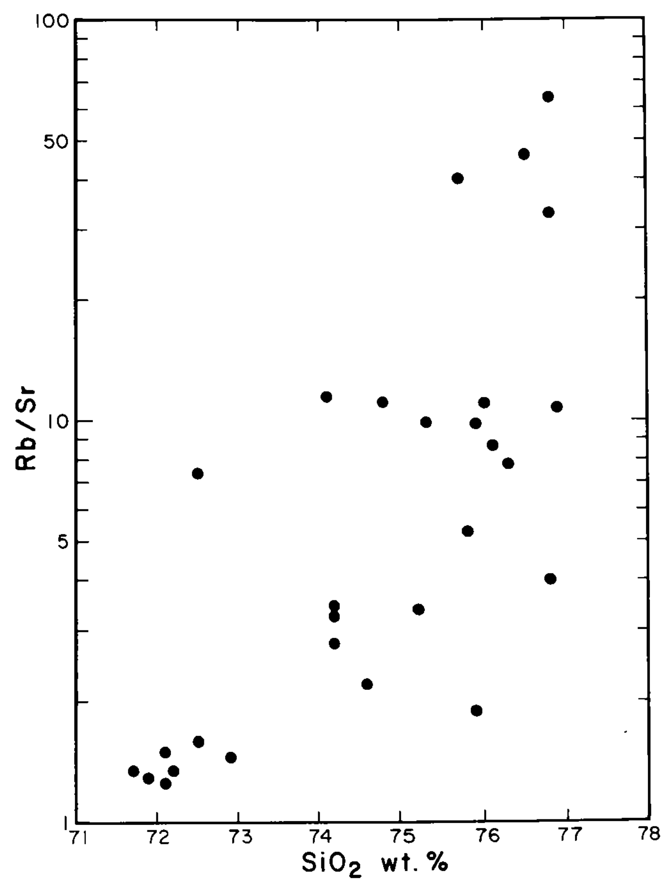

Figure 17. Variation of Rb/Sr with SiO_2 content in Wichita granites.

Xenoliths

In distinct contrast to the rhyolites, the granites commonly have inclusions. Most of these seem to be igneous inclusions derived from other known parts of the Wichita province, or sedimentary inclusions attributed to the Tillman Group. There are no known or presently recognized fragments of the lower to middle crust, or the mantle, either as rocks or as xenocrysts. Merritt (1958) and Gibson (1981) presented data and interpretations for xenoliths in the western Wichitas. The Lugert Granite in the west, and the Mount Scott Granite in the east, seem to carry the most xenoliths. Basically, there are three principal types of inclusions: basaltic, rhyolitic, and sedimentary (quartzite to graywacke). None of these has been well studied in the east, and it is increasingly clear that the significance of the whole set needs to be reevaluated. As in the west, the mafic ones are mostly fine grained, consisting of hornblende ± biotite + plagioclase and are assumed to be recrystallized basalts from the Navajoe Mountain Group (Ham and others, 1964). Coarse-grained inclusions, such as gabbros or anorthosites that could be related to the Raggedy Mountain Gabbro Group (either Glen Mountains Layered Complex or the Roosevelt Gabbros), are exceedingly rare to nonexistent. There are some fragments in granitoid dikes, but many of these occurrences are associated with the Cold Springs Breccia, whose granitoid component may not be related to the Wichita Granite Group. This lack of gabbros is not explained. Since the rocks of the layered complex are highly anorthositic, perhaps disaggregation by the silicic magma on intrusion might have contributed plagioclase as individual grains to the granite rather than as rock fragments.

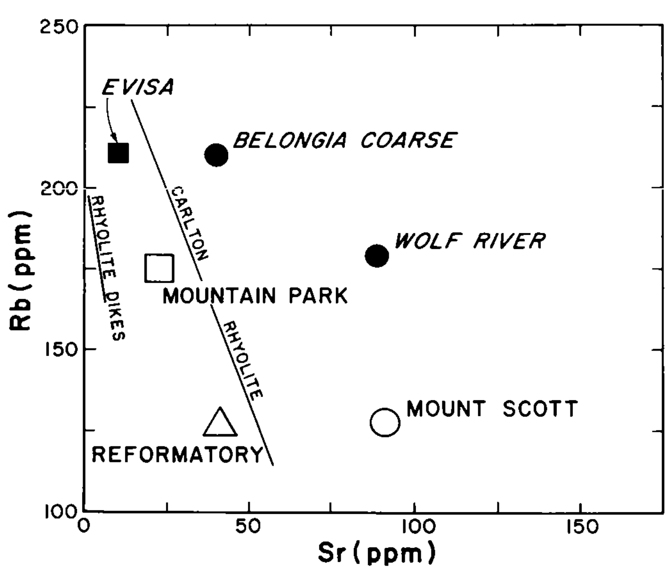

Figure 18. Averaged Rb versus averaged Sr for the three recognized chemical classes of Wichita granites. Limited data-ranges are shown for rhyolite dikes and Carlton Rhyolite Group. Data for an older, but somewhat comparable, A-type suite are presented from Wolf River Batholith of Wisconsin, from main phase and a differentiate known as Belongia Coarse (Anderson and Cullers, 1978). An average for A-type granitoids from Evisa (Corsica) also is given (Bonin and others, 1978).

The most straightforward linkage between inclusions and original rock is found in the metarhyolite. The petrographic character of these xenoliths is similar to Carlton rhyolites, except for recrystallization and a coarsening of the groundmass. As detailed mapping goes on, more of these are being found in every granite (see Stops 5 and 6).

The most puzzling are the metasedimentary xenoliths. The Meers Quartzite was recognized in the east many years ago (Taylor, 1915), and problems associated with it are discussed in the next section. Historically, highly quartz-rich metasediments usually have been found first, and those with compositions similar to graywacke have been grouped with rhyolite or fine-grained granite and not recognized until later (see Sides and Miller, this guidebook). It is not clear where or what the source terranes were. Ham and others (1964) put all these with the Tillman, but no extensive study has been done.

MEERS QUARTZITE

Background

The Meers Quartzite, as xenoliths in gabbro, was first recognized and identified by Taylor (1915) in the eastern Wichitas. However, the formal stratigraphic name dates from Hoffman (1930). Hoffman (1930), Merritt (1948), and Ham and others (1964) provided most of the descriptive material. The type outcrop was taken to be the outcrop south of Meers. Hoffman (1930) found additional outcrops of quartzite in granite, but he also decided that the largest outcrop originally mapped by Taylor, south of Mount Scott, was a granophyre. All subsequent workers until now, except Chase (Chase and others, 1956), accepted Hoffman's interpretation. My own work, plus that of Sides and Miller (this guidebook), indicates that Taylor was correct and that Hoffman was incorrect in the Mount Scott area.

How did this confusion arise, and how was it propagated? Hoffman (1930) was impressed with the granophyric textures so common in most of the granites. Some rather more fine-grained, equigranular rocks, with abundant quartz plus alkali feldspar, and noticeable "snowflake" texture (Anderson, 1969, 1970)—where quartz poikilitically surrounds and encloses alkali feldspars—were grouped by Hoffman into the Davidson Granophyre. In fact, Hoffman included two different kinds of rocks with the Davidson: hornfelsed Carlton Rhyolite, and the graywacke facies of the Meers Quartzite. Ham and others (1964) saw clearly that this hornfelsed rock resulted from reheating of rhyolite near intrusive contacts with the Mount Scott Granite. They used this as one key factor in establishing the relative ages of rhyolite and granite. During their reconnaissance surface work, they found additional outcrops and recognized that a wider range of metasedimentary types existed under the Meers designation, but they did not realize that part of the Davidson of Hoffman was metasedimentary and not all hornfelsed rhyolite. This was particularly true at Pratt Hill on the south side of Lake Elmer Thomas, where both hornfelsed rhyolite and Meers Quartzite occur intimately together (see Stops 4 and 8; and Sides and Miller, this guidebook). In correction of Hoffman, the Davidson Granophyre in the Easter Pageant (Holy City) area, NE¼ sec. 17, T. 3 N., R. 13 W., is hornfelsed rhyolite, whereas the Davidson south of Mount Scott, sec. 14, T. 3 N., R. 13 W., is metasedimentary.

Problem and Proposal

From Taylor (1915) on through Ham and others (1964) to Powell and others (1980) and Sides and Miller (this guidebook), all workers have treated the Meers Quartzite as inclusions in the igneous rocks of the Wichita province. However, since the Glen Mountains Layered Complex and Roosevelt Gabbros were recognized as separate and distinct intrusive events by Powell and others (1980), and each was thought to have quartzite inclusions, a profound problem with the Meers has emerged. What stratigraphic and structural position could the Meers have that would enable three different magmas—two gabbroic and one granitic—to acquire pieces of it, particularly with an erosional interval separating the gabbros from the granite? The only possible answer seems to be that the Meers is in the crustal column below the gabbro, at least 4 km below the present surface. This answer generates another problem: How could a low-density quartzite be found in the middle of a gabbroic lopolith, where the original tholeiitic liquid should have floated it? While this question might be answered, more complexities and improbabilities immediately arise, so that a rethinking of the basic relations is necessary.

A review yields the following situations:

1. As presently understood, Meers inclusions occur in (a) the Glen Mountains Layered Complex at only two localities, one of which is SW NE SW NW sec. 32, T. 4 N., R. 13 W.; (b) the Roosevelt Gabbros, in the Mount Sheridan member south of Meers, as the type example at NE NE SE sec. 32, T. 4 N., R. 13 W., and in nearby areas; and in the Sandy Creek member as a new report from Stockton and Giddens, Stop 3, NE NE SW sec. 4, T. 3 N., R. 15 W.; and (c) the Wichita Granite Group, in the Mount Scott Granite at several places, for example, NE SW SW SE sec. 34, T. 4 N., R. 14 W., and as a new report from Stockton and Giddens, Stop 3, SW NE NE SE sec. 8, T. 3 N., R. 15 W.; and in the Quanah Granite as a new report from Gilbert, Stop 5, SE SW SE sec. 23, T. 3 N., R. 14 W. Many of the occurrences of metasedimentary rocks in the granites of the western Wichitas (Merritt, 1958) might now have to be included within the Meers unit. The Meers is part of the Tillman Metasedimentary Group and older than the Glen Mountains Layered Complex.

2. The Meers Quartzite consists of two distinct facies, a quartzite and a "graywacke" or feldspathic sandstone. The relationship between these facies is unknown although in places they do occur together. Two different sedimentary units of different ages may have been inadvertently grouped together, and Sides and Miller (this guidebook) argue for such an interpretation. The pure quartzite facies is not known from the subsurface Tillman. Sides and Miller suggest that the dirty quartzite (graywacke facies) of Pratt Hill (Stop 8) is not Meers but a post-gabbro quartzite developed on the erosional surface, predating the rhyolite. In fact, a similar interpretation in mapping in the eastern Wichitas had been used by considering some of these quartzite–sandstone outcrops to be a volcaniclastic basal portion of the Carlton Group. However, Sides and Miller do not see much evidence for volcanic materials in the dirty quartzite.

3. Review of available information suggests a revised interpretation for the Meers. Consider the following points. From the beginning, a range of sandstone types, from pure to dirty quartzite, have been included in the Meers, although the pure type has been emphasized by most workers. Our own work shows a range in metamorphic grade for the quartzite, from chlorite-bearing through andalusite-bearing, to sillimanite-bearing. This suggests recrystallization of the same rock types along a steep temperature gradient. The only quartzite outcrops that can be seen unequivocally immersed in igneous rock are in granite and rhyolite. All of these appear to be near or along the base of the granite and rhyolite sections. The only outcrops of quartzite that had been thought to be in gabbro also occur near or *at* the granite–gabbro contact, a surface of unconformity. The high-grade metamorphism of the quartzite (sillimanite-bearing) was always thought to be due to the gabbro (Hoffman, 1930; and Merritt, 1948), but this was not the only heat source available. The granites are high-temperature types at 950°–1,000°C, as discussed earlier, and well above the low-pressure, minimum temperature of stability of sillimanite at 800°–850°C (Richardson and others, 1969). Therefore, the proposal here is that the Meers is not correlative with the Tillman but is younger than the Raggedy Mountain Gabbro Group and predates, or is basal to, the Carlton Rhyolite Group, as shown in table 10. This means that (1) the metamorphism of the quartzite is due to the granite (and rhyolite, to a lesser extent); (2) the variation in degree of metamorphism is a function of envelopment in the granite, and the lower grade samples must lie below the base of the granite; (3) the outcrops listed as in the gabbros are actually just at the unconformity, lying on the gabbro, and are not inclusions in it, contrary to all earlier discussions; and (4) the metasedimentary xenoliths common in parts of the western Wichitas (Merritt, 1958) are probably fragments of the Meers Quartzite as well.

The unusual aspect of these interpretations is the removal of the quartzite from stratigraphic position beneath the gabbros. This may have additional implications with respect to the age of the Tillman, for it is unclear how much weight Ham and others (1964) placed on the accepted surface relations in the Wichitas. A variation on the theme advanced above is the alternative that the Meers is part of the Tillman, but making all the Tillman younger than the gabbro. In any case, a large sedimentary section, pre-Reagan in age, is thought to exist in southern Oklahoma and northern Texas, from the COCORP study (Brewer and others, 1981; Brewer, this guidebook). The precise dating of these rocks becomes increasingly important in unraveling the regional tectonic history.

POST OAK CONGLOMERATE AND WICHITA MOUNTAINS GEOMORPHOLOGY

Numerous outcrops of the Post Oak Conglomerate of Permian age (Hennessey Group) are evident in the eastern Wichitas. Figure 3 shows the general relations of the Permian units on the substrate lower Paleozoic sequences. A close correlation exists between the Post Oak and the topographic forms of the mountains. Even though Taff (1904) had thought that the conglomeratic sedimentary facies surrounding the Wichitas was Permian, Hoffman (1930) considered the facies as Pleistocene gravels. Chase (1954) first treated these rocks as a separate, mappable Permian unit with the name "Post Oak." He thought that the unit represented the last tectonic movement of the Wichita Uplift. Interpretation of the origin of the rounded granite and rhyolite boulders and cobbles, so common in the facies, was largely lacking until recently. Gilbert (1979) and Al-Shaieb and others (1980) pointed out that the rounding is due to spheroidal weathering, and not transport. Gilbert (1979) was the first to recognize the topography underlain by granite as the tor type (Twidale, 1976). The following discussion is aimed at Post Oak–granite relations, whereas Donovan (this guidebook) should be consulted for aspects of Post Oak–limestone relations.

Tor topography is generated on a generally homogeneous substrate that has been fractured, horizontally and vertically, in a regular way. The shapes of the boulders that ultimately result are a function of fracture spacing; the sizes are limited by the fracture spacing and by the degree of weathering. A distinct period of tectonic quiescence is necessary, allowing weathering to predominate over erosion. Low-relief landscapes presumably form during the time interval. An important point is that the rounding process is entirely subsurface, in an essentially H_2O-saturated environment. Hydrolysis proceeds along the fracture surfaces and out into the blocks from all sides, with minimum energy configurations yielding subspherical reaction surfaces. Near the land surface, the blocks may be entirely disaggregated and disintegrated (fig. 19); at depth, the rock is nearly pristine. Between the surface and depth, an inverse gradation occurs in volume of weathered material and unweathered core–stone-sized blocks.

Eventually, the regime changes and erosion predominates over weathering. This could be due to renewed uplift and (or) to a climate change such as increased rainfall. The weathered rind of the fractured blocks is stripped off differentially to become arkosic sand, silt, and clay, with the core-stones lagging somewhat behind as (1) tors (columns of rounded boulders), (2) boulder streams, so well developed on Mount Scott, and (3) conglomeratic sheets in low-relief areas. That the conglomerates fill in valleys can be seen in the Central Lowland (Quanah Parker Lake to French Lake, secs. 16–17, 21–23, T. 3 N., R. 14 W.). This requires an original topography that was developed in several distinct stages. The valleys had to form before substantial stripping of the surrounding knobs, because debris from the knobs fills the valleys.

Finally, the Post Oak facies as well as the igneous knobs were buried in shaly material derived externally, presumably from the east. Thus, the Permian topography was buried and only now is being exhumed. Most of the present mountain forms, down to outcrop scale, are Permian. This picture helps to

TABLE 10.—PROPOSED REVISION IN PROTEROZOIC(?) TO MID-CAMBRIAN LITHOSTRATIGRAPHY

Cambrian	Wichita Granite Group	
Cambrian	Carlton Rhyolite Group	
		Meers Quartzite
?	Raggedy Mountain Gabbro Group	
Proterozoic	Tillman Metasedimentary Group	

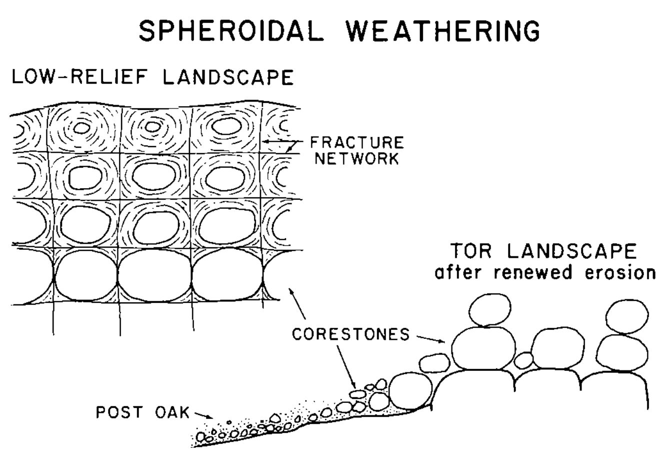

Figure 19. Drawing showing how development of spheroidal weathering can eventually lead to a tor landscape on granitoid rocks. This is origin of topography in much of Wichita Mountains and Post Oak Conglomerate. Boulders and cobbles of Post Oak are mostly corestones with shapes derived through Permian weathering before erosion rates increased. Subsequently, limited transport redeposited them as conglomerate. See Twidale (1976) for general discussion of such processes.

explain the regional distribution of the Post Oak facies. The facies is not at the present surface in the western Wichitas, because the ground surface is above the stratigraphic level of the facies. There the shaly facies occurs, dominated by illitic clays, which appears to have a Ouachita source (Stith, 1968). As erosion proceeds, the Post Oak outcrop pattern migrates to the west.

Gilbert (1979) pointed out that the Post Oak and "granite wash" of the subsurface may not be facies equivalents, as implied by many workers. Table 11 summarizes their appropriate characteristics. It appears that the Post Oak is the result of a special weathering cycle. The "granite wash" could have started with a similar cycle, but need not have, and most workers have interpreted it as a tectonic fanglomerate. This may signify two different tectonic styles in the uplift stage, with the Post Oak representing the final style. Late movement on the Meers Fault could be related to this last uplift. The Meers does appear to cut Permian units, including the Post Oak Conglomerate.

SURFACE STRUCTURE

Decker (1939) named the highest structural part of the uplifted area of the eastern Wichitas the "Fort Sill Anticline." This reflects the Pennsylvanian deformation, as primarily determined by southerly dips in the Arbuckle Group south of the igneous outcrops on Fort Sill, and northerly dips in the Slick (Limestone) Hills. Because layering in the granites, and the granite–gabbro contact, can also be used for structural control, more detailed analysis of the structure is possible, as shown in figure 20. Two anticlinal arches can be traced westward from Fort Sill, and these are designated the "North Anticline" and "South Anticline." The axial regions correspond generally to the area of most exposure of gabbro. Although the height of the gabbro is one measure of uplift, local relief on the gabbro unconformity precludes its use as the sole measure. Elevations for the granite–gabbro contact are given in slanted (italic) numerals in a few prominent locations. Elevations of the presently exposed gabbro, above which the granite–gabbro contact must lie, are given in upright numerals as additional reference points. A gentle syncline to undulating plane exists between the anticlinal axes; these axes are perhaps more akin to monoclinal flexures. Within the Carlton Rhyolite of the Fort Sill area, Schoonover (1948) identified a syncline. This feature may be Cambrian in age, rather than Pennsylvanian. There are dips in the Meers Quartzite that are discordant with those in the Carlton Rhyolite and, in both, to the granite intrusive contact.

The Wichita Mountains form a strikingly lineated terrain as seen in the field, and in topographic maps and aerial photographs. Figure 21 is a high-altitude NASA photograph taken in May 1973 across the central part of the eastern Wichitas. Quanah Parker Lake (Stop 5), in the Wichita Mountains Wildlife Refuge, is in the lower center. A section of State Highway 115 between Cache (out of view to the south) and Meers (in the far upper right), and a section of State Highway 49 running generally east-west, can be used as orientation in the photo. French Lake (Stop 6) is in the center far west. Gilbert (1982) has discussed the lineaments and their relation to the fracture system. Most of the obvious lineaments are in granite. The granite shown in the upper half of the figure is the Mount Scott sill, overlying the Raggedy Mountain Gabbro Group cropping out both on the north, and on the south in the Central Lowland

TABLE 11.—COMPARISON OF POST OAK CONGLOMERATE AND GRANITE WASH CHARACTERISTICS

	Post Oak	Granite Wash
a.	surface and near surface	subsurface
b.	Permian	dominantly Pennsylvanian and some Permian
c.	reflects local source; no significant transport	reflects more regional source, noticeable transport
d.	not directly related to faults	related to uplifted blocks and faults; higher relief sources
e.	clast size 10-100 cm; rounded and spherical igneous clasts	variable clast size with angular igneous clasts
f.	non-marine	much non-marine but with marine interruptions

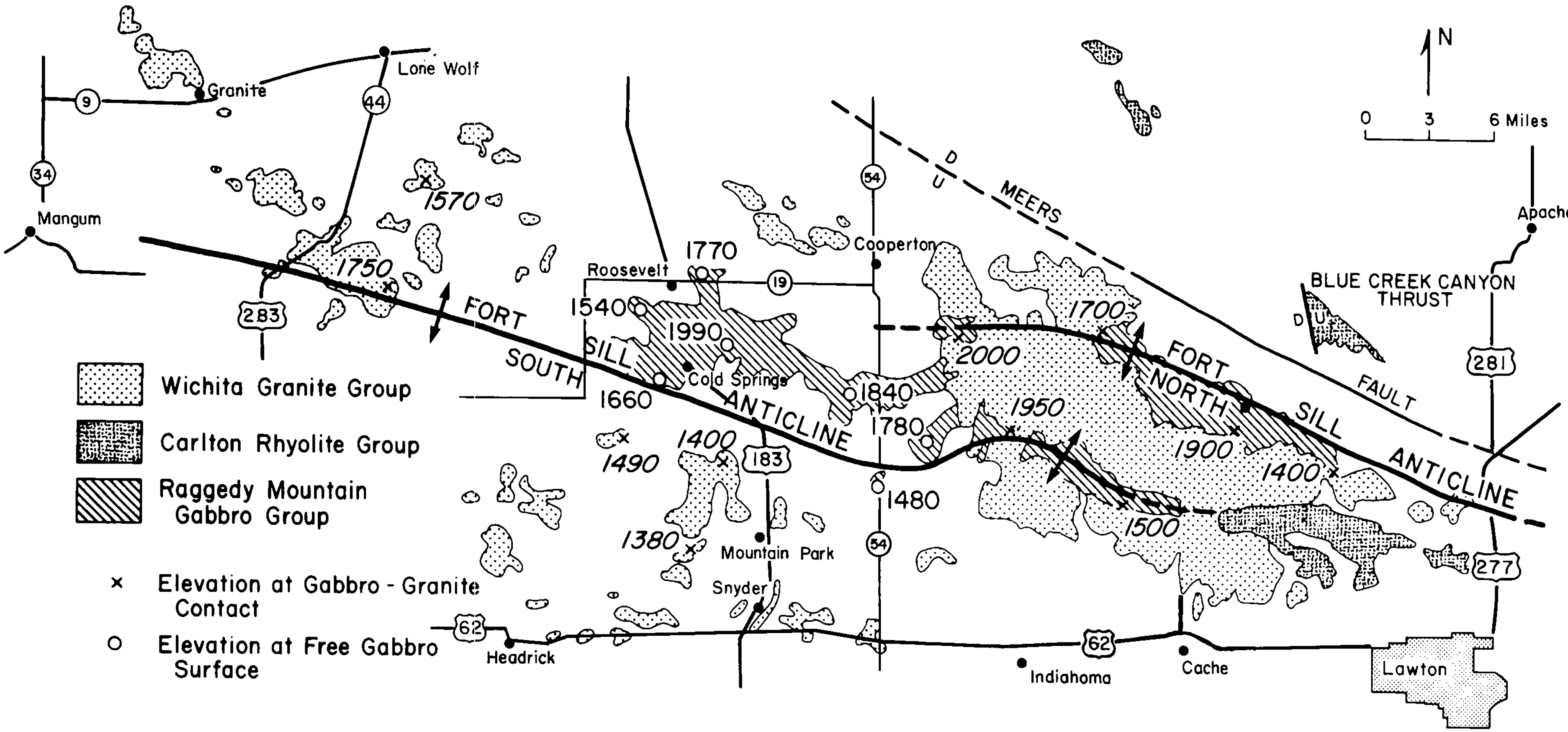

Figure 20. Major Pennsylvanian fold axes recognized within exposed igneous core of Wichitas. See text for discussion.

Figure 21. High-altitude photograph taken by NASA in May 1973 across Central Lowland of eastern Wichita Mountains. State Highway 115 transects photo from extreme upper right (where Meers is just visible) to center bottom (where road heads south toward Cache. Fort Sill Military Reservation lies across bottom of photo; Wichita Mountains Wildlife Refuge extends across center, with some private land at upper right. Quanah Parker Lake is approximately in center; French Lake is in far-west center, and Lake Jed Johnson is near but west of State Highway 115 east of center. State Highway 49 runs generally east-west across region.

(Quanah Parker Lake to French Lake). South of the Central Lowland is the Quanah Granite. Extensive deposits of the Permian Post Oak Conglomerate can also be discerned.

These lineaments clearly identify major fractures and were the basis for the fault patterns shown originally on the State geologic map of Oklahoma (Miser, 1954) and carried forward to the 1:250,000-scale map in Havens (1977). Gilbert (1982) has argued that there is no evidence for faulting (offset) on most of them and has cited evidence against faulting on certain ones. These fractures are interpreted as having been caused by Pennsylvanian deformation during the Wichita Uplift. Because the granites probably behaved as brittle sheets during uplift, relative to the underlying gabbros and overlying carbonates, strain was accommodated by breaking into regional blocks with apparently little offset. The orientation of 942 fractures of minimum 100–m length was determined from topographic maps and aerial photos in the eastern Wichitas (fig. 22). These are chiefly in units of the Wichita Granite Group. From their size, they are thought to be Pennsylvanian fractures with little contribution from the Cambrian ones discussed earlier, which are of smaller scale. Almost all of these fractures are high-angle to vertical, as seen by the way in which they transect the topography. The prominent orientation is N. 70°–80° W., but there are many at N. 30°–10° W., N. 0°–30° E., and N. 60°–90° E. The fold axes shown in figure 20 also have azimuths at N. 70°–80° W. Structural trends in the Arbuckle region are more nearly N. 60° W., whereas in the far western part of the Wichita axis, in the subsurface, they are N. 80° W. The change in trends appears to occur in this region, which is here called the Lawton Bight.

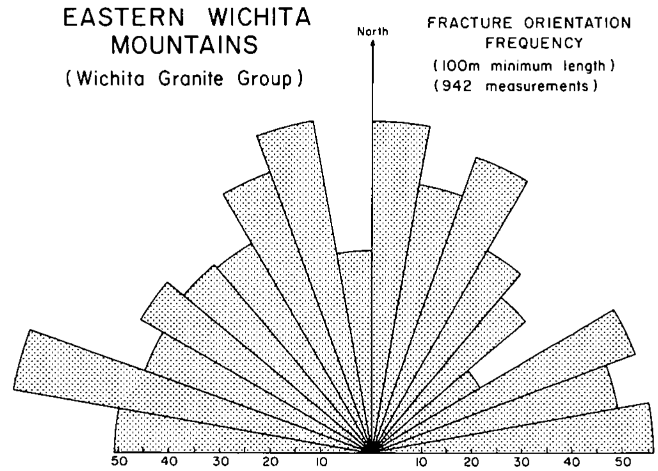

Figure 22. Fracture orientation determined from topographic maps and aerial photos.

A peculiar relationship is noted when the frequen-

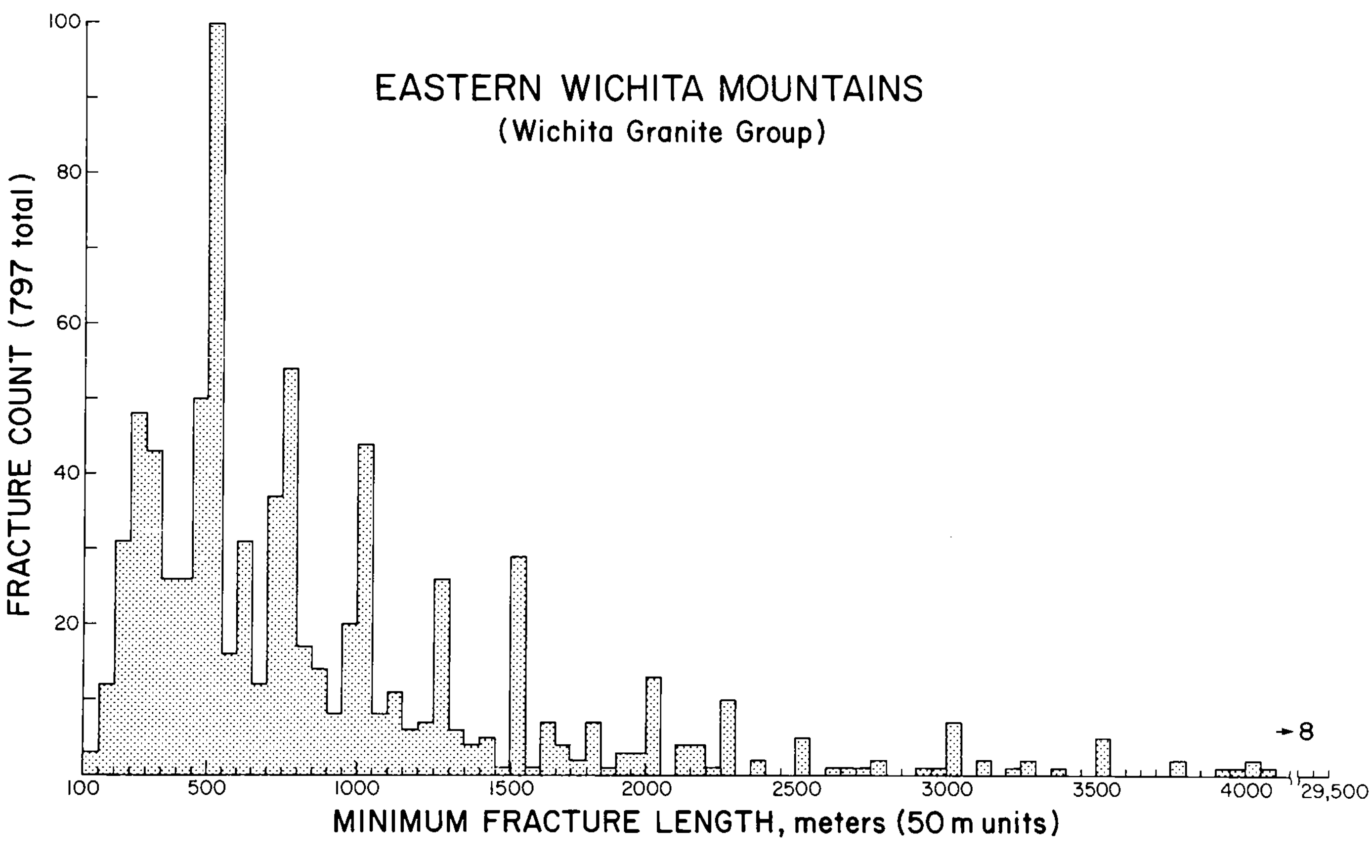

Figure 23. Fracture lengths determined from topographic maps and aerial photos.

cy of fractures is plotted against their lengths. The most prominent length is 500 m, but there are distinct peaks at 250–m intervals. There does not seem to be any artifact of the measuring process that could give this result. Lengths are obviously a function of outcrop dimensions. The granite is bounded by Permian rocks (and by gabbro), but the area measured has the greatest outcrop continuity in the Wichitas. Thus, the fracture lengths are minimums, but periodicity in lengths should not be affected. This result is provisionally interpreted here as a function of thickness of the granites. Most of the measurements are from the Mount Scott Granite, which has a demonstrable sheet form. Independent measurements of the thicknesses of Wichita granite sills range from 600 ft to 1,500 ft in wells (Ham and others, 1964). No upper boundary on the granites can be seen from surface relations. An estimate of ½ km or less for the thickness had been used independently by me on the basis of petrographic characteristics and evidence of surface-breaking at times during emplacement. The fractures appear to indicate a minimum thickness of 250 m for the granite sill, with a maximum of perhaps 500 m.

ACKNOWLEDGMENTS

Hugh E. Hunter furthered development of a basic interest in the Wichita Mountains. My co-worker in our study of the Wichita Granite Group, J. D. Myers, is responsible for most of the original chemical data presented. Many discussions with colleagues working or interested in the Wichitas have helped to sharpen and define issues, particularly B. N. Powell and R. E. Denison, as well as M. L. Stockton, J. D. Giddens III, J. A. Brewer, Nancy Scofield, J. S. Wickham, C. A. Merritt, R. N. Donovan, J. R. Sides, J. R. Miller, and D. A. Preston. None of these individuals should be held accountable for shortcomings in this presentation, nor should any reader assume they agree with all of it.

My own colleagues at Virginia Polytechnic Institute and State University, D. A. Hewitt, A. K. Sinha, and D. R. Wones, have willingly discussed problems with me when called upon. Wones willingly shared several figures from a work in preparation by Loiselle and Wones. Sharon Chiang, scientific illustrator, and her assistant, Martin Eiss, were most helpful with the illustrations.

STUDY OF SOUTHERN OKLAHOMA AULACOGEN, USING COCORP DEEP SEISMIC-REFLECTION PROFILES

J. A. Brewer

INTRODUCTION

The Southern Oklahoma Aulacogen, the type aulacogen in the United States, is a major structural feature in the southern Midcontinent region. For the purposes of this paper, I define the aulacogen in the region of the COCORP[1] traverse as including the Hardeman Basin, Wichita Mountains, and Anadarko Basin, although there is some confusion in the literature over the exact use of the term and the age of onset of the aulacogen. The Anadarko Basin is the deepest basin in the North American craton (Ham and Wilson, 1967) and the site of intensive oil and gas exploration since the turn of the century. However, relatively little is known of the deepest parts of the basin, especially in the complexly deformed area close to the Wichita Uplift; knowledge of the uplift itself is based on relatively shallow well data and studies of exposed igneous rocks.

From such data, Ham and others (1964) proposed that the first major event in the evolution of southern Oklahoma (apart from the formation of the crystalline basement) was Early Cambrian subsidence of a trough, centered beneath the present Anadarko Basin and Wichita Uplift, and thought to be filled largely with clastic metasediments (Tillman Metasedimentary Group). This trough was intruded by gabbros and overlain by basalts, subjected to uplift and erosion, and further overlain by rhyolites and intruded by granites. These intrusive rocks consolidated into what is now the Wichita block. Subsequent (Late Cambrian–Permian) subsidence was concentrated north of the Wichita block, and deformation culminated in the Pennsylvanian with uplift of the Wichita block and subsidence to the north, forming what are now the Wichita Mountains and Anadarko Basin. Thus, the present mountains and basins all lie within Ham and others' (1964) inferred Early Cambrian trough. Subsequent radiometric dating (Muehlberger and others, 1967) suggests that the Tillman Group is at least 1,000 m.y. old, or twice as old as the granites in the Wichita Mountains (500–525 m.y.; Ham and others, 1967), thus raising questions about the significance of the Tillman Group in the Paleozoic structural evolution of southern Oklahoma.

Hoffman and others (1974) interpreted Ham and others' (1964) evolutionary scheme in a plate-tectonic framework, suggesting that the inferred Early Cambrian trough formed during an extensional episode in which continental crust to the east and southeast rifted completely away from the North American craton. Although the southern Oklahoma trough failed to extend very far (a "failed rift arm"), the region continued subsiding through most of Paleozoic time. The culmination of deformation in the Pennsylvanian was related to closure of the arms that rifted successfully, and formation of the Ouachita belt. This final deformation of the Southern Oklahoma Aulacogen has been considered by most workers (for example, Harlton, 1963, 1972; Wickham, 1978) to be due to vertical or strike-slip movements along predominantly high-angle faults.

COCORP deep seismic-reflection profiling was carried out in southwestern Oklahoma to study the deep structures of the aulacogen and to determine its structural development. Three new aspects of the aulacogen are inferred from the data: (1) it is aligned along the northern margin of a hitherto unknown Proterozoic basin; (2) crustal extension occurred in late Precambrian–Early Cambrian time, with normal faulting in what is now the deepest part of the Anadarko Basin; (3) major crustal shortening occurred in Pennsylvanian time, causing the Wichita Uplift to overthrust the Anadarko Basin along moderately dipping faults. Listric thrust faulting and hanging-wall anticlines formed in the sedimentary rocks of the Anadarko Basin, which at this time was probably subsiding from thrust-loading of its southern margin. These interpretations thus suggest significant revision of ideas of the basement structural framework and style of deformation of the aulacogen.

LOCATION OF COCORP LINES

The COCORP data were recorded in three phases (figs. 24, 25): (1) the first COCORP surveys ever conducted, in 1975, in the Hardeman Basin, Hardeman County, Texas (Oliver and others, 1976); (2) in 1979, continuing the 1975 work farther north, in the Hardeman Basin and through the Wichita Mountains (Brewer and others, 1981); (3) in 1980, extending the surveys still farther north across the Frontal Fault system of the Wichita Mountains and through the Anadarko Basin, ending in Northern Dewey County, Oklahoma (Brewer and others, 1982). The surveys thus extend across the width of the Southern Oklahoma Aulacogen. The data were collected by the Vibroseis[2] technique, and field configurations and recording parameters were similar to those described by Oliver and others (1976).

[1] COCORP is an acronym denoting Consortium for Continental Reflection Profiling.

[2] Trademark of Continental Oil Co.

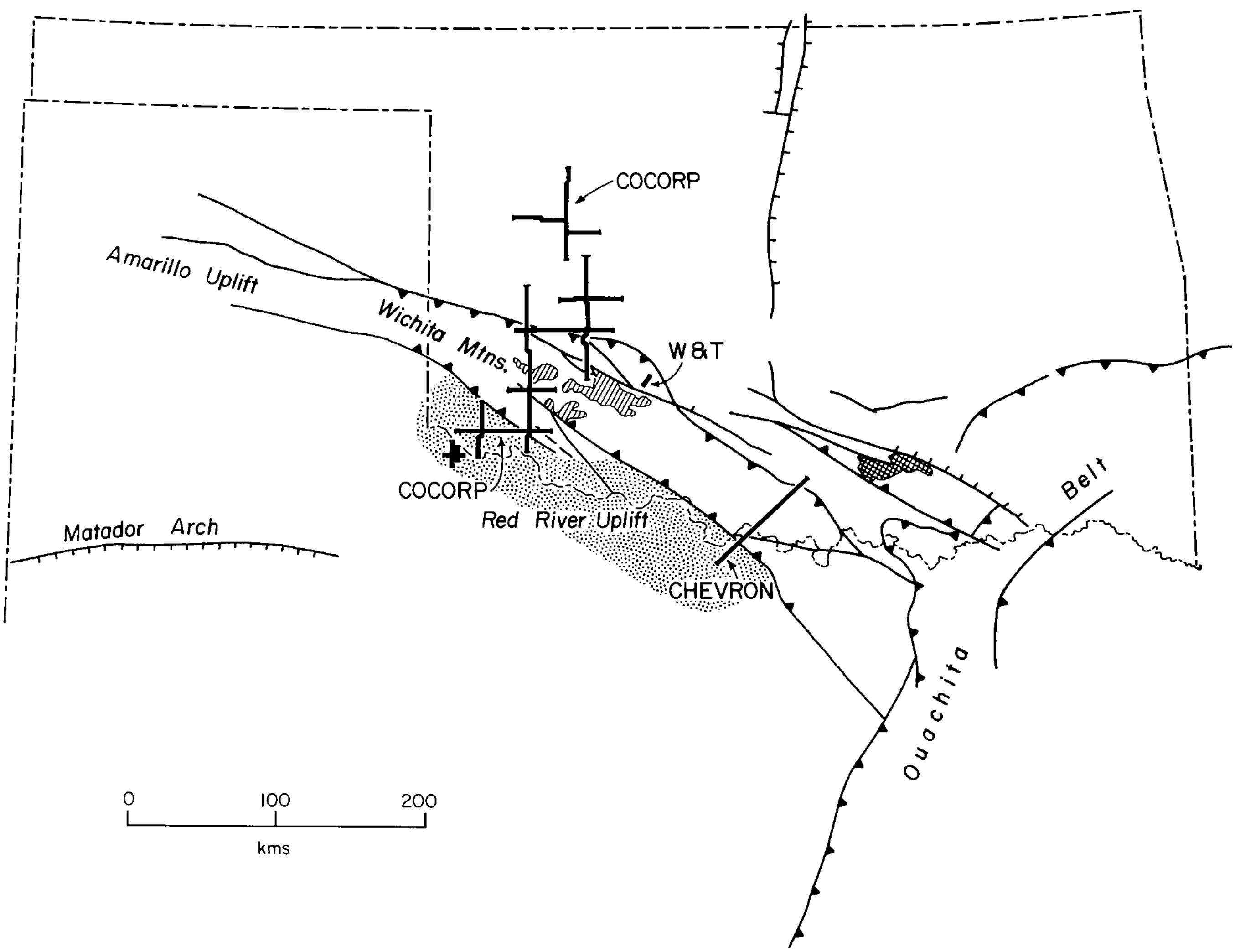

Figure 24. Major fault trends of Southern Oklahoma Aulacogen and surrounding areas of southern Midcontinent, with locations of COCORP traverse and Chevron regional seismic line. Shading patterns: diagonal stripes, granite and gabbro outcrops in Wichita Mountains; crosshatched, 1,370–1,400–m.y. old granites and granite gneisses of Arbuckle Mountains (Bickford and Lewis, 1979); dots, inferred minimum extent of relatively undisturbed Precambrian layering south of Wichita Mountains. *W & T*, location of Widess and Taylor (1959) seismic data recorded in Frontal Fault system of Wichita Mountains. These data were interpreted (Ham and others, 1964) to indicate extensive pre–Reagan Sandstone layered rocks under Anadarko Basin. These data might, however, represent thrusting along Wichita Mountain front, along moderately dipping faults.

RESULTS OF COCORP STUDIES

1. *A Proterozoic basin inferred south of the Wichita Mountains.*

This basin is inferred from pronounced, high-amplitude, laterally continuous and relatively undeformed layering in the Precambrian crust (fig. 26), seen on all COCORP data recorded south of the Wichita Mountains (Brewer and others, 1981). The layering extends over an area of at least 2,500 km^2 (based on the extent of COCORP data) and probably much more, and in places lies as deep as 13 km. The character of the layering suggests depositional processes, because there are suggestions of angular unconformities and onlapping and downlapping relationships, although other possibilities, such as layered igneous bodies (for example, Lynn, 1980), cannot be ruled out. If the depositional hypothesis is correct, the layering is most likely due to clastic sediments and felsic volcanics (probably metamorphosed to an unknown degree), since these rocks are widespread in the southern Midcontinent and in many areas are relatively undeformed (for example, Denison and others, 1981). Other rock types, such as basalts or carbonates, also could be present. A well drilled just south of the most southerly COCORP lines penetrated a micrographic microgranite porphyry, dated at 1,265 ± 40 m.y. (R. E. Denison, unpublished data), and farther north (for example, VP's 1–400 of line 1, fig. 26), Tillman metasediments lie at the top of the basement (inferred from pl. 1, Ham and

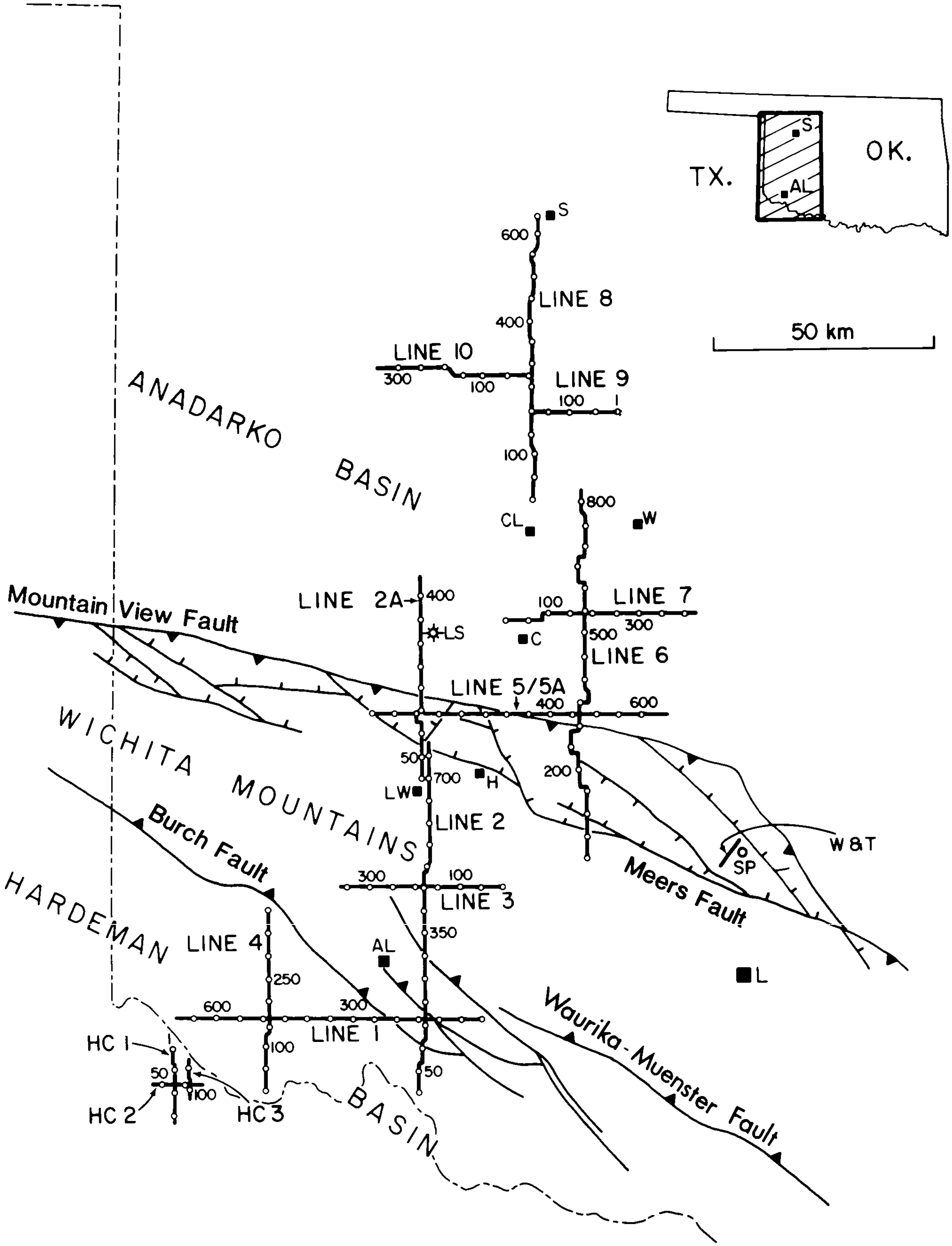

Figure 25. Location of COCORP deep seismic-reflection profiles in southwestern Oklahoma. Lines HC1–HC3 are original Hardeman County, Texas, data (Oliver and others, 1976). Numbers along profiles are ground stations or vibrator points (VP's). Towns are: *L*, Lawton; *LW*, Lone Wolf; *AL*, Altus; *H*, Hobart; *C*, Cordell; *CL*, Clinton; *W*, Weatherford; *S*, Seiling. Wells are: *LS*, Lone Star 1 Rogers; *SP*, Stanolind 1 Perdasofpy. *W & T*, Widess and Taylor (1959) seismic data.

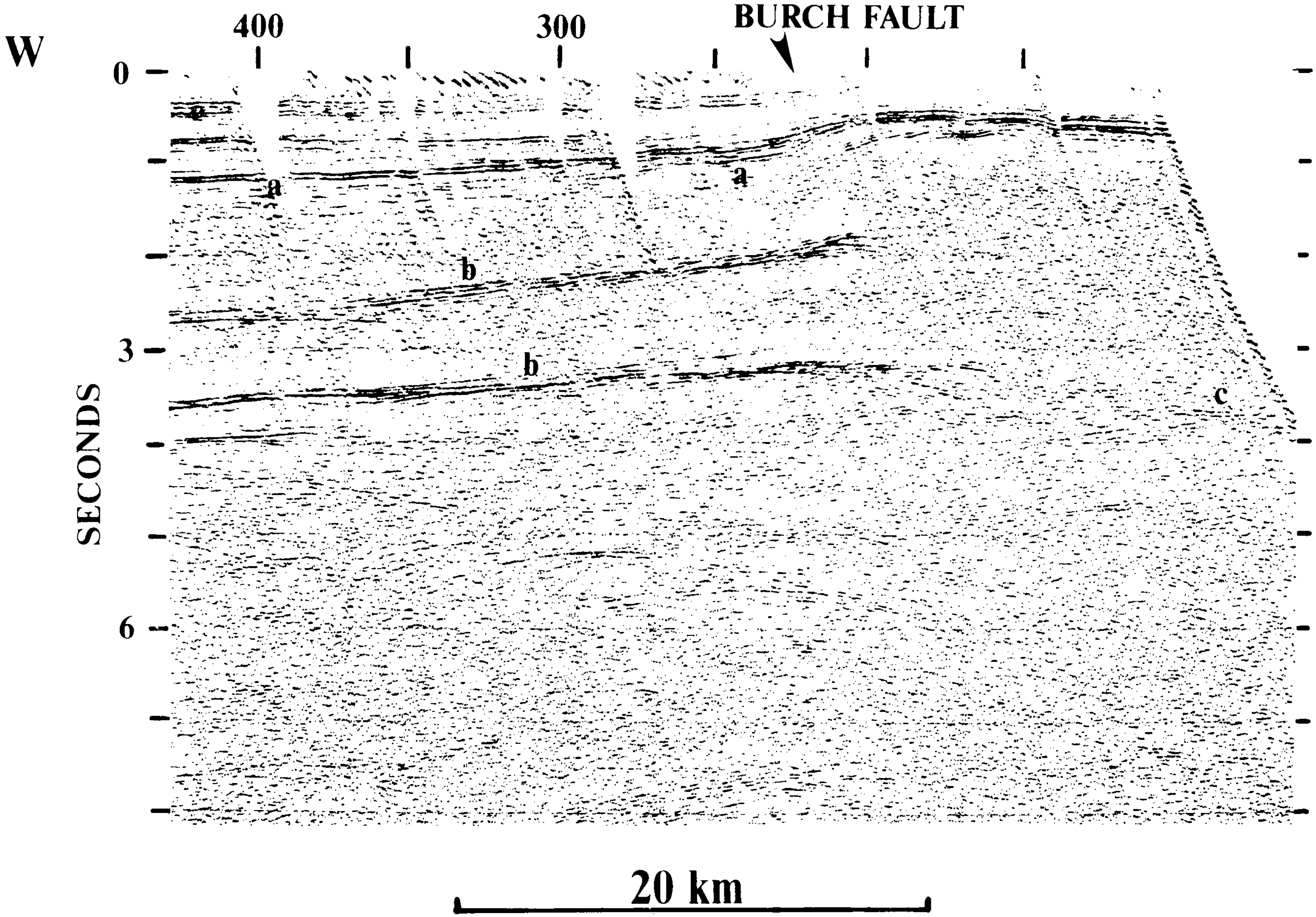

Figure 26. Detail of COCORP seismic data from Oklahoma line 1. Section is unmigrated and approximately 1:1 scale. Numbers along top are ground stations. Base of Paleozoic sedimentary section of Hardeman Basin marked by *a*; distinctive Precambrian layering south of Wichita Mountains marked by *b*. Note truncation at southern margin of Wichita Mountain block, which has been reactivated by Pennsylvanian Burch Fault in a reverse dip-slip sense. Original truncation thought to be due to late Precambrian–Early Cambrian normal faulting, because discontinuous events (for example, *c*), which also occur on south end of line 2, may represent remnants of Precambrian layering disrupted by faulting and by granitic rocks exposed in Wichita Mountains. If events such as *c* are not continuations of Precambrian layering, then distinctive truncation is most likely due to reverse faulting. To convert travel-time in seconds to approximate depth in kilometers, multiply by 3.

others, 1964). Together with other scattered well data, the most likely age of the basement layering is 1,200–1,400 m.y., although this is not a very well-constrained estimate (Brewer and others, 1981).

This Precambrian layering is seen also on a Chevron U.S.A., Inc., regional seismic line recorded 150 km to the southwest (fig. 24) (J. Fairborn, personal communication, 1981), which suggests that the inferred Proterozoic basin extends along the south side of the Wichita Mountains. North of the mountains, under the Anadarko Basin, there is no seismically distinguishable layering, in the Precambrian crust, of the thickness and character of that south of the mountains. Although this is conceivably due to total attenuation of seismic energy in the thick Paleozoic sedimentary succession, I feel it is more likely that the northern boundary of the Proterozoic basin underlies the Wichita Mountains. This northern boundary is probably fault-bounded, since basins of similar age elsewhere in the world are commonly bounded in this way (Salop, 1977).

The Precambrian layering is abruptly truncated along the south side of the Wichita Mountains (fig. 26). This truncation, seen in both the COCORP and Chevron data, occurs coincidentally with the trend of Pennsylvanian faults along the south side of the mountains (Burch and Waurika–Muenster Faults). The magnitude and sense of offset of the Precambrian layering cannot be explained just by Pennsylvanian fault movements (about 1 km, in a reverse dip-slip sense), suggesting that Precambrian or Cambrian (that is, pre-basal Upper Cambrian Reagan Sandstone) faulting, perhaps in conjunction with intrusions of granitic composition, caused the truncation. The COCORP data suggest that this faulting was normal, with downthrow to the north, because discontinuous seismic events occur within the Wichita block (north of the Burch Fault), which could then be explained as remnants of the Precambrian layering. However, equivalent events are not seen in the Chevron data, which might therefore be more consistent with major reverse faulting, with upthrow to the north. The normal-faulting interpretation is tentatively favored. Note that this prominent truncation does not correspond to the northern margin of the Proterozoic basin (assumed to be fault-bounded, but downthrown to the south), which is inferred to be farther north, under the main part of the Wichita Uplift.

The Meers Quartzite, found as inclusions in the granites and rocks of the Glen Mountains Layered Complex of the Wichita Mountains (Ham and others, 1964), is interpreted to be remnants of the Proterozoic basin. Ham and others (1964) suggested that the Meers Quartzite is part of the Tillman Group. The Tillman Group may comprise part of the Precambrian layering south of the Wichita Mountains, and my interpretation of the pre-Late Cambrian structural framework differs from Ham and others in that I believe that a large, pre-Late Cambrian basin existed south of and under the Wichita Mountains, but not farther north, under the Anadarko Basin.

2. *Thrusting along the northern flank of the Wichita Uplift.*

Major thrusting of the Wichita Mountains over the southern margin of the Anadarko Basin is suggested from dipping seismic events that can be traced from the subcrop of faults of the Frontal Fault system. The Mountain View Fault, the northern boundary of the Frontal Fault system with the relatively undeformed sedimentary rocks of the Anadarko Basin, is imaged best and can be traced to approximately 20–24 km in depth, with an approximate average south-southwesterly dip of 30°–40° (figs. 27, 28). The southern boundary of the Frontal Fault system with the massive crystalline rocks of the Wichita Mountains (the Meers Fault) is less well imaged, but it may have a similar dip. Farther south, in the middle of the Wichita Mountains, other events occur in the upper few kilometers with a dip subparallel to the Mountain View Fault. Possibly these are other thrusts, although there is little evidence for them in the exposed igneous rocks (Gilbert, 1982). Few coherent reflections are recorded from sedimentary rocks within the Frontal Fault system, which are known to be intensely folded and faulted in the upper 2–3 km (Harlton, 1963, 1972; Takken, 1968). The COCORP data are the first reported indications of the attitude and depth extent of the faults, which most workers have assumed to be nearly vertical at depth.

The dip of the faults suggests significant crustal shortening during Pennsylvanian uplift of the Wichita Mountains. Palinspastic reconstruction, based on the attitudes (poorly imaged) of the sedimentary rocks under the hanging walls of faults of the Frontal Fault system, suggests as much as 10–15 km, and perhaps more, of crustal shortening in the region of the COCORP profiles. This crustal shortening implies that subsidence of the Anadarko Basin during Pennsylvanian time was due largely to thrust-loading by the overthrust Wichita Mountains.

3. *Normal faults and hanging-wall anticlines within the Anadarko Basin.*

Sedimentary rocks are correlated from published well data, in particular the Lone Star 1 Rogers, which bottomed in carbonates of the Upper Cambrian–Lower Ordovician Arbuckle Group (Rowland, 1974). From extrapolations of the depth of the Upper Cambrian Reagan Sandstone (about 11.2 km; Rowland, 1974), there is apparently 1.5–2.5 km of seismically definable pre-Reagan Sandstone layering beneath the Anadarko Basin. Ham and others (1964) assumed that any such layering would be composed largely of Tillman metasediments and basalts; however, the thickness of this layering in the region of the COCORP profiles is much less than they suggested. The age of this layering is unknown, but it is probably either Middle Cambrian [as suggested by Ham and others (1964) from data from the Stanolind Perdasofpy well (fig. 25) in the Frontal Fault system] or perhaps similar to the inferred age of the Proterozoic

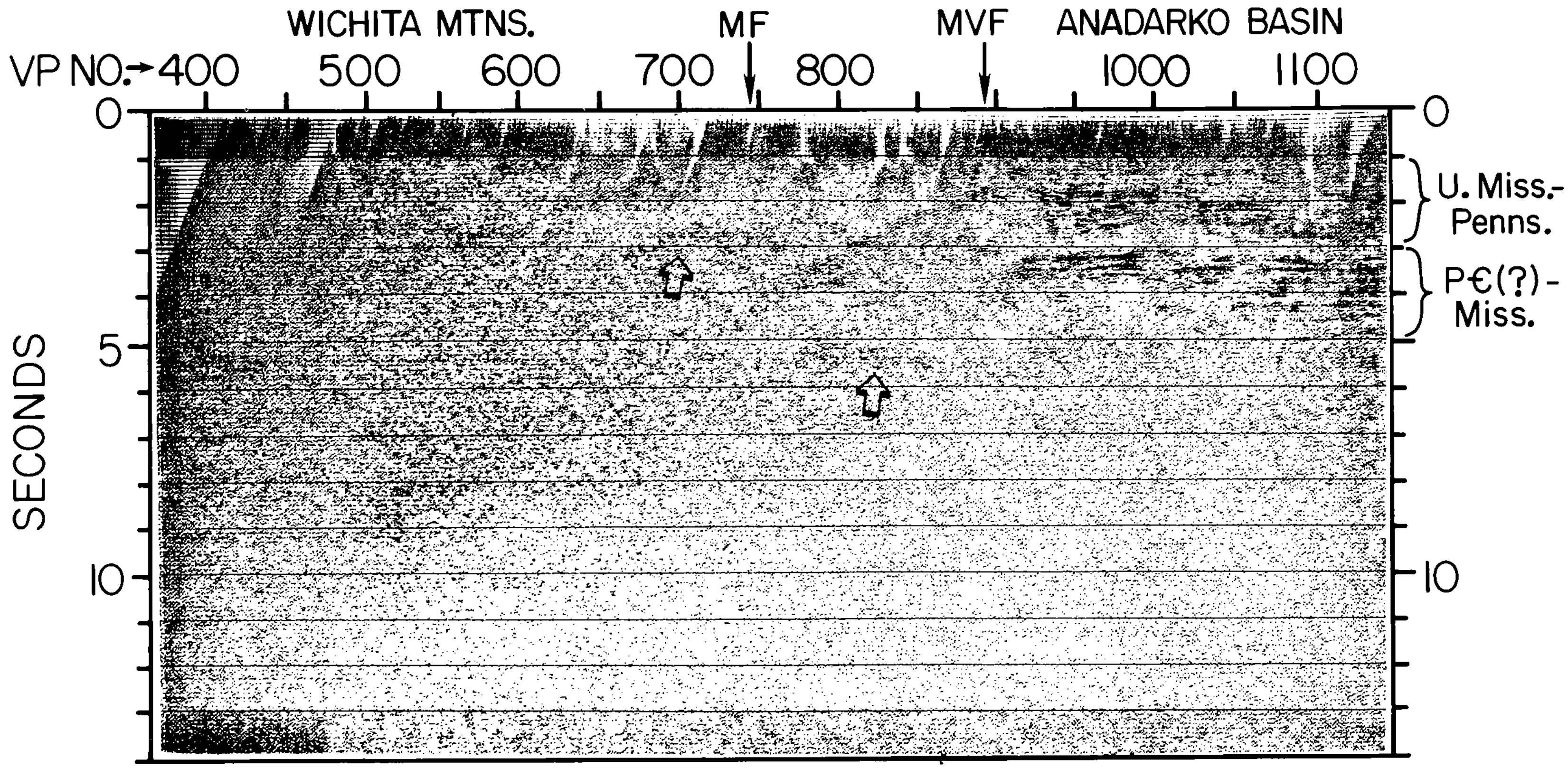

Figure 27. COCORP seismic data, Oklahoma line 2 (northern half) and 2A. Section is unmigrated and approximately 1:1 scale [100 VP's (stations) = 10 km]. Note that VP's 700–1100 are equivalent to stations 1–400 of line 2A (fig. 25). *MF* and *MVF* mark subcrop of Meers and Mountain View Faults. Band of events dipping to about 8 seconds under VP–500 is interpreted to be trace of Mountain View Fault. Note that layered sedimentary rocks of Anadarko Basin are well imaged away from mountain front, but their character rapidly deteriorates farther south. Discontinuous events marked by open arrows are interpreted as continuations of these sedimentary rocks in footwalls of Mountain View and Meers Faults. Disruption of their reflection character is probably due to faulting and perhaps to complex, near-surface structure, causing distortion of seismic energy. Cordell Anticline underlies VP–1000.

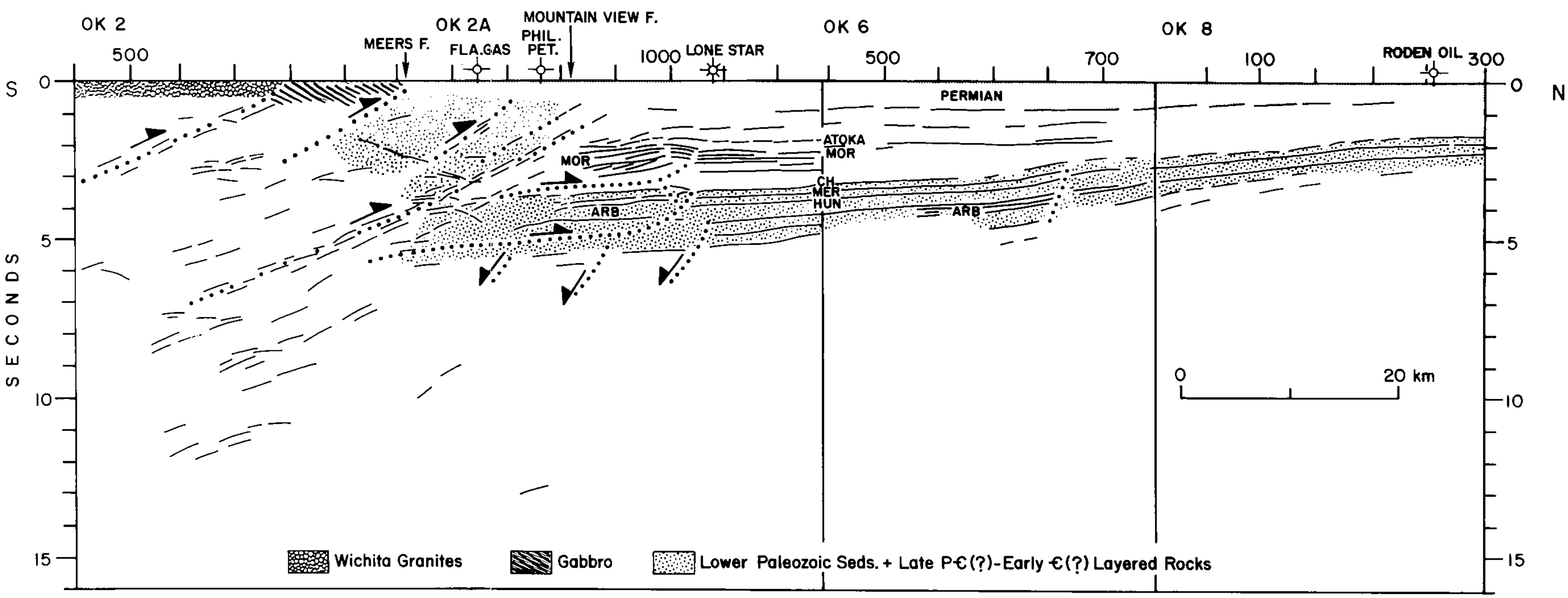

Figure 28. Interpretive line-drawing of (unmigrated) COCORP lines 2 (northern half), 2A, 6, and 8. Solid lines, seismic events (mostly reflections); dotted lines, interpreted faults with arrows indicating sense of motion. Sedimentary horizons are: *ARB*, Cambrian–Ordovician Arbuckle; *HUN*, Silurian–Devonian Hunton; *MER*, Mississippian Meramecian; *CH*, Mississippian Chesterian; *MOR*, Pennsylvanian Morrowan. Note interpreted normal faults at base of Anadarko Basin, and two levels of listric thrusting inferred to underlie Cordell Anticline (VP–1000). Evidence for lower level of thrusting is not as strong as for upper level.

basin south of the Wichita Mountains (1,200–1,400 m.y.).

The seismic character of the sedimentary rocks of the Anadarko Basin deteriorates close to the Wichita Mountain front, owing probably to wave propagation through Pennsylvanian-age granite wash, known to be a poor transmitter of seismic energy. The sedimentary rocks are inferred to extend deeply beneath the hanging wall of the Mountain View Fault (figs. 27, 28, 29), on the basis of reflections under the Lone Star well, which appear to step down to the south. These step-downs are interpreted as due to normal faults, which, on the basis of offsets in sedimentary reflectors, may have been active into Arbuckle Group time. There is little evidence for such faulting in the Arbuckle Group in places where it is exposed or has been drilled (R. E. Denison, personal communication, 1981). However, in the COCORP data, these inferred normal faults appear to be restricted to the deepest part of the Anadarko Basin, and possibly rocks from these regions have not been adequately sampled.

Anticlines occur higher in the sedimentary section (for example, Cordell Anticline). From seismic relationships, these are interpreted to be hanging-wall anticlines cored by listric thrust faults (figs. 28, 29; Brewer and others, 1982). These thrusts probably root in the Frontal Fault system and represent the response of the sedimentary layered rocks of the Anadarko Basin to crustal shortening and uplift of the crystalline rocks of the Wichita Uplift. This interpretation of these anticlines contrasts with earlier ideas of vertical or strike-slip movements along high-angle faults.

DISCUSSION: TIMING AND ORIENTATION OF PENNSYLVANIAN DEFORMATION

Structures of Pennsylvanian age along the Wichita trend are highly complex and are frequently cited as examples of left-lateral wrenching (for example, Groshong and Rodgers, 1978).

Uplift of the Arbuckle Mountains, which climaxed in early Virgilian time (Tomlinson and McBee, 1962), is usually interpreted as due to wrenching (Wickham, 1978; see Booth, 1981, for references), although Brown (1982) has shown that some structures might be equally consistent with folds and reverse faults that were formed possibly under lateral compression. The COCORP data suggest that movements on the Mountain View Fault and the listric thrust underlying the Cordell Anticline occurred mainly by the end of Atoka time, and the moderate dip and extent to depth of this fault are consistent with lateral compression normal to the Wichita trend at these times (R. E. Denison, personal communication, 1981). In this case, any later wrenching along the Wichita trend was probably along the fault trends established by earlier thrusting. A test of this hypothesis is the timing of faults along the south side of the Wichita Mountains (Burch, Waurika–Muenster trend); these faults have a sense of slip and *en-echelon* pattern consistent with left-lateral wrenching. They should be mainly Virgilian in age, and paleogeographic maps (Tomlinson and McBee, 1962) indicate that whereas some deformation along this trend occurred in Atoka time, it was most pronounced in Virgilian–Missourian time. Although this timing is reasonably consistent with earlier overthrusting followed by later wrenching, the COCORP data might be equally consistent with oblique slip (combined wrenching and thrusting) in both pre–end of Atokan and Virgilian times.

CONCLUSIONS

These interpretations of the COCORP data imply that present structures in southern Oklahoma reflect severe crustal shortening during the final stages of evolution of the aulacogen. The aulacogen has passed through a cycle of deformation in which an ancient fault trend was reactivated, first owing to crustal extension and then to crustal shortening; thus it evolved in a manner similar to aulacogens described from the Russian and Siberian Platforms (Milanovsky, 1981). These results, while not disproving the crustal updoming and radial-rifting origin of aulacogens proposed by Burke and Dewey (1973), raise the possibility that the aulacogen might have started by reactivation of the ancient fault trend under some alternative tectonic scheme.

These seismic data have started to reveal some of the fascinating details of the complex structural evolution of southern Oklahoma, yet they give little information on the equally fascinating igneous rocks that are exposed in the Wichita Mountains. Only by integrating surface and well studies with seismic and other geophysical evidence will the evolution of the basement rocks and their sedimentary cover be fully understood.

ACKNOWLEDGMENTS

This research is part of the COCORP project, funded by the National Science Foundation under grants EAR78–23673, EAR80–18363, and EAR80–25361. The data were collected by Crew 6834 of the Petty-Ray Division of Geosource, Inc. The surveys were made possible with the help of the Oklahoma Geological Survey, in particular, Kenneth S. Johnson and Charles J. Mankin. This report on the COCORP data covers work done at Cornell University, with R. Good, J. E. Oliver, L. D. Brown, and S. Kaufman. Many of the ideas benefited from discussion with many individuals, particularly R. E. Denison and M. C. Gilbert.

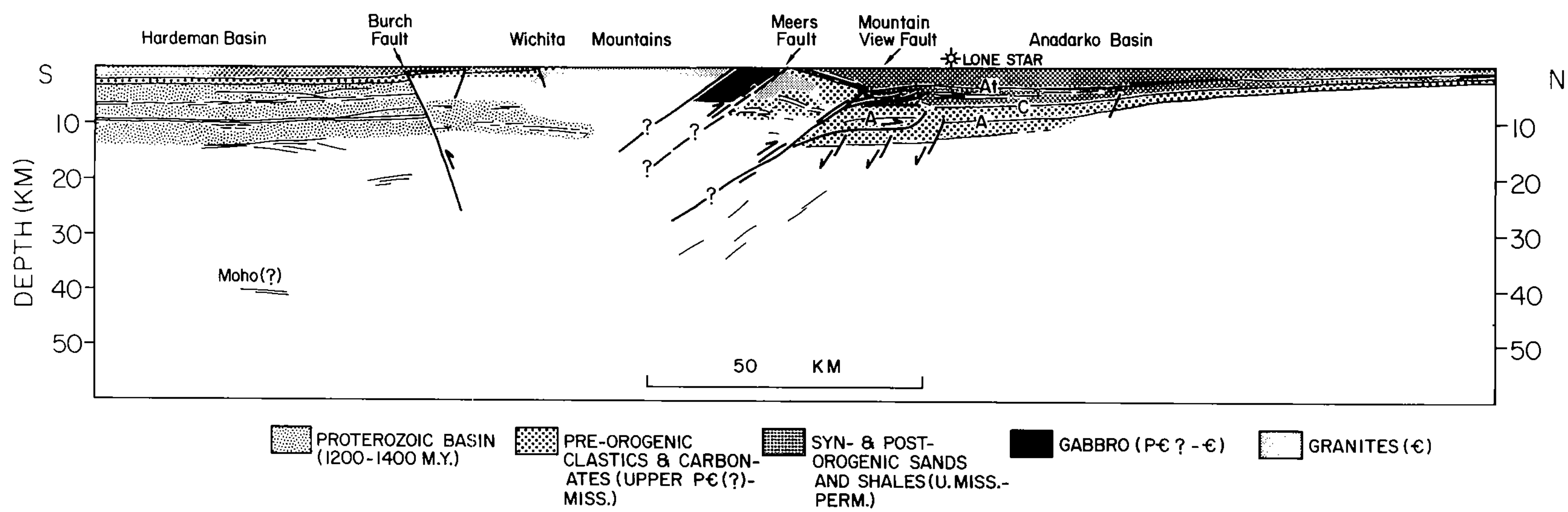

Figure 29. Section across Southern Oklahoma Aulacogen, based on COCORP data. Note (1) Proterozoic basin inferred to lie south of, and partially beneath, Wichita Mountains; (2) interpreted normal faulting near base of Anadarko Basin; (3) thrust nature of Mountain View and Meers Faults; (4) listric thrust faults in Anadarko Basin. *Lone Star*, position of Lone Star 1 Rogers. Sedimentary horizons are: *A*, Cambrian–Ordovician Arbuckle; *C*, Mississippian Chesterian; *At*, Pennsylvanian Atokan.

Oklahoma Geological Survey Guidebook 21, 1982

REINTERPRETATION OF METAMORPHIC ROCKS ALONG CARLTON RHYOLITE–MOUNT SCOTT GRANITE CONTACT WICHITA MOUNTAINS

J. Ronald Sides
James R. Miller

INTRODUCTION

Basement rocks of Oklahoma crop out in two major geologic terranes, the Wichita Mountain Uplift in the southwest and the Arbuckle Mountain Uplift in the south. These uplifts are flanked by deep Paleozoic basins that include the Anadarko, Hardeman–Hollis, Arkoma, Marietta, and Ardmore Basins (fig. 1). This structural system developed in late Proterozoic or Early Cambrian time as a rift system, called the Southern Oklahoma Geosyncline (Ham and others, 1964). Hoffman and others (1974) named it the Southern Oklahoma Aulacogen and considered it to be the type aulacogen in the United States. Burke and Dewey (1973) described the aulacogen as the failed arm of the Dallas triple junction. The aulacogen received sediments throughout most of the Paleozoic; however, Pennsylvanian deformation uplifted parts of it and left the deep basins as remnants (Ham and others, 1964). The disrupted aulacogen is marked by strong gravity, magnetic, and seismic anomalies, which are unique to North America.

Basement rocks of southern Oklahoma are divided into two provinces, the Wichita province, associated with the Wichita Mountain Uplift, and the Eastern Arbuckle province, associated with the Arbuckle Mountain Uplift (Ham and others, 1964).

The Wichita province consists mostly of Cambrian igneous and metamorphic rocks that occur over an area of at least 35,000 km^2 in Oklahoma and Texas. The province includes the most voluminous occurrence of Cambrian igneous rocks known in North America. The province consists of five major groups: Carlton Rhyolite Group, Wichita Granite Group, Raggedy Mountain Gabbro Group, Navajoe Mountain Basalt–Spilite Group, and Tillman Metasedimentary Group. Most of these units are described elsewhere in this guidebook and are not emphasized here. However, two of the units are of special significance for this paper and are described briefly below.

Carlton Rhyolite Group

The Carlton Rhyolite Group is a thick sequence of pyroclastic rocks, lavas, and agglomerates of rhyolitic composition. The unit crops out over an area of about 39 km^2 in the Bally Mountain, Blue Creek, and Fort Sill areas. Subsurface data indicate that it underlies at least 18,100 km^2 and possibly 44,000 km^2 of southern Oklahoma, and has a drilled thickness of 1.37 km (Ham and others, 1964). The enormous volume of the unit ranks it as one of the major volcanic units of North America. The Carlton Rhyolite has been studied in outcrop by Hoffman (1930), Schoonover (1948), and Ham and others (1964), who described a measured section of 1.1 km in the Bally Mountain area. The unit is correlated with the Colbert Porphyry, which crops out in the Arbuckle Mountains (Ham and others, 1964). The unit is mostly porphyritic with phenocrysts of perthite, quartz, and minor plagioclase in a quartzofeldspathic matrix (table 12). Flow-banding, spherulites, perlitic cracks, banding in water-laid tuffs, and glass shards in pyroclastic units are common (Ham and others, 1964; Powell and others, 1980). Chemically, Carlton rhyolite is highly silicic and subalkaline, and is chemically indistinguishable from rocks of the Wichita Granite Group (Adams, 1977; Hanson, 1977). Carlton rhyolite was generally intruded by the Wichita granites; however, some rhyolite dikes cut the granites, and the two units are considered to be nearly contemporaneous (Ham and others, 1964; Hanson, 1977; Powell and others, 1980). Three whole-rock Rb/Sr determinations and one zircon U/Pb determination suggest an age for the unit of 525 ± 25 m.y. The Carlton Rhyolite is considered one of the youngest major igneous units in the Wichita province because it overlies all other major igneous units.

Tillman Metasedimentary Group

The Tillman Metasedimentary Group is composed of generally low-grade metamorphosed graywackes, shales, siltstones, sandstones, arkoses, and bedded cherts. Locally, the unit consists of mica schists and hornfels (table 13). The unit is known only in the subsurface of Tillman, Jackson, and Cotton Counties of southern Oklahoma, and occurs over an area of about 3,460 km^2 (Ham and others, 1964). Correlative rocks probably occur in the subsurface of Wichita, Archer, and Clay Counties of Texas (Ham and others, 1964), in the Red River Mobile Belt of Flawn (1956). Ham and others (1964) concluded that the metasediments are flanked by, and presumably overlie, older granitic and high-grade metamorphic rocks of the Eastern Arbuckle province. They concluded that the unit is older than the Raggedy Mountain Gabbro Group, because large inclusions of Meers Quartzite (table 13) occur in the gabbros. The Meers Quartzite consists of recrystallized sandstone that contains variable amounts of microcline, sillimanite, epidote, chlorite, and biotite, and may correlate with the Tillman Metasedimentary Group. The rock is known only as inclusions within the Raggedy Mountain

TABLE 12.—MODAL ANALYSES OF CARLTON RHYOLITE AND PRATT HILL QUARTZITE, PRATT HILL

Carlton Rhyolite	ET-10	PH-26
quartz-feldspar matrix	78.7	83.7
quartz phenocrysts	5.6	4.7
orthoclase phenocrysts	10.0	9.8
chlorite	0.2	0.5
epidote	0.2	0.5
opaques	-	0.4
lithic fragments	-	0.4
vein quartz	5.3	-

Pratt Hill quartzite	PH-2	PH-10	ET-11	ET-13	PH-29	ET-12
quartz	52.4	47.3	37.4	45.7	99.+	50?
white micas	45.1	-	-	52.8	Tr	50?
matrix	-	49.6	54.1	-		
chlorite	1.3	-	-	-		
opaques	1.3	1.5	4.7	1.2		
goethite	-	1.5	2.3	0.3		

Notes: The samples also contain trace amounts of muscovite, epidote, and fluorite. Matrix refers to an intimate mixture of white micas and chlorite, which is too fine to accurately point count. The matrix ranges up to about 20% chlorite. ET-11 contains trace amounts of biotite. ET-12 is too fine-grained to accurately point count. Data shown is a visual estimate.

Gabbro Group and the Wichita Granite Group. Ham and others (1964) stated, and Powell and others (1980) reemphasized, that the Meers Quartzite does not resemble any known part of the Tillman metasediments, so that the correlation between the two and the inferred relative age of the Tillman are speculative.

Geological Development

According to Ham and others (1964), the Tillman Metasedimentary Group was deposited on a floor of Eastern Arbuckle province rocks. The original sediments were metamorphosed to the greenschist facies, probably owing to subsequent intrusion of Wichita

TABLE 13.—MAJOR FEATURES OF MEERS QUARTZITE AND TILLMAN METASEDIMENTARY GROUP

Rock Type	Description
Meers Quartzite	
chlorite, mica quartzite	Subrounded quartz grains set in a matrix of muscovite (7%), biotite (6%), and chlorite (3%). Contains zircon (1%), plagioclase (1%), and traces of magnetite and micropegmatite.
pure quartzite	Nearly pure recrystallized quartz. Partly subrounded grains. Secondary overgrowths.
feldspathized quartzite	Variable amounts of perthite, microcline and plagioclase. Small amounts of biotite and opaque minerals are common. Feldspars typically 25%.
sillimanite quartzite	5% to 10% sillimanite, 1% to 3% biotite and trace amounts of zircon, magnetite, apatite, rutile and muscovite.
Tillman Metasedimentary Group	
meta-graywacke and argillite	Quartz, various feldspars, chert and quartzite. Chert (about 5%) is universally present. Some phyllite grains. Matrix contains biotite, quartz and feldspar with some epidote, chlorite, muscovite and hornblende.
schist and hornfels	Crystalloblastic quartz, plagioclase, biotite and/or muscovite and hornblende. Hornfels consists of quartz, plagioclase, biotite and actinolitic hornblende.
bedded chert	reddish-brown and dark greenish-gray very finely crystalline chert. Up to 5% biotite or chlorite and muscovite.

Note: All data are taken from Ham and others (1964).

granite magmas. The unit is probably much more extensive than well logs now indicate, but it is buried too deep in surrounding basins to be drilled. As mentioned above, this unit could postdate the Raggedy Mountain Gabbro Group, because the presence of Meers quartzite in the gabbros is a tenuous age criterion (Powell and others, 1980).

The next(?) major event in southern Oklahoma was intrusion of the Glen Mountains Layered Complex. Layered-complex magmas may have intruded the Tillman metasediments to form a lenticular body, possibly 60 km by 200 km by 6 km thick. The complex appears to be typical of large, layered intrusions in that it was produced by crystal settling. The Navajoe

Mountain Basalt–Spilite Group may be comagmatic with the layered complex and could have been deposited on the Tillman Metasedimentary Group (Ham and others, 1964).

Layered-complex rocks were intruded by the Roosevelt Gabbros. However, the recommended age of the gabbros (535 m.y.) and their equivalence to layered-complex rocks are subject to question (Powell and others, 1980) (see Bowring and Hoppe, this guidebook). The Carlton Rhyolite and Wichita Granite Groups were emplaced almost simultaneously at about 525 m.y. Ham and others (1964) suggested that a major period of uplift and faulting occurred between emplacement of the Roosevelt gabbros and the Wichita granites.

Post–Carlton–rhyolite diabase and rhyolite dikes were the last igneous event in southern Oklahoma. Subsequent subsidence led to the deposition of at least 18 km of Paleozoic sedimentary rock during the formation of the Southern Oklahoma Aulacogen. The aulacogen was partially destroyed by Pennsylvanian uplift, which exposed the igneous rocks. This terrane was subsequently buried and is now being exhumed.

In the Fort Sill area, the Mount Scott Granite has intruded as a sill-like mass beneath the Carlton Rhyolite and above the Raggedy Mountain Gabbro, presumably along the old erosion surface. Some of the most compelling evidence that the Carlton Rhyolite was intruded by the Mount Scott Granite is in Fort Sill Military Reservation just west of Lawton, Oklahoma. In this area, the Mount Scott–Carlton intrusive contact is well exposed at a number of places. Along this contact, in the region of Lake Elmer Thomas, there occurs a large outcrop of metamorphic rock. This unit was originally included with the Davidson Granophyre (Hoffman, 1930). Ham and others (1964) reinterpreted the rock as a hornfels, which was produced when Mount Scott granite intruded overlying Carlton rhyolite. These authors presented compelling petrographic evidence that the rhyolite has been metamorphosed or hydrothermally altered. This evidence includes silicification and sericitization of the rock, with flow banding and phenocrysts still preserved. Ham and others suggested that the metamorphism gradually increases downward toward the granite. While these relationships certainly hold for some of the Carlton Rhyolite, we suggest a different interpretation for the rocks exposed on the southern shore of Lake Elmer Thomas, near the base of Pratt Hill (see map for Stops 4 and 8).

FIELD RELATIONSHIPS

The Carlton Rhyolite and metamorphic rocks are well exposed on the north side of Pratt Hill. For the sake of brevity, these metamorphic rocks are called the Pratt Hill quartzite in this paper. This is an informal field term and is not intended for use as formal nomenclature. The rhyolite caps the hill, and the contact between it and the underlying quartzite occurs near the base of the hill, along a steep slope on the north side. From this slope, the contact extends both to the east and west where the hill slopes less steeply, and in these areas the contact is generally not exposed. Our study concentrated on this steep, northern part of the hill where the contact is well exposed in several places. The contact is very sharp, and on the remainder of the hillside, where the contact is not exposed but the two rock types are in close proximity, a sharp contact is also indicated. The contact is generally east-trending across the hillside, and is irregular in elevation. It occurs at water level near the middle of the hill, and climbs to about 20 m above water level (visual estimate) toward the eastern part of the steep northern slope. Measurements taken along the contact indicate that it dips about 10° to the southeast and strikes N. 60° E. on this hillside. Near the western edge of the hill, the quartzite reappears above water level, along a small creek, and extends westward to the "Hideaway" area on the southwestern shore of the lake (see map for Stops 4 and 8). Whether the quartzite reappears along a fault or simply occurs owing to structural irregularity is unknown.

The quartzite is well exposed, and appears generally greenish-gray in outcrop. It is highly jointed, with one especially prominent joint set dipping 20° to the south and striking about N. 70° W. Although not prominently bedded, the unit contains local bands that are mineralogically inhomogeneous, which suggests crude bedding; these bands parallel the prominent joint set so that its attitude is taken to be that of the quartzite unit. The unit preserves no recognizable sedimentary structures, except that some of the jointing occurs as curved fractures that strongly suggest cross-bedding. The upper 25 cm of the unit is noticeably darker, and rocks exposed at the "Hideaway" are more brown than green-gray. These color changes are discussed below.

The Carlton Rhyolite exposed just above the contact is reddish brown and is clearly an ash-flow tuff, as indicated by the prominent occurrence of fiamme. The unit strikes N. 80° W. and dips 35° to the south, as indicated by the attitude of fiamme. The unit is porphyritic, with well-displayed phenocrysts of quartz and alkali feldspar.

PETROGRAPHY

Two thin sections of Carlton rhyolite were taken immediately above the contact with the underlying quartzite. The modes of these samples are summarized in table 12. The rock is hiatal porphyritic with phenocrysts of quartz (5 percent) and orthoclase (10 percent) in a matrix of quartz and feldspar intergrowths (fig. 30).

Quartz occurs as euhedral to subhedral phenocrysts (1 to 3 mm in diameter), rarely as oval polycrystalline aggregates (about 0.2 mm in diameter), and as microlites in the matrix. Orthoclase occurs as rectangular euhedral phenocrysts (3 to 4 mm long), as crystal fragments, and as microlites in the matrix. Phenocrysts are partially altered to white micas, clay minerals, and rarely epidote. Feldspar crystals contain small inclusions of quartz and, rarely, apatite. The matrix contains mainly quartz and orthoclase microlites (generally 0.05 mm to 20 microns in diameter) with small, rounded, opaque minerals and rare chlorite. Matrix feldspars are partially replaced by white micas. Rare aggregates of white mica and chlorite (about 1 mm long) indicate the probable presence of former mafic phenocrysts.

One sample (ET–10) contains quartz microveinlets, possibly indicating hydrothermal alteration.

The quartz and feldspar matrix was originally the glassy matrix of an ash-flow tuff, now devitrified. The quartz veinlets, and replacement of feldspar by clays and white micas, support the conclusion of Ham and others (1964) that the rhyolite has been locally metamorphosed or hydrothermally altered.

Microscopically, the Pratt Hill quartzite is variable in composition, although quartz and white micas are the dominant minerals (figs. 31–33). Quartz ranges from a low of 37 percent to more than 99 percent (table 12), and averages about 50 percent. Quartz is angular to subangular, and where grains

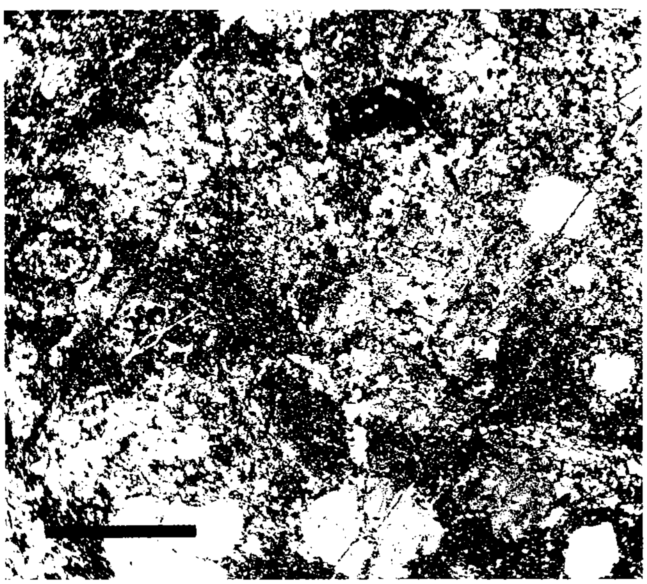

Figure 30. Photomicrograph (crossed polars) of Carlton rhyolite showing quartz and partly altered alkali feldspar phenocrysts. Sample (ET–10) collected at basal contact of rhyolite. Bar is 2.5 mm.

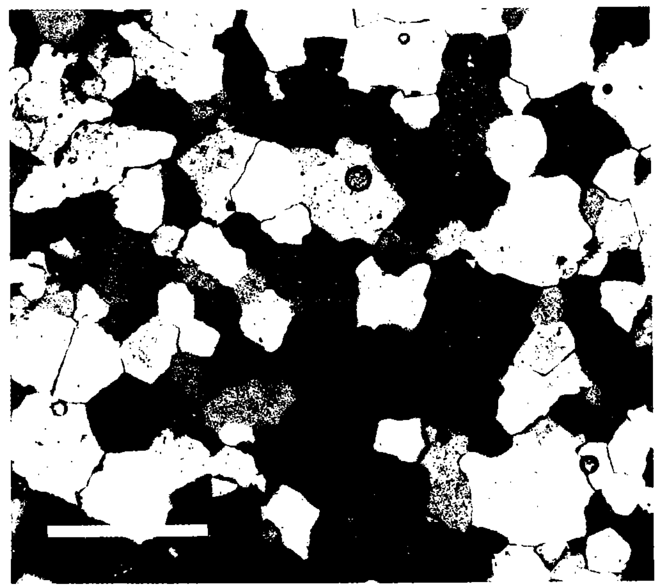

Figure 32. Photomicrograph (crossed polars) of pure quartzitic zone of Pratt Hill quartzite (PH–29). Bar is 0.25 mm.

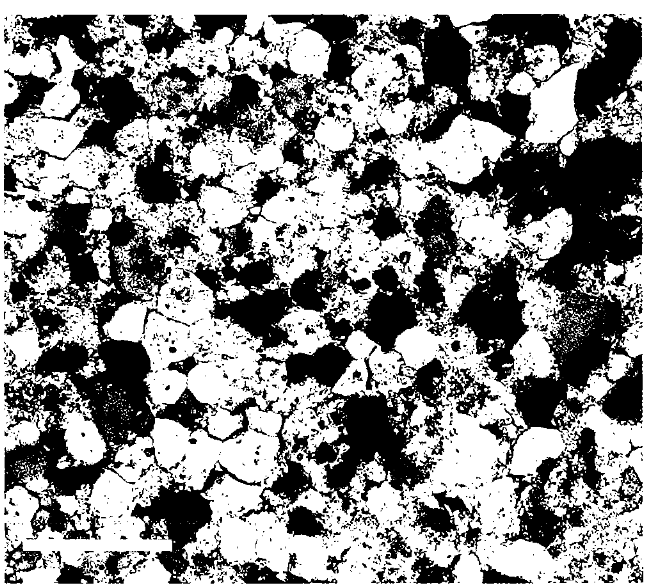

Figure 31. Photomicrograph (crossed polars) of Pratt Hill quartzite (PH–2), showing quartz and white-mica assemblage typical of this unit. Bar is 0.25 mm.

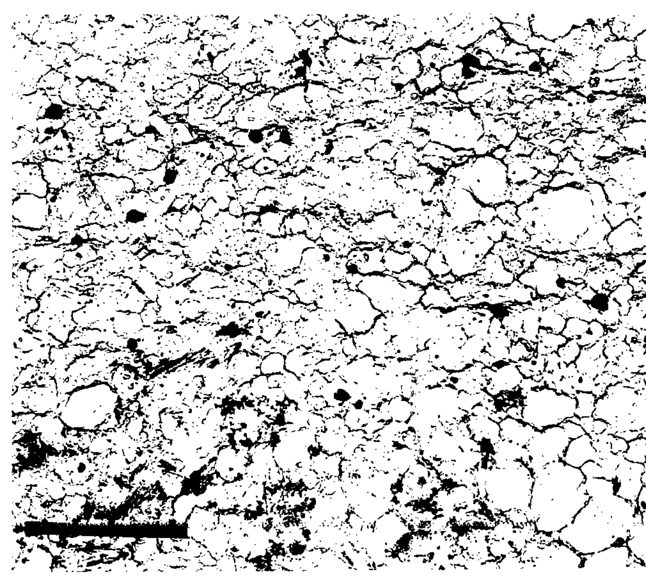

Figure 33. Photomicrograph (plane light) of Pratt Hill quartzite showing equant quartz grains in a chlorite-rich matrix. Sample (ET–11) collected immediately below upper contact of unit. Bar is 0.25 mm.

are in contact they display excellent crystalloblastic, mosaic texture, clearly indicating metamorphic growth. The grain size of quartz is remarkably uniform, generally 0.1 to 0.3 mm in diameter, and rarely down to 10 microns. Out of all the thin sections studied, there are only one or two larger quartz fragments (about 0.5 to 1 mm long) and only a few oval polycrystalline aggregates (0.3 to 0.5 mm).

The remainder of the rock is mostly white micas (45 to 54 percent) and variable amounts of chlorite. The grain size of these minerals (generally less than 0.05 mm long) is so small that they cannot easily be distinguished, and they occur as ragged flakes. Rarely, larger (about 0.1 mm) crystals of chlorite and muscovite occur. Magnetite, as small, angular to rounded grains (0.1 to 0.01 mm in diameter), is the only other major component of the quartzite (as much as 5 percent). Additionally, trace amounts of hematite, epidote, and secondary goethite(?) occur.

Some samples of the unit are homogeneous and some are crudely banded, owing to nonuniform mineral content. Whether these bands reflect flow banding or a depositional feature is undetermined.

Conspicuous by their absence in the quartzite are feldspars (except in one sample) and any high-grade metamorphic minerals such as biotite, sillimanite, or garnet. The rock is clearly metamorphic, as indicated by the crystalloblastic texture of quartz; however, the rock was subjected only to low-grade metamorphism. As albite–epidote hornfels (or greenschist) facies metamorphism progresses, chlorite first increases in size and then converts to biotite. The fine grain size of chlorite, the presence of fine-grained white micas, and the nearly total absence of biotite imply that the metamorphism did not exceed the lower greenschist facies. It might be argued that chlorite has retrograded from original biotite, but no chlorite pseudomorphs after biotite occur.

The uppermost 25 cm of the Pratt Hill quartzite is darker than the rest of the unit. Two samples of this darker band were studied to determine its origin (ET–11, ET–12). One sample (ET–11) is unusually high in chlorite, but the other is chlorite-poor and has few dark minerals. Therefore, the dark color of the band remains unexplained.

The quartzite exposed near the "Hideaway" is brownish rather than grayish green. One sample of this rock (ETL–2) contains about 21 percent orthoclase, which is altered to clay minerals and rarely to white micas, and is clouded by hematite dust. Feldspar grains are generally smaller than quartz grains (0.2 mm to 10 microns) and occur mostly as single grains interstitial to quartz. Also interstitial are less abundant polycrystalline aggregates of feldspar (0.2 to 0.1 mm). Quartz grains are typical of those in the rest of the unit, in size and shape, except that they are commonly coated with hematite. The sample contains rare chlorite, muscovite, and biotite crystals as much as 0.2 mm long. The occurrence of biotite and feldspar, and the abnormally large grain size of chlorite, are anomalous in comparison with the rest of the unit. The origin of this rock is discussed below.

DISCUSSION

Data Interpretation

Partial alteration of feldspars to white micas and clay minerals demonstrates that the Carlton Rhyolite has been metamorphosed or hydrothermally altered, as discussed by Ham and others (1964). However, the abrupt changes in texture and mineral content suggest that the exposed contact on Pratt Hill also involves a lithologic change and not just a gradual increase in metamorphic grade.

Well-defined phenocrysts in the basal part of the Carlton Rhyolite do not occur below the contact, and thus the precursor of the Pratt Hill quartzite must have been aphanitic. Two obvious choices for this precursor are a fine-grained sedimentary rock or a volcanic tuff, perhaps an air-fall tuff. This latter possibility was mentioned briefly by Ham and others (1964). Air-fall tuff initially would have been glassy but would have devitrified to a fine-grained intergrowth of quartz and feldspar. Low-grade metamorphism could have converted the feldspar to white micas, producing the mineral assemblage of the quartzite. However, the presence of both phenocryst and matrix feldspar immediately above the contact, and absence of feldspar below the contact (except in sample ETL–2), argue against this interpretation. Moreover, the locally abundant chlorite in the quartzite also is inconsistent with this model, because Carlton rhyolite contains only trace amounts of chlorite and other ferromagnesian minerals (Ham and others, 1964). Presumably, tuffaceous equivalents of the Carlton Rhyolite would be similarly deficient in ferromagnesian minerals.

An alternative we prefer is that the quartzite was originally a sedimentary rock. Compositionally, it would have been a somewhat immature, fairly well-sorted clastic rock with a bimodal size distribution that included generally fine quartz sand (Wentworth scale) in a clay matrix. It might be argued that the rare occurrence of slightly larger fragments and oval polycrystalline aggregates of quartz is more consistent with a volcanic precursor for the quartzite. However, these features would not be unexpected in a clastic rock of the kind described. Lack of sedimentary structures in the quartzite, except possibly for relict cross-bedding, is not consistent with a clastic origin for the unit. However, the quartzite also does not preserve evidence of volcanic features such as flow banding, fiamme, and foliations which commonly occur in air-fall tuff.

Although the evidence is far from unequivocal, we prefer a sedimentary origin for the Pratt Hill quartzite. Slight discordance of the contacts with overlying and underlying units implies an erosional interval between their deposition.

Sample ETL–2 represents an anomaly, because biotite, orthoclase, and muscovite do not occur elsewhere in the quartzite. There are several ways to interpret this rock: (1) it could be a feldspar-rich sedimentary facies of the Pratt Hill quartzite; (2) it could represent normal quartzite that has been feldspathized, as in the Meers Quartzite (see below); or (3) it could represent Carlton rhyolite that was intensely altered. Factors that make interpretation of this sample difficult include poorly exposed contact relationships in the "Hideaway" area, and a sample location that is very close to the microgranite contact and farther west than any other sample. The interstitial occurrence of the feldspar, hematite coatings on quartz grains, and larger grained biotite and muscovite argue for the second hypothesis; however, lack of high-grade metamorphic minerals argues against this model. Because of poorly exposed contacts, the third hypothesis cannot be ruled out. If the first model is correct, feldspar could represent original detrital grains or could have grown in place metamorphically. Which one, if any, of these models is correct cannot be determined without additional sampling and analysis of rocks from the "Hideaway" area.

Possible Correlations

We note that the sedimentary precursor for the Pratt Hill quartzite is generally similar in composition to two other units that occur in the Wichita Mountains, the Tillman Metasedimentary Group and the Meers Quartzite. The major features of these units are summarized in table 13. Most authors include the Meers Quartzite in the Tillman Metasedimentary Group. Powell and others (1980) pointed out that this correlation is tentative and divide the units at the formational level. For purposes of this paper, these units are discussed separately.

The Pratt Hill quartzite does not appear to be correlative with either of these two units. Meers quartzite occurs as large inclusions in rocks of the Raggedy Mountain Gabbro and Wichita Granite Groups. Clearly, lack of sillimanite and abundant feldspar in the Pratt Hill quartzite preclude correlation with sillimanite quartzite and feldspathized quartzite. The Pratt Hill quartzite more closely resembles the chlorite- and mica-bearing variety of Meers quartzite. Obviously, the pure quartzite varieties of these units might be correlative except that pure quartzite represents only a small portion of the Pratt Hill quartzite. The presence of subrounded quartz, and biotite, and the abundance of muscovite in the chlorite- and mica-bearing Meers Quartzite argue against correlation of these rocks. The Tillman Metasedimentary Group (table 13) contains significant amounts of chert, and either biotite, hornblende, or actinolite, and therefore probably cannot be correlated with the Pratt Hill quartzite.

The Pratt Hill quartzite may have originated as a sedimentary unit that has not yet been recognized in the Wichita Mountains. As stated previously, the Carlton Rhyolite was presumably deposited on an erosion surface of the Raggedy Mountain Gabbro. The Wichita granites were injected above this surface. This post-gabbro, pre-Carlton interval should have allowed for deposition of significant quantities of sediment. Evidence of this sediment has not been found, along either the gabbro-granite contact or granite–rhyolite contact, and hence this material was presumably mostly swept beyond the central Wichita Mountains region. It is possible that Pratt Hill quartzite represents sediment deposited during this interval. It would have formed a low hill on gabbroic rocks until buried by the Carlton Rhyolite. The Mount Scott Granite would have intruded as a sill-like mass along the gabbro-sediment contact. It is possible that the darker band at the top of the Pratt Hill quartzite represents a pre-Carlton soil horizon.

CONCLUSIONS

A sharp contact, which trends easterly along the northern face of Pratt Hill, separates moderately altered Carlton rhyolite from an underlying quartz- and white-mica–bearing rock. This rock was originally aphanitic and has been subjected to low-grade metamorphism, probably from intrusion of the underlying Mount Scott Granite. This rock, informally called "Pratt Hill quartzite," could have originated as a fine-grained, tuffaceous equivalent of the Carlton Rhyolite. However, the almost complete absence of feldspar below the contact, and lack of pseudomorphs after feldspar phenocrysts, suggest a metasedimentary origin for the unit. The contact between the two units does not parallel either of them, suggesting that it is an unconformity. We suggest that the Pratt Hill quartzite originated as a submature, clastic sediment composed of fine quartz sand in a clay matrix.

This quartzite does not appear to be correlative with either the Meers Quartzite or the Tillman Metasedimentary Group. If not, the precursor of the quartzite would most likely be a pre-Carlton and post–Raggedy Mountain Gabbro sediment. This sediment would have existed as a low hill on gabbro. The sediment could have originated in one of many ways. It could have originated from weathering of some early phase of the Carlton Rhyolite. This weathering would necessarily have been extensive enough to convert original feldspar to clay minerals. However, no hiatus of this magnitude in the deposition of the Carlton Rhyolite has thus far been reported. Alternatively, the sediment could have been derived from the preexisting gabbroic units, because quartz is reported in sediments produced from rocks that are even this mafic. As in the previous model, feldspar would need to have been converted to clay minerals. The mineralogy of the quartzite is more compatible with a source that was high in Al and alkalis, rather than high in Mg and Ca. However, given the limited data now available, either source is entirely possible.

The Pratt Hill quartzite crops out over a small area that belies its possible regional significance. The purpose of this paper is to report its occurrence and to stimulate further study.

IGNEOUS GEOLOGY OF COOPERTON QUADRANGLE WICHITA MOUNTAINS

Marjorie L. Stockton
Joe D. Giddens III

INTRODUCTION

Three of the major divisions of the Wichita igneous complex crop out in the Cooperton Quadrangle. These are the Glen Mountains Layered Complex, the Roosevelt Gabbros, and the Mount Scott Granite. Other rock types occur in minor amounts (fig. 34). Chase (1950b) prepared a map that included most of this region, but his lithostratigraphy has been superseded by that described in Powell and others (1980).

The Cooperton 7.5-minute Quadrangle lies along the boundary between Kiowa and Comanche Counties. It covers parts of Ts. 3, 4, and 5 N., Rs. 15 and 16 W., and includes the western edge of the Wichita Mountains Wildlife Refuge.

GEOLOGY

Glen Mountains Layered Complex

The Glen Mountains Layered Complex forms the hills and low-lying outcrops in the southwestern quarter of the quadrangle. This sequence of anorthositic cumulate rocks is characterized by variably developed igneous lamination and rhythmic layering. The body strikes west-northwesterly and dips about 10° to the north-northeast. Local variations in strike are common.

The Glen Mountains Layered Complex was first mapped in detail in the Glen Mountains Quadrangle to the west, and was subdivided into sequential stratigraphic zones by M. C. Gilbert (1960) and A. B. Spencer (1961). The zones in the Cooperton Quadrangle are essentially similar to those previously described.

The lowermost zone, called the K Zone, is present only in the southwestern corner of the Cooperton Quadrangle and in the northwestern corner of the Odetta Quadrangle to the south (NW¼ sec. 11 and NE¼ sec. 15, T. 3 N., R. 16 W.). It consists of alternating layers of anorthosite and olivine gabbro, with isolated occurrences of coarse-ophitic pyroxene. The L Zone, stratigraphically overlying the K Zone, also has only a small outcrop area. It is predominantly anorthosite, and contains irregular masses of coarse-ophitic clinopyroxene as much as 25 cm in diameter. Igneous lamination is pronounced. The M Zone, overlying the L Zone, consists of anorthosite, anorthositic gabbro, and olivine gabbro, and is characterized by spherical, 1-6-cm fine-ophitic pyroxenes. The uppermost zone, the N Zone, has not been previously described (table 14). It consists of anorthositic gabbro with irregularly shaped subophitic pyroxenes, sparse olivine, and minor amounts of quartz, which may be secondary. Unlike the underlying zones in which no primary hydrous phases occur, traces of late-magmatic biotite and brown hornblende can be found locally in the N Zone.

Roosevelt Gabbros

The Roosevelt Gabbros are intrusive into the Glen Mountains Layered Complex. Two distinct bodies of these gabbros occur in the Cooperton Quadrangle: the Sandy Creek Gabbro, and a rock unit informally called the Mount Baker hornblende gabbro.

The Sandy Creek Gabbro, described by Powell and others (1980, p. 1935–1944), is a biotite, two-pyroxene gabbro that locally is olivine rich. It crops out in secs. 3, 4, 5, and 9, T. 3 N., R. 15 W.

The Mount Baker hornblende gabbro forms the base of Mount Baker and can be seen on the lower slopes, in secs. 17, 18, and 19, T. 4 N., R. 15 W. This biotite–hornblende, two-pyroxene gabbro is variable in grain size and texture and is much finer grained than the Sandy Creek body. Olivine is absent. Quartz is generally present, both as interstitial grains and as small microcrystalline pods. In some places, the rocks contain cavities filled with quartz and potash feldspar. Magnetite crystals as much as 15 cm in diameter have been found as float in areas peripheral to the Mount Baker gabbro. Their origin or relation to the gabbroic rocks is unknown. The Mount Baker body is nowhere in contact with the Sandy Creek body, and their relative ages have not been established.

Numerous dikes of biotite microgabbro, considered to be related to the Roosevelt Gabbros, cut the Glen Mountains Layered Complex throughout the outcrop area.

Mount Scott Granite

The Mount Scott Granite is a quartz–perthite granite containing some primary plagioclase, hornblende as the dominant mafic mineral, and magnetite, biotite, apatite, zircon, and sphene. Gray, ovoid feldspar phenocrysts are characteristic. The texture is variably micrographic.

The Mount Scott is younger than the mafic rocks. It was emplaced as a sill, as evidenced by a generally horizontal gabbro floor and, farther to the east, a cover of rhyolite. (The rhyolite has been eroded away over all of the Cooperton Quadrangle.) The Mount Scott Granite caps the mountains in the eastern half of the quadrangle.

Quaternary & Permian undifferentiated		Intertonguing Post Oak Conglomerate and Hennessey shale facies dominate. Post Oak forms higher ridges radiating away from mountains. Only minor flood plains along some of the streams.	
Permian		Tepee Creek facies of Post Oak shown separately.	
Cambrian	Wichita Granite Group	Hale Springs pegmatites	
		Quanah	
		Saddle Mountain	
		Hybrid rocks	
		Mt. Scott	
		Cold Springs Breccia	
	Raggedy Mountain Gabbro Group	Roosevelt Gabbros	Biotite microgabbro dikes & plugs
			Mt. Baker hornblende gabbro
			Sandy Creek Gabbro
Cambrian (?) to Proterozoic (?)		Glen Mountains Layered Complex	Undifferentiated (Probably mostly N Zone)
			N Zone hydrothermally altered
			M Zone
			L Zone
			K Zone
Proterozoic		Meers Quartzite	

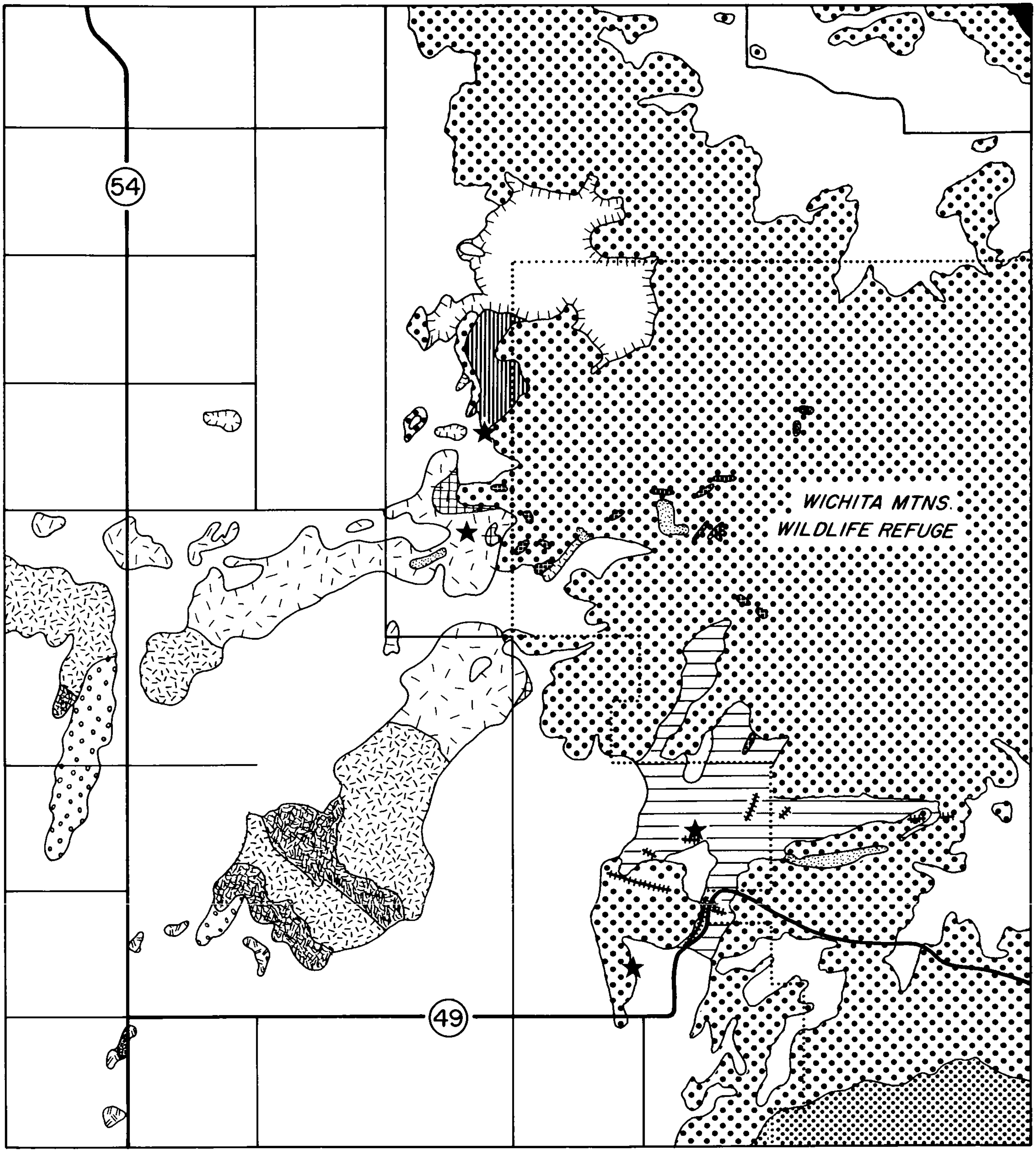

Figure 34. Geologic map of part of Cooperton 7.5-minute Quadrangle. Geology principally by Giddens and Stockton, with additions by M. C. Gilbert and from Chase (1950b). Section-line roads are at 1-mile intervals and indicate cardinal directions.

Hybrid Rocks

Rocks of intermediate composition and varying color and texture occur along the contacts between the gabbroic rocks and the granite. Some of these are merely contaminated granites. Others, however, exhibit unusual coarse textures, with plagioclase, pyroxene, and magnetite crystals several centimeters in length. The mechanism by which these rocks were formed is not yet clear.

Hale Spring Pegmatite

This sodic amphibole-bearing, quartz-feldspar pegmatite occurs as strikingly banded dike rocks in secs. 3, 4, and 9, T. 3 N., R. 15 W. The Hale Spring pegmatite is thought to be nearly the youngest igneous rock in the area, and to have formed from the last-stage fluids of the Quanah Granite.

Miscellaneous Dikes

Granitic and aplitic dikes are ubiquitous throughout the outcrop area of the Glen Mountains Layered Complex. One such dike in secs. 1 and 2, T. 3 N., R. 16 W., marks the site of a fault that produces a repeated section of the L and M Zones.

Diabase dikes cut the Roosevelt Gabbros and the granite in several places. An interesting example can be seen below Mount Baker, in the SW SE NE sec. 19, T. 4 N., R. 15 W.

Meers Quartzite

Four new localities of the Meers Quartzite have been identified: (1) SE NW NE SE sec. 8, T. 3 N., R. 15 W., in Mount Scott Granite; (2) NW NE NE SW sec. 4, T. 3 N., R. 15 W., on Sandy Creek Gabbro; (3) SE NW NE sec. 30, T. 4 N., R. 15 W., on N Zone, Glen Mountains Layered Complex; and (4) NW SW NE sec. 19, T. 4 N., R. 15 W., at the contact between Mount Scott Granite and the Mount Baker hornblende gabbro. These localities are symbolized on the map (fig. 34) as a star. Some of these are sillimanite-bearing (for example, no. 2). See the discussion by Gilbert (this guidebook) concerning the significance of the Meers outcrops.

TABLE 14.—CHARACTERISTICS OF N ZONE, COMPARED TO UNDERLYING M ZONE GLEN MOUNTAINS LAYERED COMPLEX

1) Clinopyroxene typically is sub-ophitic, irregularly shaped with a strung-out, "chicken-wire" appearance on outcrop. Size varies from 2 to 20 cm. Absence of characteristic fine ophitic clinopyroxene with chadocryst plagioclase randomly oriented and smaller than laminated cumulus plagioclase.

2) Chunky, round, coarse-ophitic clinopyroxene common at the M-N Zone transtion.

3) Orthopyroxene more common.

4) Olivine generally absent.

5) Poikilitic magnetite is ubiquitous.

6) Laminated plagioclase distinctive locally.

ROOSEVELT GABBROS (RAGGEDY MOUNTAIN GABBRO GROUP) WICHITA MOUNTAINS

Benjamin N. Powell

INTRODUCTION

Intrusive into the Glen Mountains Layered Complex, the lower formation of the Raggedy Mountain Gabbro Group, is a series of biotite-amphibole–bearing gabbroic rocks of tholeiitic affinity, collectively given the formation name "Roosevelt Gabbros" by Powell and others (1980). Three members have been formally named: Mount Sheridan Gabbro, Sandy Creek Gabbro, and Glen Creek Gabbro (table 2; figs. 2, 7). The latter two are discussed in some detail in this guidebook and are included among the scheduled stops. Another member, the Mount Baker hornblende gabbro, has been recognized informally (Stockton and Giddens, this guidebook).

GENERAL CHARACTERISTICS

The Roosevelt Gabbros form dikes, sills, and irregular bodies within the Glen Mountains Layered Complex. They are in turn intruded by younger intermediate rocks (Otter Creek Microdiorite and Cold Springs Breccia; table 2) as well as by granitic rocks, some of which belong to the Wichita Granite Group; others are presently unclassified and may or may not belong to the Wichita Granite Group (fig. 6).

In contrast to the Glen Mountains Layered Complex, with its *anhydrous* primary mineral assemblages, the Roosevelt Gabbros are characterized by primary magmatic hydrous phases. Biotite (or phlogopite), readily discernible on fresh rock surfaces, provides a distinctive field criterion for recognition. Amphibole and octahedral mica are typically present, the two collectively ranging in abundance from about 1 percent to 25 percent of the mode. Although they are late in the crystallization sequence relative to olivine, plagioclase, clinopyroxene, and orthopyroxene, the hydrous phases have every appearance of being primary magmatic, and not deuteric or hydrothermal. This characteristic, together with the comparatively great abundance and larger grain sizes, sets these hydrous magmatic phases and the rocks that contain them apart from the strictly deuteric, phlogopitic biotite found in trace amounts in some rocks of the Glen Mountains Layered Complex.

Where relatively abundant in the Roosevelt Gabbros, the amphibole and (or) micas form large poikilitic crystals enveloping unaltered plagioclase, olivine, pyroxene, and Fe–Ti oxides. In extreme cases (uncommon), pyroxene may be lacking in olivine-rich gabbro, with its textural position occupied instead by amphibole and phlogopite (see later section on the Glen Creek Gabbro). In a single thin section, olivine may be rimmed by orthopyroxene, amphibole, and (or) phlogopite, illustrating variable behavior of the residual liquid relative to the olivine peritectic reaction. Accessory phases, variably present in the Roosevelt Gabbros, include ilmenite, magnetite, apatite, pyrite, chalcopyrite, pyrrhotite, and sporadic pleonaste spinel. Fractionated lithologies contain quartz, K-feldspar, and zircon.

Amphibole compositions in the Roosevelt Gabbros range from titanian–magnesian hastingsite to kaersutite ($TiO_2 > 4.5$ percent); mica ranges from phlogopite (4 to 6.6 percent TiO_2) in olivine-bearing rocks, to titaniferous biotite ($TiO_2 > 5.5$ percent) in olivine-free rocks.

Bulk compositions of the Roosevelt Gabbros (table 15) resemble the high-TiO_2–high-P_2O_5–low-Al_2O_3 magmas recognized in the Keweenawan of Upper Michigan (Wilband and Wasuwanich, 1980). Their hydrous character could have been derived from melting of hydrous upper-mantle source rock, or it could be the result of contamination in the crust. Their principal interest lies in their crystallization behavior as hydrous olivine tholeiites, and in their chemical contrast to the probable parental magma for the Glen Mountains Layered Complex (anhydrous high-Al_2O_3 tholeiite) (Powell, 1981). This suggests a bimodality of basic magmatism that is becoming more widely recognized in other provinces (for example, Weiblen and Morey, 1980).

DIFFERENTIATION

Larger bodies of the Roosevelt Gabbros are internally differentiated. Both the Sandy Creek Gabbro (Powell and others, 1980) and the Mount Sheridan Gabbro (Powell and Fischer, 1976; Powell and others, 1980) are internally fractionated and show continuous gradation, with concomitant cryptic variation, from olivine gabbro to quartz-bearing gabbro–diorite or ferrogranodiorite. This observation is critical to the understanding of gabbro–granite relations in the Wichita province. Where contact zones are visible between gabbro and sizable bodies of younger Wichita Granite, the latter generally lie above the former. This relationship, together with the presence of granophyric texture in some granite bodies, has contributed to earlier interpretations of a direct fractionation relationship between the two rock groups (for example, Hoffman, 1930; Hamilton, 1956, 1959). Quite aside from the fact that granitic material in the province is much too voluminous relative to the basic rocks to have been derived from the latter by differentiation, the intrusive relations—both regional and local—demonstrate that the gran-

TABLE 15.—AVERAGE BULK COMPOSITIONS OF BIOTITE GABBROS (ROOSEVELT GABBROS) INTRUSIVE INTO GLEN MOUNTAINS LAYERED COMPLEX, WICHITA PROVINCE, OKLAHOMA

	1	2	3	4	5	6	Analytical Uncertainty*
SiO_2	47.5	46.7	47.6	46.3	50.0	45.8	0.24
TiO_2	1.39	2.95	2.49	3.42	2.66	5.06	0.10
Al_2O_3	16.1	12.9	18.3	14.1	15.9	12.5	0.16
FeO†	9.81	13.9	8.81	11.9	12.6	15.6	0.06
MnO	0.16	0.27	0.16	0.18	0.21	0.25	0.01
MgO	11.9	10.6	6.23	7.75	5.79	6.65	0.07
CaO	10.5	8.97	11.7	13.3	8.24	10.3	0.06
Na_2O	1.82	1.81	2.40	1.59	2.44	1.87	0.09
K_2O	0.25	0.62	0.23	0.13	0.59	0.35	0.01
P_2O_5	0.17	0.37	0.16	0.09	0.27	0.23	0.01
Total	99.60	99.09	98.08	98.76	98.70	98.61	
Atomic Fe/(Fe+Mg)	0.317	0.425	0.443	0.463	0.550	0.567	
Normative mol % An	66.3	56.1	62.8	67.4	54.8	56.7	

*Average estimated analytical uncertainty in absolute % of oxide; does not include sampling error.

†Total Fe expressed as FeO.

Samples:

1. Sandy Creek Gabbro, NE¼NW¼ sec.9, T.3N., R.15W., Comanche County County (WM-152).
2. Biotite-olivine gabbro dike, on boundary between sec.33, T5N.,R.17W. and sec.4, T.4N.,R.17W., Kiowa County (WM-154).
3. Glen Creek Gabbro, N½SE¼ sec.14,T.4N.,R.17W., Kiowa County (WM-266).
4. Glen Creek Gabbro, adjacent to olivine-magnetite-ilmenite segregation, NE¼SW¼ sec.14, T.4N.,R.17W., Kiowa County (MP-22).
5. Mount Sheridan Gabbro (olivine-bearing), NE¼SE¼ sec.5,T.3N., R.13W., Comanche County (T-49).
6. Mount Sheridan Gabbro at contact with Glen Mountains Layered Complex, NE¼SW¼ sec.32,T.4N.,R.13W., Comanche County (WM-117).

ites invariably crosscut and are considerably younger than the basic rocks, which are commonly (though not always) hydrothermally altered near the contacts. These and other observations germane to this question were discussed by Ham and others (1964), Powell and Fischer (1976), and Powell and others (1980). The Sandy Creek Gabbro, described in some detail later in this guidebook, provides some evidence supporting the interpretation of a considerable time hiatus between its crystallization and crystallization of the Wichita Granite Group.

RELATIVE AGES

Relative ages of the Roosevelt Gabbros are generally well established through intrusive relations in the Wichita province: younger than the Meers Quartzite and the Glen Mountains Layered Complex, and older than the Otter Creek Microdiorite, Cold Springs Breccia, Wichita Granite Group, and Carlton Rhyolite Group. (See table 2 and fig. 6.) The relationship of the Roosevelt Gabbros to the Navajoe Mountain Basalt–Spilite Group remains unclear, owing to the restriction of the latter to subsurface occurrences. Although it is perhaps logical to assume that the Navajoe Mountain basalt is the volcanic equivalent of either the Roosevelt Gabbros or the Glen Mountains Layered Complex (as did Ham and others, 1964), one should remember that the evidence is meager at best, model-dependent, and purely circumstantial. For one thing, the Navajoe Mountain basalt lacks olivine and orthopyroxene, both of which are typically present in the Raggedy Mountain Gabbro Group as a whole. A definitive study of the Navajoe Mountain Basalt–Spilite Group would make a significant contribution to Wichita geology.

ABSOLUTE AGES

In contrast with the well-established *relative* ages of the principal rocks of the Wichita province, the picture with regard to *absolute* ages remains incomplete and in places equivocal. Ham and others (1964) summarized the available data, firmly establishing the age of the Wichita Granite Group and the Carlton Rhyolite Group as 525 ± 25 m.y. [All ages given in this guidebook are corrected for the modern IUGS-recommended decay and abundance constants, after Steiger and Jager (1977) and Dalrymple (1979).] Previous radiogenic age determinations on the basic rocks of the Raggedy Mountain Gabbro Group, including the Roosevelt Gabbros, are much more limited in number and are subject to interpretation.

Rb/Sr measurements by Tilton and others (1962) on biotite of the Mount Sheridan Gabbro indicate an age of 530 ± 30 m.y. Burke and others (1969) performed K/Ar determinations on biotite samples of the Mount Sheridan Gabbro and on one whole-rock sample of the Sandy Creek Gabbro, reporting ages of 498–519 ± 10 m.y. and 514–527 ± 10 m.y., respectively. Given the magnitude of the subsequent granite–rhyolite magmatic episode in the Wichita province, the possibility of thermal overprinting on these radiogenic systems in the older basic rocks is very real. The geologic evidence requires a considerable time hiatus between the older gabbroic and the younger granitic magmatism, as discussed by Ham and others (1964) and Powell and others (1980).

New evidence on the probable crystallization age of the Mount Sheridan Gabbro is discussed by Bowring and Hoppe (this guidebook). On the basis of general lithologic characteristics and ages relative to the older Glen Mountains Layered Complex and the younger Wichita Granite Group (and Carlton Rhyolite), the Roosevelt Gabbros were grouped together in the lithostratigraphic classification by Powell and others (1980). This grouping also serves the interest of petrologic simplicity; it does not, however, necessarily indicate the same absolute age for all members of the Roosevelt Gabbros. Two points should be borne in mind. First, intrusive contacts between members of the Roosevelt Gabbros are not visible to establish relative ages within the group; second, how *much* older the Glen Mountains Layered Complex is than the Roosevelt Gabbros has not been established by radiogenic geochronology.

U/PB ZIRCON AGES FROM MOUNT SHERIDAN GABBRO WICHITA MOUNTAINS

Samuel A. Bowring
Wendel J. Hoppe

INTRODUCTION

In the last 10 years it has become apparent that a major hindrance to full understanding of the geology of the Wichita province is the lack of precise ages of crystallization for some of the igneous rocks exposed in the Wichita Mountains. Detailed field, petrographic, and chemical studies of the rocks have led to assignment of relative ages for the major units (Powell and others, 1980); however, there is considerable uncertainty regarding their crystallization ages. We are currently involved in a comprehensive U/Pb zircon study of many of the rocks in the Wichita province, and the preliminary results from the Mount Sheridan Gabbro are reported here.

GEOLOGY

Field and subsurface observations indicate that the rocks of the Glen Mountains Layered Complex are the oldest igneous rocks of the Wichita province; however, its age of crystallization is not certain (Powell and others, 1980). The Roosevelt Gabbros comprise a series of biotite-bearing rocks that intrude the Glen Mountains Layered Complex and are lithologically distinct from it. The largest exposure of Roosevelt Gabbros in the Wichita Mountains has been formally named "Mount Sheridan Gabbro" by Powell and others (1980), who also gave petrographic and chemical information. Excellent exposures of the Mount Sheridan Gabbro are found in the Rowe Quarry along Medicine Creek (fig. 35). Dikes and pods of pegmatitic material within the gabbro (fig. 36) are well exposed in the quarry.

The pegmatitic material is composed dominantly of green hornblende, alkalic feldspar, and quartz, with variable amounts of biotite, augite, magnetite, and accessory apatite and zircon. Zircon is found as an accessory mineral in both the Mount Sheridan Gabbro and the pegmatite. Powell and Fischer (1976) suggested that the pegmatites could represent either late-stage segregations of residual liquid from the crystallizing Mount Sheridan Gabbro or the products of assimilate reaction and recrystallization of xenoliths of the Meers Quartzite. Powell and others (1980) stated that the petrographic similarity between the pegmatite and the mesostasis of the gabbro favors a magmatic origin for the pegmatites. Our samples of the Mount Sheridan Gabbro and associated pegmatite pods, for zircon chronology, were obtained from the Rowe Quarry.

PREVIOUS GEOCHRONOLOGIC STUDIES

Several geochronologic studies, including U/Pb zircon studies from the Wichita Mountain granites and Carlton Rhyolite (Tilton and others, 1957, 1962), were conducted in the Wichita Mountains during the late 1950's and 1960's. All ages discussed here are approximately recalculated to modern IUGS decay constants after Steiger and Jager (1977) and Dalrymple (1979). The Glen Mountains Layered Complex has been dated by the K/Ar method on whole-rock samples and plagioclase separates (Burke and others, 1969). These measurements yielded average calculated ages of 730 ± 15 m.y. from a troctolite and 509 ± 10 m.y. from a gabbro. The age of the Mount Sheridan Gabbro has been determined by K/Ar dating of whole-rock and biotite samples (Burke and others, 1969) and by the Rb/Sr method on biotite (Tilton and others, 1962). The K/Ar measurements by Burke and others (1969) suggest an age for the Mount Sheridan Gabbro in the range of 498 to 520 ± 10 m.y., and the Rb/Sr data of Tilton and others (1962) give an age of approximately 530 ± 30 m.y. However, as Powell and others (1980) pointed out, all the samples dated were collected very close to intrusive contacts with the younger granite bodies and thus were susceptible to thermal overprinting.

The significance of the published radiometric ages is further complicated by the recent paleomagnetic data of Roggenthen and others (1981) on rocks from the Glen Mountains Layered Complex and the Mount Sheridan Gabbro. These samples indicate paleopole positions that correspond to an age of either 1,300 m.y. or 800 m.y. An older age for the Glen Mountains Layered Complex is favored by Powell and Phelps (1977) on the basis of petrologic arguments relative to the amount of erosion of the upper part of the layered complex.

GEOCHRONOLOGY

Magnetic fractions of zircon from the Mount Sheridan Gabbro and its associated pegmatite were dated by the U/Pb method, using standard techniques for isotopic analysis. Techniques for dissolution and chemical separation of U and Pb were modified from those reported by Krogh (1973). Isotopic ratios were measured on a 9–inch-radius (NIMA) mass spectrometer with on-line digital processing. Lead and uranium separates were analyzed on a single rhenium filament, using H_3PO_4 and silica gel. Arrays of an-

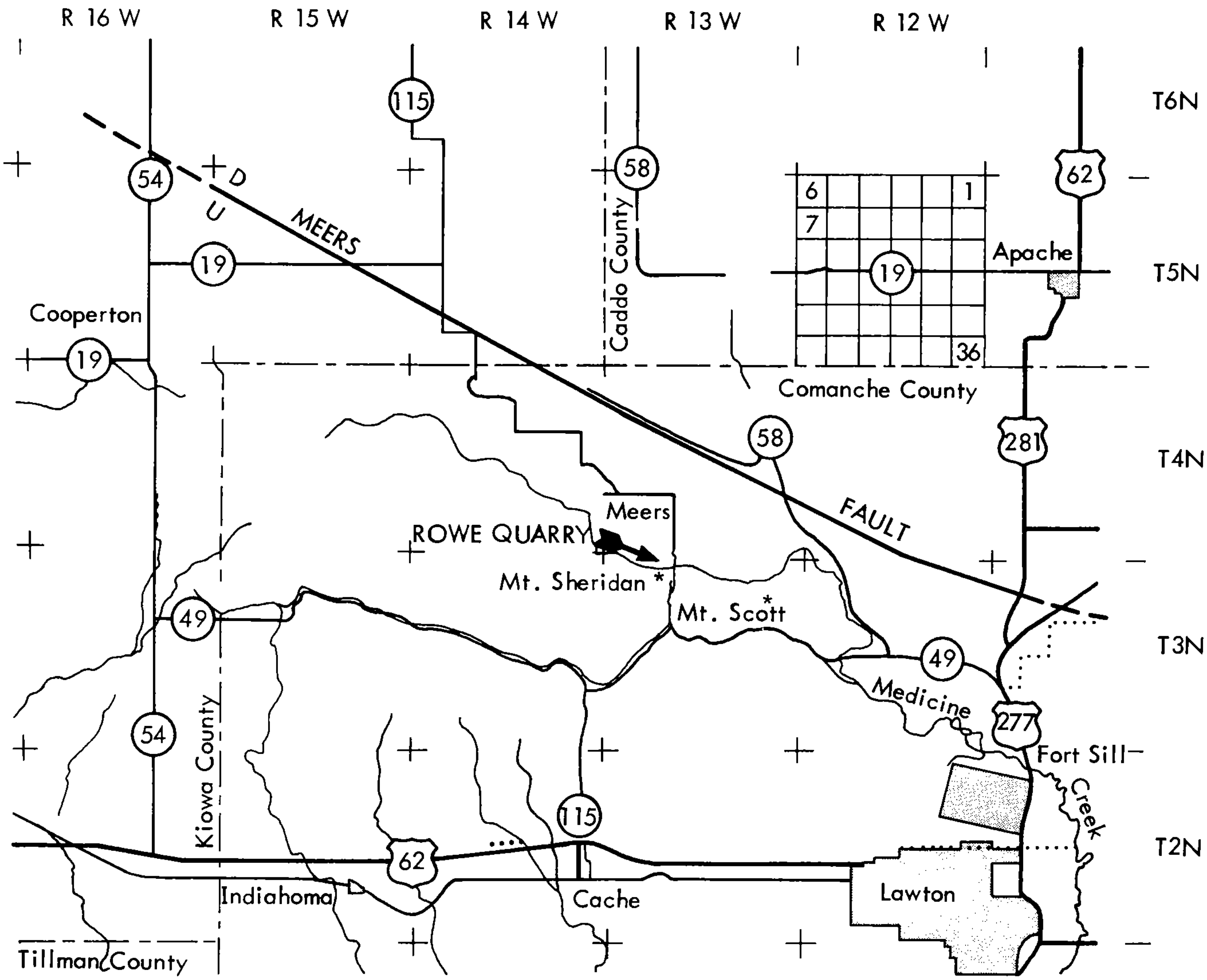

Figure 35. Location map of principal localities in the Wichita Mountains showing Rowe Quarry, where samples were collected. (After Powell and others, 1980.)

alytical data were interpreted by fitting a line to the data points, using the least-squares-cubic method of York (1966), and solving for the intersection with concordia (Wetherill, 1956).

Nine magnetic fractions of zircon from the Mount Sheridan Gabbro and its associated pegmatitic pods were analyzed. The zircons from both the gabbro and pegmatite are similar in morphology, being mostly clear and euhedral and relatively free of inclusions (fig. 37). Zircon was much more abundant (approximately 200 times) in the pegmatite than in the gabbro.

The U/Pb data from the individual fractions (table 16) define separate chords on a U/Pb concordia diagram (fig. 38). The chord defined by data from the pegmatite intersects concordia at 552 ± 7 m.y. This age is believed to represent the time of crystallization of the Mount Sheridan Gabbro pegmatite. The chord

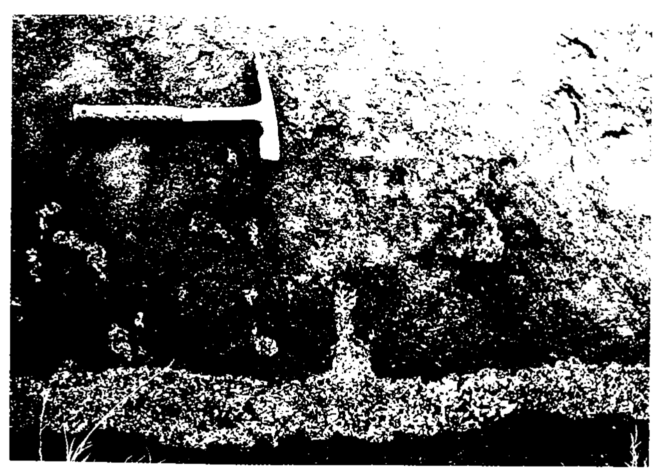

Figure 36. Pegmatitic pods in Mount Sheridan Gabbro, Rowe Quarry. (Photograph courtesy of M. C. Gilbert.)

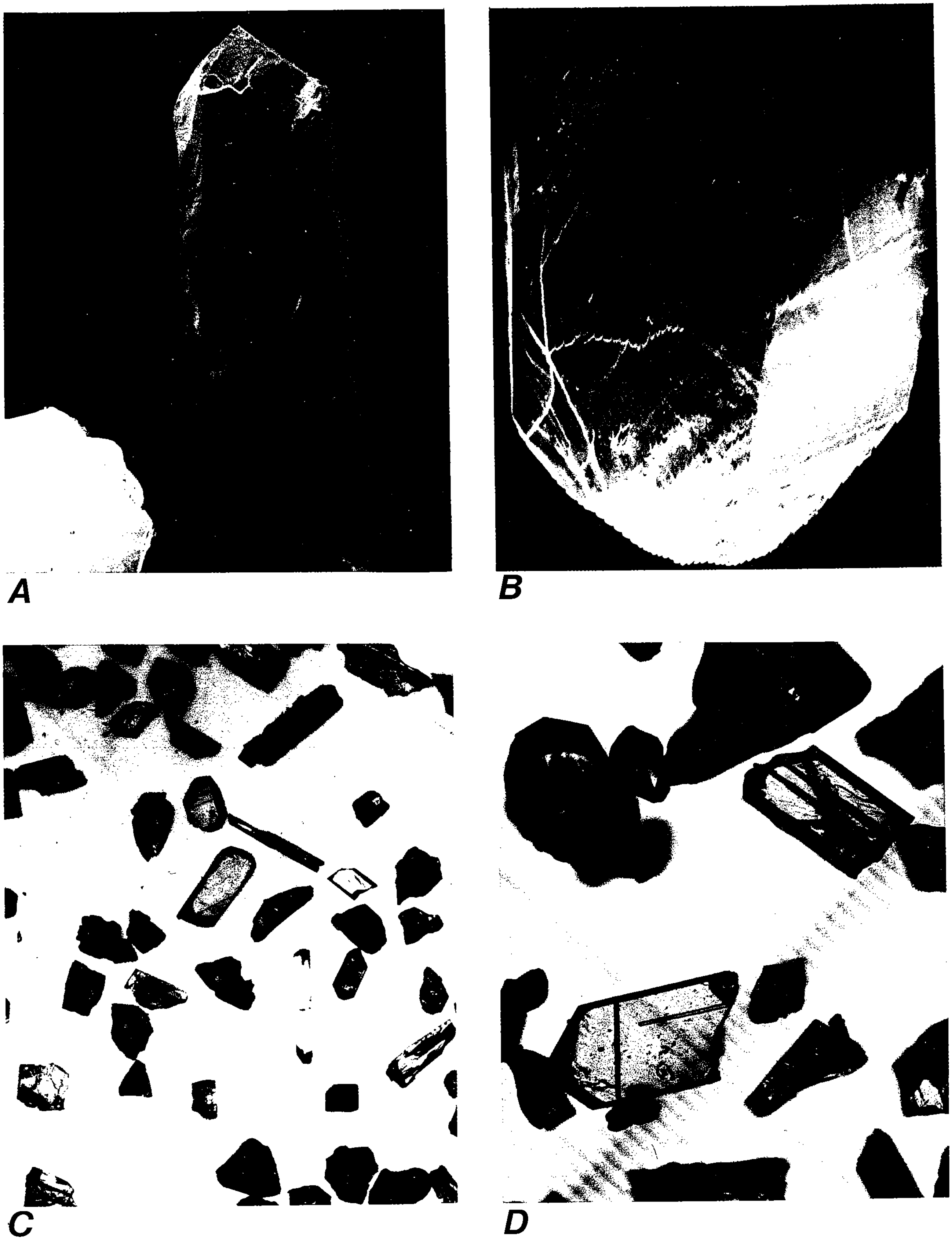

Figure 37. Zircon crystals. Scanning electron microscope (SEM) photographs of zircons separated from pegmatite (*A*, 320 ×) and gabbro (*B*, 640 ×). Photomicrographs of zircons from gabbro (*C*, 30 ×) and pegmatite (*D*, 60 ×).

defined by data from the gabbro is distinct from that of the pegmatite, and has concordia intercepts of 507 ± 1 m.y. and 2,000 ± 100 m.y. The lower intercept is well defined because all points plot close to the concordia curve, whereas the upper intercept is more uncertain.

The chord defined by the gabbro data is interpreted by us to be the result of a mixture of two components of zircon: an older component, and a younger component that is presumably the same age as the pegmatite zircon. The lower intercept of 507 m.y., clearly younger than the age of the pegmatite zircon, must be largely due to discordance of the young component.

Microscopic examination of the gabbro zircon in oils of high refractive index has not revealed any obvious cores in the zircons that might be interpreted as the older component. However, the clustering of the gabbro data near the lower intercept indicates that the younger component greatly dominates the mixture, and the older component may be present as small, unidentifiable inclusions within the crystals.

The upper intercept of 2,000 ± 100 m.y. for the gabbro chord must be interpreted as a maximum average age of the contaminating zircon. This age is interesting because it is much older than any reported on igneous rocks from the Wichita Mountains or in the adjacent subsurface of the Midcontinent region (Bickford and Lewis, 1979; Bickford and others, 1981b). The most likely source of the contaminant zircon is believed to be the Meers Quartzite, because large, partly digested xenoliths of it are found in the Mount Sheridan Gabbro near Rowe Quarry (Powell and Fischer, 1976). Ham and others (1964) reported as much as 1 percent detrital zircon in the Meers Quartzite, and thus it represents an

TABLE 16.—ISOTOPIC DATA FOR ZIRCON FROM MOUNT SHERIDAN GABBRO (WM–1) AND ASSOCIATED PEGMATITE (WM–2)

Sample	zircon fraction⊕	Concentrations+ (ppm)		Measured Ratios*			Calculated Ratios##			Age (m.y.)#
		U	Pb	$^{206}Pb/^{208}Pb$	$^{206}Pb/^{207}Pb$	$^{206}Pb/^{204}Pb$	$^{206}Pb^{**}/^{238}U$	$^{207}Pb^{**}/^{235}U$	$^{207}Pb^{**}/^{206}Pb^{**}$	$^{207}Pb^{**}/^{206}Pb^{**}$
WM-1	A	587.1	58.42	3.66	15.77	7,751	0.08625	0.73166	0.06153	658
	B	678.5	67.41	3.35	16.22	12,048	0.08469	0.70596	0.06046	620
	C	1137.7	115.41	2.92	16.62	15,625	0.08385	0.68494	0.05925	576
	E	1872.8	194.27	2.60	16.78	17,543	0.08331	0.67519	0.05878	559
	F	2045.3	215.81	2.51	15.59	2,632	0.08316	0.67221	0.05863	553
WM-2	A	116.7	10.61	4.80	15.38	2,141	0.08216	0.65975	0.05824	539
	B	186.6	16.31	5.33	15.46	2,242	0.08042	0.64531	0.05820	537
	C	579.7	54.49	3.72	11.04	447	0.07694	0.61561	0.05803	531
	D	1404.0	125.57	4.03	15.76	2,674	0.07866	0.62920	0.05801	530

⊕ Zircons were separated for analysis according to differing magnetic suseptibility: A = least magnetic, F = most magnetic.

\+ Zircons were analysed by methods similar to those described by Krogh (1973). Total analytical Pb blank during this study was 1.5 ng. Concentrations for U and Pb ± 1%.

* Isotopic ratios corrected for analytical blank. Precision for measured ratios is ± 0.1% or better except for $^{204}Pb/^{206}Pb$ ratios for which absolute precision is ± 0.00001.

** Indicates radiogenic Pb.

\# Constants used for age calculations: $^{238}U = 1.5513 \times 10^{-10}$/yr; $^{235}U = 9.8485 \times 10^{-10}$/yr. (Steiger and Jäger, 1977).

\## Common Pb corrections were made according to Stacey and Kramer (1975).

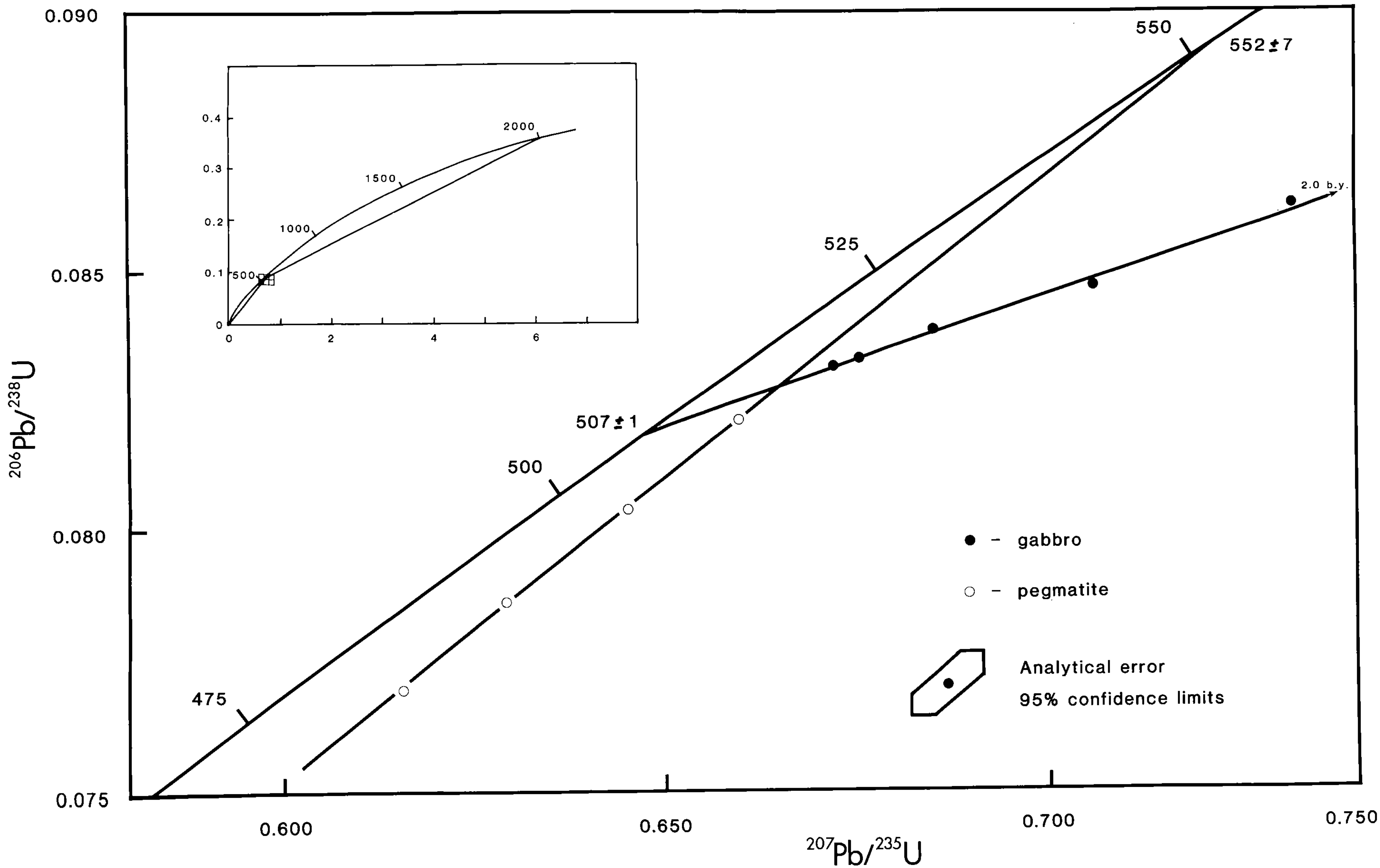

Figure 38. Concordia plot of zircons from Mount Sheridan Gabbro and its associated pegmatitic pods. Location of points relative to concordia curve is shown in inset. See table 16 for analytical data.

obvious source. The zircon determinations reported here strengthen the suspicion of Powell and Fischer (1976) that the Meers Quartzite contaminated the Mount Sheridan Gabbro, but do not support the possibility that the pods represent recrystallization of the quartzite. Analysis of zircon from the Meers Quartzite will be undertaken in the future to test this hypothesis. If the older contaminating zircons are indeed from the Meers Quartzite, and yield middle Proterozoic ages, it would indicate a much older source than is known in the subsurface to the north. An alternative hypothesis for the origin of the contaminant zircon is that it was incorporated during production and rise of the gabbroic magma, and thus was derived from some unknown lower crustal source.

If the pegmatitic pods are late-stage fractionation products of the Mount Sheridan Gabbro, the older contaminant fraction must have been mostly incorporated in the initial stage of crystallization of the gabbro. Bickford and others (1981a) and Aleinikoff and others (1981) have reported similar relationships in which young magmas have been contaminated with older zircons and the coarsest (first to crystallize) fractions have the highest proportion of older core material, whereas the fine fractions have the smallest amount.

CONCLUSIONS

U/Pb isotopic studies of zircon from the Mount Sheridan Gabbro and its associated pegmatitic pods indicate that the gabbro and pegmatite crystallized approximately 552 ± 7 m.y. ago. The gabbro zircons contain an older xenocrystic component, which indicates that the parental magma was contaminated with crustal material during emplacement. We plan to test zircons from the Meers Quartzite as a possible source of the contaminating zircon. A crystallization age of 552 ± 7 m.y. for the Mount Sheridan Gabbro suggests that available Rb/Sr and K/Ar calculated ages in the Wichita province are approximately correct, and that they were not reset by the intrusion of the Wichita granites.

ACKNOWLEDGMENTS

This research was supported by a special grant from the Department of Geology of the University of Kansas, and by National Science Foundation grant EAR 79–19544. M. E. Bickford critically read the manuscript and suggested many improvements. Susan C. Kent helped collect the samples, and John E. Gray prepared the thin sections.

Oklahoma Geological Survey Guidebook 21, 1982

ALKALI AMPHIBOLES OF THE WICHITA MOUNTAINS

Nancy Scofield
M. Charles Gilbert

INTRODUCTION

Within and cutting the granites of the Wichita Mountains are irregular bodies, dikes, and pegmatites of alkali amphibole-bearing granitoids and aplites. These dikes and pegmatites represent the last differentiates of the granitic magmas. Thus, their mineral and chemical compositions should help in determining the path of crystallization of the granites. A report of some of our work is presented here.

Seven sample sites from these amphibole dikes and pegmatites were chosen for study. Their locations are shown on the maps in figures 2 and 39. Sample 7 is from the Lugert Granite of the western Wichita Mountains, and can be compared with the other six samples, which are all from the eastern area. Sample 5 is from the main Hale Spring pegmatite (fig. 40) (dike 1 of Johnson, 1955), and sample 2 is from a related dike, both of these cutting the Roosevelt gabbro but presumed related to the Quanah Granite (see Stop 3). The other samples are from dikes cutting the Quanah Granite, with the exception of sample 4, which cuts the Mount Scott Granite near the Quanah–Mount Scott contact.

The Quanah Granite is coarse grained and equigranular. Averaged modal proportions are 30 to 40 percent quartz and 55 to 65 percent perthite. The Lugert Granite has nearly identical modal proportions, but it is texturally much more variable and commonly is reported to contain a few percent plagioclase. All the Wichita granites have very low contents (1.5–5 percent) of ferromagnesian minerals, which are green hornblende, mainly brown biotite, and magnetite. Only the Quanah commonly carries sodic amphiboles in some of its facies (Myers and others, 1981).

The amphibole-bearing granitoid dikes and pegmatites consist mainly of albite, K-spar, quartz, sodic amphiboles and pyroxenes, and, in places, magnetite. The sodic pyroxene present in all the samples from the eastern Wichitas is aegirine, but in the western sample it is aegirine–augite.

SODIC AMPHIBOLES

This study concentrated on the composition of the amphiboles. They range in size and habit from fine (< 0.1 mm) needles of riebeckite to coarse (several cm) euhedra of black arfvedsonite. The dikes and pegmatites commonly show banding and alignment of these sodic amphiboles and pyroxenes.

Polished thin sections were studied petrographically and then by electron microprobe. Several photomicrographs (figs. 41–45) show typical relationships.

Electron-microprobe analyses were performed at the Institute of Mineral Research, Michigan Technological University, and at the Department of Geological Sciences, Virginia Polytechnic Institute and State University. A MAC–400 electron microprobe with Kevex 5100 energy dispersive system, with dedicated PDP 11/03 minicomputer, was used at Michigan Tech. Wavelength spectrometers using a TAP crystal were employed for Mg, Al, and F, with a thin window detector for F. The Virginia facility is an ARL SEMQ with three variable- and six fixed-wavelength spectrometers using data reduction methods of Bence and Albee.

Compositions are tabulated in tables 17 and 18, and the range of compositions from the eastern samples can be compared with those from the western sample (*M* = analysis from Michigan Tech; *V* = Virginia Tech). The blue needles of riebeckite were too small for analysis, and commonly were plucked out during sample polishing. All the analyzed sodic amphiboles are extremely iron-rich (32–35 weight percent as FeO). Amphibole from the west is much lower in F and Na_2O and somewhat lower in SiO_2 than eastern samples. K_2O is generally lower in the west, but overlaps the lower part of the range of eastern amphiboles. TiO_2 and MgO have wider ranges in the west, with TiO_2 ranging lower. Al_2O_3 can be higher in the west, and CaO and MnO are much higher in the west.

A wet-chemical analysis by S. S. Goldich, given in Johnson (1955), is provided for reference to a calculated formula. Formulae are not given for the microprobe determinations, owing to the lack of ferric–ferrous determinations. The real totals of these latter determinations will be higher on determination of H_2O and Fe_2O_3. Nevertheless, the trends are clear. These are very sodic, very iron-rich, and with as much as half the OH-position replaced by F.

Compositions of individual crystals were reasonably homogeneous in the east. All of these samples are members of the riebeckite–arfvedsonite series. In the west, the amphiboles appear to show zoning from arfvedsonitic cores to ferrorichteritic rims.

DISCUSSION

Ernst (1962) determined stable phase relations for bulk compositions between end-members riebeckite, $Na_2Fe^{+2}_3\ Fe^{+3}_2\ Si_8O_{22}(OH)_2$, and riebeckite–arfvedsonite solid solution, $Na_{2.4}$

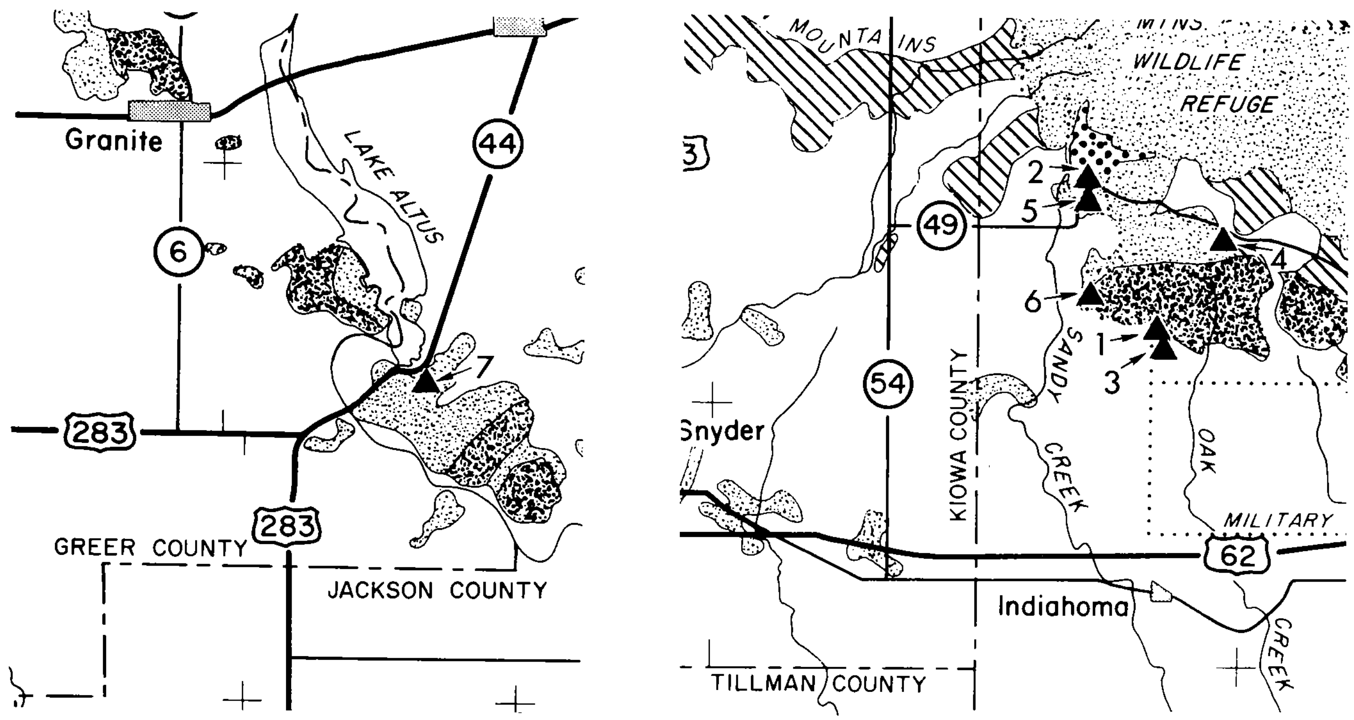

Western Wichitas

Eastern Wichitas

Figure 39. Index map for sample areas from figure 2.

$Fe^{+2}_{4.9}Fe^{+3}_{0.7}Si_{7.7}Fe^{+3}_{0.3}O_{22}(OH)_2$, under hydrothermal conditions, depending on temperature, oxygen fugacity, and fluid pressure. Under relatively oxidizing conditions, with oxygen fugacity defined by the hematite–magnetite buffer, fine-grained, blue riebeckite is stable up to about 500°C, depending on fluid pressure. When the oxygen fugacity is defined by the magnetite–fayalite–quartz buffer, high-temperature stability is elevated, and the experimental amphibole crystals were coarser grained and greenish. This reflects solid solution toward the more ferrous arfvedsonite, with formation of about 5 percent quartz. With still greater reducing conditions, as defined by the wustite–iron buffer, the maximum thermal stability extends to nearly 700°C at 1,000 bars fluid pressure. The amphibole is green, has the approximate composition of $Na_{2.4}Fe^{+2}_{4.9}Fe^{+3}_{0.7}Si_{7.7}Fe^{+3}_{0.3}O_{22}(OH)_2$, and coexists with 10 to 15 percent quartz. However, the high-temperature thermal stability is presumably elevated considerably when fluorine replaces hydroxyl (Ernst, 1962).

Thus, in the sample from the western Wichitas, the lower fluorine content of the arfvedsonitic amphiboles, and the presence of fine, blue riebeckite (fig. 44) surrounding titanomagnetite, suggest reaction of the titanomagnetite and quartz with the residual fluid as the temperature dropped under relatively oxidizing conditions. Samples from the eastern locations 1, 2, 3, and 5, with their higher fluorine contents and more arfvedsonitic compositions, suggest relatively greater reducing conditions and perhaps

Figure 40. Photograph of Hale Spring outcrop, dike 1—sample WM5 (Stop 3).

Figure 41. Sample 2. Dark lower part is small part of a large sodic amphibole that almost covers thin section (2 × 3 cm); at three places on border the relationship with aegirine (middle part of field) can be seen. Amphibole and pyroxene appear to be crystallographically continuous. Upper part of field is mostly feldspar, nearly pure albite and microcline, with some quartz. Width of field ~1 mm. See table 18 for albite and microcline analyses.

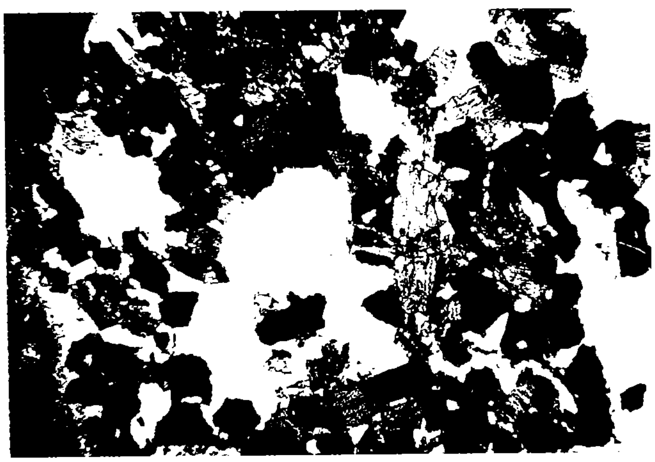

Figure 42. Sample 5. Elongate aegirine and equant amphibole (black) scattered through matrix, which is mostly feldspar. Width of field ~4 mm.

Figure 43. Sample 4. In samples 4 and 6, all sodic amphibole has been oxidized to magnetite in matrix of quartz or feldspar. Some magnetite is surrounded by needles of riebeckite. Width of field ~ 1 mm.

Figure 44. Sample 7. Titanomagnetite (black) with needles of blue riebeckite crystals along its margins in quartz (white). Gray phase is feldspar. Width of field 0.4 mm.

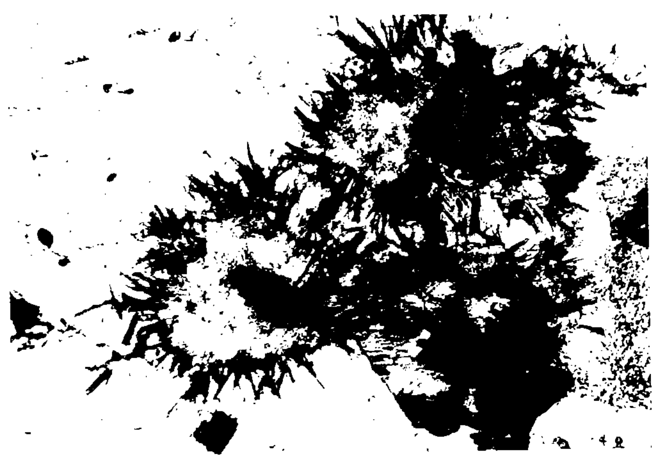

Figure 45. Sample 7. Large aegirine–augite (right side) showing varying degrees of resorption and reaction rim of magnetite. Width of field ~1 mm.

higher temperatures. However, amphiboles in samples from eastern locations 4 and 6 have been oxidized to magnetite with some acicular blue riebeckite crystals. Figure 43 shows an amphibole oxidized to magnetite (plus some riebeckite, which cannot be seen in the photomicrograph), and suggests an increase in oxygen fugacity.

The minerals, their composition, and the assemblage can be used to place some constraint on conditions of formation. The presence of magnetite + quartz places the fO_2 range below the hematite–magnetite phase boundary and above magnetite + quartz = fayalite. The pyroxene in the assemblage is almost pure $NaFeSi_2O_6$, Ti being the principal contaminant. The alkali feldspars have essentially no Ca. There are really no extraneous major phases present to complicate the relations. Thus, Ernst's data (1962; see his figs. 5 and 11b especially) can be applied directly. He showed the variation of Si/(Na + Fe + Si) with fO_2 and temperature. This ratio for

TABLE 17.—SODIC AMPHIBOLE ANALYSES—WICHITA GRANITE GROUP

	Hale Spring Locality					
	Dike #1 Johnson, 1955	WM5	WM2	Quanah WM3	Lugert WW7	
		V	V	M	M	V
SiO_2	50.58	50.8	49.8	49.4	46.0	48.5
TiO_2	.82	.8	1.2	.7	.7	.2
Al_2O_3	1.40	.5	.7	.6	2.5	.2
Fe_2O_3	13.54					
FeO	19.74	32.4	34.6	34.4	32.0	27.9
MnO	.52	.9	.9	1.1	4.5	2.8
MgO	.44	.5	.2	nd	1.2	.5
CaO	.14	.2	.5	nd	5.6	14.9
Na_2O	8.50	8.5	7.4	11.81(?)	4.8	3.8
K_2O	1.49	1.7	1.6	1.48	0.9	.05
Li_2O	.44			nd	nd	
H_2O+	.48			nd	nd	
H_2O-	.04			nd	nd	
F	2.16	1.9	1.8	1.3	0.5	.07
Cl	.02	.07	.02	nd	nd	.01
	100.31	98.3	98.7	100.8	98.7	98.9
less O for F & Cl	.91	.8	.8	.6	.2	.03
	99.40	97.5	97.9	100.2	98.5	98.9

Formula: Analyzed sample from Johnson

$$(K_{.3}Na_{2.6}Ca_{.03})(Fe^{2+}_{2.6}Mg_{.1}Mn_{.1}Li_{.3})(Fe^{3+}_{1.6}Al_{.3}Ti_{.1})(Si_{7.9})O_{22}(OH)_{.5}F_{1.1}Cl_{.01}$$

Theoretical formulae: riebeckite-arfvedsonite

$$oNa_2Fe^{2+}_3Fe^{3+}_2Si_8O_{22}(OH,F)_2 - Na_3Fe^{2+}_4Fe^{3+}Si_8O_{22}(OH,F)_2$$

Hale Spring amphiboles is 0.537, which is on the high-fO_2 side of the stability range. Further, if the total pressure during intrusion of the source granite were assumed to have been low (see Gilbert, this guidebook, for a summary of the arguments), at no more than 500 bars (1.5 km overburden), then the maximum temperature possible for the pegmatite would be about 500°C.

Because the MgO content is so low, the discussion of Wones (1981, fig. 5) is pertinent as well. The reactions riebeckite = acmite + quartz + magnetite and sanidine + magnetite = annite intersect, forming a lower temperature, relatively oxidizing phase space within which the pegmatite must lie. This is completely consistent with the compositions of the coexisting feldspars, which are almost pure albite

TABLE 18.—MINERAL ANALYSES, SODIC AMPHIBOLE DIKES

	WM2			WM5
	Acmite (aegirine)	Albite	Microcline	Microcline
	V	M	M	V
SiO_2	52.4	68.2	64.6	65.2
TiO_2	2.0			
Al_2O_3	0.4	18.4	17.4	17.2
FeO	29.5	1.1	1.0	1.0
(Fe_2O_3)	(32.4)			
MnO	0.2			
MgO	0.0			
Na_2O	13.7	11.7	0.4	0.5
K_2O	-	0.3	15.1	16.7
CaO	0.3			0.03
BaO	0.1			
Total	98.7	99.7	98.5	100.6
(Total)	(101.6)			

and pure K-spar. K-spar has less than 5 mole percent Ab component, and so it must be microcline in structural state. Perthite is limited, implying that original crystallization did not occur high on the solvus. These relations are consistent with low temperatures of formation and equilibration, down to 350°C or lower.

For these reasons, the Hale Spring pegmatites are thought to be derived from hydrothermal fluids, not granitic magma. To be sure, these fluids are late-stage emanations from a granite, presumably the Quanah, but they did crystallize below the solidus. Relevant textural relations include the following: (1) strong mineralogic layering, wherein sodic amphibole layers alternate with layers dominated by the reaction products; (2) sodic amphiboles in some layers are strongly poikilitic; (3) the long axes of sodic amphiboles in some layers are perpendicular to the layering, appearing to have grown out into fluid space; and (4) amphiboles and pyroxenes in other bands lie in the plane of layering, with axes aligned in some cases and randomly oriented in others. These features are compatible with formation from water-rich fluids, pulsating in flow rate and alternating between rapidly moving and stationary as discharge and crystallization go on.

ACKNOWLEDGMENT

Todd Solberg, in charge of the microprobe facility at Virginia Polytechnic Institute and State University willingly assisted in generating part of the data reported here.

Oklahoma Geological Survey Guidebook 21, 1982

GEOLOGY OF BLUE CREEK CANYON WICHITA MOUNTAINS AREA

R. Nowell Donovan

INTRODUCTION

Lower Paleozoic carbonates crop out extensively in two areas of southern Oklahoma: the Arbuckle–Criner Hills region and the Slick or Limestone Hills north of the Wichita Mountains. The latter area lies in the complex fault zone that separates the Amarillo–Wichita Uplift from the Anadarko Basin. The Arbuckle and Criner areas have received much attention from geologists, but the Slick Hills are less well known. Recent studies have included detailed mapping of parts of the area (Barthelman, 1968; Brookby, 1969) and delineation of major structural units and their bounding faults (Harlton, 1951, 1963, 1972). Harlton's work established two important tectonic elements in the Slick Hills, the Lawtonka Graben and the Blue Creek Horst. The graben is bounded on the south by the Meers Fault and on the north by the Blue Creek Canyon Fault. The latter forms the southern boundary of the horst, which to the north is bounded by the Mountain View Fault (fig. 46). Lower Paleozoic rocks are comprehensively folded, particularly in the graben.

The present study focuses on the exposed part of the Blue Creek Canyon Fault, in Blue Creek Canyon. Recently exhumed from beneath a cover of Permian fanglomerates, this area is beautifully exposed ground. The fault juxtaposes the Carlton Rhyolite Group and overlying Cambrian sedimentary rocks against Ordovician formations of the Arbuckle Group (in the graben). An interpretation of fault movement is offered here that differs from those of previous workers.

A map and outcrop sections (figs. 154 and 155) of the area are given in the account of Stop 10.

GEOLOGIC SUCCESSION

Carlton Rhyolite Group

The Carlton Rhyolite Group, well exposed in this area, comprises lava flows and tuffaceous sandstones. In addition, a pebbly conglomerate (presumably of fluvial origin) occurs between two of the flows. Close to the Blue Creek Canyon Fault, the volcanic rocks clearly have been involved in folding associated with the fault movement.

Timbered Hills Group

The unconformity between the Carlton Rhyolite Group and the overlying Timbered Hills Group, which records a widespread Franconian transgression (Stitt, 1978), is of interest because it shows evidence of considerable relief. In the southern part of the area, the Carlton Rhyolite is overlain by the upper formation of the Timbered Hills Group, the Honey Creek Formation. In the northern part of the area, the rhyolite is overlain by the Reagan Sandstone. The total overlap (onlap) from north to south appears to involve about 200 ft of strata (fig. 47). In detail, the unconformity shows considerable minor relief. In the north, where the Carlton consists of tuffaceous sandstones, the unconformity is planar. In the southern part of the area, where the Carlton consists of lava flows, the unconformity is irregular in detail and shows features characteristic of rocky shorelines (fig. 159). This unconformity also shows great relief where it is exposed in the Arbuckle Mountains (Ham, 1969).

Three distinct facies are developed in the Reagan Sandstone. The first facies is a basal conglomerate consisting of small (average size, 1 inch diameter) pebbles of rhyolite, and is overlain by the second facies, which consists of dark-green, fine-grained,

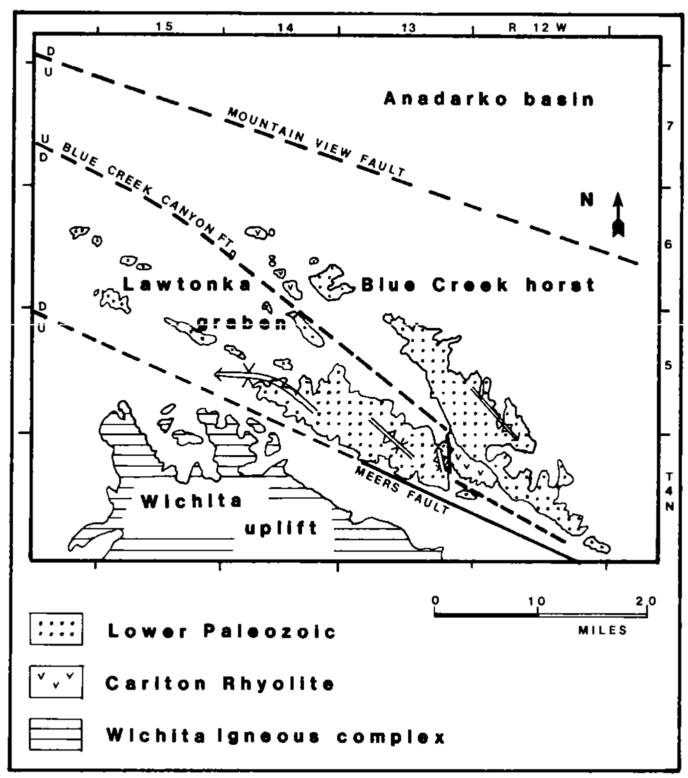

Figure 46. Simplified map of Slick Hills area, showing principal tectonic elements. Terms "graben" and "horst" are followed even though bounding faults of these units are no longer considered normal. Principal fold trends also shown.

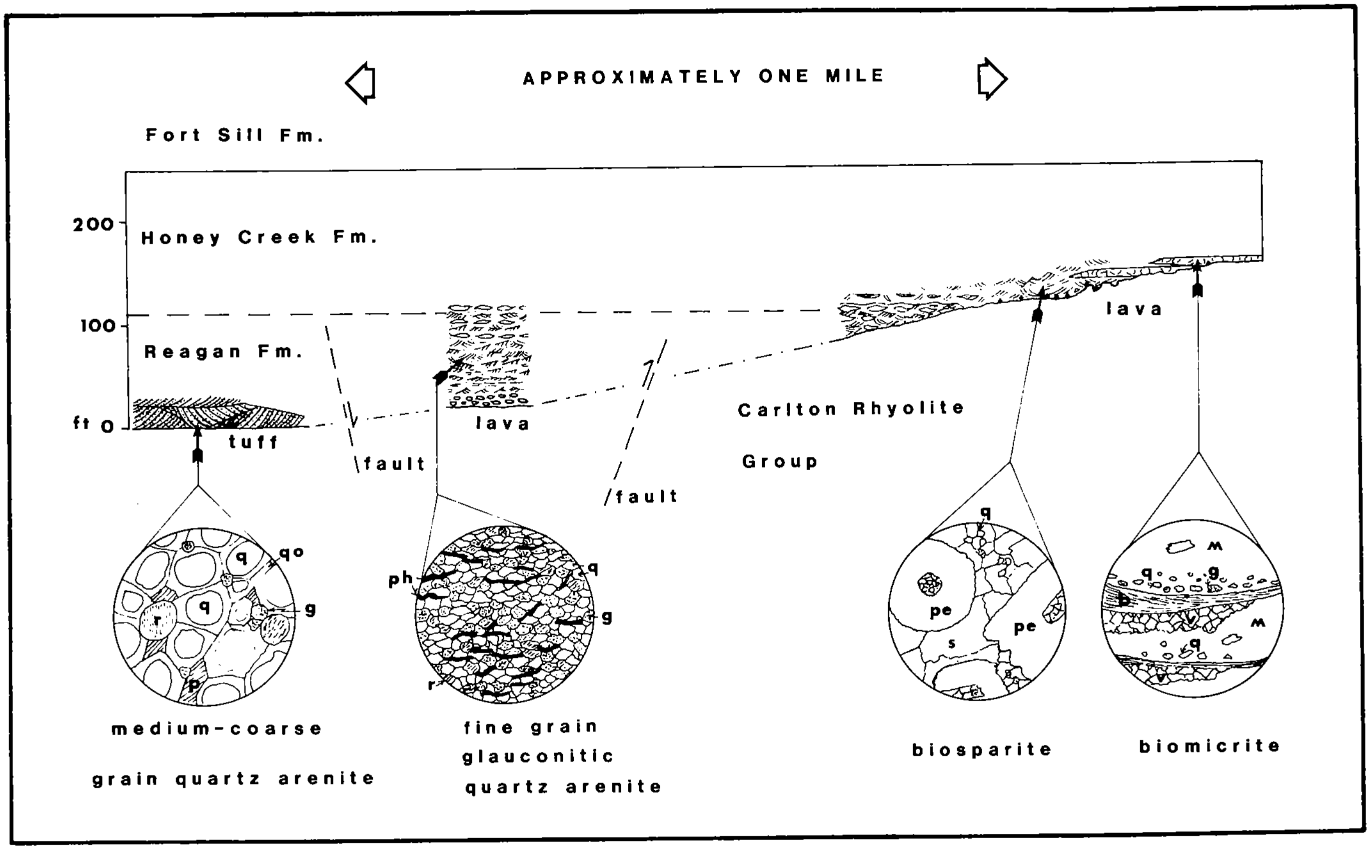

Figure 47. Schematic diagram showing overlap (onlap) relationships and facies variations in Blue Creek Canyon area. North is to left. Sequence has been broken by faults, which may have affected present relationships. Key to thin-section sketches: *q*, quartz; *qo*, syntaxial quartz overgrowth; *g*, glauconite; *r*, rhyolite grain; *p*, porosity; *ph*, phosphatic fragment; *pe*, pelmatozoan fragment; *s*, sparite; *m*, micrite; *b*, brachiopod valve; *v*, shelter porosity now filled with sparite.

moderately well-sorted sandstones characterized by small- and medium-scale cross-bedding. Mineralogically, these sandstones consist of more or less equal amounts of granular glauconite and quartz together with subordinate feldspar and rhyolite fragments, the whole being intensively cemented by quartz (fig. 48). This facies is interpreted as a shallow-marine shoreline deposit. The third facies of the Reagan is restricted to an area where the underlying Carlton Rhyolite consists of tuffaceous sands and where the basal unconformity is planar. This facies consists of medium- to coarse-grained, well-rounded and very well-sorted sandstones characterized by medium- to large-scale cross-bedding (to 3 ft). Mineralogically, these sandstones consist largely of quartz grains with minor amounts of rhyolite and glauconite. They are tentatively interpreted as either eolian coastal dunes or marine sand ridges. This facies also is intensively cemented by secondary silica, which forms spectacular syntaxial overgrowths (fig. 49).

The upward passage from the Reagan Sandstone into the Honey Creek Formation records a gradual change from quartz–glauconite shoreline sands to a carbonate, sand-dominated shoreline. The boundary between the two formations is gradational and has been obscured by diagenesis. As a result of the diagenetic loss of calcium carbonate, a wavy texture has formed in which discontinuous lenticular, carbonate-sand bodies are enveloped by quartz–glauconite sandstones (figs. 47, 50).

In the southern part of the area, where the Honey Creek rests directly on a rugged surface of Carlton Rhyolite, three distinct facies are developed. The first of these, a very thin (0–12–inch) breccia of rhyolite fragments cemented by sparite (fig. 51), passes abruptly upward into medium-scale cross-bedded, bioclastic sandstones (fig. 52) consisting mostly of pelmatozoan fragments with lesser amounts of brachiopods, trilobites, quartz, and glauconite. The cement is sparite (syntaxial on pelmatozoan fragments), later generations of which are slightly ferroan (fig. 53). Subsequent loss of calcite is indicated by many sutured grain contacts. A third, more restricted facies consists of mounds of orthid brachiopods. These mounds were apparently shell banks of some stability, because individual shells acted as baffles that trapped calcareous mud and small amounts of quartz–glauconite silt particles (fig. 54).

Arbuckle Group: Area *A* (East of Blue Creek Canyon Fault)

The three members of the Fort Sill Formation, lowermost component of the Arbuckle Group, are

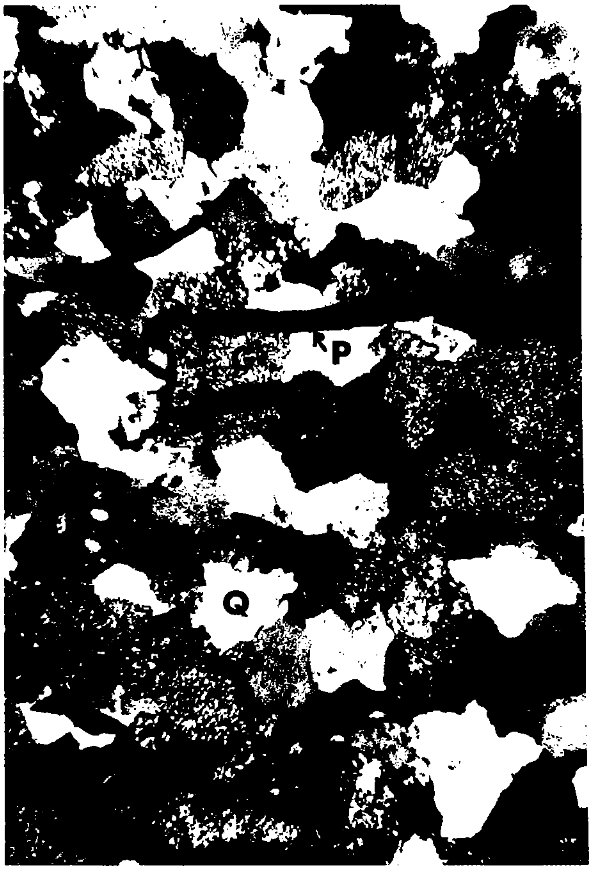

Figure 48. Reagan facies, composed of fine-grained sandstone largely cemented by quartz that has grown syntaxially on original grains. *Q*, quartz; *G*, glauconite; *P*, phosphate (collophanite). Polarized light; view 2 × 1 mm.

Figure 49. Reagan facies, composed of coarse-grained sandstone dominated by rounded quartz grains (highlighted) and showing fine, syntaxial overgrowths. *Q*, quartz grains; *G*, glauconite; *S*, syntaxial overgrowths. Ordinary light; view 2 × 1 mm.

(following Nelms, 1958; Brookby, 1969): (a) Lower Limestone unit, (b) Middle Silty Limestone unit, and (c) Upper Massive-bedded Limestone unit. The total thickness of the formation is about 600 ft.

The units of the Fort Sill Formation are dominantly micritic and generally unfossiliferous. Small-scale (ripple) cross-bedding is present in the Middle unit, and stromatolites are in the Upper unit. Although the Royer Dolomite is absent, the Middle unit is partly dolomitic. The formation seems to record a period of low-energy sedimentation in shallow water of restricted circulation.

The contact between the Upper unit of the Fort Sill Formation and the overlying Signal Mountain Formation is sharp and locally has controlled the trend of the Blue Creek Canyon Fault. The massive Upper unit is succeeded by medium-gray, thinly bedded, fossiliferous limestones, and calcareous shales and mudstones that do not form prominent relief. Thin intraformational conglomerates occur. Brookby (1969), working on sequences exposed to the northeast, was able to place the Cambrian–Ordovician boundary (on fossil evidence) about 400 ft above the base of the formation. Although at least this thickness is exposed, the boundary has not yet been located in the Blue Creek Canyon outcrop. Furthermore, measured thicknesses in this section are highly suspect, because much tectonic movement has occurred along bedding horizons in the fissile shales.

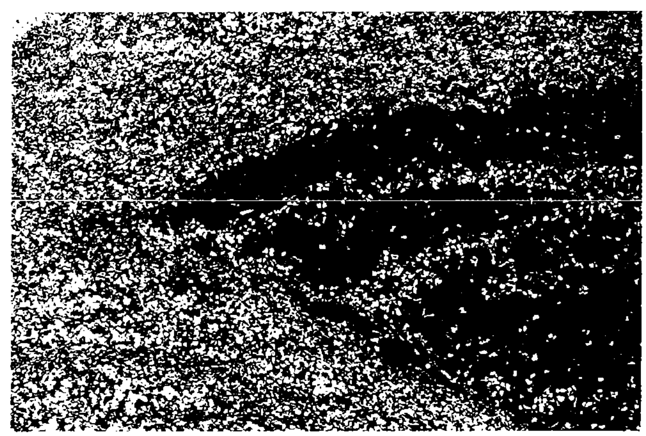

Figure 50. Timbered Hills Group. Transitional rock at Reagan–Timbered Hills contact shows lenticular sparite body resulting from diagenetic loss of calcite. Sediment originally was interlayered carbonate and quartz–glauconite sand; carbonate has been lost from most of rock, leaving a fine-grained quartz–glauconite sandstone. Carbonate is stained. View 3 × 2 cm.

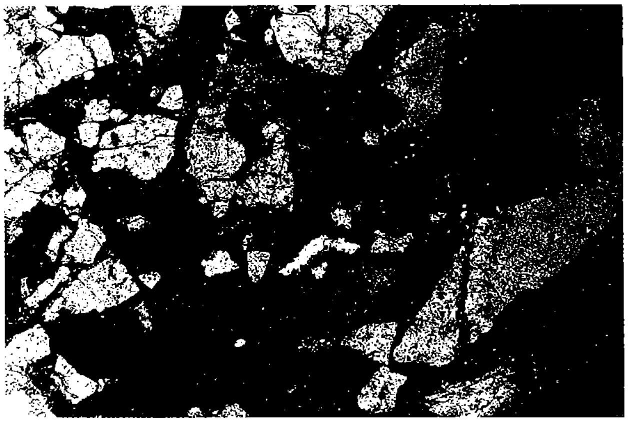

Figure 51. Honey Creek Formation; basal breccia. Rock composed of angular rhyolite fragments, shell fragments, and quartz and glauconite grains that have been cemented by sparite. Carbonate is stained. View 3 × 2 cm.

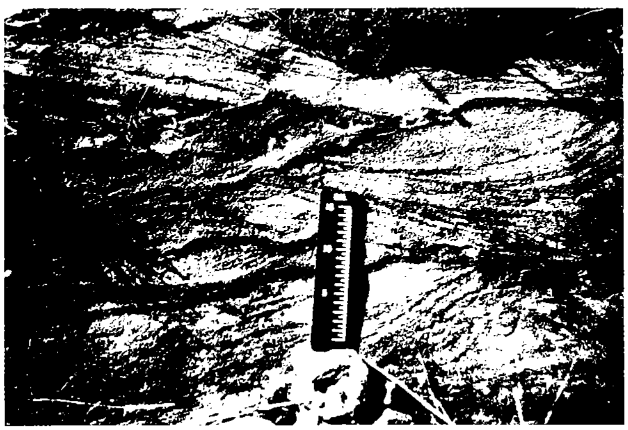

Figure 52. Honey Creek Formation; medium-scale trough cross-bedding. Rock consists of interlayered shell fragments (mostly pelmatozoans and brachiopods) and quartz–glauconite silt (interlayering visually defines cross-bedding, owing to differential weathering). Cement is sparite.

Figure 53. Honey Creek Formation; biosparite. Pelmatozoan fragments are cemented by sparite; minor quartz silt and glauconite are present. Considerable diagenetic loss of carbonate is indicated by sutured grain contacts. Carbonate is stained. View 4 × 2.5 cm.

This is particularly the case toward the northern end of the exposure, where the formation is sandwiched between two important branches of the Blue Creek Canyon Fault (fig. 160). Intraformational conglomerates apparently are more common toward the top of the formation (Brookby, 1969), hinting that a small thickness of Ordovician rocks may be present. The depositional environment is somewhat enigmatic; mudstones, and the absence of stromatolites, may indicate a little deeper water than had occurred previously.

Arbuckle Group: Area *B* (West of Blue Creek Canyon Fault)

The two Ordovician elements of the Arbuckle Group encountered are the McKenzie Hill and (overlying) Cool Creek Formations. In mapping the former, Brookby (1969) was able to recognize a lower noncherty member and an upper cherty member. The first appearance of chert is apparently a chronostratigraphic marker. Only the upper member is present in the area under consideration here.

The cherts of the upper member represent the oldest conspicuous cherts in the Arbuckle Group, and occur mostly as ovoid nodules elongated along bedding. Siliceous sponges are a probable source of the silica. The carbonates of the member are a monotonous sequence of well-bedded, medium- to light-gray mudstones, punctuated by intraformational conglomerates and calcareous skeletal sandstones. Small amounts of patchy dolomite are present. Fossils are not common, although stromatolites are present.

The Cool Creek Formation, which is more than 1,000 ft thick (Brookby, 1969), is the most varied of the Arbuckle Formations. The base of the formation is clearly marked by the sudden appearance of quartz sand, which persists throughout the lowest 150 ft of section. Quartz constitutes as much as 30 percent of some sections, and is mixed with ooliths, intraclasts of micrite pellets, and minor shell fragments. Gastropods are the most commonly seen macrofossils. Sedimentary structures include small-scale cross-bedding (fig. 157), symmetrical ripple marks, in-

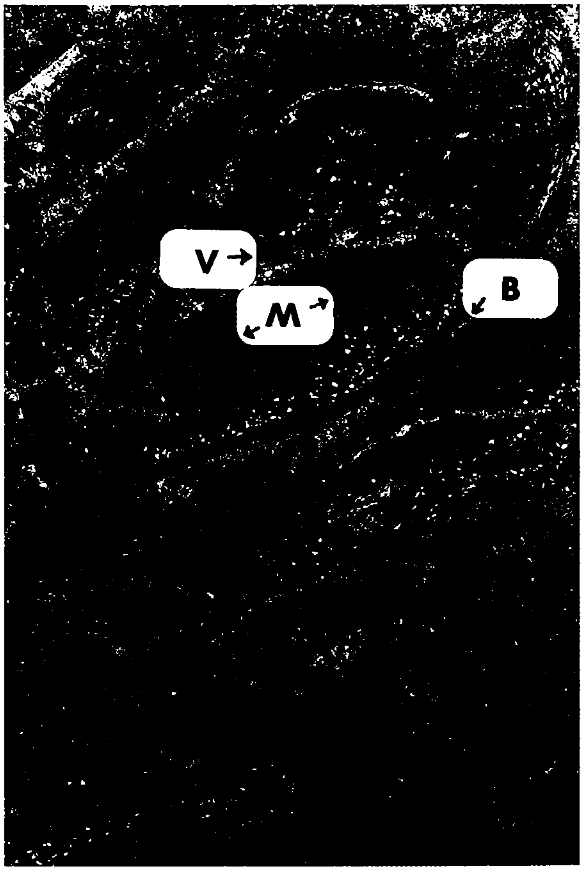

Figure 54. Honey Creek Formation; biomicrite. Rock consists of more or less complete orthid brachiopod valves (*B*) (with fibrous texture), micrite (*M*), and minor quartz, glauconite, and sparite (*V*). Brachiopod valves formed a stable shell bank that trapped carbonate mud, quartz, and glauconite. Each valve acted as a sediment baffle (note grading in fines above some valves). Following shrinkage of carbonate mud, shelter porosity developed beneath some valves; pores were later filled with drusy sparite, later generations of which are ferroan. Carbonate is stained. View 4 × 2.5 cm.

Figure 55. Cool Creek Formation; oosparite. Allochems are ooliths (nucleated on pellets and other carbonate fragments) and intraclasts of lime mud with quartz grains (*L*); rounded quartz grains (*Q*) are present. Cemented first by silica (evidenced by syntaxial overgrowths (*O*) against existing pore space) and then by sparite (*S*). Ordinary light; view 4.5 × 3 mm.

traformational conglomerates, and some graded units. A variety of forms of stromatolites is present, most of which are massive; delicate branching forms are rare. Major build-ups are not present. The depositional environment is interpreted as a somewhat restricted shallow-water carbonate setting. Whereas the general level of energy was not great, the frequent occurrence of intraformational conglomerates and the absence of delicate stromatolites suggests that the area was subjected to storms. The origin of the quartz is uncertain; most of the grains are of medium size and appear to have been moderately to well rounded before diagenesis (fig. 55). In addition, quartz grains are widely scattered through lime mudstone. Where quartz and oolitic grains are mixed, it is noteworthy that quartz grains have rarely acted as nuclei for oolite growth. These two observations suggest that the carbonate sediment and quartz had separate histories before coming together. One is tempted to regard some of the quartz as an eolian contribution, subsequently reworked to varying degrees in shallow waters.

Secondary silica is abundant in this formation, taking a variety of forms, the most common of which is chert nodules and lenses. These lenses commonly are intimately associated with siliceous sponges. Other examples of silicification were fabric-controlled and appear to be related to the presence of aragonite. Thus, oolitic calcarenites may show selective silicification of ooliths rather than carbonate cement (figs. 56, 57). Presumably, aragonite macrofossils such as gastropods may be silicified (fig. 58), and stromatolites may have silicified interiors. Some of the silicification was penecontemporaneous, because reworked chert nodules occur in some intraformational conglomerates. In a few examples, these nodules have been stacked in an imbricate fashion (fig. 59).

POST–LOWER PALEOZOIC–PRE-PERMIAN STRUCTURAL GEOLOGY

In the northern part of the Wichita Mountains (fig. 46), the principal faults are the Meers, Blue Creek Canyon, and Mountain View Faults (Harlton, 1951, 1963, 1972). These three faults have an overall trend

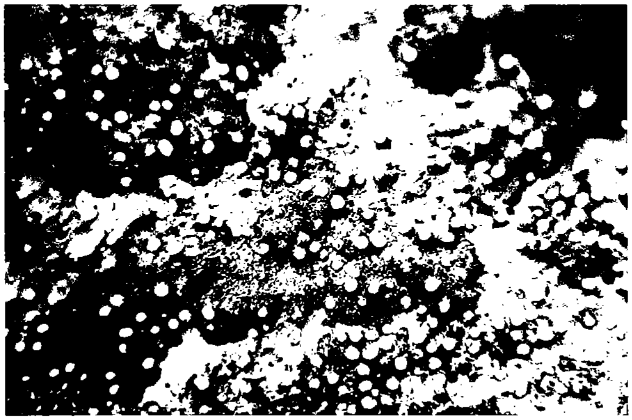

Figure 56. Cool Creek Formation; oosparite. Sample shows selective silicification of ooliths, which are approximately 0.75 mm in diameter.

Figure 59. Cool Creek Formation; chert nodules. Some nodules are stacked in an imbricate fashion, suggesting reworking.

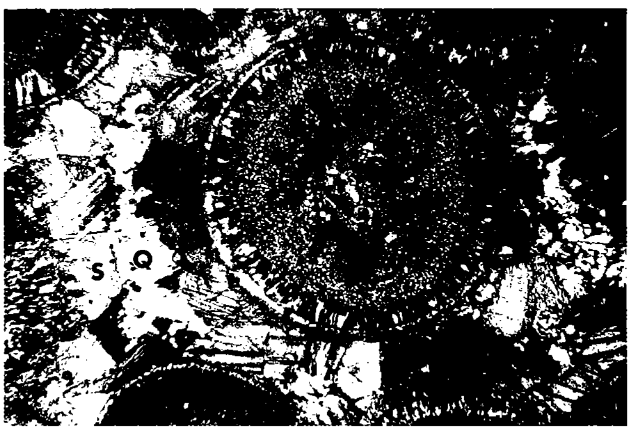

Figure 57. Cool Creek Formation; silicified oosparite. Large oolith is chalcedony (both fibrous and nonfibrous), and nucleus is calcite. Cemented first by drusy sparite (*S*), and then by void-filling microquartz (*Q*). Silicification may have been related to aragonite dissolution (indicating early diagenesis). Polarized light; view 2 × 1.5 mm.

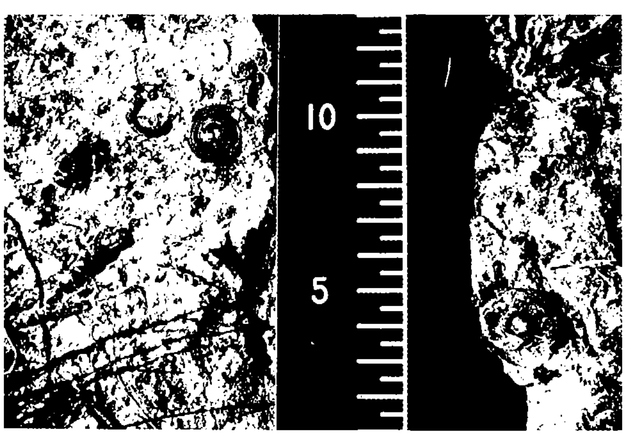

Figure 58. Cool Creek Formation; silicified gastropods. Photo courtesy of M. Munsil.

of N. 40°–60° W., in common with many minor structures. However, in the area of the canyon itself, the Blue Creek Canyon Fault is well exposed as a north-trending structure. Segments of the Mountain View and related fault show similar anomalous trends (Harlton, 1972).

In the Slick Hills, the three major faults bound two complex tectonic units (fig. 46), termed the "Blue Creek Horst" and "Lawtonka Graben" by Harlton (1951). Lower Paleozoic strata in both units, particularly the graben, are comprehensively folded.

Blue Creek Canyon Fault

The principal structural feature of the Blue Creek Canyon area is the braided complex of faults known as the Blue Creek Canyon Fault. The net effect of this complex is to juxtapose the Carlton Rhyolite Group and overlying Cambrian formations with the Ordovician members of the Arbuckle Group (figs. 154 and 155). Fault movement was clearly pre-Permian. In general, the stratigraphic throw of the fault decreases from 2,400 ft to 1,800 ft to the north, whereas the dip increases from 45° to vertical (fig. 155).

Stratigraphic relationships and the attitude of the fault planes make it clear that the Blue Creek Canyon Fault is a high-angle reverse fault, approximately north-trending, which has variable downthrow to the west. This interpretation differs from that of previous workers (notably Harlton, 1951, 1963, 1972), who have interpreted the structure as a normal fault, with downthrow to the west. It is noteworthy that the main line of faulting lies within the limestones of the Arbuckle Group, and not at the Carlton Rhyolite–Timbered Hills contact, as indicated by the geologic map in Havens (1977).

The line of Blue Creek Canyon itself is a trench with considerable relief, now entirely occupied at the surface by alluvium of recent origin. The Post Oak Conglomerate certainly lies beneath this alluvium at the northern end of the canyon and may persist throughout. Although no fault plane can now be seen, spatial considerations indicate that the valley was eroded (in Permian time) along a branch of the Blue Creek Canyon Fault (fig. 154).

Fold Patterns

West of the Blue Creek Canyon Fault, within the Lawtonka Graben, Ordovician members of the Arbuckle Group are comprehensively folded (Barthelman, 1968; Babaei, 1980). Fold trends throughout most of the graben are N. 50° W. Anomalous trends occur adjacent to the Blue Creek Canyon Fault (see below) and in the southwestern part of the graben, where the Saddle Mountain Syncline bends from N. 40° W. to N. 70° E. (Barthelman, 1968). Folding is present in the Blue Creek Horst but is less intense than in the graben (Harlton, 1951, 1963; Brookby, 1969); in general, fold trends are similar to the dominant trend in the graben.

Close to Blue Creek Canyon, two orders of fold size are present: major first-order folds have amplitudes of 600 to 3,000 ft; minor second-order folds have amplitudes of 5 to 30 ft. First-order folds trend N. 20° W. adjacent to the Blue Creek Canyon Fault, but tend to become more westerly (N. 50° W.) in the western part of the area. All folds plunge to the northwest at angles of 18° to 32° (fig. 154).

In the vicinity of the Blue Creek Canyon Fault, first-order folds are asymmetrical, with the steeper (and more disturbed) limb to the east (fig. 60). Immediately adjacent to the fault, some beds on the downthrown side are overturned and generally dip more than 60°.

Fold types include parallel folds and similar folds, with the latter type usually associated with the tighter, closed folds. The larger folds generally tend to parallel one another. Measurements of bed-thickness variation in similar folds (fig. 61) indicate thickness changes of 2:1 to 4:1 (Babaei, 1980). Some folds show disharmony as a consequence of parallel form. An *en-echelon* fold pattern is present in the first-order folds. Because of the consistent plunge of folds in the area, this *en-echelon* pattern can be seen clearly in both lateral and vertical dimensions (figs. 62, 63). Structural terraces are developed in the slack areas between such *en-echelon* folds.

Minor second-order folds (figs. 61, 64) are more variable in orientation than their major folds. They are developed in two principal positions relative to major first-order-fold geometry: in the hinge zones of first-order folds, and in the slack areas between *en-echelon* folds.

In areas close to the Blue Creek Canyon Fault, where folds are closed with steep limbs, some minor-fold axes show cleavage. This cleavage involves recrystallization of calcite from compression in well-defined cleavage planes perpendicular to principal stress (fig. 156). In addition, quartz grains in limestones generally are cataclastically shattered by tension joints normal to compressional stress (fig. 65); calcite fragments (for example, pellets) show con-

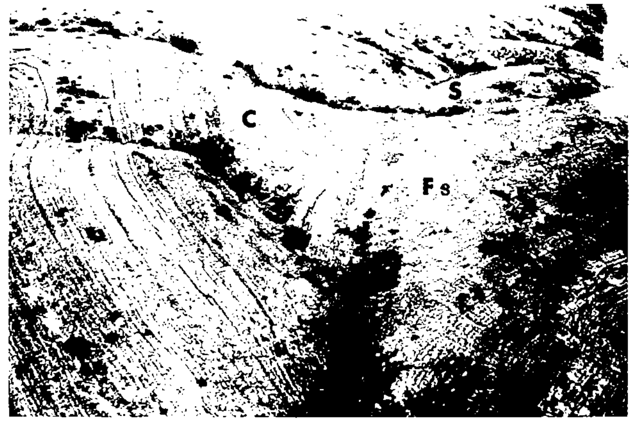

Figure 60. View northward, showing trace of Blue Creek Canyon Fault following line of tree-filled gully. East (right) of fault are Cambrian formations on western limb of hanging-wall anticline; this limb is greatly disturbed by small, east-trending faults. West of fault are north-plunging folds in Ordovician Cool Creek Formation; eastern limb of syncline closest to fault has been partly overridden by fault movement. *F1*, *F2*, *F3*: lower, middle, and upper members of Fort Sill Formation; *S*, Signal Mountain Formation; *C*, Cool Creek Formation.

Figure 61. Similar fold developed in Cool Creek limestone. Fold is a minor second-order syncline plunging steeply northward. Bed *X* is approximately 2.75 times thicker in hinge zone than it is on limb. Scale shown by quarter (see arrow).

Figure 62. View eastward, showing geometry of first-order folds developed in graben immediately west of Blue Creek Canyon Fault (*B*). Note how north-plunging anticline (*Z*) bifurcates, "sprouting" two anticlines (*X* and *Y*) at a higher structural level. Fold *X* becomes major structure seen in figure 161 when traced northwestward. Spatially above sharp axis of fold *Z*, a structural terrace (*U*) (or "broad-bottomed" syncline) develops to north. *R*, Carlton Rhyolite; *C*, Cambrian rocks of hanging-wall anticline.

Figure 63. View northward along axis of north-plunging anticline (described in fig. 62), showing upward passage from sharp-crested anticline (*Z*) to a structural terrace (*U*) and bifurcation of original fold into anticlines *X* and *Y*. Note localized disharmony (*D*).

Figure 64. Minor second-order fold in Cool Creek limestone. Structure plunges northward. Note cleavage in bed *H*.

Figure 65. Axial-plane cleavage in axis of minor second-order anticline. Rock is a silty pelsparite in Cool Creek Formation. Bedding is horizontal, cleavage perpendicular. Note how pellets (dark areas) are flattened in plane of cleavage, whereas quartz grains are shattered along tension cracks perpendicular to cleavage (cracks are sparite-filled). Ordinary light; view 2 × 1 mm.

spicuous flattening parallel to cleavage. Ratios of flattening indicated by these pellets vary from 2:1 to 5:1, that is, similar to values obtained from bed-thickness ratios (see above).

Interpretation of the Structure

The study area coincides with part of the hinge between the eastern part of the Lawtonka Graben and the Blue Creek Canyon Horst (Harlton, 1951, 1963, 1972). The southern boundary of the Lawtonka Graben is the Meers Fault.

All major folds and faults in this area trend between N. 5° E. and N. 30° W., whereas over most of the graben area the majority of the folds trend N. 50° W. (fig. 66). This latter direction is more or less parallel to the Blue Creek Canyon Fault as mapped in the subsurface to both the north and south of Blue Creek Canyon (Havens, 1977) (fig. 67). However, this trend is about 10° north of the Meers Fault trend.

Anomalous Trend of Blue Creek Canyon Fault

Sudden deflections in fault trends are usually of interest because they may afford insights into the geometry. In the Blue Creek Canyon area, the following departures from regional attitude are noted (figs. 66, 67):

1. The fault trend changes from N. 50° W. to north.
2. Axes of first-order folds trend N. 20° W. as opposed to N. 50° W. elsewhere in the Lawtonka Graben and Blue Creek Horst.
3. Fold limbs steepen toward the fault. As a consequence, the axial planes of the folds adjacent to the fault dip to the east, whereas folds elsewhere are upright.
4. Northwesterly fold plunge is consistent in direction close to the fault and less so elsewhere.
5. Cleavage is developed close to the fault but is rare elsewhere.

In addition, fold limbs are truncated by the fault, and field observations show that the fault is a high-angle reverse structure. It is worth noting that, although the Oklahoma Geological Survey (Havens, 1977) connects the fault that crops out in Blue Creek Canyon with faults in the subsurface north and south of the canyon, there is no direct field evidence to support this interpretation.

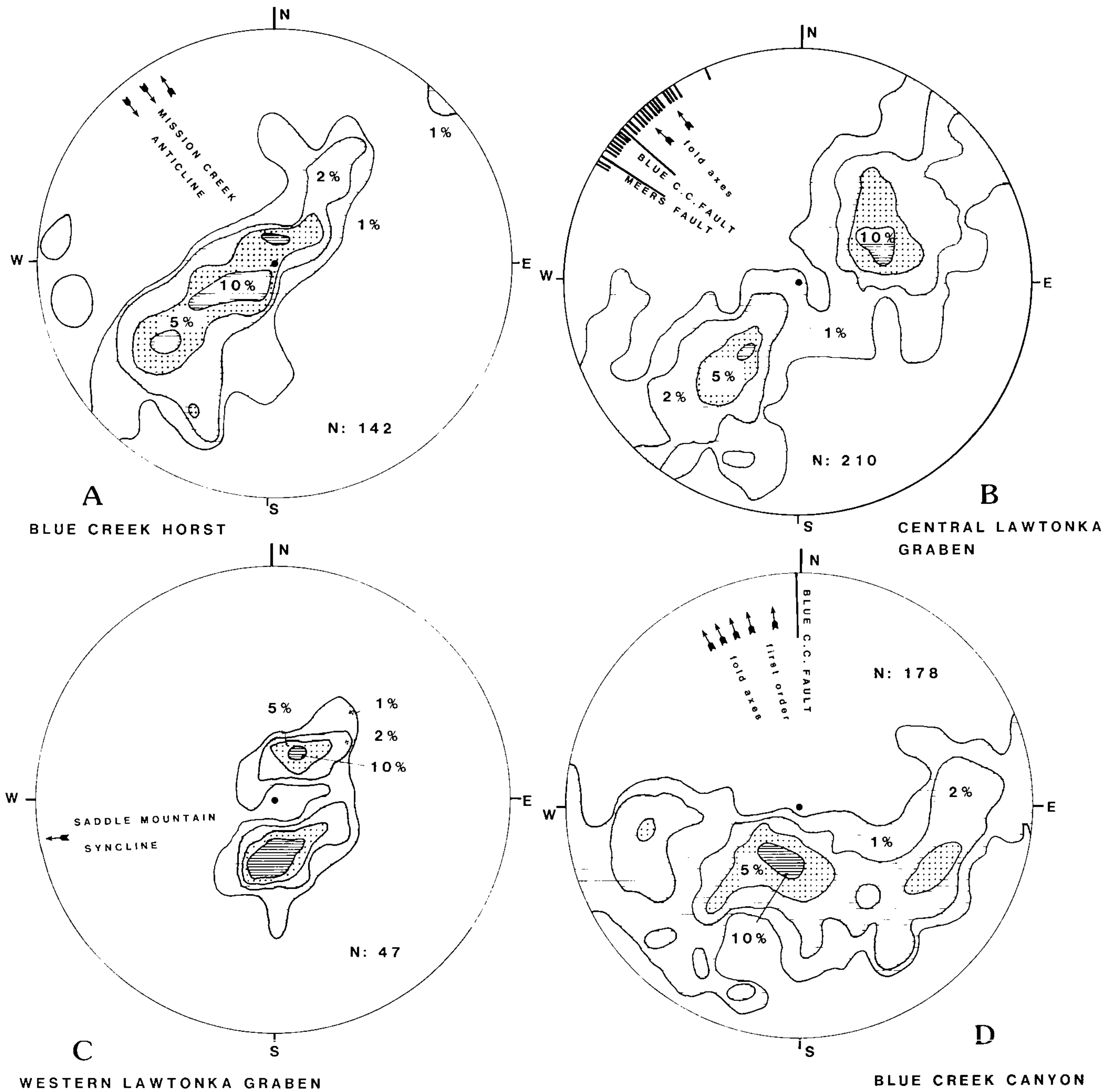

Figure 66. Contour diagram of poles to bedding from traverses in Slick Hills. Data from present author, Babaei (1980), Barthelman (1968), and Brookby (1969). Also plotted are principal faults and fold axes (plunge indicated where appropriate). Data illustrate (1) relatively gentle folding and variable plunge of structures in horst, (2) consistency and intensity of folds in central graben, (3) slight departure of fold axes from trend of Meers Fault in graben, (4) "anomalous" trend of Saddle Mountain Syncline, and (5) "anomalous" trend, consistent plunge, and steepness of folds near Blue Creek Canyon.

Fold and Fault Genesis

The most obvious analysis of the stresses that produced the folding and faulting is that maximum principal stress was oriented approximately N. 40° E., that is, perpendicular to the average fold-axis trend and to the usual (nonanomalous) trend of the Blue Creek Canyon Fault. Within the Lawtonka Graben, the degree of crustal shortening from folding alone, parallel to this trend, is approximately 60 to 80 percent at the present level of erosion.

However, the Lawtonka Graben is wedge shaped (fig. 46), and both the fold axes and the Blue Creek Canyon Fault diverge by 10° to 15° from the Meers Fault to the south (figs. 46, 66, 67). The latter is a more substantial structure than the Blue Creek Canyon Fault, and has a trend (N. 70° W.) that is more characteristic of major faults elsewhere in southern

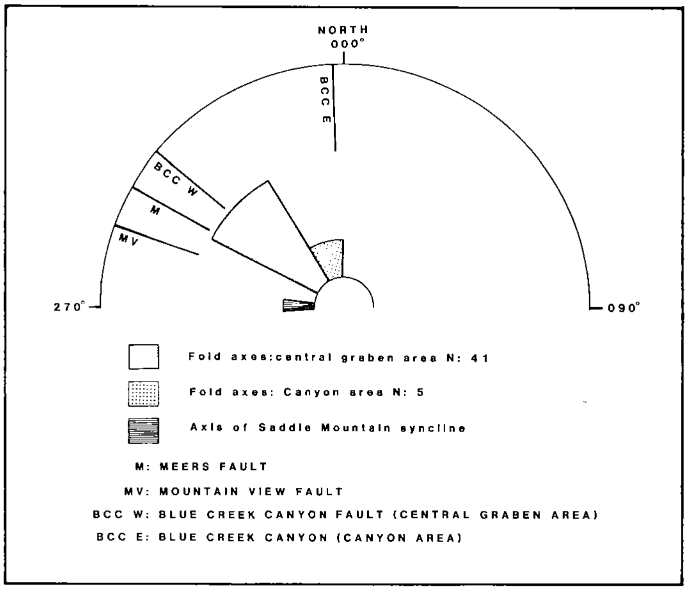

Figure 67. Synopsis of trends of major structures in the area.

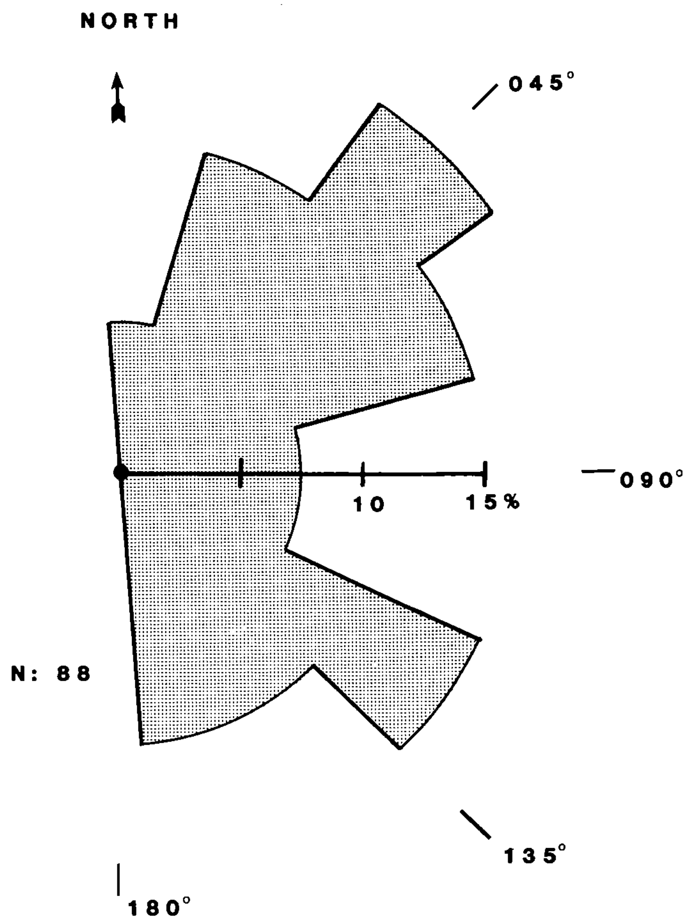

Figure 68. Joint directions in granitic terrain 5 miles west of Meers (replotted from Miller, 1981).

Oklahoma. Thus, it is probable that a principal stress oriented N. 40° E. is of local significance only. If the Meers Fault is considered to be a reverse fault involving simple vertical displacement, a regional maximum principal stress oriented N. 20° E. is indicated.

Recent work (Brewer, this guidebook) has shown that the Meers and Mountain View Faults are thrusts of considerable magnitude, involving basement, that have moved the Wichita Mountains block over the southern margin of the Anadarko Basin. This interpretation is consistent with the analysis of crustal shortening discussed above.

An alternative model is one that involves left-lateral wrench movement on principal faults in the region (Pruatt, 1975; Wickham, 1978). If theoretical resolutions of stress for this model are applied, the maximum principal stress was oriented at about N. 80° E. Studies of major wrench-fault zones (for example, Groshong and Rodgers, 1978) indicate that a common element of the basic wrench pattern is *en-echelon* folds inclined at a low angle to the wrench zone. Such fold patterns and related phenomena have been recognized in the Arbuckle Mountains, and certainly occur in parts of the Lawtonka Graben (Wickham and others, 1978). However, there is some difficulty in applying this model to all folds in the Lawtonka Graben; in particular, the Saddle Mountain Syncline (one of the principal folds in the graben) shows a variation in trend that could be consistent with either left- or right-lateral movement (figs. 46, 66, 67). Furthermore, this model cannot account for the deep-seated thrusting that occurs at depth on the Meers and Mountain View structures (Brewer, this guidebook).

It is now pertinent to discuss the anomalies in structural trend associated with the Blue Creek Canyon Fault (see above). The simplest interpretation of these anomalies is that, in this area, the fault is a high-angle reverse structure involving movement of the Blue Creek Canyon Horst over the Lawtonka Graben. This movement postdates folding in the graben and, as a result, folds adjacent to the fault have been distorted. In particular, fold limbs are disturbed, truncated, and steepened nearer to the fault. Furthermore, both a decreasing stratigraphic throw to the north and a consistent northwestward plunge are consequences of reorientation of fold-axis trends from N. 50° W. to N. 20° W. (fig. 69). The maximum principal stress required for this movement is a vector from approximately N. 80° E. This stress could have induced left-lateral wrench movement on both the Meers Fault and the "nonanomalous" Blue Creek Canyon Fault.

Conclusions

The preferred interpretation of pre-Permian structure in this region involves two stress orientations. An early compression, oriented N. 20° E. and more or less at right angles to the Southern Oklahoma Aulacogen, produced folding along N. 50° W. axes, particularly in the Lawtonka Graben, and substantial thrust movements along major bounding faults. Subsequently, compression oriented N. 80° E. produced high-angle reverse faulting along north-trending structures (for example, the Blue Creek Canyon Fault as mapped here) and initiated left-lateral movements on major faults parallel to the aulacogen axis in the region.

This late compression received some support from an analysis of joints conducted by Miller (1981) in an area some 10 miles west of Blue Creek Canyon; major modes can be interpreted as left- and right-lateral shears, respectively (fig. 68). The model is also in accord with the interpretation and timing of movement advanced by Brewer (this guidebook). It is possible that the north-trending segment of the Blue Creek Canyon Fault is an outlying representative of the Broxton Fault complex, which crops out to the east near Elgin and Apache (Harlton, 1972). The overall trend of faults in this complex is N. 20° W.

The analysis offered above differentiates two stress components. It must be noted, however, that some of the structural complexities could be the result of an oblique (and perhaps shifting) stress field.

A further "wild card" may be some unknown influence that rejuvenated early Paleozoic faults (associated with the initial development of the Southern Oklahoma Aulacogen) may have had on local structures.

SUB-PERMIAN UNCONFORMITY AND THE POST OAK CONGLOMERATE

The Permian Post Oak Conglomerate, facies-equivalent of the Hennessey Shale (Havens, 1977) and Wellington Formation (Chase, 1954), oversteps all the lower Paleozoic rocks exposed in the canyon. The unconformity is extremely irregular, and it is clear that the present topography of the Slick Hills is a slightly modified Permian inheritance. Because conglomerate is present on the floor of the northern part of the canyon, the valley is inferred to be a partially exhumed Permian feature (fig. 69).

Beneath the unconformity, lower Paleozoic limestones may show karst fissures and small cave sys-

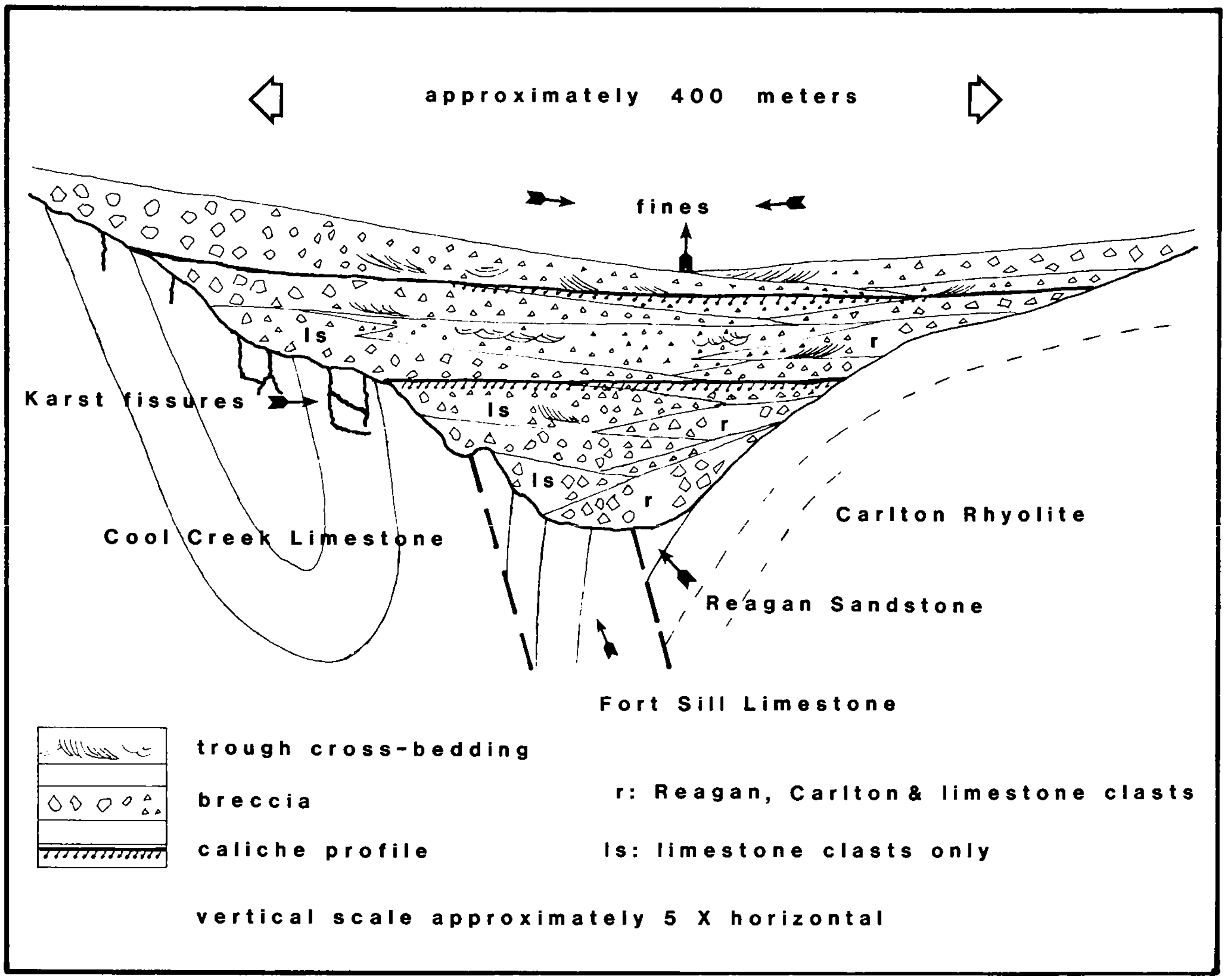

Figure 69. Schematic diagram showing nature of sub-Permian unconformity and fanglomerate infilling of northern part of Blue Creek Canyon.

tems (figs. 163, 164, and 165). Karst fissures are infilled with a reddened micrite, interpreted as eolian dust and limestone fragments derived from the fissure walls (that is, they were in contact with the Permian land surface). Cave systems are filled with a variety of types of flowstone, indicating a strong vadose imprint.

The Post Oak Conglomerate in the Wichita area mantles all of the exposed older rocks; its composition is closely related to the type of substrate. Chase (1954) was able to recognize four general categories of conglomerate: (1) Ppo–1—limestone conglomerate, (2) Ppo–2—granite-boulder conglomerate, (3) Ppo–3—rhyolite porphyry conglomerate, and (4) Ppo–4—granite–gabbro conglomerate with zeolite–opal cement.

Ppo–2 and Ppo–3 received some attention from Al-Shaieb, Hanson, and others (1980). In essence, these facies have a complex diagenetic history that involves two principal facets: an early phase of localized calcrete (caliche) formation, and a continuing breakdown of labile silicates with subsequent reprecipitation as clay minerals and ferric oxides.

The limestone conglomerate Ppo–1 has been largely ignored but is the sole facies occurring around the Slick Hills. In the area of Blue Creek Canyon, the composition of the conglomerate is closely related to the underlying geology; representative clasts of all the exposed lower Paleozoic formations are found in predictable locations. The basal conglomerate may be a coarse breccia, and shows some evidence of having been deposited adjacent to fault scarps (fig. 154, site q). The conglomerate fines upward and outward (that is, away from the Permian relief) and formed as talus and small alluvial-fan deposits. The Permian Blue Creek Canyon was filled with breccio-conglomerates that were debouched from both sides of the valley (fig. 69); the contribution from the west side was greater, and in places conglomerate composed of limestone fragments oversteps onto the Carlton Rhyolite. For the most parts, the conglomerate is massive and devoid of primary bed forms. However, finer conglomerate facies may show parallel lamination and poorly defined, medium-scale trough cross-bedding (the latter indicating transport away from exhumed Permian relief).

Some calcrete (caliche or "corn-stone") zones are developed. These pedogenic carbonates are seen as rubbly weathering micritic deposits that cement limestone pebbles (figs. 70, 71, 162). The micrite in common with other calcretes is cut by small, irregular veins of sparite (fig. 71). By uniformitarian analogy, the calcretes record periods of fan-surface stability in a semiarid environment (Leeder, 1975; Steel, 1974). The tops of the calcretes are reddened by ferric oxides that probably accumulated as eolian dust during these periods of stability. The lower parts of some calcrete profiles are characterized by green coloration; this change in color presumably records plugging of the calcrete zone and local development of reducing conditions (with consequent reduction of ferric oxide dust).

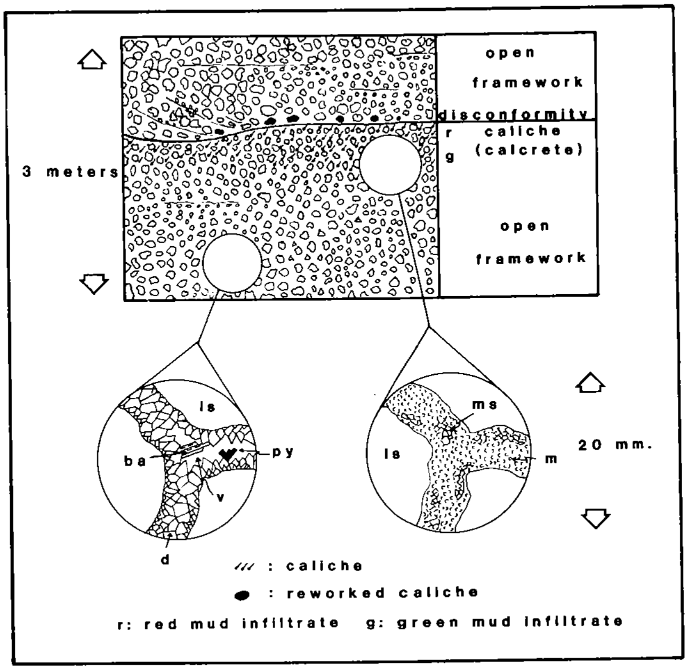

Figure 70. Schematic representation of calcrete profile developed on stable surface in Post Oak Conglomerate. A pedogenic calcrete formed at and beneath this surface. Key to thin-section sketches: *ls*, lower Paleozoic limestone clasts; *d*, drusy sparite cement; *v*, void (porosity); *py*, pyrite; *ba*, barite; *m*, micrite; *ms*, microsparite veins.

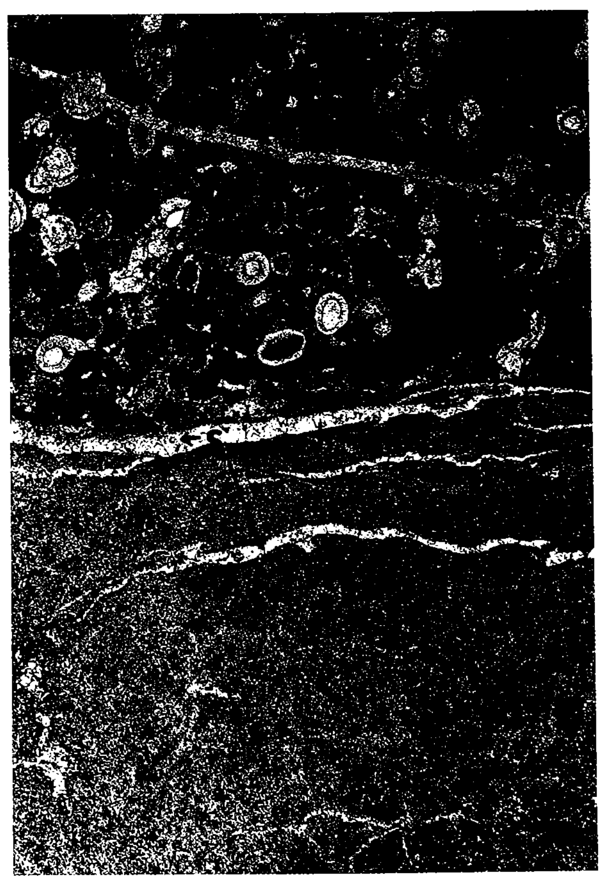

Figure 71. Post Oak Conglomerate calcrete, showing pebble of lower Paleozoic oosparite (*LP*), micrite cement (*M*), and later sparite veinlets (*S*). View approximately 2 × 1.3 cm.

Figure 72. Post Oak Conglomerate. Originally open-framework texture of angular, lower Paleozoic blocks (*LP*) cemented by drusy sparite (*D*). Absence of fines mainly reflects solution weathering of Permian limestone land surface. View 6 × 4 cm.

Subsequent cementation of the carbonates has been by drusy sparite (forming dogtooth-spar crystals as much as 5 mm across in cavities between pebbles). This sparite records phreatic precipitation of carbonate (fig. 72); cathode-luminescence studies (Donovan and Al-Shaieb, in preparation) show a variable redox condition with respect to iron content in this cement. Minor late-stage cements are euhedral pyrite and barite. The latter mineral is also found in other Post Oak facies (Al-Shaieb, Hanson, and others, 1980).

ACKNOWLEDGMENTS

It is a pleasure to record the great hospitality of Mr. and Mrs. Charlie B. Oliver of the Kimbell Ranch; they have afforded me constant access to their land and have always expressed interest in the work.

I benefited from discussions in the field with David Sanderson, Abdolali Babaei, Richard Hanson, Richard Thomas, and Steve Culver. John Shelton and Zuhair Al-Shaieb were supportive in analysis of the Permian rocks. Wayne Pettyjohn reviewed aspects of the work.

STOP DESCRIPTIONS

M. Charles Gilbert
Benjamin N. Powell
Marjorie L. Stockton
Joe D. Giddens III
James R. Miller
J. Ronald Sides
R. Nowell Donovan
A. Babaei
D. J. Sanderson

STOP 1—REID'S PIT

Relationships among Glen Mountains Layered Complex, Glen Creek Gabbro, Cold Springs Breccia, and late diabase. Secs. 13–14, T. 4 N., R. 17 W., Kiowa County, Oklahoma. **B. N. Powell** and **M. C. Gilbert.**

Introduction

This stop beautifully displays many key relations within the Raggedy Mountain Gabbro Group. Deep Permian weathering in a coarsely recrystallized zone along the upper intrusive contact of the Glen Creek Gabbro with the host Glen Mountains Layered Complex has provided material useful for road bases and drilling pads. Excavation over the past 20 years has exposed many intrusive and structural relations. In order to simplify the discussion, and to key the illustrations to exposures within the excavated area, the pit has been arbitrarily divided into reference segments as shown in figure 73. The geology is shown in figures 74 and 75, with the approximate outline of the excavated area. The "west" pit is that part in sec. 14 west of Glen Creek. This is the oldest area of excavations, where attention was centered on a magnetite prospect. There are now 11 separate pit centers in the west segment alone.

The "east" pit represents all the excavated area east of Glen Creek. This is the most recently excavated, with the latest activity far to the east in sec. 13. E–14 refers to the segment east of Glen Creek that lies in sec. 14. Three distinct levels of quarrying require additional breakdown into lower, middle, and upper sections. The lower E–14 is almost at the level of Glen Creek. E–13 refers to the rest of the pit area, where removal is still in progress, and where, in general, less impressive features are seen. Figure 76 is the view westward from E–13 showing the excavated contact between the underlying darker, intrusive Glen Creek Gabbro and the overlying slightly altered and whiter M Zone of the Glen Mountains Layered Complex, dipping to the north.

The area shown in figure 74 was originally mapped and described by Chase (1950a), followed by Gilbert (1960), Hiss (1960), and Spencer (1961). The nomenclature used in the lithostratigraphy has been revised by Powell and others (1980) and is given in table 2. The Glen Mountains Layered Complex is the oldest formation in the Raggedy Mountain Gabbro Group, and both the L and M Zones of the complex are exposed in the area. The complex is the host rock into which the Glen Creek Gabbro intruded. Two modifications of the geologic relations have been made since the original mapping: (1) what we now recognize as the Glen Creek Gabbro was called "olivine diallage gabbro" by Chase, and was called the "biotite–olivine facies of the L Zone" by Gilbert, and (2) a "basic pegmatite" recognized by Gilbert may be a late-stage offshoot of the hydrous Glen Creek Gabbro or local, remelted pods of the layered complex.

Most of the terrane is in the M Zone, dominated by plagioclase and olivine cumulates. Layering is commonly defined by plagioclase lamination and by alternating bands of anorthosite and gabbro (grating structure). Finely ophitic augite, which may stand out in relief, and olivine, which weathers to pits, dominate the surface features of the outcrops. These textures are well displayed on the north-dipping, dip slope exposed in $SW\frac{1}{4}$ sec. 14. Loose boulders of M Zone rock are found in the E–14 middle section of the pit, where these features can be studied in three dimensions (figs. 77, 78). Clumps of ophitic pyroxenes may represent paths of migrating liquid through the accumulating magmatic deposit.

Modal data on the rocks of the area were extracted from Hiss (1960) and are presented in table 19. Chemical and modal data from outcrops of the M Zone were taken from Alipouraghtapeh (1979) and are shown in table 20. The significance of bulk chemical determinations from rocks that are highly

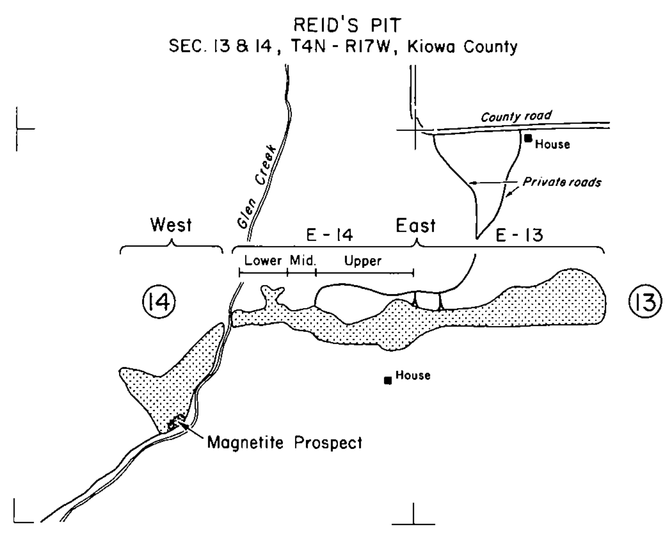

Figure 73. Location map for features in Reid's Pit.

EXPLANATION

PERMIAN	Hennessey Group		Includes minor amounts of soil cover and Quaternary alluvium, undifferentiated
CAMBRIAN			Late diabase dike
			Cold Springs Breccia; includes Otter Creek microdiorite and granitoid facies
PROBABLE CAMBRIAN	Raggedy Mountain Gabbro Group	Roosevelt gabbros	Biotite microgabbro dikes
			Glen Creek; includes magnetite-olivine body
CAMBRIAN TO PROTEROZOIC (?)		Glen Mountains Layered Complex	M Zone
			L Zone

A———*A*′
Line of cross section

x WG60
Sample locality; WG from Alipouraghtapeh (1979), H from Hiss (1961), W from Gilbert.

Excavated area

Geology by M. C. Gilbert, after Gilbert (1960) and Spencer (1961)
Base from U.S. Geological Survey, Glen Mountains, 1:24,000, 1956

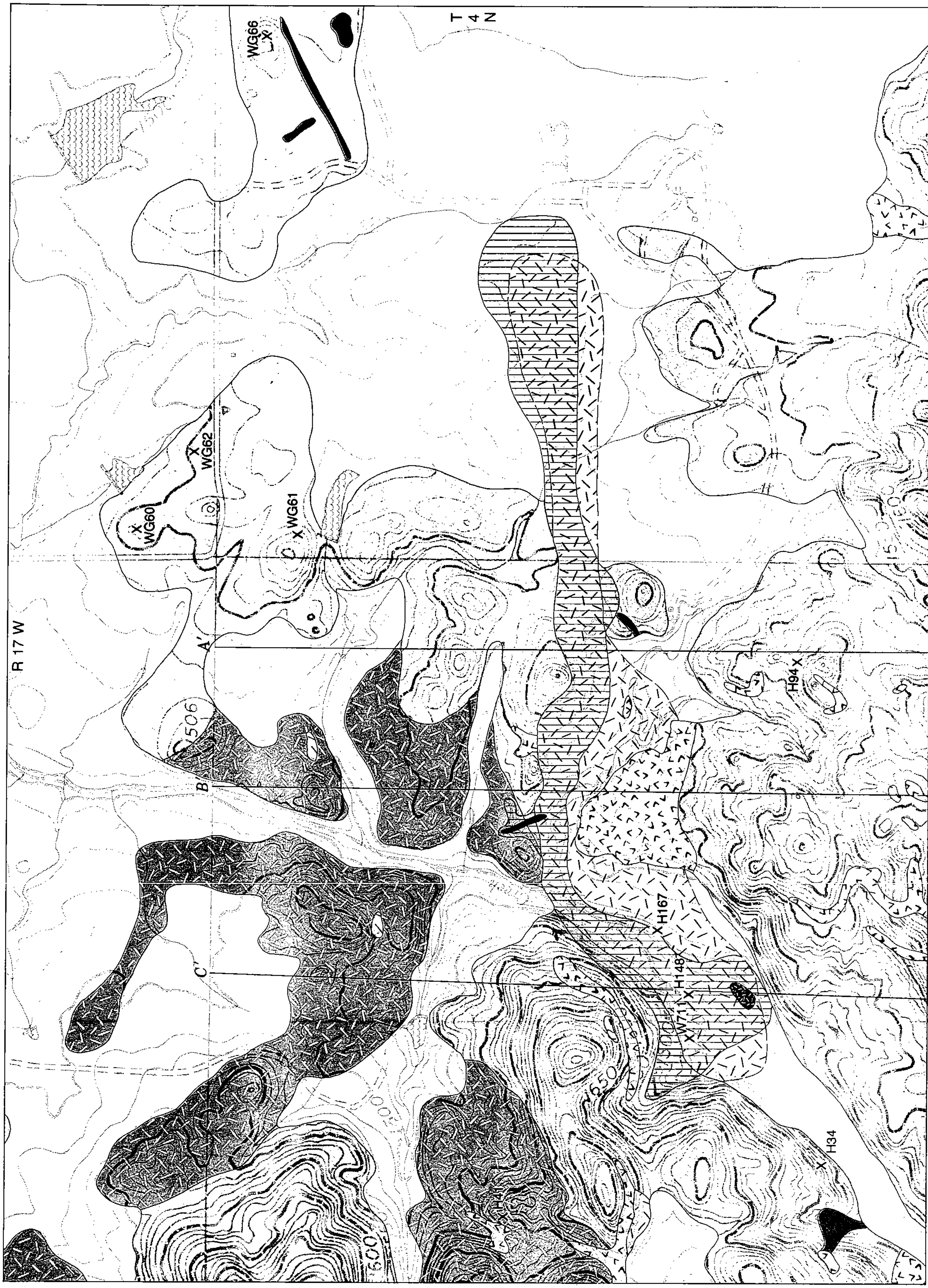

Figure 74. Geologic map of Reid's Pit area, Stop 1. Map scale, 1:12,000.

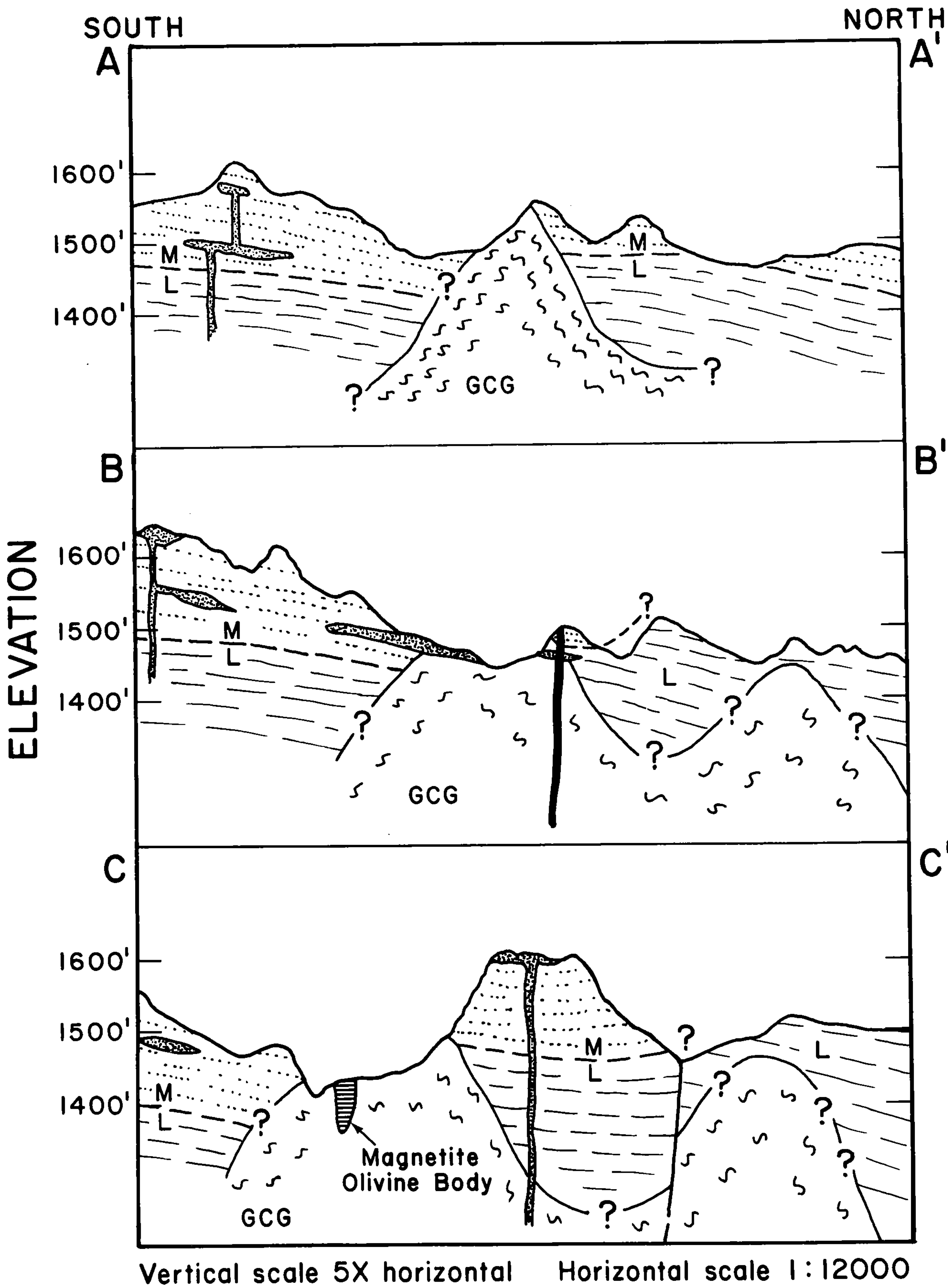

Figure 75. Geologic cross sections of Reid's Pit area.

Figure 76. Photograph from E–13 area of Reid's Pit (T. O. Materials Co.), looking westward. On skyline 1½ mi away is highest point in Glen Mountains (1,993 ft), capped by M Zone. Hill (1,600+ft) in middleground is partially excavated on south side; Glen Creek Gabbro is exposed along flank and almost to top of hill before M Zone of Glen Mountains Layered Complex is intersected. M Zone is anorthositic and weathers white; contact can be seen dipping north.

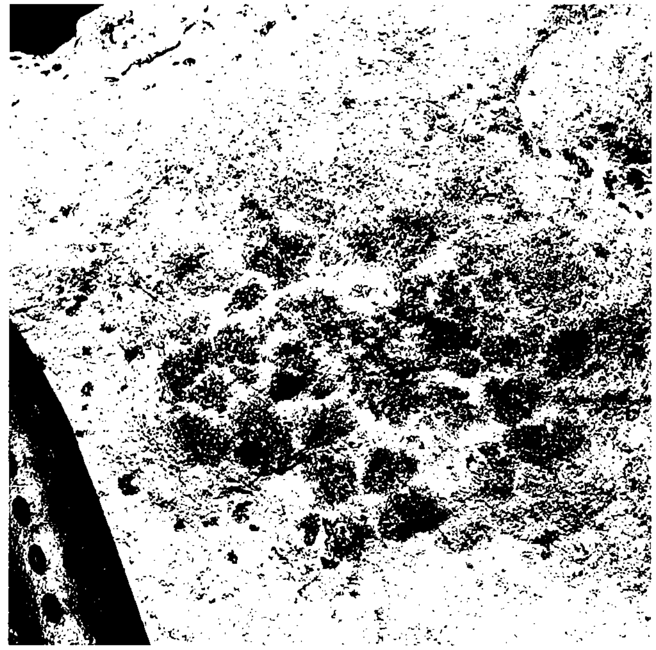

Figure 78. Clusters of finely ophitic clinopyroxene. Area is E–14 Middle.

Figure 77. Alternating anorthositic (plagioclase-rich) and gabbroic (plagioclase + clinopyroxene ± olivine) layers characteristic of M Zone. Plagioclase is cumulus phase in both. Finely ophitic clinopyroxene is generally post-cumulus, but "cotectic" crystallization has been suggested where some 1–2–cm-sized grains contain randomly oriented plagioclase (Karns, 1961). Area is E–14 Middle.

Figure 79. Outcrop face where darker Glen Creek Gabbro has intruded lighter M Zone of Glen Mountains Layered Complex, showing nature of angular, sharp contact. This photograph figured in Powell and others (1980, Pt. II) and by Gilbert in Oklahoma Geology Notes (1978, no. 4). Area is E–14 Middle.

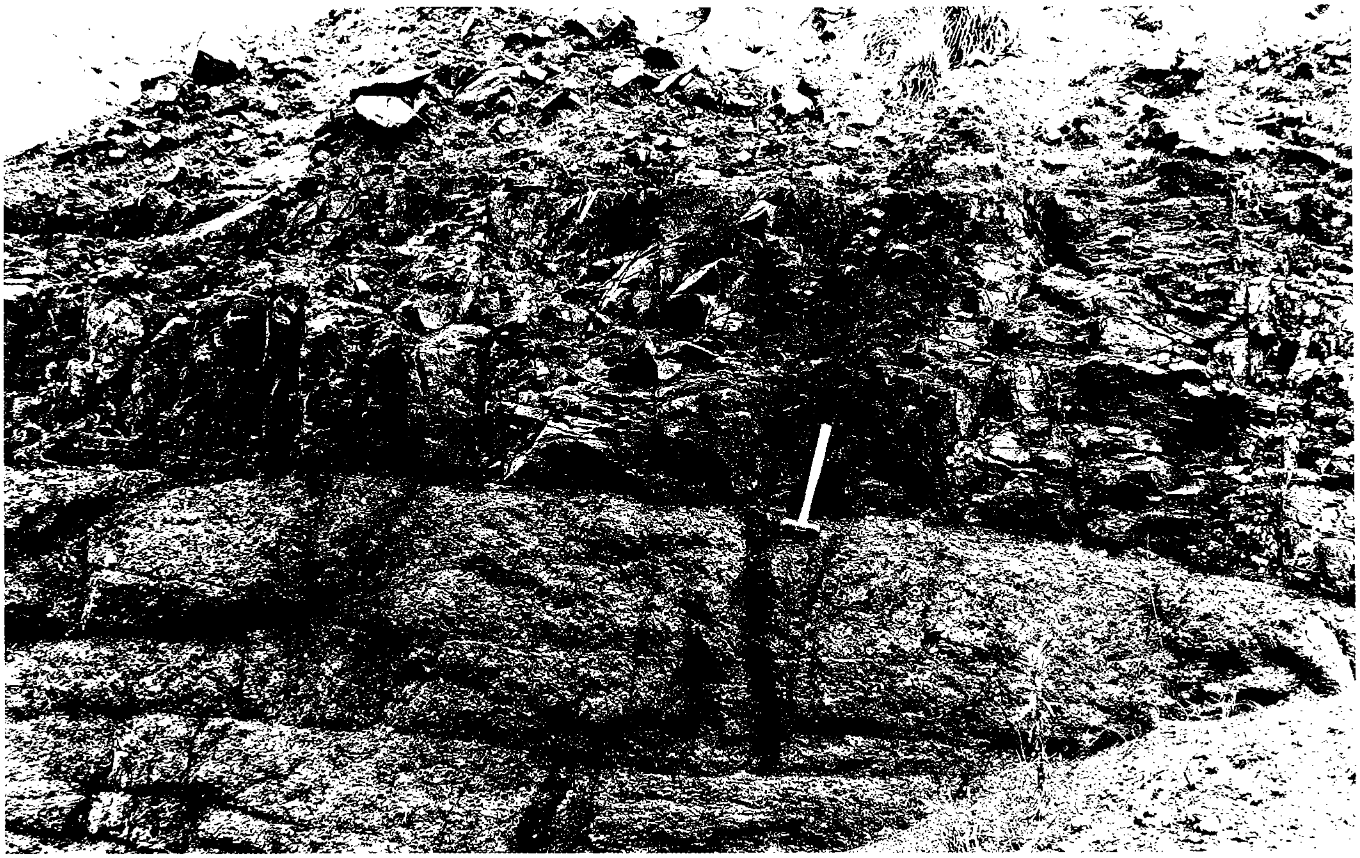

Figure 80. Horizontal sill of Cold Springs Breccia has intruded Glen Creek Gabbro. Hammer head is just below lower contact of sill. Vertical late diabase dike cuts both previous units just left of hammer. Diabase subsequently offset along small strike-slip fault. This outcrop was partially buried in 1981 when excavation increased. Photograph faces east. Area is E–14 Lower.

TABLE 19.—MODAL ANALYSES OF IGNEOUS ROCKS FROM REID'S PIT AREA (STOP 1)

(From W. L. Hiss, 1960)

	Glen Mountains Layered Complex			Roosevelt Gabbros		
	L-Zone	M-Zone		Glen Creek Gabbro		
	#H41 (Rock 124) NW SW SW NW 14-4N-17W	#H34 (Rock 110) SW NE SW SW 14-4N-17W	#H94 (Rock 262) SE NW SE SE 14-4N-17W	#H148 (Rock 377) NE SW NE SW 14-4N-17W	#H167 (Rock 380) NW SE NE SW 14-4N-17W	#H168 (Rock 381) NW SE NE SW 14-4N-17W
Plag	75	60	60	60	32	34
Cpx (ophitic)	15	20	20	20	45	20
Opx	2	10 (d)	15 (d)	tr	-	tr
Ol	5 (poik + react rims)	-	-	6 (rr)	5 (p)	20 (p+rr)
Oxide (discrete)	1	1	2	8	2	4
Oxide (skeletal)	2 (intergrowth)	9	3	2	8	11
Hb	-	-	-	tr	3	tr
Biot	-	-	-	4	5	10
Ap	-	-	-	tr	tr	1

d = discrete
rr = reaction rims
p = poikilitic

Figure 81. Horizontal Cold Springs Breccia dike bifurcates on north wall of excavation. Area is E–14 Lower.

Figure 82. Glen Creek Gabbro cut by series of genetically related biotite microgabbro dikes. These in turn are cut by granitoid offshoots of Cold Spring Breccia dikes, with contemporaneous faulting. Area is E–14 Lower.

TABLE 20.—ANALYSES OF M ZONE SAMPLES GLEN MOUNTAINS LAYERED COMPLEX

(From Alipouraghtapeh, 1979)

Field Trip Stop #1

Wt %	WG-60	WG-61	WG-62	WG-66
SiO_2	46.00	45.75	47.75	48.00
TiO_2	0.66	0.46	0.74	0.41
Al_2O_3	30.00	29.60	24.50	31.00
FeO^1	3.97	3.40	4.58	3.10
MgO	3.12	2.92	5.18	2.28
MnO	0.04	0.02	0.07	0.05
CaO	11.00	11.80	12.00	10.00
Na_2O	2.56	2.82	2.27	3.56
K_2O	0.27	0.22	0.27	0.34
P_2O_5	0.34	0.22	0.32	0.22
ppm				
Cu	88	22	45	51
Cr	5	10	43	16
Zn	58	30	49	30
Pb	20	20	30	20
Ni	20	22	18	20
Ba	70	60	45	120
Sr	534	622	441	573
Rb	nd	nd	nd	4
V	160	90	140	90
Total	97.96	97.21	97.69	98.96

1 = all Fe as FeO

Modes %	WG-60	WG-61	WG-62	WG-66
Plagioclase	93		65	
Olivine	tr		tr	
Clinopyroxene	5		25	
Orthopyroxene	tr		tr	
Opaques	2		10	
Others	tr		tr	

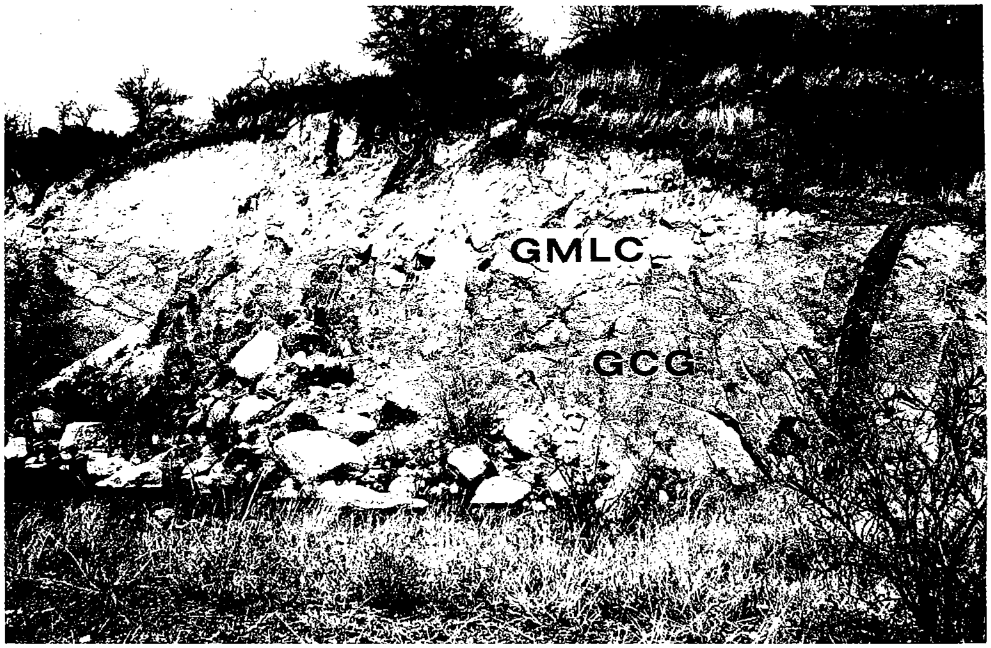

Figure 83. Glen Creek Gabbro Member (*GCG*) of Roosevelt Gabbros intrusive into the M Zone of the Glen Mountains Layered Complex (*GMLC*) in SE¼SW¼NE¼ sec. 14, T. 4 N., R 17 W., Kiowa County. Excavated face is about 10 m high. Note Cold Springs Breccia dike on right side.

layered and locally variable is unclear. Either very large samples (about 1 m^3) or samples taken from a well-defined sequence of layers seem necessary for adequate characterization at the outcrop scale. Nevertheless, they are presented for reference and do show how Al_2O_3-rich these anorthositic gabbros are.

A brief summary of events affecting the rocks of Stop 1 yields:

Youngest

8. Deep Permian weathering along regional fractures during burial in shale.
7. Regional Pennsylvanian fracturing and faulting.
6. Later faulting (Cambrian to Pennsylvanian?).
5. Intrusion by late diabase.
4. Formation of the Cold Springs Breccia and intrusion by related granitoids and Otter Creek Microdiorite, with some local faulting along dikes.
3. Selective recrystallization of the Glen Mountains Layered Complex near the contact and (or) formation of basic pegmatoid pods.
2. Intrusion by the Glen Creek Gabbro.
1. Formation of L and M Zones of the Glen Mountains Layered Complex.

A summary of features in the pit area is given in table 21.

Glen Creek Gabbro

The Glen Creek Gabbro is demonstrably intrusive into the older Glen Mountains Layered Complex (both the L and M Zones) and in turn is intruded by narrow dikes and "sills" of Cold Springs Breccia, granitoid, and late diabase. Although a logical first assumption is the correlation of the granitoid dikes with the Wichita Granite Group, another possibility must be considered. In the exposures of Glen Creek Gabbro, and in exposures to the west in the SE¼ sec. 15, T. 4 N., R. 17 W. where the Cold Springs Breccia intrudes the Glen Mountains Layered Complex, the intimate association of granitoid dikes and breccia intrusions, and the close resemblance of the dikes to the granitoid phase of the Cold Springs Breccia, strongly suggest a genetic relationship. Correlation of the pink granitic phase of the Cold Springs Breccia with any particular unit of the Wichita Granite Group is uncertain. Substantial exposures of Wichita Granite nearest to the principal occurrences of the Cold Springs Breccia are more than 5 km to the north. These granite occurrences were mapped as Lugert Granite by Taylor (1915), as Mount Scott Granite by Merritt (1967), and are now called Cooperton by Myers and others (1981). The pink granite in and associated with the Cold Springs Breccia, however, has a higher plagioclase content than the Wichita granites. The significance of this distinc-

TABLE 21.—GENERAL FEATURES OF REID'S PIT AREA (STOP 1)

Reference Segments	Feature
E-13	Excavation within the GCG but apparently reaching the eastern terminus of the body. Features not studied in this area.
E-14 Upper	Includes most prominent hill (1600+') with intrusive contact between GCG and GMLC well displayed just south of the crest of the hill. A prominent dipping granitoid dike exposed in pit south of hill. "Basic pegmatoid" and Permian-altered GMLC (Tepee Creek-style weathering) on east slope of hill. On SW excavated side, spheroidally weathered GCG boulders in place. In saddle between E-14 Upper and Middle, where road enters pit, is a subhorizontal dike of Cold Springs Breccia cut by nearly vertical late diabase.
E-14 Middle	Our best exposure of GCG intruding GMLC. Figured in Powell and others (1980, Part II, fig. 14), by Oklahoma Geology Notes as the cover, v. 38, #4 (Gilbert, 1978), and here as Fig. 79. The sharp contact overall dips steeply to the north cross-cutting layering in the GMLC. The contact is highly angular in places. Local layering in GCG is at a low angle to the contact. Small fragments of GMLC, elongated parallel to internal layering, are now aligned with GCG layering. Well-displayed, in place, spheroidal corestones of GCG in excavated wall. Subhorizontal dike of Cold Springs Breccia cuts both GCG and GMLC.
E-14 Lower	The pit here drops in elevation 3 to 10 m and has a projection off to the north. Figure 80 shows a horizontal dike of Cold Springs Breccia intruding GCG, both subsequently cut by a thin vertical late diabase dike on which there is offset. The Cold Springs dike bifurcates subhorizontally at the GMLC-GCG contact on the north wall of the pit (Fig. 81). To the immediate east of that figure, in a NE corner of the excavation, are biotite microgabbro dikes cutting GCG, themselves cut and offset by granitoids associated with the Cold Springs (Fig. 82). To the west, the GCG-GMLC intrusive contact is again beautifully clear (Fig. 83). The excavated projection to the north exposes a vertical late diabase dike on the eastern wall cross-cutting both vertical and horizontal parts of the Cold Springs Breccia (Fig. 84). Fractures in the late diabase dikes are perpendicular to walls (Fig. 85) presumably due to cooling against quite lower temperature host rocks, implying considerable time hiatus since Cold Springs and earlier igneous events. The steeply dipping, large Cold Springs Breccia dike on the west wall of the excavated arm shows some left-lateral strike-slip offset (Fig. 86, and cover of Guidebook). This dike T's into the horizontal Cold Springs dikes, and its granitoid offshoots contain fragments of the host GMLC (Fig. 87). Finally, spheroidal weathering of GMLC rocks yields rounded but more angular blocks due to the stronger internal layering (Fig. 88) compared to the somewhat more homogeneous GCG (Fig. 89).
West-14	"Basic pegmatoid" pods are common. The Ti-Fe oxide-olivine prospect (magnetite pit) is exposed (Fig. 96). A Cold Springs Breccia dike with granitoid offshoots, sample locality W711, is being studied, and chemical data will be available later.

Figure 84. Host rock is Glen Mountains Layered Complex cut by horizontal dike of Cold Springs Breccia. Breccia dike is exposed at base of cut at bottom of photograph. Above the hammer, vertical late diabase dike cuts the breccia. Elsewhere in the cut, small granitoid offshoots of breccia also are cut by stringers of late diabase. Area is E–14 Lower, north projection.

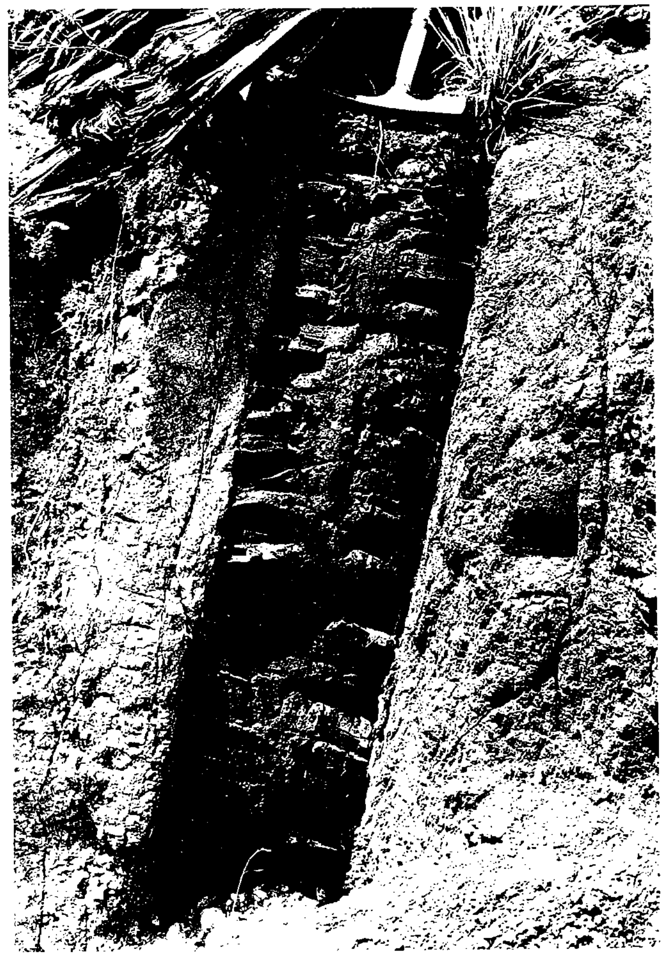

Figure 85. Late diabase dike cutting gabbro, showing fractures in dike perpendicular to walls. Area is E–14 Lower, at beginning of north projection.

Figure 86. Cold Springs Breccia dike, subhorizontal to subvertical, cutting Glen Mountains Layered Complex and showing strike-slip fault. Area is E–14 Lower, north projection.

Figure 87. Granitoid dike offshoot of Cold Springs Breccia, with inclusion of host (Layered Complex). Area is E–14 Lower, north projection.

Figure 88. Glen Mountains Layered Complex showing result of spheroidal weathering in strongly layered rocks. Area is E–14 Lower, north projection.

Figure 89. Glen Creek Gabbro showing spheroidal weathering, typical of its more homogeneous nature. Area is E–14 Lower, north projection.

tion is clouded by the possibility that assimilative reaction has affected even the pinkest (least contaminated) granitoid components of the Cold Springs Breccia. For the present, the origin of the Cold Springs Breccia and the associated granitic dikes—both of which transect the Glen Creek Gabbro—remains uncertain. (See also Powell and others, 1980.)

The Glen Creek Gabbro is exposed along an easterly trend for about 1.5 km; the outcrop width reaches about 0.4 km. The body is undoubtedly larger than this, because it is covered in places by surficial deposits and is overlain by the Glen Mountains Layered Complex. Although the body appears to be tabular and sill-like at the surface, probably owing to horizontal dikes, its exact form is unknown. That the Glen Creek is not strictly conformable is seen where it intrudes both the L and M Zones of the Glen Mountains Layered Complex. The thickness of the body is not known, but it does exceed 30 m.

Unlike the enveloping rocks of the Glen Mountains Layered Complex, which weather to light-gray, blocky slabs, the Glen Creek Gabbro weathers to comparatively smooth and rounded surfaces, a characteristic of the Roosevelt Gabbros in general. The weathered Glen Creek Gabbro forms olive-brown, friable masses, of considerable thickness in places, which exfoliate in layers from rounded masses of remarkably fresh, dark-brown gabbro. In one particular excavation, these weathering patterns convey the impression that their size, shape, and distribution are controlled by subtle structures that may relate to stresses formed during magma cooling.

The Glen Creek Gabbro is generally medium grained, although its grain size is variable. It is readily distinguished from the Glen Mountains Layered Complex by the higher color index and presence of biotite (or phlogopite) in the gabbro. Interesting ultramafic concentrations of olivine, magnetite, and ilmenite occur locally in the Glen Creek Gabbro. The genesis of these ultramafic concentrations is discussed below.

A coarse-grained rock resembling gabbro ("basic") pegmatite occurs in the northwestern and eastern parts of the Glen Creek Gabbro exposures. Its close spatial relationship to Glen Creek Gabbro strongly suggests a genetic connection, at present not worked out in any detail. Whether it represents an initial facies of the gabbro or is the result of secondary processes is unknown. Current investigation is being focused on this question. In the section below on the Sandy Creek Gabbro is a discussion of the origin of a similar-looking rock type within that body, with remarks about the interpretation of these and other occurrences in the Raggedy Mountain Gabbro Group.

The characteristic texture of the Glen Creek Gabbro is hypautomorphic-granular, locally ophitic to subophitic, with large (1 to 5 cm), anhedral augite grains (5–53 percent) enclosing lath-shaped labradorite crystals (30–70 percent) and subhedral to anhedral, rounded olivine grains (2–22 percent) (fig. 90). Magnetite and ilmenite are ubiquitous and occur

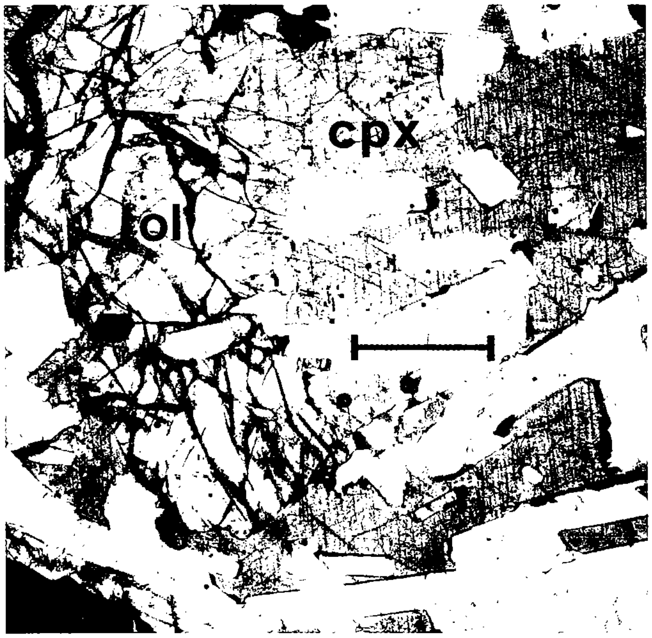

Figure 90. Photomicrograph of Glen Creek Gabbro showing rounded, anhedral olivine grains (*ol*) and plagioclase laths (white) ophitically enclosed by augite (*cpx*). Pyroxene is optically continuous over entire picture. Bar is 1 mm. (Sample MP–12.)

in subequal amounts, together commonly totaling 5 percent of the mode. Primary red-brown phlogopite and primary pale-pinkish-brown amphibole (titanian magnesian hastingsite) are ubiquitous but vary in amount. Phlogopite ranges from 0 to 6 percent, and amphibole, from 0 to 21 percent; one or the other hydrous phase—usually both—is invariably present. They appear to be relatively late in the crystallization sequence, forming interstitial, sometimes subpoikilitic grains and, where less abundant, thin rims on pyroxene and oxide grains (fig. 91).

The amphibole locally exceeds 20 percent and occupies the textural position of augite in other samples, forming large poikilitic grains enclosing olivine and oxide crystals (fig. 92). The amphibole is invariably well crystallized and clearly a primary magmatic phase, unlike the fibrous, uralitic amphibole formed locally in hydrothermally altered rocks of the Raggedy Mountain Gabbro Group. (See the section on the Sandy Creek Gabbro, Stop 3.)

Orthopyroxene is less abundant than clinopyroxene in the Glen Creek Gabbro, ranging from 0 to 10 percent (average 1–2 percent). Typically, it forms discrete grains and only rarely occurs as reaction

Figure 91. Photomicrograph of Glen Creek Gabbro showing thin rims of amphibole *(a)* along grain boundaries of plagioclase *(pl)*, olivine *(ol)*, magnetite (opaque), and augite. Note platelets of ilmenite exsolved from augite. Bar is 0.5 mm. (Sample WM–138.)

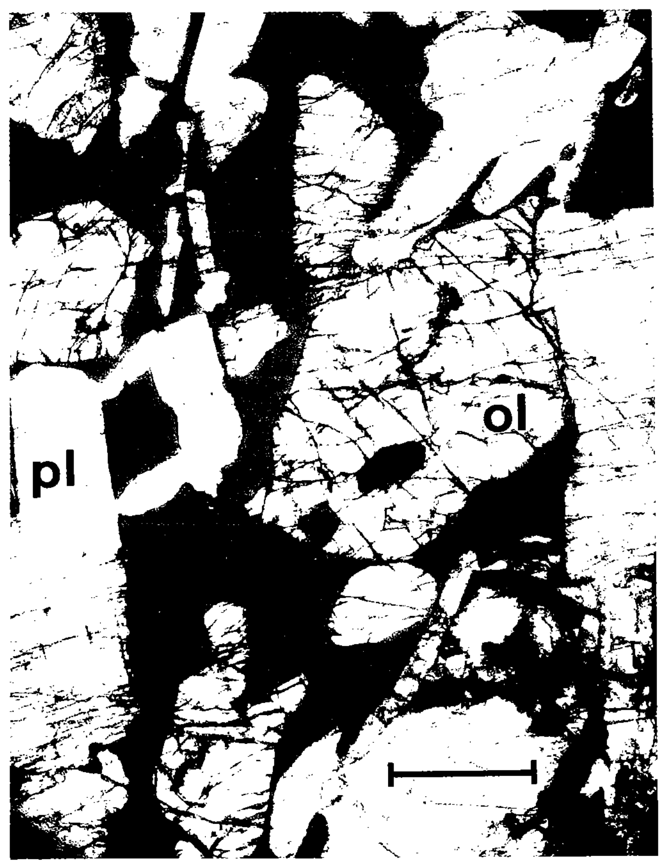

Figure 92. Photomicrograph of Glen Creek Gabbro showing abundant optically continuous kaersutitic amphibole (*a*) poikilitically enclosing olivine (*ol*), plagioclase (*pl*), and ilmenite and magnetite (opaque). Sample is from a lens of gabbroic material surrounded by ultramafic material; it contains abundant phlogopite, and the illustrated kaersutite, but contains no pyroxene. Bar is 1 mm. (Sample MP–27.)

rims around olivine. Accessory minerals include apatite and pyrite, plus sporadic pyrrhotite, chalcopyrite, and pleonaste spinel (rare), the latter occurring typically as tiny cores in magnetite grains.

Olivine, magnetite, and ilmenite concentrations in the Glen Creek Gabbro have given rise to unusual ultramafic masses that have been described petrographically by Powell and Fischer (1976) and Hanks (1978). Olivine (20–60 percent), magnetite (21–60 percent), and ilmenite (2–17 percent) together compose 72 to 99 percent of the mode (fig. 93). (Modal data reported in this section are based on 1,000 point-counts, each in transmitted and reflected light, on 30 ultramafic, 3 "transitional," and 26 gabbro samples.) Other phases in the ultramafic masses are interstitial to olivine and oxides, and include clinopyroxene (0–6 percent), orthopyroxene (0–1.2 percent), plagioclase (0–16 percent), pinkish-brown, kaersutitic amphibole (0.3–10.7 percent), and pleonaste spinel (0.1–1.6 percent). Trace amounts of red-brown phlogopite and sulfides also are present.

Representative pyroxene and olivine compositions from the Glen Creek Gabbro (gabbroic portions) are listed in tables 22 and 23, respectively, and are plotted in figure 94 along with some compositions from an ultramafic sample. Amphibole and phlogopite compositions from gabbro and ultramafic material are shown in tables 24 and 25, respectively. Systematic differences in Mg/(Mg + Fe) ratios of mafic silicates, between the gabbro and ultramafic rock as well as the gradational changes through modally transitional rocks, are illustrated in figure 95. The plagioclase composition averages An_{62} in both the gabbroic and ultramafic rocks.

Although their modes are exotic, the ultramafic masses have essentially the same mineralogy as the "ordinary" Glen Creek Gabbro that envelopes them. In mapping detailed relationships in the excavation known locally as Reid's magnetite pit (fig. 74), Hanks (1978) demonstrated the interfingering of gabbro and ultramafic rock (fig. 96) and the gradational "contacts" between the two tock types. Although smoothly gradational, the transition between them occurs on the scale of a few inches. The ultramafic masses are enveloped by gabbroic material that also occurs as small lenses or pods surrounded by the ultramafic material (fig. 96). These observations indicate an intimate genetic relationship between the olivine-oxide rock and the Glen Creek Gabbro, the former representing segregations within the latter. The ver-

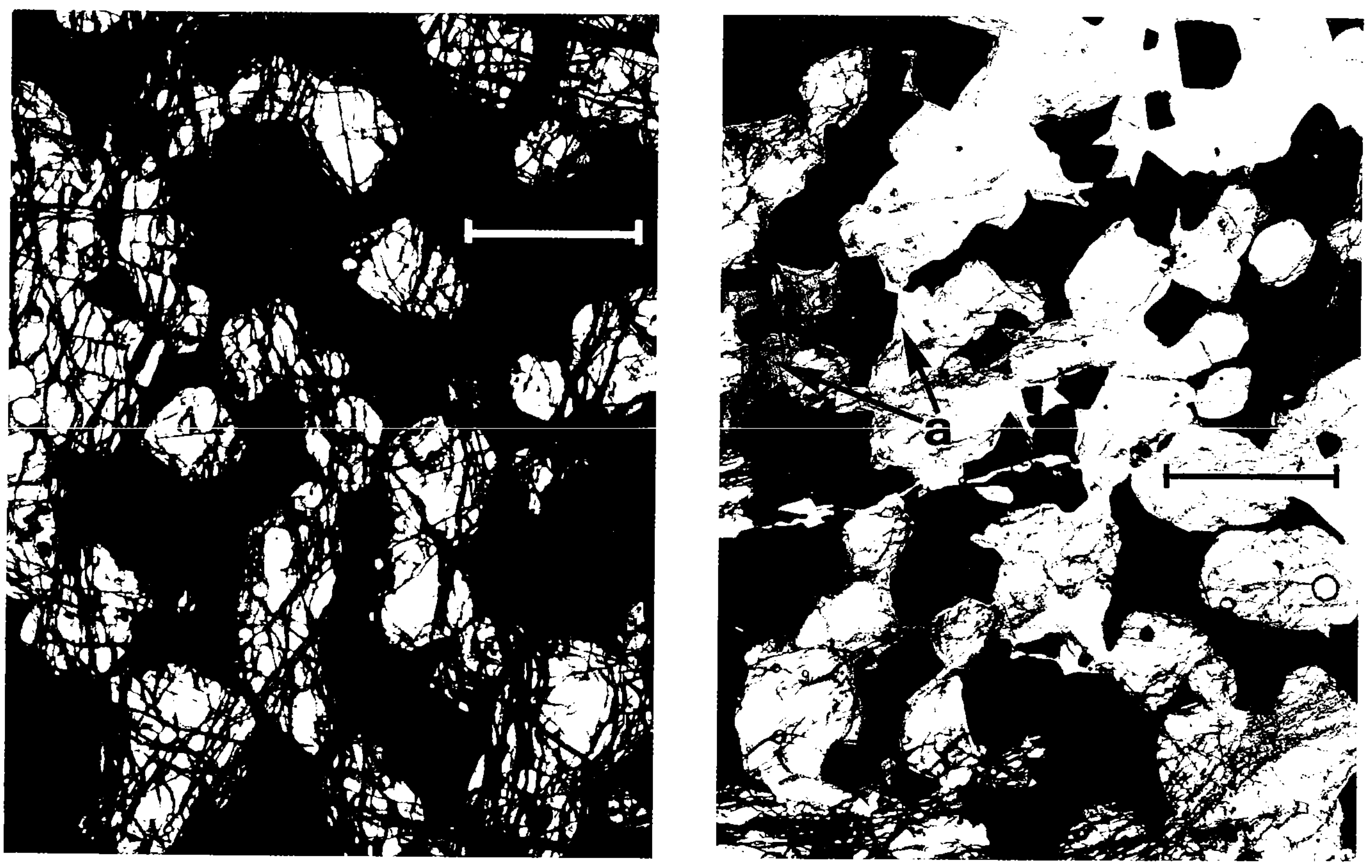

A *B*

Figure 93. Photomicrographs illustrating ultramafic segregation within Glen Creek Gabbro. *A*, magnetite–ilmenite-rich area; transparent grains are olivine. *B*, olivine-rich area; opaques are magnetite and ilmenite; note minor amphibole (*a*). Bar is 0.5 mm. (Sample WM–136.)

TABLE 22.—REPRESENTATIVE PYROXENE COMPOSITIONS FROM GABBROIC AND ULTRAMAFIC LITHOLOGIES ASSOCIATED IN GLEN CREEK GABBRO

(Microprobe analyses in weight %)

	1	2	3	4	5
SiO_2	52.5	52.6	52.4	52.1	51.3
TiO_2	0.45	0.39	1.11	1.23	1.19
Al_2O_3	1.60	0.97	3.01	3.26	3.14
FeO*	10.5	21.8	8.53	7.51	7.14
NiO	0.00	0.04	N.D.	N.D.	0.00
MgO	14.3	22.3	14.3	13.8	14.7
CaO	20.3	1.44	20.6	21.5	21.3
Na_2O	N.D.	N.D.	N.D.	N.D.	0.48
Total	99.65	99.54	99.95	99.40	99.25
Wo (mol %)	41.9	2.9	43.8	46.1	45.0
En (mol %)	41.1	62.7	42.1	41.3	43.2
Fs (mol %)	17.0	34.4	14.1	12.6	11.8
Atomic Mg/(Mg+Fe)	0.708	0.645	0.749	0.767	0.786
*Average Mg/(Mg+Fe)	0.712	0.646	0.754	0.756	0.786

Note: Averages are for several grains in the indicated sample. Total Fe is expressed as FeO.

Samples (all from Reid's magnetite pit, NE¼SW¼ sec. 14, T. 4 N., R. 17 W., Kiowa County):

1. Augite in gabbroic lithology (MP-2).
2. Hypersthene coexisting with augite no. 1, this table (MP-2).
3. Augite in gabbroic lithology close to ultramafic lithology (MP-22).
4. Salite in ultramafic lithology adjacent to gabbroic lens (MP-29).
5. Salite in ultramafic lithology (MP-24).

TABLE 23.—REPRESENTATIVE OLIVINE COMPOSITIONS FROM SANDY CREEK AND GLEN CREEK GABBROS

(Microprobe analysis in weight %)

	1	2	3	4	5	6	7
SiO_2	37.8	36.5	35.5	36.4	36.8	37.6	39.2
FeO*	28.8	31.9	39.0	34.7	33.7	27.9	25.2
MnO	0.37	0.50	N.D.	N.D.	0.37	0.33	N.D.
NiO	0.12	N.D.	0.01	0.08	0.19	0.04	0.10
MgO	32.5	30.9	25.0	27.9	29.3	34.4	36.1
CaO	0.02	0.03	0.04	0.05	0.05	0.05	0.08
Total	99.61	99.83	99.55	99.13	100.41	100.32	100.68
Fo (mol %)	66.8	63.3	53.4	58.9	60.7	68.7	71.9
*Average Fo (mol %)	67.5	66.6	53.6	58.3	60.8	68.6	71.5
*Average NiO	0.12	N.D.	0.03	0.06	0.07	0.07	0.10

Note: Averages are for several grains in the indicated sample. Total Fe is expressed as FeO.

Samples: (All Glen Creek Gabbro Samples are from Reid's magnetite pit, NE¼SW¼ sec. 14, T. 4 N., R. 17 W., Kiowa County.)

1. Sandy Creek Gabbro, olivine-rich, NE¼NW¼ sec. 9, T. 3 N., R. 15 W., Comanche County (WM-152).
2. Sandy Creek Gabbro, olivine-rich, SE¼NE¼ sec. 4, T. 3 N., R. 15 W., Comanche County (WM-309).
3. Glen Creek Gabbro, gabbroic lithlolgy (MP-2).
4. Glen Creek Gabbro, small amphibole-phlogopite-rich gabbroic lens within ultramafic segregation (MP-27).
5. Glen Creek Gabbro, gabbroic lithology close to ultramafic segregation (MP-22).
6. Glen Creek Gabbro, ultramafic lithology close to gabbroic lens (MP-25).
7. Glen Creek Gabbro, ultramafic segregation (MP-24).

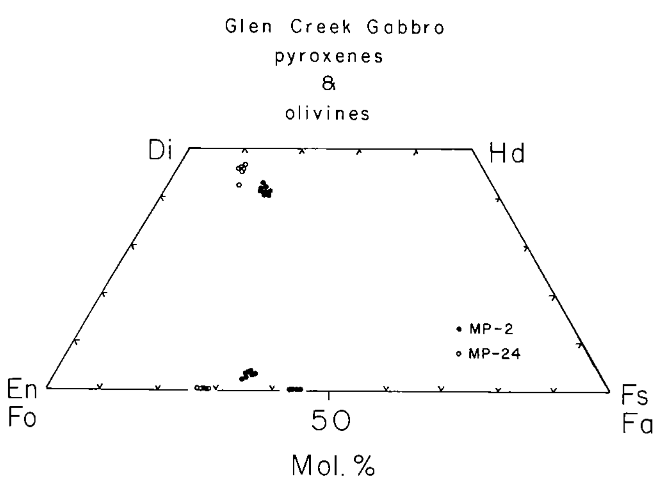

Figure 94. Pyroxene and olivine compositions from Glen Creek Gabbro. Olivines are plotted along base of diagram. Solid circles are from gabbroic rock (MP-2), and open circles are from ultramafic rock (MP-24). Note systematically higher magnesian compositions in latter (see text). Low-Ca pyroxenes are primary hypersthene, not inverted pigeonite. Sample locations are shown in figure 96.

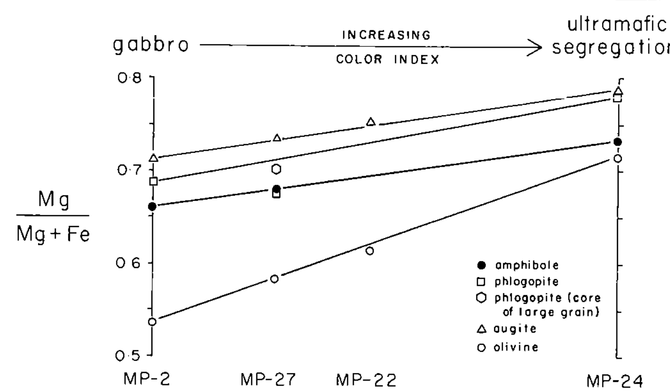

Figure 95. Systematic differences in Mg/(Mg + Fe) ratios in silicate phases in Glen Creek Gabbro and its ultramafic segregations. Horizontal "axis" (color index) is not quantified, lateral positions of samples MP-27 and MP-22 being determined by best fit of a given vertical array of plotted points on "lines" defined by "end-members" MP-2 (gabbro with minor olivine and oxides) and MP-24 (olivine–oxide rock). (Qualitatively, the positions of MP-27 and MP-22 are correct in a relative sense.) Diagram illustrates systematically higher magnesian compositions of silicate phases in ultramafic segregations and magnitude of differences. (See text for discussion and figure 96 for sample locations.)

tical extent of the ultramafic concentration in Reid's pit is not known, but test drilling indicated a minimum thickness of 15 m (H. E. Hunter, personal communication, 1974).

The high Mg values from amphibole, phlogopite, pyroxene, and olivine in the ultramafic segregations are considered to represent magmatic compositions and are attributed to locally elevated fO_2. Virtually identical plagioclase compositions suggest that liquidus temperatures were similar in the two contrasted rock types. In contrast to the silicates, the coexisting ilmenite and magnetite (determined by microprobe) have equilibrated to subsolidus temperatures (700°–800° C) and fO_2 values near the fayalite–magnetite–quartz buffer curve (modified Buddington–Lindsley fO_2–T thermobarometer), thus eliminating any oxide "fingerprint" of initial heterogeneities in magmatic fO_2 values (see fig. 97).

Mechanical aspects of the crystallization environment probably played some role in the formation of the ultramafic masses. The form and distribution of the olivine–oxide concentrations suggest flow segregation rather than simple gravitational accumulation under quiescent conditions. The concentration process was substantially influenced by

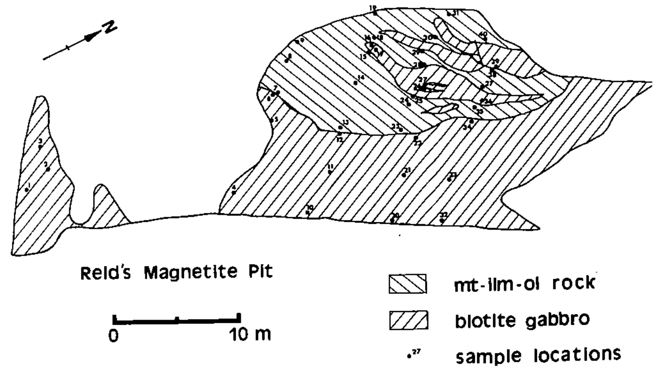

Figure 96. Map of Glen Creek Gabbro exposures in Reid's magnetite pit, NE¼SW¼ sec. 14, T. 4 N., R. 17 W., Kiowa County, illustrating relationship of ultramafic segregations and gabbro. (Glen Creek Gabbro is exposed over a much wider area than shown here.) Unpatterned areas are surficial cover. Rock type labeled "biotite gabbro" contains amphibole and phlogopite (not biotite) and refers to average Glen Creek Gabbro (see text for variations); ultramafic segregations within gabbro are labeled "*mt–ilm–ol* rock" (see text for petrographic description). Note interfingering of the two rock types, which are gradational (over distances of a few inches or less) across indicated "contacts." Map and sampling by C. L. Hanks. (All sample numbers are prefaced with *MP*.)

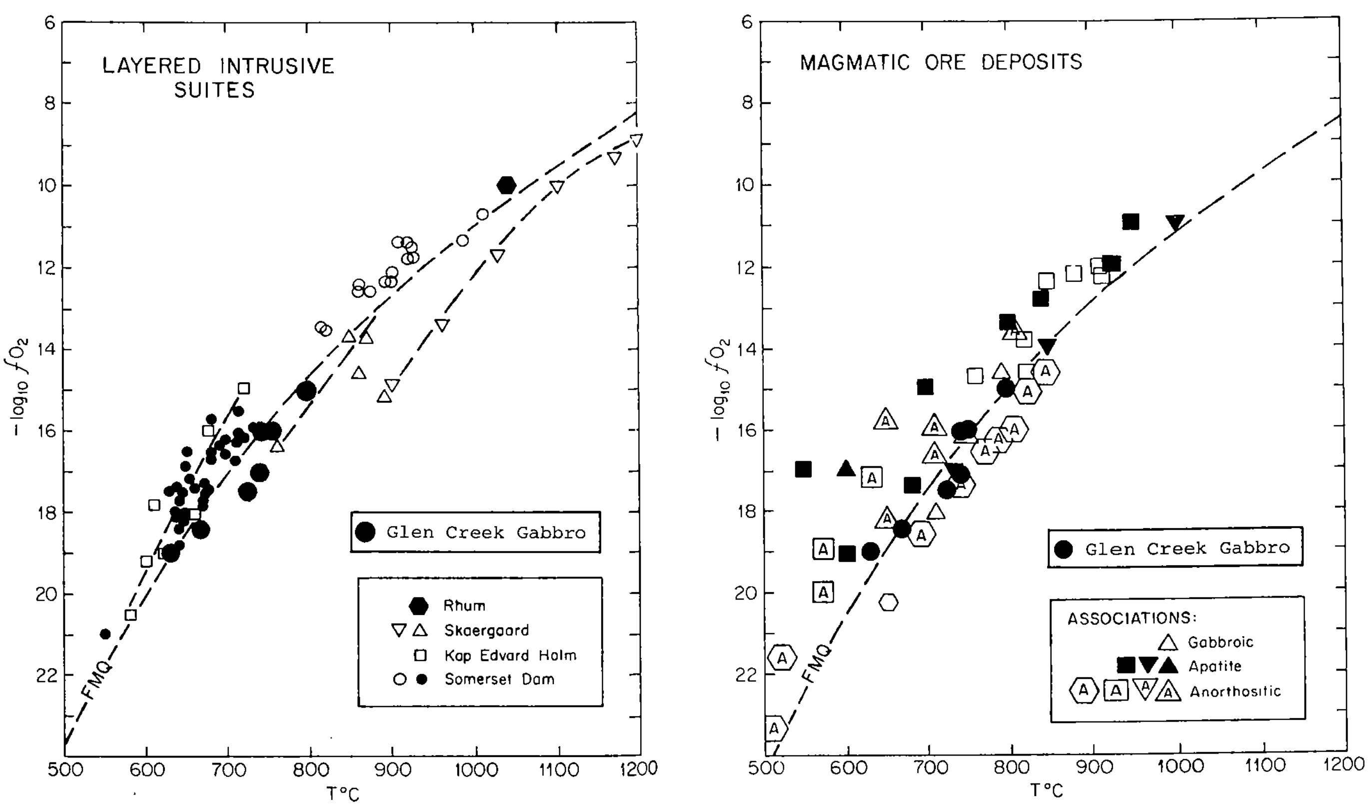

Figure 97. Temperature fO_2 determinations of Glen Creek Gabbro and its ultramafic segregations (both shown as large solid circles), using modified Buddington–Lindsley ilmenite–magnetite thermobarometer. Diagrams are after Haggerty (1976, figs. Hg–44c, Hg–45). Oxides in the two types of Glen Creek Gabbro have equilibrated to a similar range of subsolidus T–fO_2 values near the fayalite–magnetite–quartz *(FMQ)* buffer curve, not unlike Fe–Ti oxides in other basic intrusive rocks and associated ore deposits.

TABLE 24.—ANALYSES OF AMPHIBOLES IN GLEN CREEK GABBRO

	1		2		3		4	
	MP-2		MP-27		MP-24		WM-154	
SiO_2	42.2		41.0		39.7		42.0	
TiO_2	3.51		4.61		4.68		3.53	
Al_2O_3	11.0		11.2		12.9		11.0	
Fe_2O_3	2.31		2.10		1.68		2.25	
FeO	11.8		10.7		8.54		11.5	
MgO	12.8		12.8		13.0		12.2	
CaO	11.5		11.4		12.3		11.3	
Na_2O	2.10		2.35		2.66		2.18	
K_2O	1.10		1.19		0.99		1.01	
SUM†	98.32		97.35		96.45		96.97	
Si	6.233	8.000	6.113	8.000	5.927	8.000	6.276	8.000
Al^{iv}	1.767		1.887		2.073		1.724	
Al^{vi}	0.141		0.074		0.203		0.211	
Fe^{3+}	0.258		0.235		0.189		0.253	
Ti	0.390	5.000	0.517	5.000	0.525	5.000	0.397	5.000
Mg	2.830		2.841		2.895		2.707	
Fe^{2+}	1.381		1.333		1.066		1.432	
Fe^{2+}	0.076						0.005	
Ca	1.814		1.821		0.122		1.815	
Ca		2.000		2.000	1.839			2.000
Na	0.110		0.179		0.161	2.00	0.180	
Na	0.492	0.700	0.500	0.726	0.608	0.796	0.452	0.644
K	0.208		0.226		0.188		0.192	
$Mg(Mg+Fe^{2+})$	0.660		0.681		0.731		0.653	

NOTES TO TABLE

*Fe_2O_3 calculated assuming $Fe^{3+}/(Fe^{3+}+Fe^{2+}) = 0.15$

†Analyses are by microprobe and do not include H_2O, F, Cl.

Analyses (averages of several in each sample):

1. Titanian magnesian hastingsite from olivine-gabbro (MP-2). Olivine Fo_{54}.
2. Kaersutite from amphibole-rich olivine-gabbro lens within untramafic segregation (MP-27). Olivine Fo_{58}.
3. Kaersutite from ultramafic segregation (MP-24). Olivine Fo_{72}.
4. Titanian magnesian hastingsitic hornblende from olivine gabbro dike probably related to Glen Creek Gabbro (WM-154). Olivine Fo_{52}.

TABLE 25.—PHLOGOPITE AND BIOTITE ANALYSES FROM GLEN CREEK AND SANDY CREEK GABBROS

	1	2	3	4	5	6	7	8
	MP-2	MP-27	MP-24	WM-152	WM-337	WM-309	WM-359	WM-360
SiO_2	37.2	37.0	38.2	37.5	37.6	38.3	37.5	38.0
TiO_2	4.60	6.59	4.80	4.95	4.54	4.07	6.37	5.66
Al_2O_3	15.2	14.6	15.8	14.8	14.6	14.0	13.1	13.3
Fe_2O_3*	0.73	0.72	0.51	0.66	0.75	0.61	0.93	0.97
FeO*	12.5	12.3	8.72	11.26	12.8	10.4	15.9	16.7
MgO	16.2	15.4	18.5	16.7	16.5	17.8	12.9	12.7
CaO	0.04	0.03	0.13	0.03	0.07	0.04	0.03	0.03
Na_2O	0.28	0.52	0.59	0.32	0.61	0.78	0.05	0.10
K_2O	9.59	9.07	8.49	9.20	9.02	8.09	9.38	9.19
SUM†	96.34	96.23	95.74	95.42	96.49	94.09	96.16	96.65
Mg/(Mg+Fe)	0.686	0.679	0.782	0.714	0.684	0.743	0.578	0.563

*Fe_2O_3 calculated assuming $Fe^{2+}/(Fe^{3+}+Fe^{2+}) = 0.05$

†Analyses are by microprobe and do not include H_2O, F, Cl (about 4-5% in phlogopite).

1. Phlogopite in Glen Creek Gabbro (olivine Fo_{54}). (MP-2)
2. Titaniferous phlogopite in olivine gabbro lens within ultramafic segregation in Glen Creek Gabbro (olivine Fo_{58}). (MP-27)
3. Phlogopite in ultramafic segregation in Glen Creek Gabbro (olivine Fo_{72}). (MP-24)
4. Phlogopite in olivine-bearing (Fo_{68}) Sandy Creek Gabbro. (WM-152)
5. Phlogopite in olivine-bearing (Fo_{66}) Sandy Creek Gabbro. (WM-337)
6. Phlogopite in olivine-bearing (Fo_{67}) Sandy Creek Gabbro. (WM-309)
7. Titaniferous biotite in quartz-bearing Sandy Creek Gabbro. (WM-359)
8. Titaniferous biotite in Sandy Creek Gabbro with interstitial "granophyre". (WM-360)

nucleation mechanisms in an inhomogeneous (at least with respect to fO_2) magma.

The cause of locally elevated fO_2 in the Glen Creek Gabbro magma remains unclear. That it relates to heterogeneities in H_2O content is suggested by the presence, within the olivine–oxide rock, of small lenses and pods of gabbroic lithology that are abnormally enriched in amphibole (kaersutite) and phlogopite to the exclusion of pyroxene, but with the other phases—olivine, plagioclase, oxides, and others—present in their usual abundances (fig. 98). The source of the extra H_2O is not known, although the implication that its concentration is localized suggests a local source. This is problematic, however, because the rock enveloping the Glen Creek Gabbro (at least at the exposed level) is the anhydrous Glen Mountains Layered Complex, which is nonporous and unlikely to contain much meteoric water. For the present, the question remains unresolved.

Ultramafic material petrographically similar to that in the Glen Creek Gabbro was reported by Ham and others (1964, p. 266) in the subsurface in sec. 35, T. 7 N., R. 18 W., Kiowa County, indicating that olivine–magnetite–ilmenite rock is not unique to the Glen Creek locality. According to Ham and others, the rock has the following modal abundances: "iron ore" (28 percent), olivine (27 percent), pyroxene (20 percent), calcite (8 percent), chlorite (9 percent), iddingsite (2 percent), apatite (2 percent), plagioclase (2 percent), and "basaltic hornblende" (1 percent). The rock is relatively altered, and we do not know from the brief description whether it originally contained primary biotite or phlogopite. Associated rock types were not reported, and its origin is not known. We mention it here to point out that the ultramafic occurrence at the Glen Creek locality may not be unique in the province, although such lithologies are rare in rocks available for sampling.

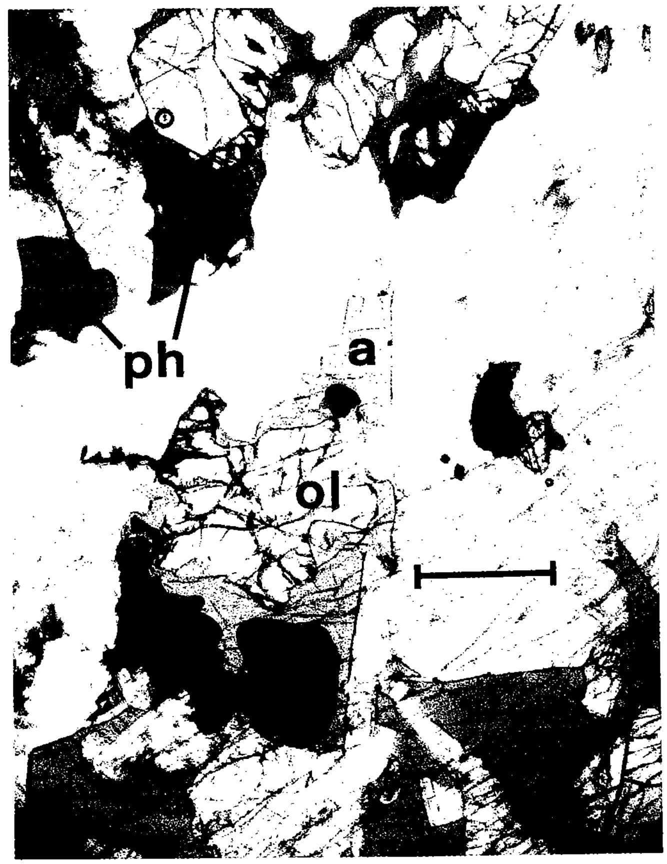

Figure 98. Photomicrograph of sample of gabbroic lens surrounded by ultramafic material in Glen Creek Gabbro (sample MP–27). (See figure 96 for sample location.) Abundant kaersutitic amphibole (*a*) and phlogopite (*ph*) occupy usual textural position of pyroxene, which is absent from this sample. White grains are plagioclase; opaques include magnetite and ilmenite. Phlogopite and amphibole are optically continuous over their respective areas shown (and larger). Bar is 1 mm.

STOP 2—HIGHWAY 54 AREA

Transition between M and N Zones of Glen Mountains Layered Complex. Secs. 25–27, 34–36, T. 4 N., R. 16 W., Kiowa County, Oklahoma. **M. L. Stockton** and **J. D. Giddens III.**

Introduction

Parking locations for the M and N Zones are marked as P on the accompanying map (fig. 99). Access to the Willis Ranch (sec. 34 and most of sec. 27) and to the NW¼ sec. 35 is controlled by Jerry Treadwell. The NW¼ and the NW¼SW¼ of sec. 26 are owned by James Raasch.

The remainder of sec. 26, the NE¼ sec. 35, and the S½ sec. 25 may be entered by permission of James or Nick Callen. The Callen ranch house is located in the center, NE¼ sec. 26. Access is from the section-line road to the north, ¾ mile east of State Highway 54.

The only earlier map available for this area is by Chase (1950b). He located many of the outcrops, but his definitions of the mappable units have been superseded by later work. Alipouraghtapeh (1979) did a reconnaissance geochemical study of the Raggedy Mountain Gabbro Group in this area. Table 26 lists three bulk-rock determinations of samples noted on the map (fig. 99).

Geology

M Zone rocks in the Cooperton Quadrangle are essentially similar to those in the Glen Mountains Quadrangle, described by Gilbert (1960) and Spencer (1961).

Rock types are anorthosite, anorthositic gabbro, and olivine gabbro. The characteristic pyroxenes are of fine-ophitic texture; that is, the plagioclase crystals within the pyroxene are anhedral, randomly oriented, and much smaller than those of the surrounding matrix (fig. 100). The pyroxenes are nearly spherical, ranging in size from 1 to 6 cm. They typically stand out in relief, and the rocks have very rough, lumpy surfaces where weathering has been severe. In many places, the pyroxenes occur in layers or bands, or small, ophitic crystals may cluster together in larger masses (fig. 101).

Olivine is abundant, although it is not present in all rocks. Crystals are small (2–5 mm) and are most commonly represented as weathered pits on rock surfaces (fig. 102). Olivine may accumulate in layers, as discrete grains or in combination with fine-ophitic pyroxenes, but more commonly they are randomly distributed.

Plagioclase lamination is well developed in many outcrops and is present to some degree in most.

Within the map area, a number of outcrops are transitional to the N Zone.

Overlying the M Zone is a section of rock that does not crop out to the west in previously mapped areas. It is here indicated as the N Zone.

The N Zone bears some resemblance to both the M and L Zones. The predominant rock type is anorthositic gabbro with a few occurrences of anorthosite.

The N Zone is characterized by clinopyroxene of two textural types. The first type shows zoned ophitic crystals with distinct cores and marginal halos (figs. 103, 104). The dense, pyroxene-rich core encloses small, anhedral plagioclase grains, and is similar to the fine-ophitic pyroxene common in the M Zone. The core is rimmed by an optically continuous halo in which the pyroxene is less abundant and is interstitial among larger, subhedral plagioclase crystals. This type is common where present, but it is found in only a few areas in the Cooperton Quadrangle.

TABLE 26.—ANALYSES OF SAMPLES FROM GLEN MOUNTAINS LAYERED COMPLEX

(From Alipouraghtapeh, 1979)

	M-Zone	N-Zone	
Wt %	WC-31	WC-32	WC-33
SiO_2	48.73	49.71	47.40
TiO_2	0.15	0.56	0.20
Al_2O_3	34.50	32.00	30.00
FeO[1]	0.80	2.10	2.95
MgO	0.38	1.63	1.34
MnO	0.02	0.02	0.02
CaO	11.97	12.00	(3.70)
Na_2O	2.73	3.68	3.10
K_2O	0.19	0.23	0.23
P_2O_5	0.16	0.30	0.27
ppm			
Cu	21	34	50
Cr	3	5	14
Zn	26	26	30
Pb	10	20	30
Ni	16	16	25
Ba	60	65	70
Sr	567	494	460
V	30	70	90
Total	99.64	102.23	(99.10)

1 = all Fe as FeO

EXPLANATION

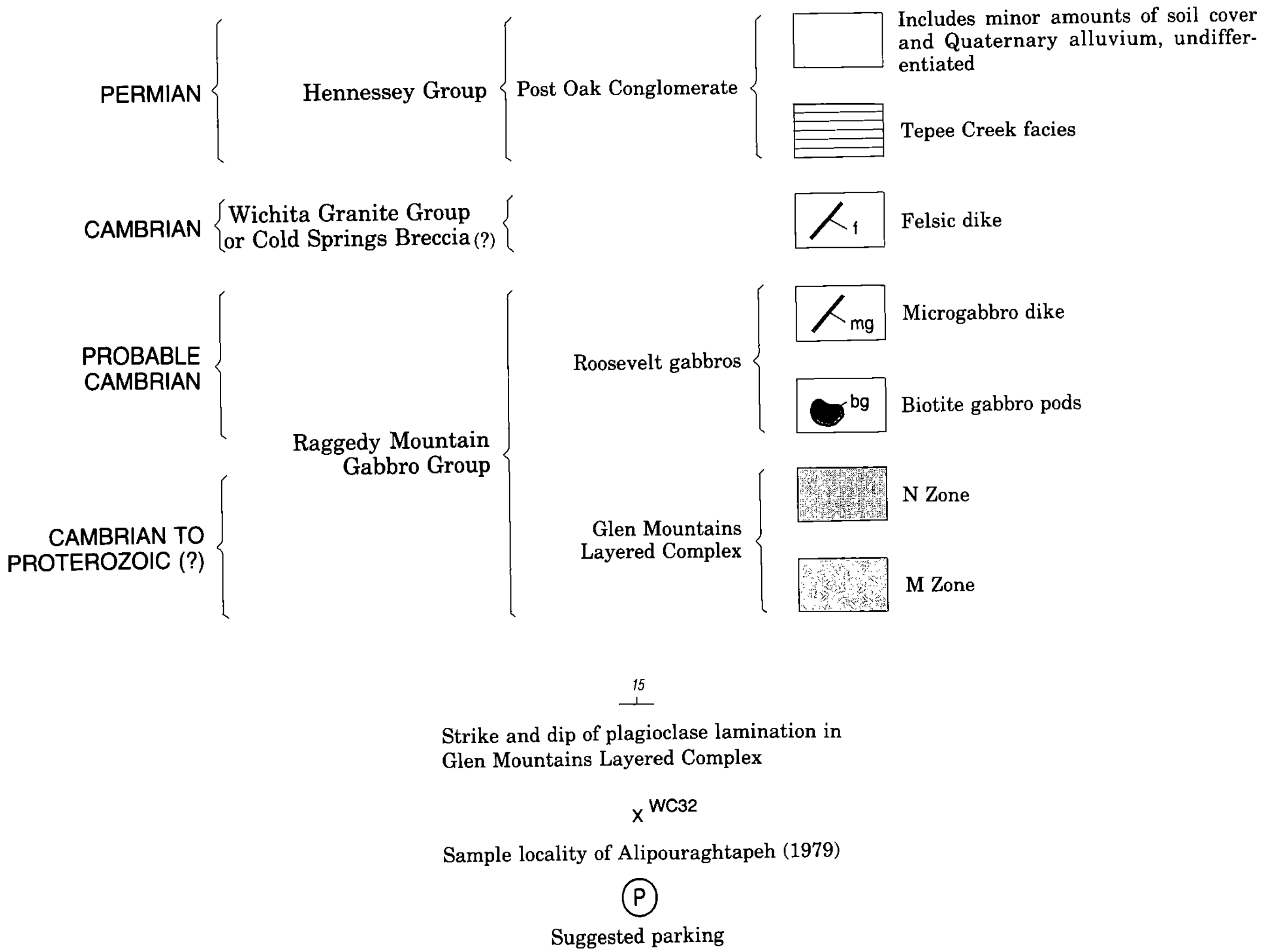

Geology by M. L. Stockton and J. D. Giddens III

Base from U.S. Geological Survey, Cooperton, 1:24,000, 1956
Photorevisions as of 1975

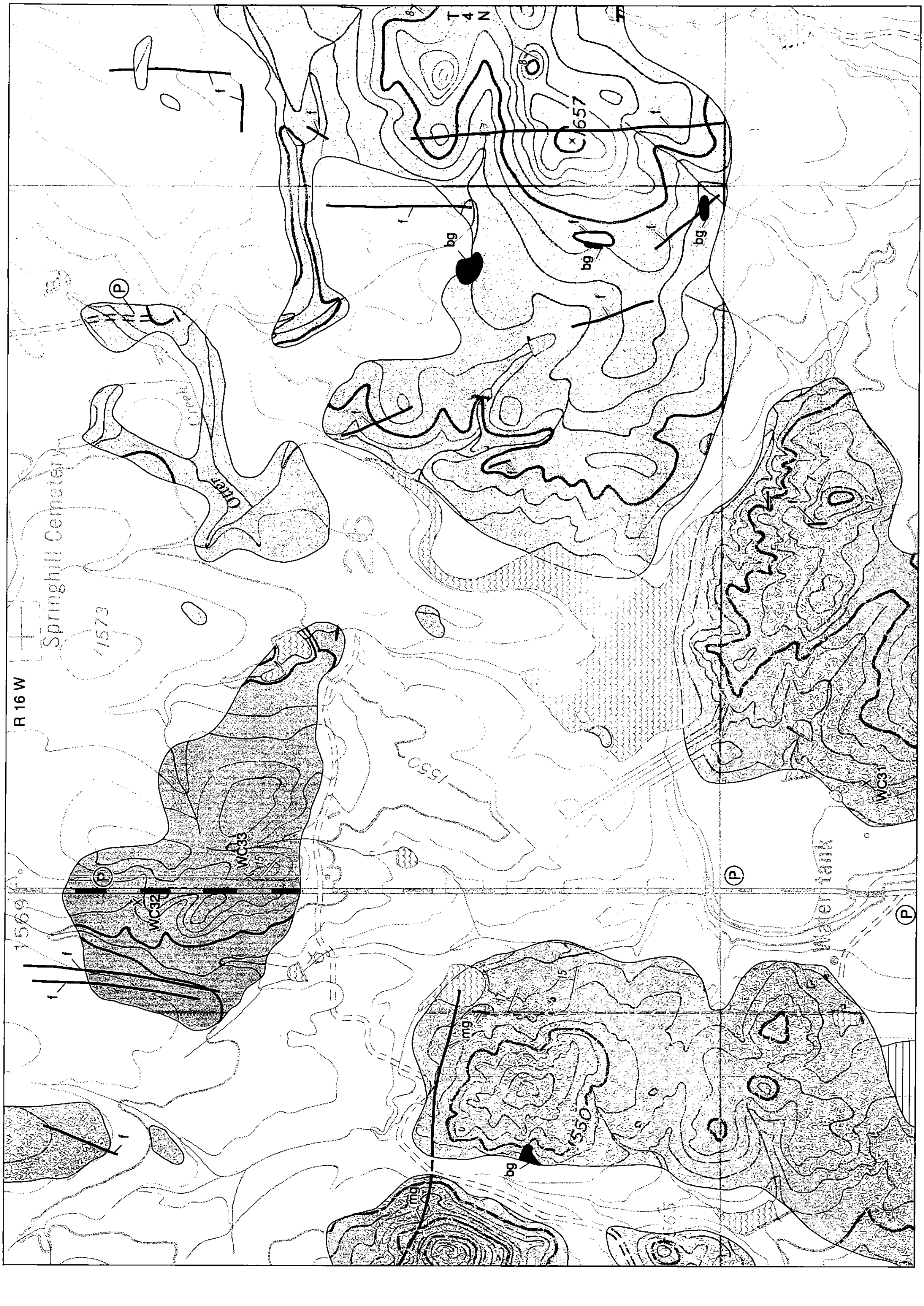

Figure 99. Map showing igneous geology of M–N transitional area of Glen Mountains Layered Complex, Kiowa County, Oklahoma (Stop 2). Map scale, 1:12,000.

Figure 100. Photomicrograph of whole thin section from olivine gabbro of M Zone. Fine-ophitic pyroxenes enclose plagioclase grains which are anhedral and smaller than those in the surrounding matrix.

Figure 101. Ophitic pyroxenes in M Zone. Dark spots are clusters of two to five individual grains, elongated in plane of layering.

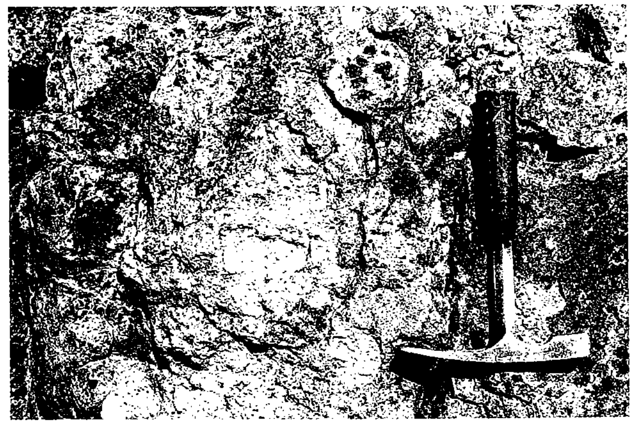

Figure 102. Olivine gabbro of M Zone exhibiting pits from weathered olivine.

Figure 103. Anorthositic gabbro of N Zone in which reflecting cleavage faces outline clinopyroxene of first textural type.

The second textural type is ubiquitous throughout the N Zone. These pyroxenes are subophitic or interstitial, and have a starved, "chicken-wire" appearance on rock surfaces. They are irregularly shaped and vary in size from 2–3 cm to 20 cm. Pyroxene of this type has more chadocrysts in the N Zone than in the L Zone.

Although the plagioclase in the N Zone is generally subhedral and lath-shaped, the grains in a number of localities are anhedral and have a disorganized, "crystal-mosaic" texture.

Olivine is absent in all but a few localities in the N Zone. Where it does occur it is abundant and clustered in masses.

Magnetite is extremely abundant and ubiquitous in the N Zone. It occurs as interstitial grains, as poikilitic crystals enclosing plagioclase, and as intergrowths with pyroxene that commonly form red lumps 5 to 10 mm across on rock surfaces.

Orthopyroxene is more common in the N Zone than in the M Zone of this area. It occurs as intergrowths with clinopyroxene and magnetite. Olivine, where present, commonly bears reaction rims of orthopyroxene.

Traces of late-magmatic quartz, biotite, and brown hornblende are found locally. These minerals do not occur in the lower zones.

The N Zone is characterized by igneous lamination that is more poorly defined than the lamination in underlying zones. Obvious rhythmic layering is rarely found. Boulders are rounded and rock surfaces are smoother than in the M Zone.

Much of the N Zone rock appears to have been subjected to hydrothermal alteration. Mafic minerals are altered to chlorite, tremolitic amphibole, and epidote. Three miles east and northeast of the map area, the layered complex is so intensely altered that it cannot be assigned to a zone.

An unusual nonigneous rock occurs in the southwestern part of the map area (center S½NE¼ sec. 34), on a ridge west of State Highway 54. This is a brick-red, well-indurated arkose, thought to represent the Permian Tepee Creek lithofacies of the Post Oak Conglomerate (Merritt and Ham, 1941; Mayes, 1947; Chase, 1950, 1954).

The rock, 0.5 to 3 mm in grain size, is composed of quartz, perthite, plagioclase, magnetite, and white mica, as well as both granitic and anorthositic rock fragments, in a very fine-grained matrix. It has a vuggy, honeycombed texture from weathering of unstable minerals (fig. 105).

Figure 104. Photomicrograph of thin section from N Zone exhibiting part of a zoned ophitic pyroxene.

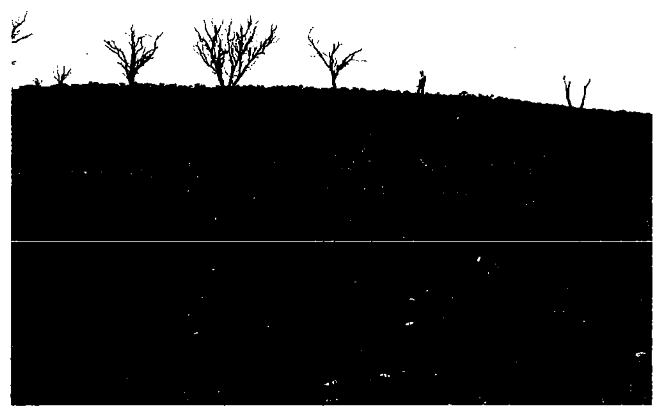

Figure 105. Ridge-forming Tepee Creek facies of Post Oak Conglomerate.

STOP 3—HALE SPRING LOCALITY

Relationships among Sandy Creek Gabbro, Mount Scott Granite, pegmatites of Quanah Granite, and Meers Quartzite. Secs. 3–5, 8–10, T. 3 N., R. 15 W., Comanche County, Oklahoma. **B. N. Powell, M. L. Stockton, J. D. Giddens III**, and **M. C. Gilbert**.

Introduction

Suggested parking locations are marked as P on accompanying maps (figs. 106A, 106B). Do not block ranch gates.

Access to the privately owned portions of this area is controlled by John Phelan (W½ sec. 4, E½ and SW¼ sec. 9, all of sec. 8, SE¼ sec. 5) and Jim Snell (E½ sec. 4, NW¼ sec. 9). The wildlife refuge north of State Highway 49 (sec. 3 and northern portion of sec. 10) is a special-use area, not accessible to the public. The area is regularly patrolled, and trespassers are fined. Access is by permit from the refuge manager, and generally permission is granted only for research purposes. This stop has a wealth of fascinating and key geologic features. The substrate in the immediate area is the Sandy Creek Gabbro Member of the Roosevelt Gabbros (figs. 106A, 106B, 107). Figure 108 is a photograph taken in June 1978, looking eastward across the gabbro body toward the pronounced outcrop "V" which is defined by erosion into the overlying Mount Scott Granite. The subhorizontal nature of the contact is clear. One of the type areas that Merritt (1965) used to define the Mount Scott Granite is the Ira Smith Quarry, just south of the photograph and along State Highway 49. This quarry was figured in earlier guidebooks (Stone, 1967; Powell and Fischer, 1976). However, the gabbro–granite contact, and local character of the Mount Scott, also are items of special interest here. The Hale Spring pegmatites (Johnson, 1955) are a series of pegmatoid dikes or veins cutting the Sandy Creek Gabbro and the Mount Scott Granite. Because these dikes are so similar to numerous others throughout the Quanah Granite terrane of the eastern Wichitas, they are assumed to be late emanations from a subjacent lobe of Quanah and are so shown on the cross section (fig. 107). Scofield and Gilbert (this guidebook) discuss the mineralogy of the dikes. Stockton and Giddens (this guidebook) report two new occurrences of Meers Quartzite in the area, one underlain by the Sandy Creek and one by the Mount Scott. Gilbert, and Sides and Miller (this guidebook), discuss occurrences of Meers and revisions in previous interpretations.

This stop reports on the most detailed mapping and work now available for the area. The only previous work was that of Chase (1950), whose study was more regional, and Johnson (1955), who studied the pegmatites. Alipouraghtapeh (1979) did a reconnaissance geochemical survey of part of the Raggedy Mountain Gabbro Group. The data he reported for the Sandy Creek Gabbro are given in table 27, approximately keyed to the outcrop numbers used on our map. The more detailed data generated by Powell, and reported shortly, can be used more effectively for petrogenetic interpretations. Al-Shaieb (1978) also reported new data on U and Th concentrations and their distributions in mineral phases of the Hale Spring pegmatites and Quanah Granite.

Sandy Creek Gabbro

The Sandy Creek Gabbro Member of the Roosevelt Gabbros (table 2) occurs in sec. 4 and the N½ secs. 3 and 9, T. 3 N., R. 15 W., Comanche County (see figs. 106, 119, 120). The gabbro is exposed over approximately 5 km^2. It weathers to a dark-reddish-black, very hard and dense rock, commonly with a scalloped, rough surface (fig. 109).

Although the lower boundary is not exposed, the upper limit is defined by the Mount Scott Granite, which nonconformably overlies the gabbro, forming the higher elevations on three sides of the gabbro exposure.

The contact between older gabbro and younger granite can be closely located in the SE¼NE¼NW¼ sec. 9, T. 3 N., R. 15 W. Here, the gabbro is olivine-rich, and the granite is Mount Scott. In the SW¼NE¼ sec. 3, T. 3 N., R. 15 W., the approximate contact lies between quartz–alkali feldspar–bearing gabbro and younger granite, here containing aegerine. Dips of laminated olivine gabbro in the SE¼NE¼NW¼ sec. 9, T. 3 N., R. 15 W., are approximately 20°–30° to the east-southeast (fig. 110). Assuming that the layering originally was broadly horizontal, the quartz-bearing gabbro in sec. 3 must be upsection, which is consistent with differentiation of a tholeiitic gabbro by gravitational crystal fractionation. An important implication of this interpretation is that the gabbro body must have been structurally tilted prior to granite emplacement, offering indirect evidence for a considerable time lag between the gabbroic and granitic intrusions.

The Sandy Creek Gabbro on average is a medium-grained rock with hypautomorphic-granular texture. Plagioclase is generally the most abundant phase and commonly forms euhedral laths 1 to 5 mm long. Olivine is abundant in some samples, forming rounded and embayed grains that are commonly rimmed by orthopyroxene (fig. 111). Augite typically surrounds plagioclase and olivine, forming subophitic to ophitic texture (fig. 112). Some olivine-bearing samples exhibit lamination formed by plagioclase (fig. 113). Pinkish-brown amphibole and red-brown mica—primary magmatic phases—are ubiquitous and interstitial (fig. 114). The former is typically titanian magnesio-hastingsitic hornblende in olivine-bearing rocks; the latter is phlogopite (4–5 weight percent TiO_2) in olivine gabbro, and titaniferous biotite (5.5–6.5 weight percent TiO_2) in quartz-bearing gabbro. (See tables 25 and 28.) Representative pyroxene compositions are listed in table 29 and plotted in figure 115. The relatively Fe-rich, low-Ca pyroxenes plotted in figure 115 occur in fractionated quartz-gabbro and are primary hypersthene, not inverted pigeonite. In typical differentiated gabbroic intrusions, the primary (liquidus) low-Ca pyroxene

EXPLANATION

Age	Group	Unit	Map unit
PERMIAN	Hennessey Group	Post Oak Conglomerate	Includes minor amounts of soil cover and Quaternary alluvium, undifferentiated
CAMBRIAN	Wichita Granite Group		Diabase dike (d)
			Hale Spring pegmatites (Quanah Granite)
			Aplite dike (a)
			Hybrid rocks
			Mount Scott

UNCONFORMITY

Age	Group	Unit	Map unit
PROBABLE CAMBRIAN	Raggedy Mountain Gabbro Group	Roosevelt gabbros	Sandy Creek
CAMBRIAN (?) TO PROTEROZOIC		Glen Mountains Layered Complex	Xenoliths in Sandy Creek Gabbro
	Tillman Metasedimentary Group		Meers Quartzite

A———————*A′*

Line of cross section

(P)

Parking area for field trip

Sandy Creek Gabbro Sample Localities of Powell:

○ 300 Much altered, precursor type not specified

▲ 311 Fresh, "Saturated" (no olivine, no quartz)

■ 323 Fresh, quartz-bearing

● 372 Fresh, olivine-bearing

≻— Adit

Geology by M.L. Stockton; J. D. Giddens III, B. N. Powell, and M. C. Gilbert
Additional Information from Chase (1950b) and Johnson (1955)

Base from U. S. Geological Survey, Cooperton-Odetta, 1:24,000, 1956
Photorevisions as of 1975

(See pages 104 and 105 for maps.)

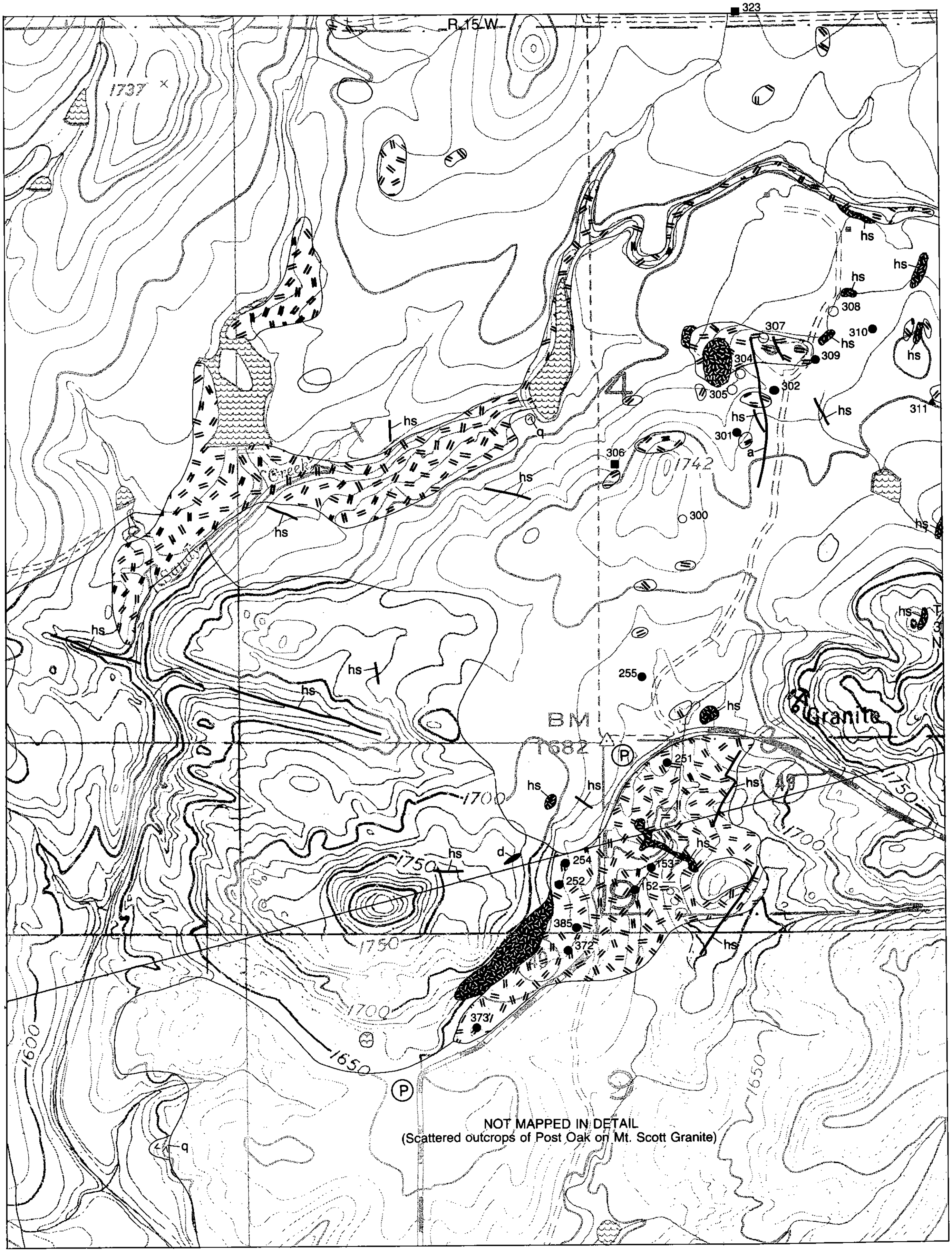

Figure 106A. Geologic map (west part) for Stop 3. Map scale, 1:12,000. See page 103 for explanation.

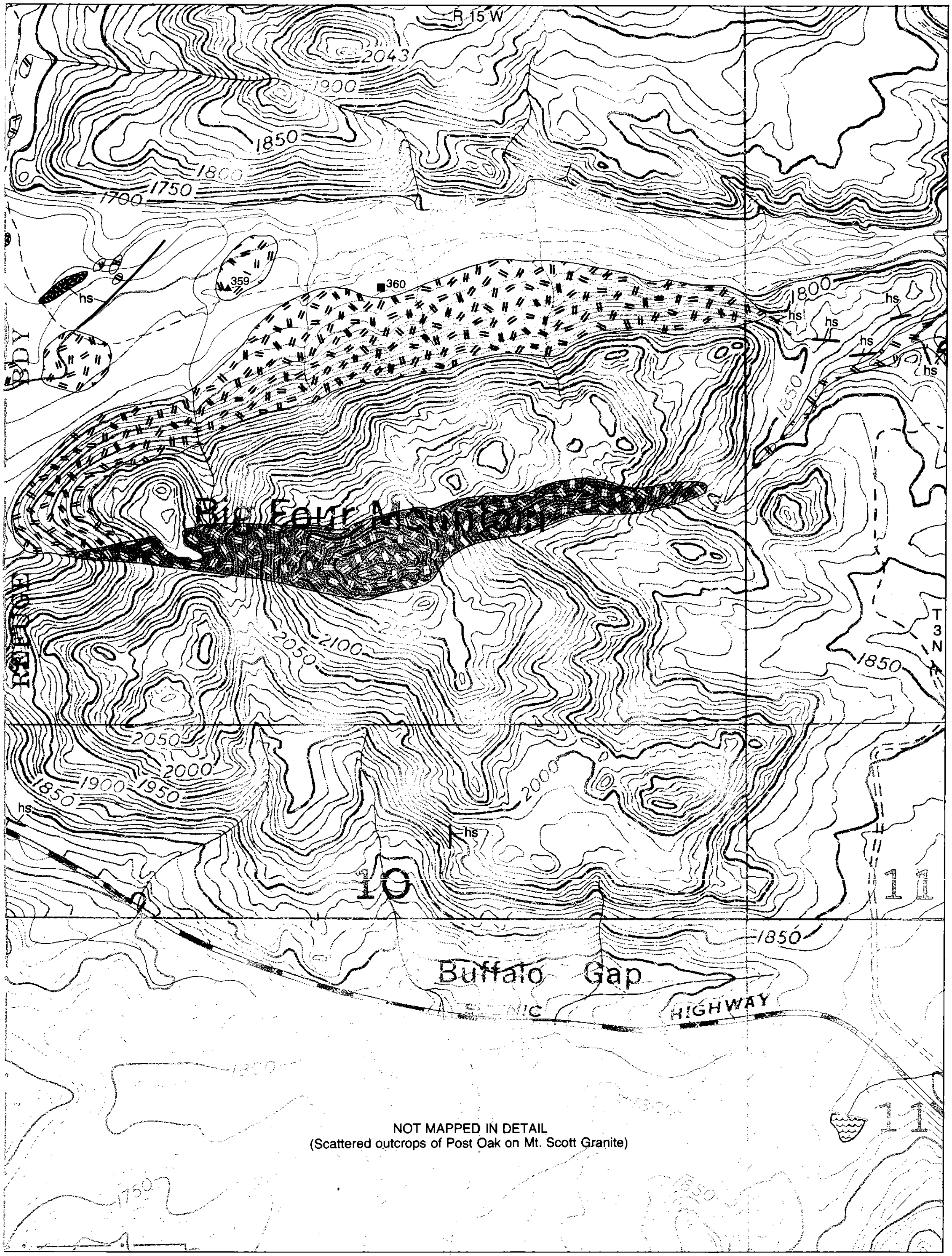

Figure 106B. Geologic map (east part) for Stop 3. Map scale, 1:12,000. See page 103 for explanation.

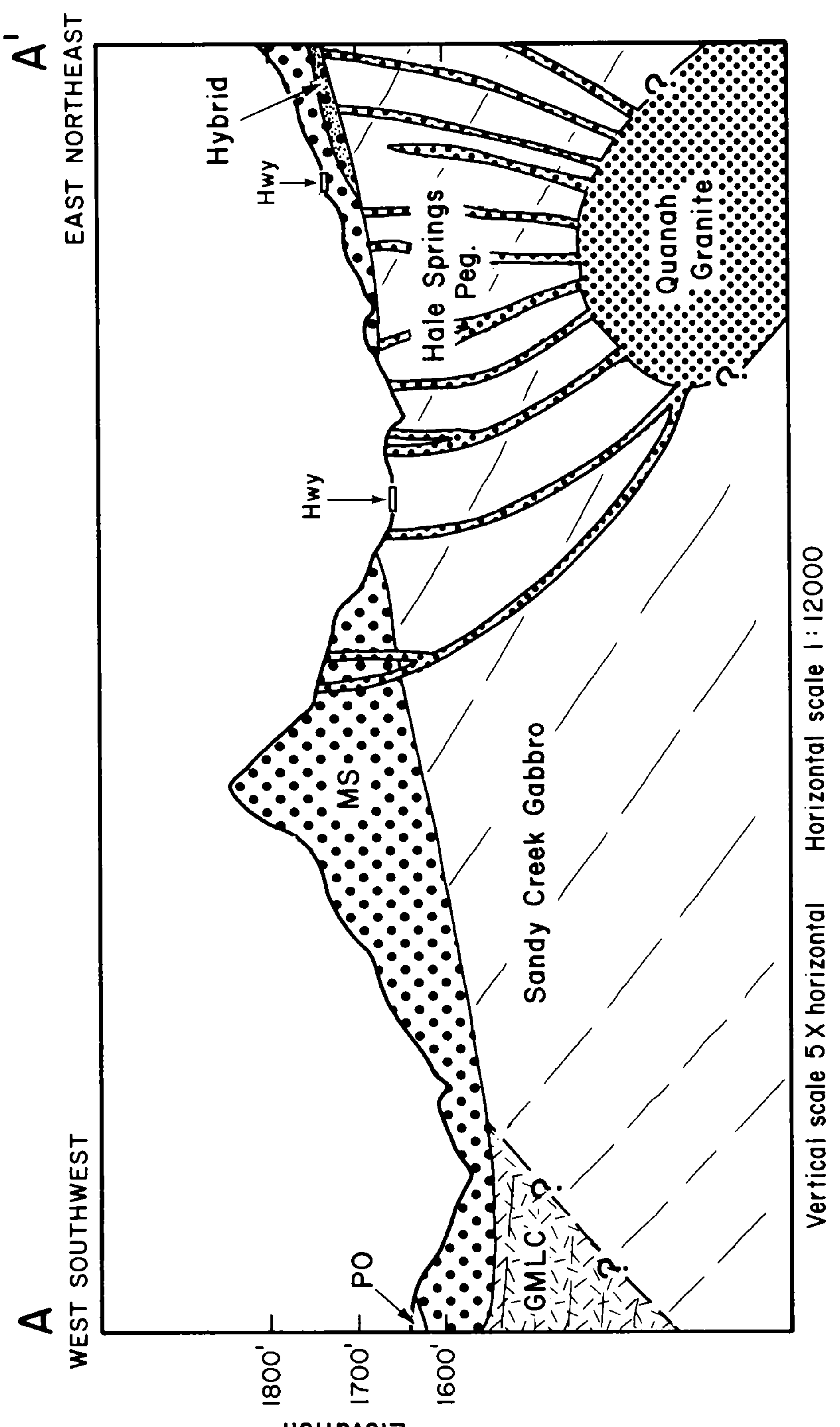

Figure 107. Geologic cross section across figure 106.

Figure 108. Aerial photograph taken in June 1978, looking eastward across main mass of Sandy Creek Gabbro. Black Bear Mountain on left (north) of tree-covered valley; Big Four Mountain on right (south). Mountains are part of Mount Scott Granite sill on substrate gabbros. Surface of Antelope Flat within Wichita Mountains Wildlife Refuge to east is partially formed by Post Oak Conglomerate.

TABLE 27.—BULK-ROCK ANALYSES OF SANDY CREEK GABBRO
(From Alipouraghtapeh, 1979)

Wt %	WC-108(372,385)	WC-16(252,254)	WC13(153)	WC15((153)	WC11(251)	WC12(251)
SiO_2	45.5	47.9	45.5	45.6	46.1	46.0
TiO_2	1.36	1.47	1.55	1.31	1.01	1.22
Al_2O_3	17.50	16.80	16.2	18.0	18.6	17.39
FeO	10.00	8.60	12.0	10.0	8.9	10.6
MgO	13.40	10.40	11.0	11.4	.07	.05
MnO	.05	.04	.08	.08	11.6	4.54
CaO	9.00	9.69	8.8	9.8	9.6	12.0
Na_2O	1.74	2.53	1.93	2.55	2.36	2.10
K_2O	.47	.55	.67	.44	.41	.45
P_2O_5	.20	.72	.64	.33	.46	.38
ppm						
Cu	140	87	54	195	154	147
Cr	152	127	115	171	165	128
Zn	87	90	100	87	80	93
Pb	15	20	20	20	10	20
Ni	122	83	88	109	105	114
Ba	190	140	110	70	110	50
Sr	282	350	379	359	338	324
Rb	4	5	2	7	2	nd
V	140	200	190	160	150	160
Mode						
plagioclase		45	40	45	53	40
olivine		20	25	27	20	28
clinopyroxene		27	27	20	15	24
orthopyroxene		tr	tr	tr	tr	tr
opaque		5	3	5	7	5
biotite		3	5	3	5	2
others		tr	tr	tr	tr	tr

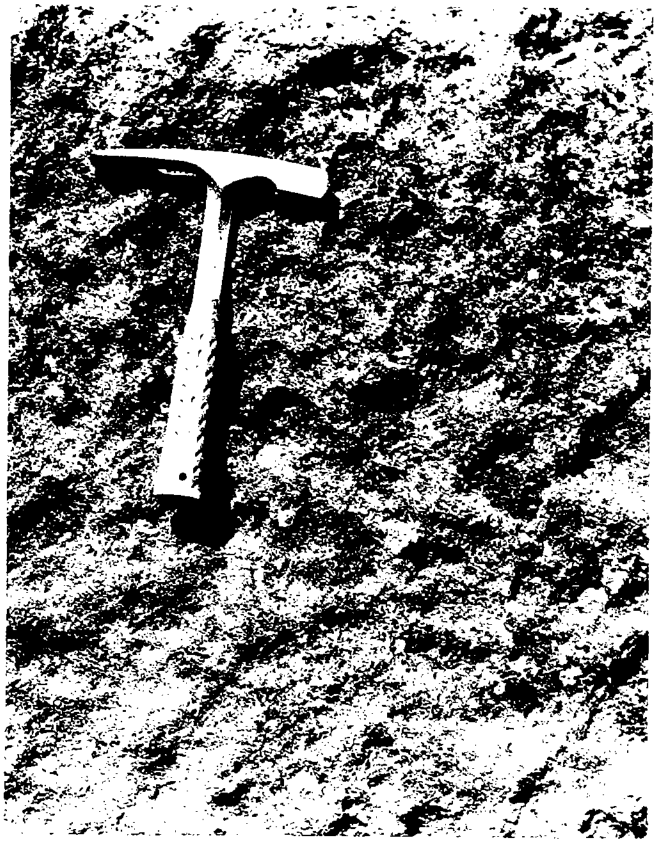

Figure 109. Typical scalloped weathering of Sandy Creek Gabbro.

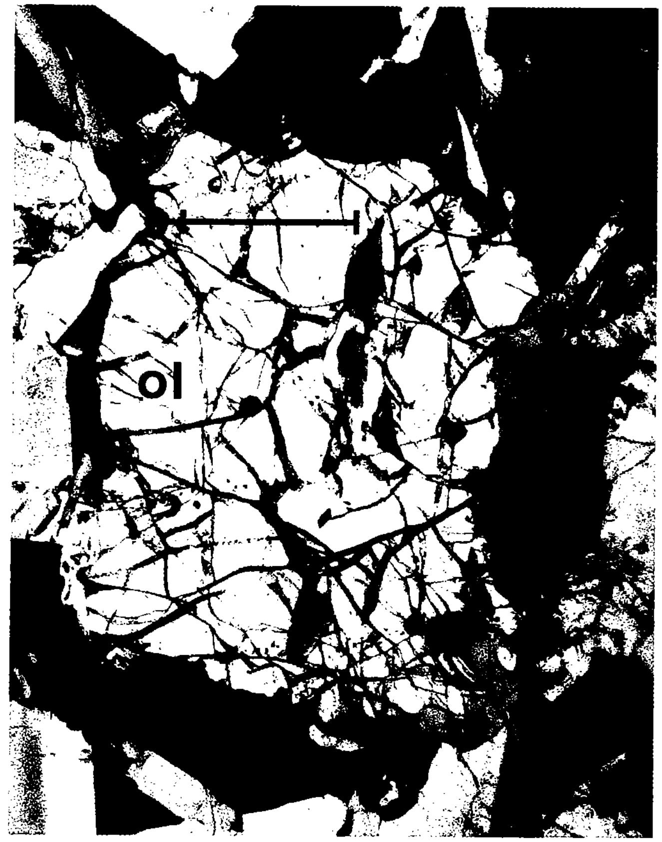

Figure 111. Photomicrograph of Sandy Creek Gabbro Member of the Roosevelt Gabbros showing olivine (*ol*) peritectic reaction. Note embayments in olivine and nearly continuous rim of bronzite (*opx*). Polarizers are partially crossed to highlight orthopyroxene which here appears dark gray. Plagioclase, magnetite, and ilmenite also are in picture. Bar is 0.5 mm. (Sample WM–385.)

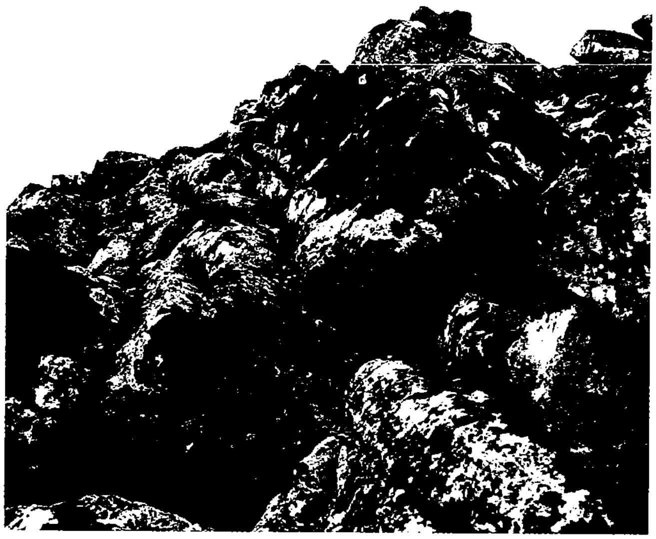

Figure 110. Looking northward at east-dipping, layered Sandy Creek Gabbro (SE¼NE¼NW¼ sec. 9, T. 3N., R. 15 W.), which is prominent west of State Highway 49.

becomes pigeonite after Fe/(Fe + Mg) ratios have evolved to about 0.30 or 0.35, because the temperature–composition curve for the magma passes into the stability field of pigeonite. A lower liquidus temperature for a given Fe/(Fe + Mg) ratio would keep orthopyroxene on the liquidus to more evolved (higher) Fe/(Fe + Mg) compositions. This appears to have been the case with the Sandy Creek Gabbro magma, and is tentatively attributed to its higher than average H_2O content.

Plagioclase ranges in composition from An_{72} in olivine gabbro to An_{52} in quartz-bearing gabbro. The feldspars are zoned, and the figures given are average core compositions. Representative olivine compositions are listed in table 23. Additional minor and accessory phases in the Sandy Creek Gabbro include ilmenite, Ti-magnetite, apatite, pyrite, chalcopyrite, and pyrrhotite.

Some samples of gabbro from secs. 3 and 4 lack olivine and contain intergranular quartz and (or) "granophyre" in the mesostasis (fig. 116). In fresh rocks, such occurrences appear to be primary and

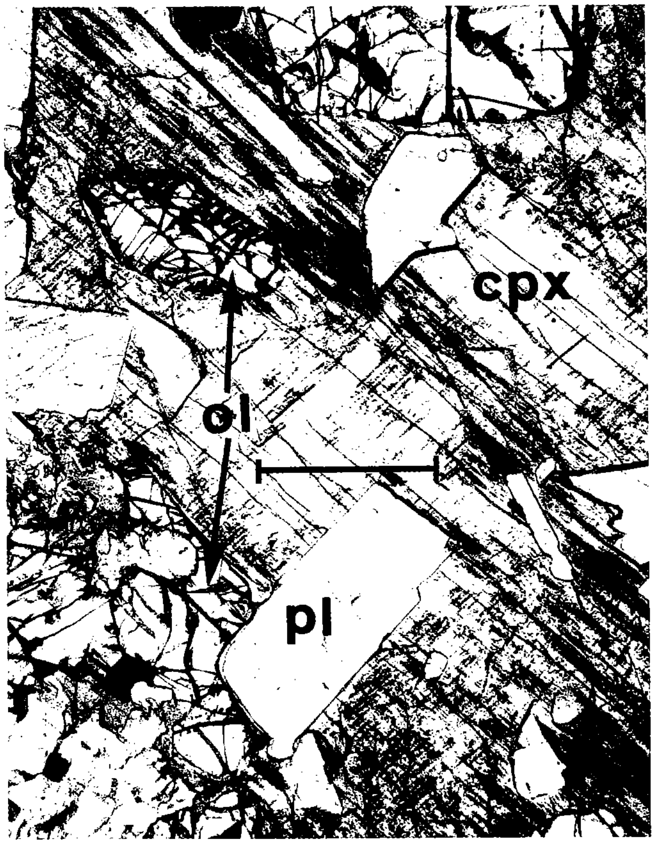

Figure 112. Photomicrograph of Sandy Creek Gabbro showing optically continuous augite (*cpx*) ophitically enclosing plagioclase (*pl*) and olivine (*ol*). Bar is 0.5 mm. (Sample WM–385.)

Figure 113. Photomicrograph of Sandy Creek Gabbro, showing plagioclase lamination; olivine (*ol*). Bar is 1 mm. (Sample WM–372.)

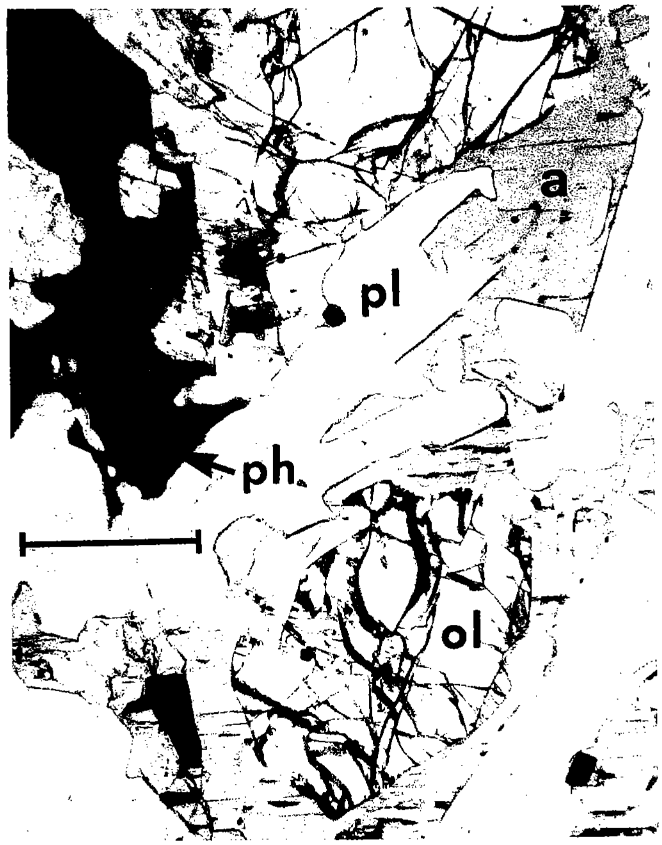

Figure 114. Photomicrograph of Sandy Creek Gabbro showing interstitial, well-crystallized amphibole (*a*) and phlogopite (*ph*); olivine (*ol*); plagioclase (*pl*); opaque is ilmenite. Bar is 0.5 mm. (Sample WM–385.)

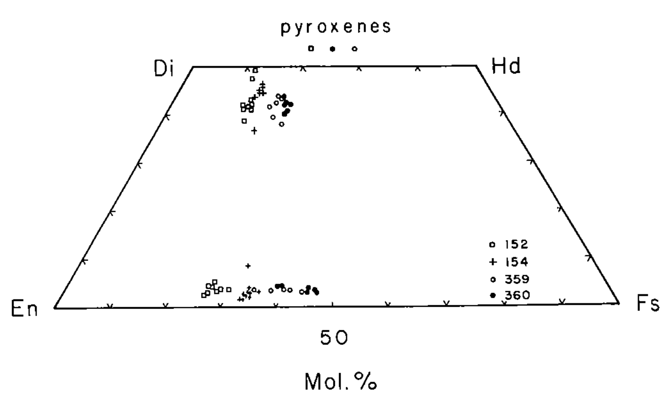

Figure 115. Pyroxene compositions in Sandy Creek Gabbro and a separate dike of biotite–olivine gabbro (WM–154, an unnamed member of Roosevelt Gabbros). Sample WM–152 is olivine-bearing; WM–359 lacks olivine and quartz; WM–360 contains quartz and K-feldspar as granophyric intergrowth in mesostasis (see fig. 116). All low Ca pyroxenes plotted for Sandy Creek Gabbro (squares, and filled and open circles) are primary orthopyroxenes, not inverted pigeonite. (See text for discussion.)

reflect differentiation in the intrusion. They should not be confused with hydrothermally altered gabbro, common in sec. 4, which probably was altered in response to granite emplacement. (See more on this below.) Differentiation of the Sandy Creek Gabbro is further reflected in the range of bulk compositions (table 30) and in systematic phase chemical variations (cryptic variation) (figs. 115, 117).

Exposures in the eastern half of sec. 4, T. 3 N., R. 15 W., reveal intrusive relationships that are a key to the relative age of the Sandy Creek Gabbro. Meter-sized xenoliths of unaltered gabbroic anorthosite of the Glen Mountains Layered Complex occur in the Sandy Creek Gabbro (fig. 106A), fixing the younger age of the latter. In addition to the granite contacts referred to above, a north-trending aplite dike approximately 2 m wide can be traced for about 250 m in the eastern half of sec. 4 (fig. 106A). Over much of the meadow east of this dike are low, discontinuous outcrops of gabbro and banded granite pegmatite, the latter containing riebeckite–arfvedsonite ± aegerine. Many exposures of the gabbro are relatively light in color in comparison with its more typical appearance (almost black) and locally resemble gabbro pegmatite. This material, in thin section, is seen to be rather pervasively altered. Plagioclase is variably replaced by sericite, calcite, and "clays"; original mafic phases are totally altered to mixtures of pale green, acicular to fibrous amphibole, chlorites, calcite, epidote–zoisite minerals, and traces of sphene (fig. 118).

Feldspar grain boundaries are highlighted in the outcrop by the alteration, which also lightens the color of the matrix (originally interstitial or ophitic mafic minerals). These effects impart a (basic) pegmatitic appearance to the coarse-textured altered gabbro, although fine- to medium-grained rocks are locally altered also. The grain-size variation in the Sandy Creek Gabbro appears to be primary and does not in any obvious way correlate with the alteration process.

Although the alteration, together with observed and inferred contact relations, fixes the age of the Sandy Creek Gabbro relative to the younger Wichita Granite Group, the observed alteration patterns and contact relations have wider relevance. Similar rocks are found elsewhere in the Wichita province where the precursors belong to lithostratigraphic units other than the Sandy Creek Gabbro. In the vicinity of Meers, Oklahoma, and in the central portion of the Wichita Mountains Wildlife Refuge, outcrops of the Glen Mountains Layered Complex are similar in alteration and appearance to the altered, coarser grained Sandy Creek Gabbro (see figs. 2 and 7 for

TABLE 28.—ANALYSES OF AMPHIBOLES IN SANDY CREEK GABBRO

	1		2		3	
	WM-152		WM-337		WM-309	
SiO_2	43.2		45.3		43.8	
TiO_2	3.42		2.08		2.60	
Al_2O_3	10.7		8.78		9.96	
Fe_2O_3	1.99		2.14		2.02	
FeO	10.2		11.0		10.3	
MgO	13.6		14.8		14.6	
CaO	11.3		11.7		11.4	
Na_2O	1.84		1.54		2.19	
K_2O	1.08		0.67		0.76	
SUM+	97.33		98.01		97.63	
Si	6.367		6.618		6.434	
Al^{iv}	1.633	8.000	1.382	8.000	1.566	8.000
Al^{vi}	0.218		0.132		0.161	
Fe^{3+}	0.221		0.236		0.223	
Ti	0.379	5.000	0.229	5.000	0.288	5.000
Mg	2.994		3.222		3.198	
Fe^{2+}	1.188		1.181		1.130	
Fe^{2+}	0.064		0.158		0.133	
Ca	1.789	2.000	1.840	2.000	1.789	2.000
Na	0.147		0.002		0.078	
Na	0.379	0.583	0.434	0.559	0.546	0.689
K	0.204		0.125		0.143	
$Mg/(Mg+Fe^{2+})$	0.705		0.706		0.717	

NOTES TO TABLE

*Fe_2O_3 calculated assuming $Fe^{3+}/(Fe^{3+}+Fe^{2+}) = 0.15$

+Analyses are by microprobe and do not include H_2O, F, Cl.

Analyses (averages of several in each sample):

1. Titanian magnesio-hastingsitic hornblende from olivine gabbro (WM-152). Olivine Fo_{68}.
2. Edenitic hornblende from olivine gabbro (WM-337). Olivine Fo_{66}.
3. Titanian magnesio-hastingsitic hornblende from olivine gabbro (WM-309). Olivine Fo_{67}.

locations). Alteration in the Meers area is most likely due to the Mount Sheridan Gabbro Member of the Roosevelt Gabbros, although the Mount Scott Granite cannot be discounted. In the wildlife refuge occurrence, the cause of alteration is not immediately obvious, but Mount Scott Granite and (or) Quanah Granite are the most likely agents (fig. 2).

Similar rocks occur in association with the Glen Creek Gabbro in the Glen Mountains. Such textures are found here in the Glen Creek Gabbro itself, next to small granitic intrusions, and also in rocks that *may* belong to the Glen Mountains Layered Complex (uncertain at present). In the latter case, the Glen Creek Gabbro could have been responsible for the alteration, although this interpretation is problematic because elsewhere the Glen Creek Gabbro exhibits sharp intrusive contacts against the older Glen Mountains Layered Complex, with no visible alteration in the latter.

Clearly, alteration in the Wichita province is complex and arises from more than one source. Such a situation should be expected, of course, where multiple magmatic episodes have occurred. An important caveat offered here is that similar (but not necessarily identical) alteration processes acting on similar (but not necessarily identical) precursor rock types can produce very similar results. This must be borne in mind when mapping in complex magmatic terranes like the Wichita Mountains. A definitive study of alteration—genetic as well as descriptive and focused on causes and effects—in the Wichita province would be very challenging, with excellent prospects for important contributions.

One must also be aware in studying Wichita geology that various "intermediate" rocks in contact zones between basic rocks of the Raggedy Mountain Gabbro Group and the Wichita Granite probably have a variety of origins with different detailed pet-

TABLE 29.—REPRESENTATIVE PYROXENE COMPOSITIONS FROM SANDY CREEK GABBRO

(Microprobe analyses in weight %)

	1	2	3	4	5	6	7	8
SiO_2	51.6	55.1	50.0	53.6	52.5	52.9	52.9	51.9
TiO_2	1.48	0.48	1.29	0.04	0.34	0.40	0.22	0.29
Al_2O_3	3.78	1.31	3.48	0.96	1.05	0.81	0.61	0.55
FeO*	9.25	16.4	10.2	19.4	11.5	24.7	12.8	27.2
MnO	0.25	0.44	0.22	0.46	N.D.	N.D.	N.D.	N.D.
MgO	15.7	23.4	14.3	25.5	12.9	19.8	13.0	18.4
CaO	18.4	1.63	20.1	0.63	21.3	1.60	20.1	1.44
Na_2O	N.D.	N.D.	0.21	0.00	0.23	0.19	0.36	0.00
Total	100.46	98.76	99.80	100.59	99.82	100.40	99.99	99.78
Wo (mol %)	38.8	3.5	42.0	1.2	44.1	3.3	41.8	3.0
En (mol %)	46.0	69.3	41.4	69.2	37.3	56.9	37.5	53.5
Fs (mol %)	15.2	27.2	16.6	29.6	18.6	39.8	20.7	44.0
Atomic Mg/(Mg+Fe)	0.752	0.718	0.714	0.700	0.667	0.589	0.644	0.547
*Average Mg/(Mg+Fe)	0.757	0.726	0.751	0.708	0.669	0.595	0.641	0.561

*Note: Averages are for several grains in the indicated sample. Total Fe is expressed as FeO.

Samples:

1. Augite, olivine-gabbro, NE¼NW¼ sec. 9, T. 3 N., R. 15 W., Comanche County (WM-152).
2. Bronzite coexisting with augite no. 1 this table (WM-152).
3. Augite, olivine-gabbro, SE¼NE¼ sec. 4, T. 3 N., R. 15 W., Comanche County (WM-309).
4. Bronzite coexisting with augite no. 3 this table (WM-309).
5. Augite, gabbro with neither olivine nor quartz, SE¼NW¼ sec. 3, T. 3 N., R. 15 W., Comanche County (WM-359).
6. Hypersthene coexisting with augite no. 5 this table (WM-359).
7. Augite, gabbro with "granophyre" in the mesostasis, SW¼NE¼ sec. 3, T. 3 N., R. 15 W., Comanche County (WM-360).
8. Hypersthene coexisting with augite no. 7 this table (WM-360).

Figure 116. Photomicrograph of fractionated Sandy Creek Gabbro showing granophyric intergrowth of quartz (white) and K-feldspar (gray) in mesostasis. Note crystal of primary, iron-rich hypersthene (*opx*). Large dark grain in lower right is augite; twinned grains are sodic labradorite. Polarized light. Bar is 0.5 mm. (Sample WM–360.)

Figure 118. Photomicrograph of hydrothermally altered Sandy Creek Gabbro showing replacement of pyroxene by fibrous amphibole mixed primarily with chlorite and "epidote." Plagioclase shows only incipient alteration (more pervasive in other samples). Bar is 0.5 mm. (Sample WM–307.)

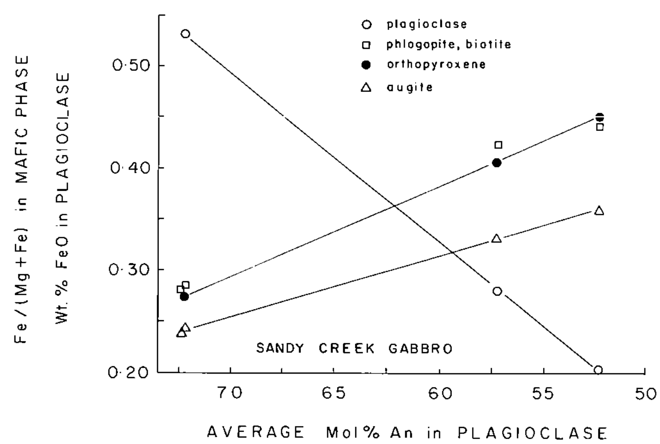

Figure 117. Cryptic variation in differentiated Sandy Creek Gabbro revealed in average compositions of coexisting ferromagnesian phases and plagioclase. Points to left ($An_{72.5}$) are from olivine gabbro; points at about An_{57} are in "saturated" gabbro (no olivine or quartz); points to right (An_{52}) are in quartz–K-feldspar-bearing gabbro. Line defined by open circles (plotting weight percent FeO in plagioclase, using same vertical scale) reflects declining FeO in magma with fractionation. Both trends are typical of tholeiitic systems.

rogeneses. Quartz and K-feldspar-bearing Sandy Creek Gabbro, as we have seen, is fortuitously intruded by granite. A similar situation exists on Mount Sheridan in the eastern Wichitas, where the rocks involved are ferrogranodiorite (fractionated from the Mount Sheridan Gabbro) and Mount Scott Granite. (See Powell and Fischer, 1976.) Elsewhere, quartz-bearing intermediate rocks in gabbro–granite contact zones probably resulted from assimilative reaction between older gabbroic rocks and younger granitic liquids. [Some of Huang's (1955) cited occurrences fall into this latter category, whereas others perhaps do not.] Both petrogeneses may be combined in a given situation, alteration/assimilation being imposed on rocks that already possessed an intermediate character from older, purely magmatic processes. Unfortunately, the two importantly different petrogeneses are not always readily distinguishable.

The possibility exists that the Sandy Creek Gabbro and the Glen Creek Gabbro are connected at depth or at least share a common origin. Perhaps they are separate intrusions from the same parental magma.

Local subsurface information does not resolve this question, and Powell and others (1980) named them as separate members of the same formation (Roosevelt Gabbros). Exposures of biotite–olivine gabbro along a creek in the north-central part of sec. 33, T. 4 N., R. 15 W., are taken to be Sandy Creek Gabbro, but this is presently under investigation.

Mount Scott Granite

The Mount Scott Granite is nonmicrographic in this area, as reported earlier by Merritt (1965). A modal analysis of sample W–76 occurring west of the diabase dike in the SW¼NE¼NW¼ sec. 9 yields 34.5 percent quartz, 55.25 percent alkali feldspar, 2.25 percent plagioclase, 3 percent hornblende (some may be secondary), 2.25 percent biotite (some also secondary), 1.5 percent oxides, 0.75 percent sphene, and traces of fluorite, epidote, zircon, and apatite. The grain size varies between 1 and 4 mm. This rock is as even grained and coarse as the Mount Scott is known to be (fig. 119). Ovoid feldspars are present, but they are not as outstanding as in other exposures, particularly those farther east. This may mean that the sill and (or) overburden was thicker in this region, and the sill cooled more slowly. The later intrusion of Quanah Granite nearby also may have acted to keep temperatures high while permeating the rock with fluid, thus promoting crystallization adjustments.

Hybrid Rocks

These rocks of intermediate composition occur in an east-trending band across the crest of Big Four Mountain. The band can be seen in the aerial photograph (fig. 108), oriented from the map (figs. 106A, 106B), as heading eastward from a small pond, up a tree-lined gully. The rocks vary in mafic content, ranging in color from pink and gray to dark gray. The rocks are fine to medium grained, with quartz and pink feldspar phenocrysts and xenoliths of biotite gabbro.

Similar hybrid rocks have been interpreted as resulting from partial recrystallization and melting

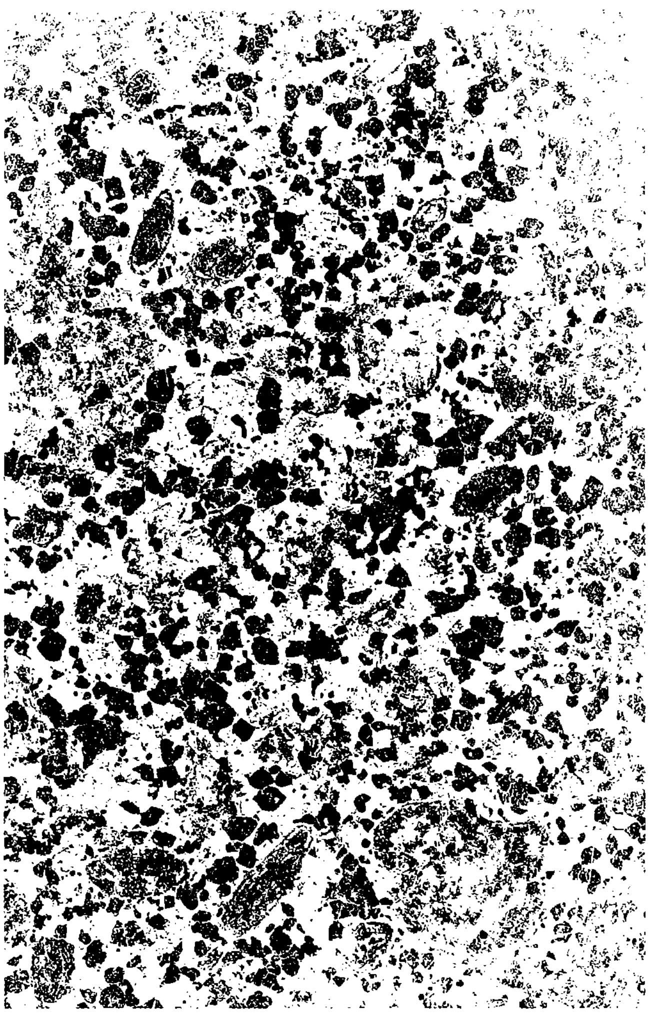

Figure 119. Photograph of thin section (width about 1 inch) of Mount Scott Granite (W–76). Note characteristic ovoid feldspar and nonmicrographic texture.

Figure 120. Photograph of thin section (width about 1 inch) across several layers of Hale Spring pegmatite, no. 1 dike of Johnson (1955). White areas are quartz and feldspar. Dark and gray areas are arfvedsonite. Acmite is present but too fine to be seen at this scale.

that occurred when the granite sill was intruded into an area of weathered and previously reworked gabbroic regolith (Myers and others, 1981). The intermediate rocks in this locality are surrounded on all sides by massive Mount Scott granite. Interpreting them as a contact zone requires several hundred feet of structural displacement across the mountain, or considerable relief on the underlying gabbro surface. No intermediate rock has been found along the granite–gabbro contact on the north slope of the mountain. The slope is covered with granite float, however, and in many places the contact is obscured.

A deep prospect pit beside a small tank on the east side of Big Four Mountain (SE¼NE¼SE¼ sec. 3) reveals a dark, coarse-grained gabbroic rock (0.5–2–cm plagioclase, 1–3–cm mafic minerals) with blebs and veins of secondary quartz and white feldspar. Similar coarse-grained mafic rocks have been seen in isolated outcrops elsewhere in the Cooperton Quadrangle. Their relation to the intermediate rocks is not clear.

Hale Spring Pegmatites

Numerous dikes of Hale Spring pegmatite cut the Sandy Creek Gabbro in the central part of the N½ sec. 9 and the central part of the E½ sec. 4. Fragments of a Hale Spring dike can be seen cutting Mount Scott granite in the west-northwest-trending stream canyon in the southwestern corner of sec. 4. Veins and dikelets occur also on the granite hill in the NW¼ sec. 9.

These quartz–albite–microcline pegmatites bear large crystals of a sodic amphibole commonly referred to as riebeckite but more properly as arfvedsonite (Scofield and Gilbert, 1980; and this guidebook). The Hale Spring rocks occur in both pegmatitic and aplitic facies. These facies commonly exhibit conspicuous banding and alignment of amphibole crystals (figs. 120, 121, 122). Figure 122 is a photograph taken parallel to the layers. Parts of four separate layers can be seen, with alignment of crystals in each.

Al-Shaieb and others (1980) generated a large amount of trace-element data from pegmatoid samples. Some of these are shown in table 31. Comparison of these data with those for the Sandy Creek Gabbro (table 27) shows the expected contrast between mafic and silicic rocks. The gabbro is high in Sr, V, and Cu, whereas the pegmatoids are low in these. The Cu mineralization reported with the Hale Spring bodies may be due to remobilization of Cu

Figure 121. Typically banded portion of no. 1 pegmatoid dike of Johnson (1955). Light areas are feldspar and quartz, dark areas are abundant arfvedsonite and (or) acmite.

Figure 122. Photograph view is parallel to layers in pegmatite. Four different amphibole-rich layers can be discerned. Amphiboles in each layer are aligned consistently, although orientation changes as much as 10° to 30° among layers. Alignment thought to be due to crystallization from moving fluids.

TABLE 30.—AVERAGE BULK COMPOSITIONS OF SANDY CREEK GABBRO AND ASSOCIATED QUARTZ-BEARING BIOTITE GABBRO

(Microprobe analyses in weight %)

	1	2	3	4	5	6	7	8	9
SiO_2	47.5	46.6	47.8	53.9	49.0	44.7	47.6	56.5	55.2
TiO_2	1.39	1.91	1.76	2.74	2.60	5.02	4.99	2.89	3.34
Al_2O_3	16.1	14.2	16.0	14.7	17.8	13.5	12.7	14.1	13.0
FeO*	9.81	13.7	12.1	11.6	11.1	16.5	15.6	11.5	12.8
MgO	11.9	13.1	11.3	6.11	5.13	6.49	6.06	4.36	4.09
CaO	10.5	7.96	9.43	7.73	11.2	10.5	9.66	6.89	7.47
Na_2O	1.82	1.85	1.60	2.51	2.28	2.04	2.11	2.53	2.46
K_2O	0.25	0.40	0.25	1.04	0.36	0.48	0.53	1.54	1.50
P_2O_5	0.17	0.21	0.14	0.31	0.56	0.21	0.28	0.26	0.37
S	n.d	0.04	n.d	n.d	0.06	0.07	0.05	n.d	n.d
Total	99.44	99.97	100.38	100.64	100.09	99.51	99.58	100.57	100.23
Atomic Fe/(Fe+Mg)	0.317	0.370	0.375	0.516	0.547	0.587	0.592	0.596	0.638

*Total Fe expressed as FeO. (Samples were prepared using the method described by Brown, 1977).

Samples:

1. Sandy Creek Gabbro, olivine-bearing, NE¼NW¼ sec. 9, T.3N., R.15W., Comanche County (WM-152).
2. Sandy Creek Gabbro, olivine-bearing, SE¼NE¼ sec. 4, T.3N., R.15W., Comanche County (WM-309).
3. Sandy Creek Gabbro, olivine-bearing, SE¼NE¼NW¼ sec. 33, T.4N.,R.15W., Comanche County (WM-337).
4. Quartz-bearing biotite gabbro, SW¼NE¼ sec. 21, T.4N.,R15W., Comanche County (WM-330).
5. Sandy Creek Gabbro, quartz-bearing, NW¼SE¼ sec. 4, T.3N.,R15W., Comanche County (WM-306).
6. Sandy Creek Gabbro with neither olivine nor quartz, SE¼NW¼ sec. 3, T.3N.,R.15W., Comanche County (WM-359).
7. Sandy Creek Gabbro with quartz and K-feldspar (granophyre in mesostasis), SW¼NE¼ sec. 3, T.3N.,R.15W., Comanche County (WM-360).
8. Quartz-rich biotite gabbro-diorite, NW¼ sec. 29, T.4N.,R15W., Comanche County (WM-363).
9. Sandy Creek Gabbro, quartz-bearing, SE¼ sec. 33, T.4N.,R.15W., Comanche County (WM-323).

TABLE 31.—ANALYSES OF HALE SPRING PEGMATITES

(Uranium prospect 21 of Al-Shaieb and others, 1980)

Sample #/ppm	U_3O_8	Ti	V	Mn	Cu	Zn	Li	Ba	Sr	Y	Zr	Nb
118	54	167	80	370	5	356	16	110	50	149	12277(?)	226
119	138	1400	50	350	3	358	54	70	70	323	6865	335
120	45	188	85	180	2	209	261	10	30	127	5417	136
201	60	2800	15	129	43	136	18	120	20	110	4100	189

118, 119, 120 are west of Highway 49, SE NE NW-9-T3N-R15W.
201 is east of Highway at main pegmatite dike (#1 of Johnson), SW NW NE-9-T3N-R15W.
(Note: locations of these samples are listed incorrectly in the original report.)

from the gabbro by later fluids, rather than original introduction by those fluids. Zn is higher in the pegmatoids than in the gabbro. Li concentration is interesting because the wet analysis of the sodic amphibole (table 17) shows noticeable Li; most of the Li in the rock must be in the amphibole. Al-Shaieb (1979) showed that U is associated with the mafic phases and zircon, but he could not tell its exact form.

These rocks are the youngest in the area and are believed to be derived from the Quanah Granite.

Meers Quartzite

Metaquartzite has been found in two exposures: the SE¼NW¼NE¼SE¼ sec. 8, T. 3 N., R. 15 W., and the NW¼NE¼NE¼SW¼ sec. 4, T. 3 N., R. 15 W. The first of these is bounded by Mount Scott Granite on two sides, and probably on three, although not so clearly. The Post Oak Conglomerate overlies the quartzite and granite, bounding the upper surface. This is nearly pure quartzite, composed of partially reconstituted quartz grains, traces of metamorphic sillimanite and muscovite, and detrital zircon, apatite, rutile, and sphene (figs. 123, 124).

The second of these outcrops is surrounded by Sandy Creek Gabbro and is much smaller, exposed only in a prospect pit (NW¼NE¼NE¼SW¼ sec. 4, T. 3 N., R. 15 W.). This outcrop is near the southeastern end of an earthen dam at a larger stock pond (in foreground of the aerial photograph, fig. 108). Sillimanite is quite prominent in some of these samples (W–977): 69.5 percent quartz, 18 percent sillimanite, 10.5 percent perthite, 0.25 percent plagioclase, 1.25 percent muscovite, 0.25 percent biotite, and 0.25 percent oxides (fig. 125).

Figure 124. Photomicrograph of quartzite from Mount Scott Granite, showing polygonal (recrystallized) quartz.

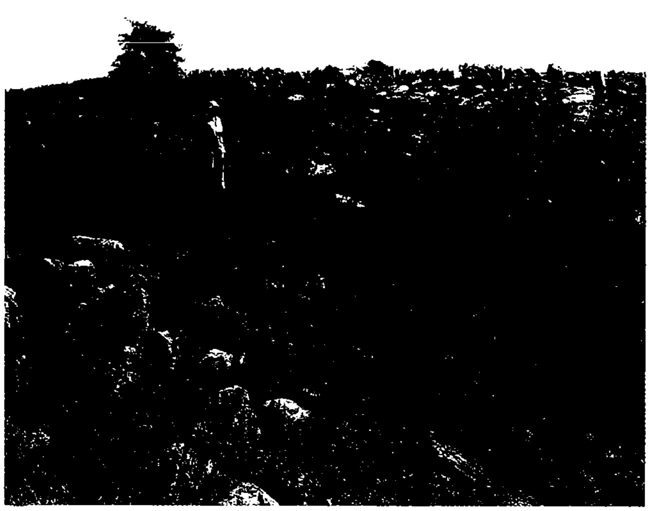

Figure 123. Mount Scott Granite in foreground. Person is standing at contact with Meers, which caps the skyline. Post Oak Conglomerate overlies these two units beyond hill, out of sight.

Figure 125. Photomicrograph of sillimanite-rich quartzite from Sandy Creek Gabbro. View 1.75 × 2.6 mm.

STOP 4—MOUNT SCOTT CAMPGROUND

Contact relations at base of Mount Scott Granite sill, Mount Scott Campground and vicinity. NW¼ sec. 14, T. 3 N., R. 13 W., Comanche County, Oklahoma. **M. C. Gilbert.**

This stop illustrates two contact relations and one key structural relation: (1) the Carlton Rhyolite–Meers Quartzite contact; (2) the Meers Quartzite–Mount Scott Granite contact; and (3) the basal Mount Scott intruded *over* both the rhyolite and quartzite. The geologic map for Stops 4 and 8 (fig. 126) and the three cross sections (fig. 127) show these relations.

This revised geology corrects an error dating from Hoffman (1930), who had assigned rocks that Taylor (1915) originally mapped as Meers, south of Mount Scott, to a new unit called the "Davidson granophyre." This nomenclatural problem is discussed in the first article of the guidebook. A substantial amount of the terrane from here southward to Stop 8 exposes Meers. Many excellent outcrops occur directly south of the Mount Scott picnic area. Stop 8 presents more of the data that have been generated on the quartzite from localities south of Lake Elmer Thomas at Pratt Hill. Sides and Miller (this guidebook) should be consulted for a detailed description of these latter samples.

A correction of the structure and contact relations involving the Mount Scott Granite can also be made on the basis of new mapping. Schoonover (1948) thought that the Mount Scott overlay the Carlton Rhyolite. However, most other workers, especially Ham and others (1964), thought that the granite intruded between the substrate Raggedy Mountain Gabbro Group and the Carlton Rhyolite, thus lying *beneath* the rhyolite. While there is abundant evi-

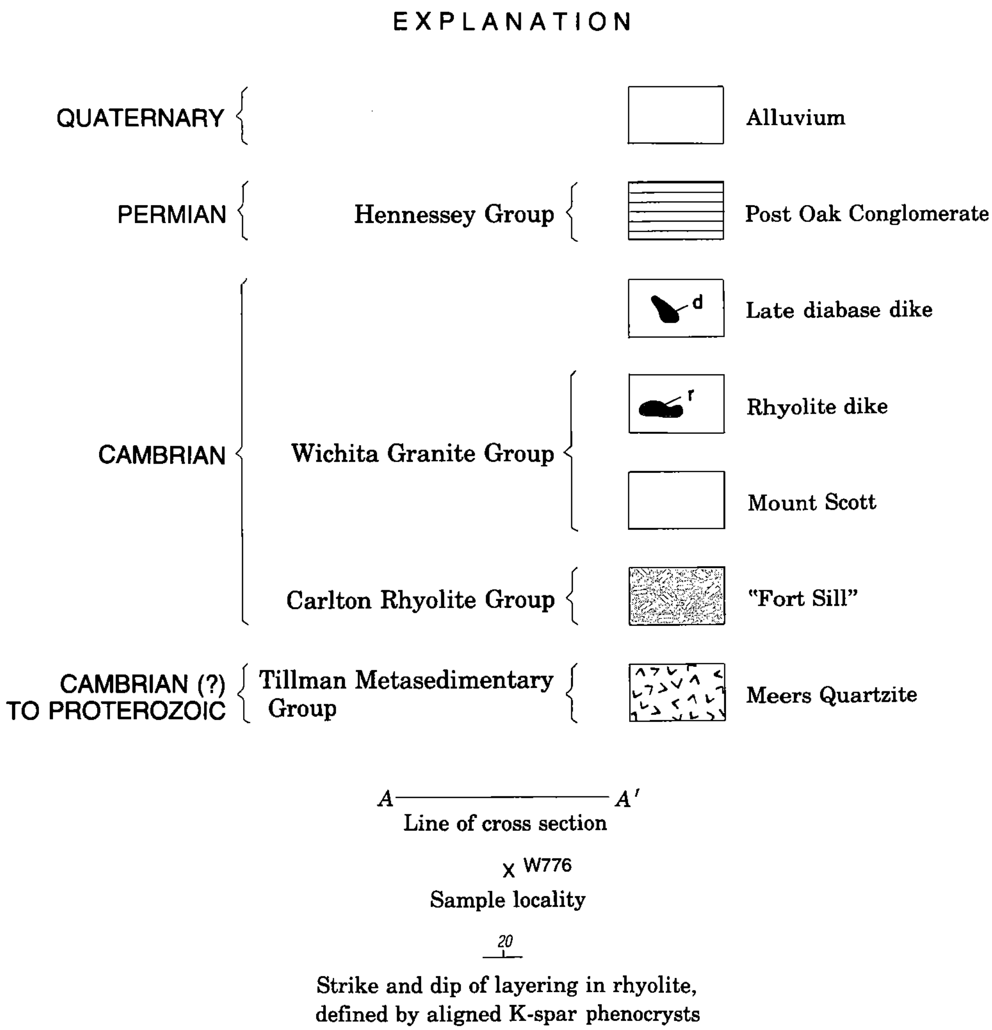

Geology by M. C. Gilbert and J. R. Miller, after Hoffman (1930), Schoonover (1948), and Chase (unpublished data, OGS files)

Base from U.S. Geological Survey, Mount Scott, 1:24,000, 1956
Photorevisions as of 1970

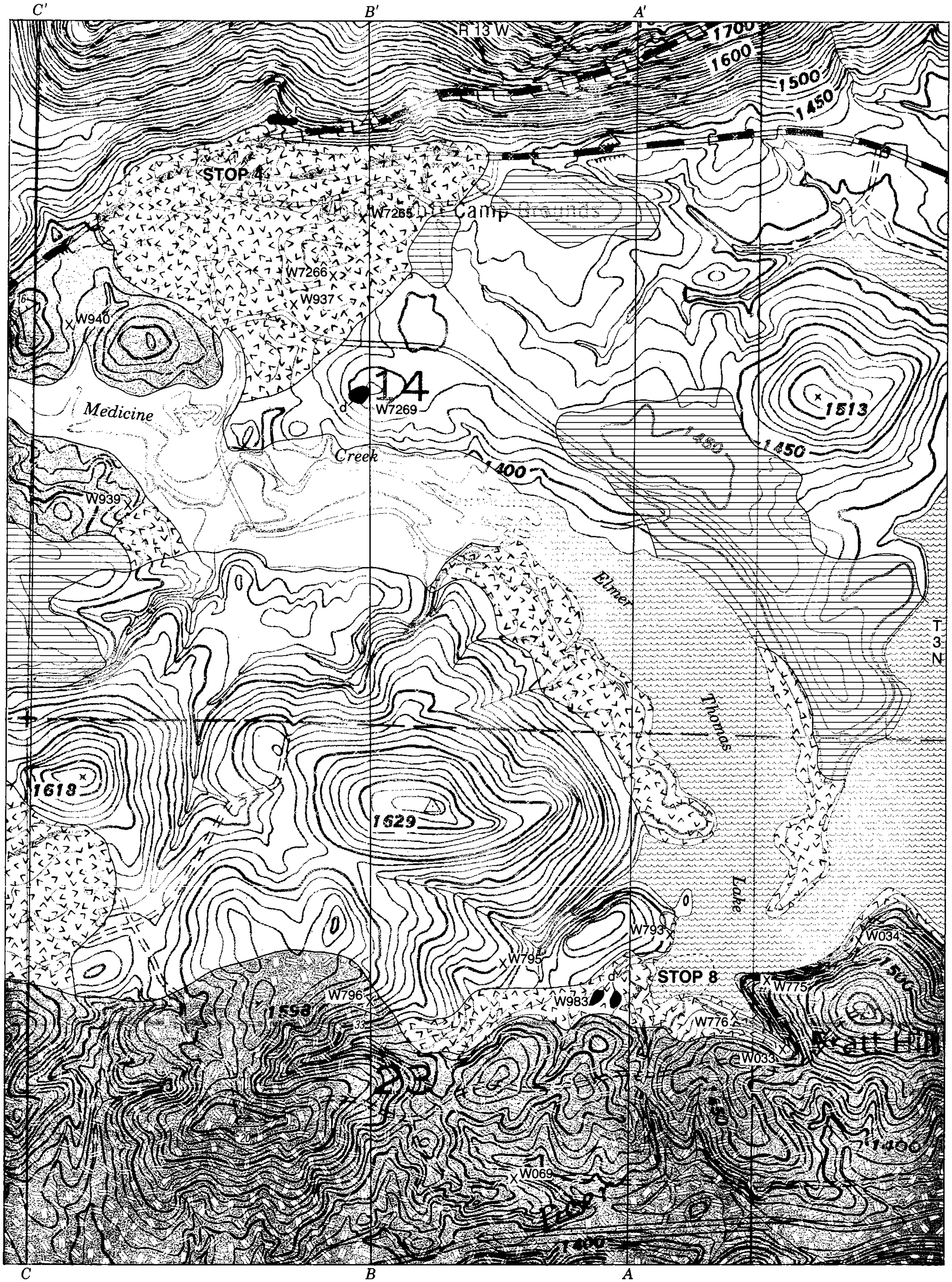

Figure 126. Geologic map for Stops 4 and 8. Map scale, 1:12,000.

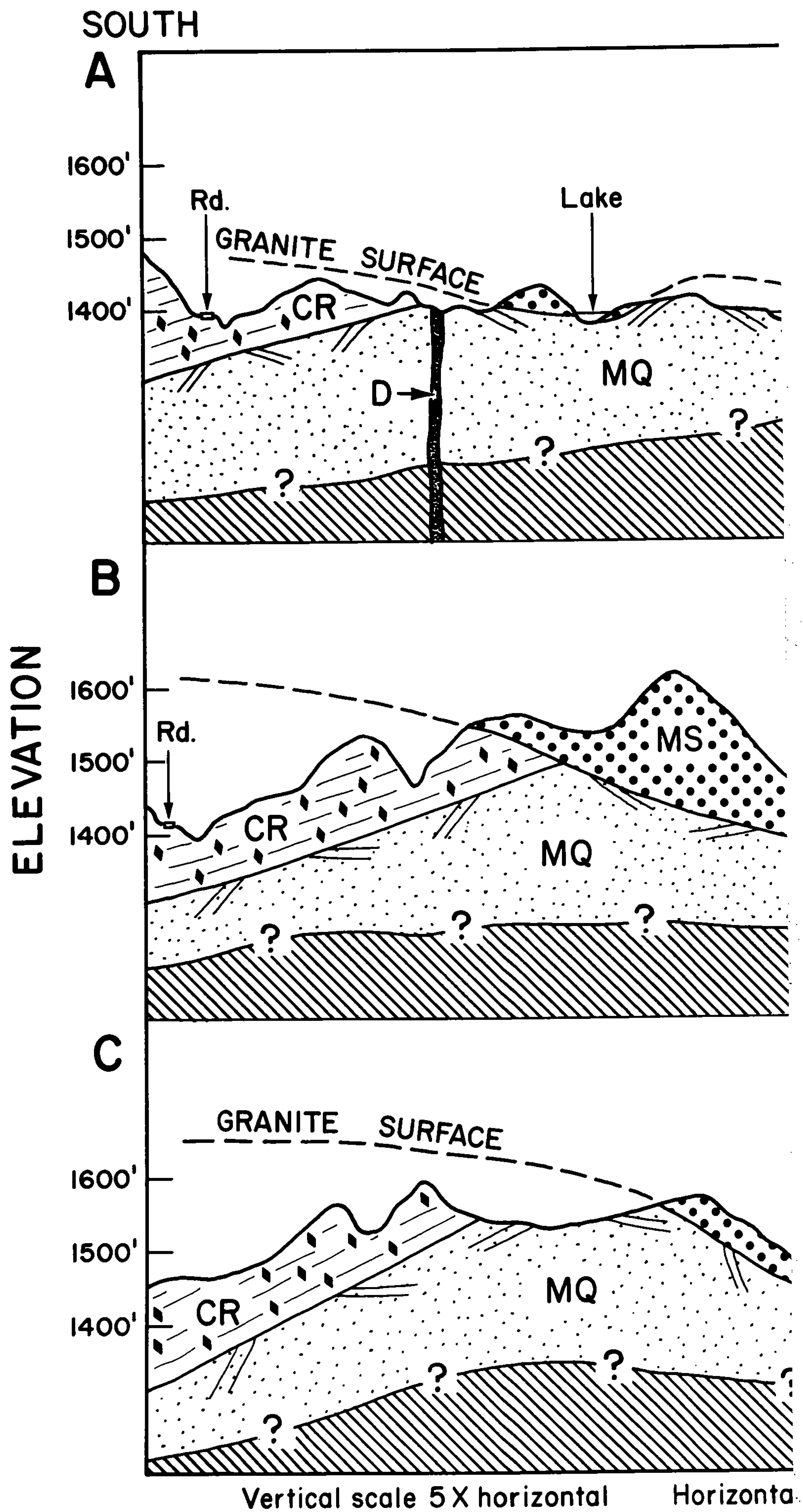

Figure 127. South-north geologic-profile sections across figure 126.

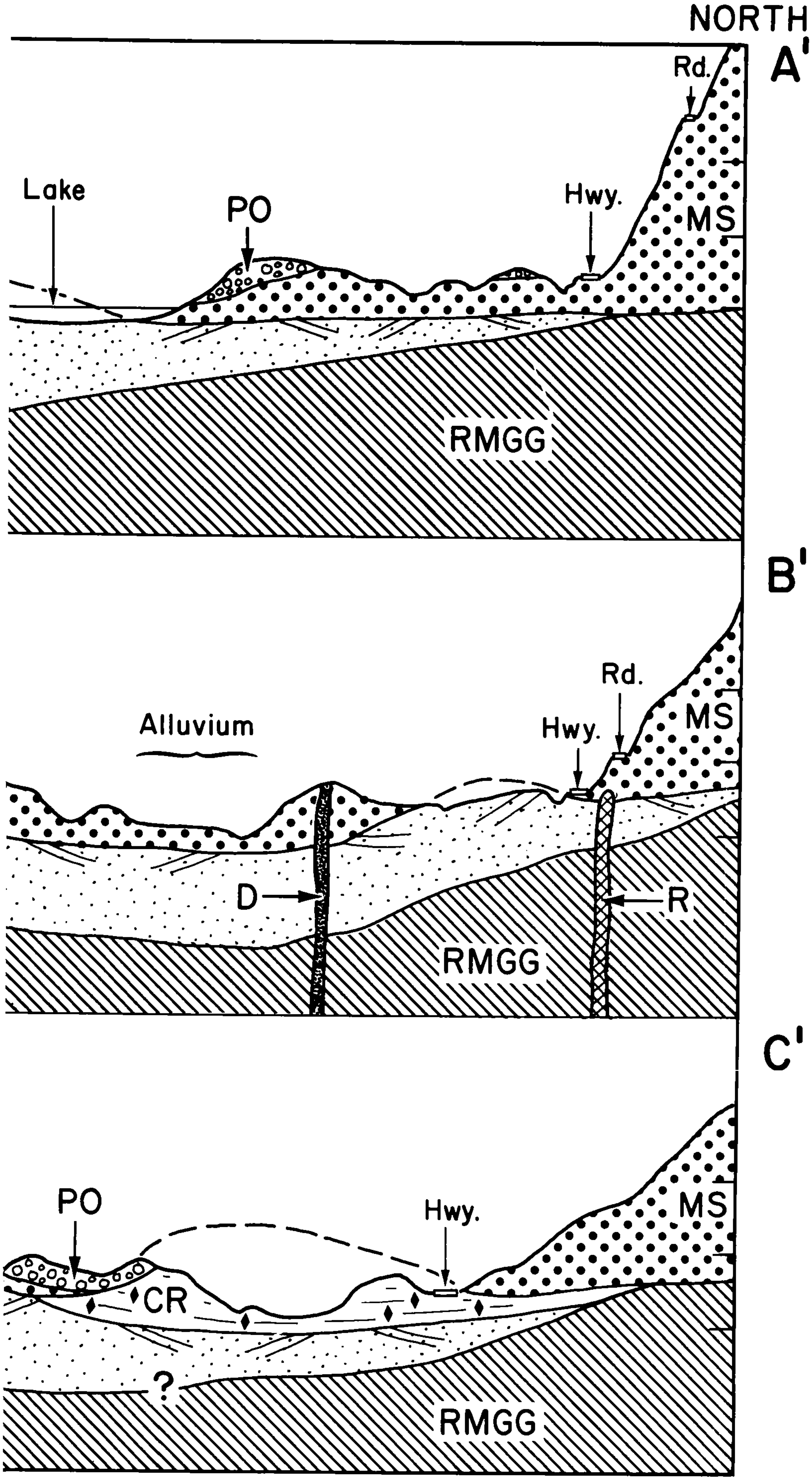

scale 1 : 12000

dence for this view on a regional scale, the specific relations in the Mount Scott–Lake Elmer Thomas–Ketch Lake area are different. The Mount Scott Granite sill lies on Mount Sheridan Gabbro on the north side of Mount Scott, but going southward it rises above the gabbro surface and can be traced upsection into the rhyolite on the south side of Mount Scott. Consequently, there is a wedge of Carlton Rhyolite (and Meers Quartzite) separating the gabbro and granite.

These relations can be confirmed easily and quickly by short traverses in the immediate vicinity of the intersection of the Mount Scott summit road and State Highway 49. Figure 128 is a photograph looking northeastward toward Mount Scott. The present thickness of the granite sill is fully displayed. A small stream, or gully, flows southward off the mountain and out under the summit road, exiting just east of the entrance (on-ramp) to the summit road, and then crosses the main road. Along this gully between the roads are outcrops of the dirty or graywacke facies of the Meers Quartzite. Just south of the culvert of the summit road, Mount Scott granite crops out. This is the base of the sill. For about the first 10 m upsection, the granite is finer grained and called "facies B" by Myers and others (1981) (table 5). A fault cannot be responsible for this outcrop configuration, because the granite behaves as a sheet extending southward across the main highway, just ¼ mi to the east (see figs. 126, 128). To the southwest, the granite overlies the northwest-trending contact between quartzite and rhyolite. The rhyolite–granite contact is clear at the map scale, but not at the outcrop scale, and is better studied farther south.

Table 32 presents modal data for the main rock types in the vicinity. The Meers in this area is mostly fractured, greenish gray and gritty in hand specimen, and dominated by fine-grained, white to yellow-green micas and quartz. Banding is not uncommon. The Carlton is a salmon to dark-red-brown, fractured, massive rhyolite. Phenocrysts of red-orange alkali feldspar and dark-gray quartz are prominent. The feldspars are typically aligned rather consistently over single outcrops, so that mapping of flow directions may be possible. Figure 129 is a photograph of part of a thin section (W–940) showing the

Figure 128. Aerial photograph (taken in June 1978) of Mount Scott, looking northeast. Stop 4 is in vicinity of intersection of State Highway 49 and on-ramp to Mount Scott summit road. Prominent fracture pattern crisscrossing western side of mountain is striking. Many spheroidally weathering boulders, or core-stones, which have toppled from small tors on mountainside, have accumulated in ravines following fractures. All these features, including boulder streams, are interpreted to be Permian.

characteristically broken and corroded phenocrysts (quartz appears black). The thin-section scale (1 in. by 2 in.) is not adequate to describe the rock quantitatively. Two sections of the same rock were point-counted and the data listed in table 32, with noticeable differences in phenocryst ratio. Mount Scott Granite normally contains primary hornblende, although some specimens show late or secondary biotite. A typical late diabase plug cuts granite about ⅓ mi to the south. A rhyolite dike, similar to the one on State Highway 49 by Medicine Creek, cuts granite north of the road.

The largest boulder streams in the Wichitas are developed on Mount Scott (fig. 128). These probably developed in Permian time and do not appear to be recent. Prominent fractures cut the mountain in an unexplained pattern. A combination of this pattern and apparent subtle rock differences yields a surface topography of quite varied character.

The cross sections (fig. 127) drawn to accompany the map show no faults. Although zones of intense brecciation are common, discernible offsets along regional lineaments have not been identified in the igneous terranes. Until more control is available, it seems better to leave this possibility open.

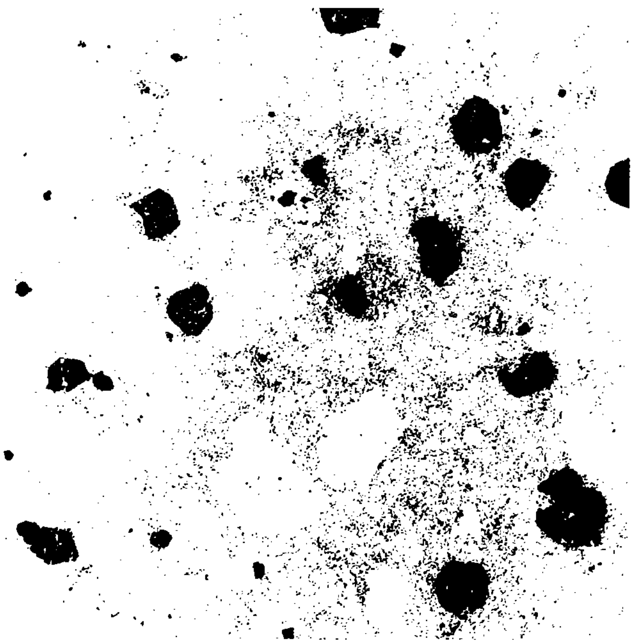

Figure 129. Photograph of thin section of Carlton Rhyolite from sample W–940. Width of section is about 1 in. Phenocrysts of quartz are dark, and those of alkali feldspar are light.

TABLE 32.—MODAL ANALYSES OF ROCKS FROM MOUNT SCOTT CAMPGROUND AREA (STOP 4)

	Meers (Gray type - Davidson) Schoonover 14-3N-13W	Carlton Rhyolite W939 NE SW NW SW 14-3N-13W	Carlton Rhyolite W940 NE NW SW SW NW 14-3N-13W	Carlton Rhyolite W940 14-3N-13W	Mt. Scott Schoonover 14-3N-13W	Mt. Scott W7269A	Late Diabase W7269B SW NE NE NE SW 14-3N-13W
Qtz-P		4.25	7.5	4		1.75	
Alk-F-P		4.75	6	10.75		18.75	
Qtz-G	55	} 87.25	} 83	} 80.75	29.8	31.5	
Alk-F-G					} 64.8	43.25	
Plag (Free)						.5	33.75
Hornbl					3.8	.25	25 (px)
Biotite						.25	19
Opaques	7	2.25	2.75	2.5	1.5	1.5	13
Apatite					tr		tr
Sphene	tr				.05	tr	1.75
Zircon	tr				tr	tr	
Fluorite	1	.5	tr	.25	tr	.25	
Alteration		tr		tr		tr	2.25
Hematite					tr		
Chlorite/Mica	36	.75	.75	1.5		2	5
Epidote		.25	tr	.25		tr	

STOP 5—QUANAH PARKER LAKE AREA

Character of Quanah Granite and its relation to Glen Mountains Layered Complex, Quanah Parker Lake Dam, Little Baldy, and Camp Doris Campground. SW¼ sec. 23, T. 3 N., R. 14 W., Comanche County, Oklahoma. **M. C. Gilbert.**

Introduction

Many of the features seen in this area can be reached from either the Camp Doris Campground or the parking area for Lake Quanah Parker Dam. The discussion here will begin from the dam. Note that sample collection is specifically prohibited in the wildlife refuge without a permit. An overview of most of the features that make this area important can be gained by hiking over trails from the dam, west to Little Baldy and Camp Doris.

Geology

The geologic relations in the area are shown in figure 130 and the accompanying cross section, figure 131. At the damsite, typical coarse Quanah granite

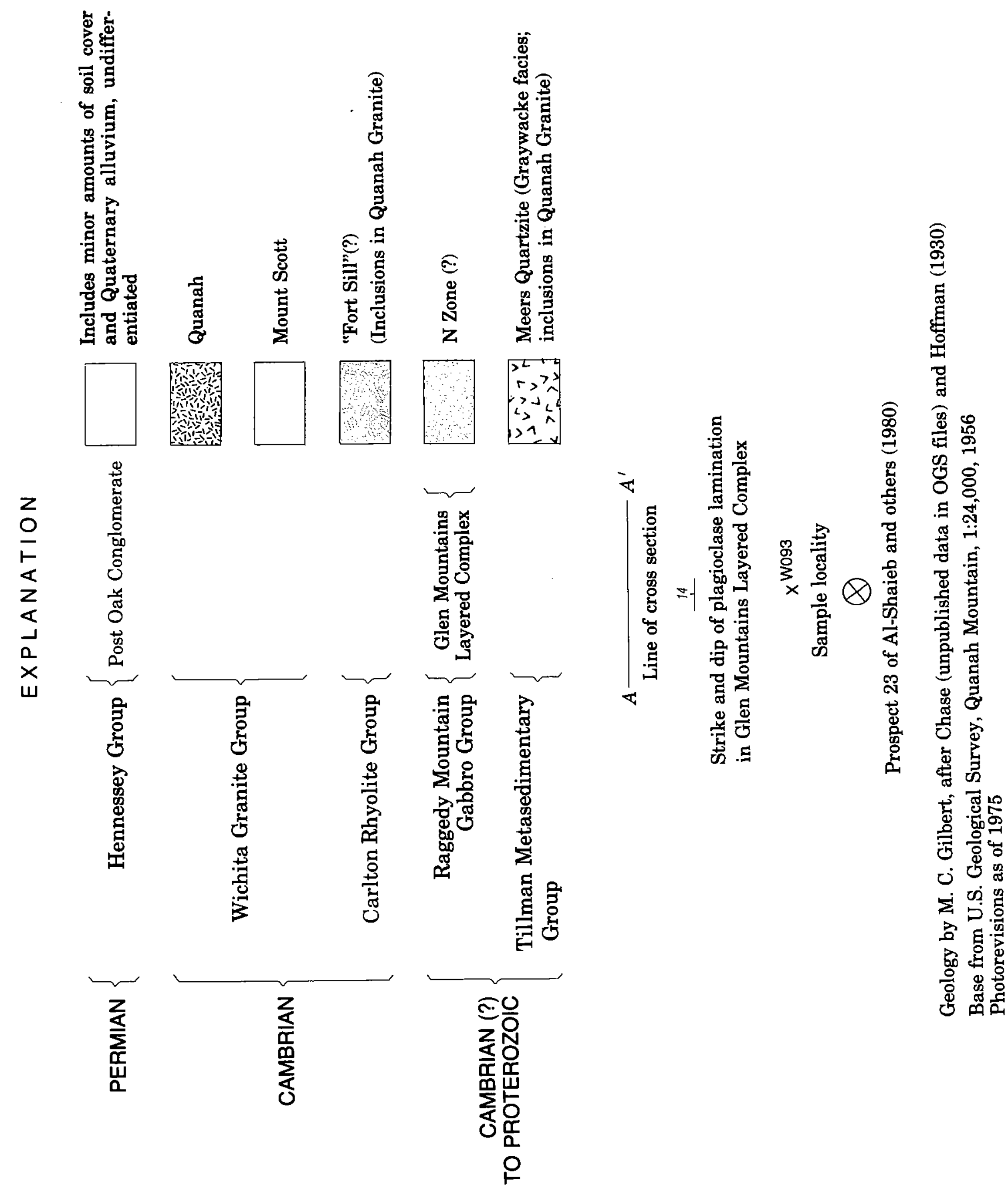

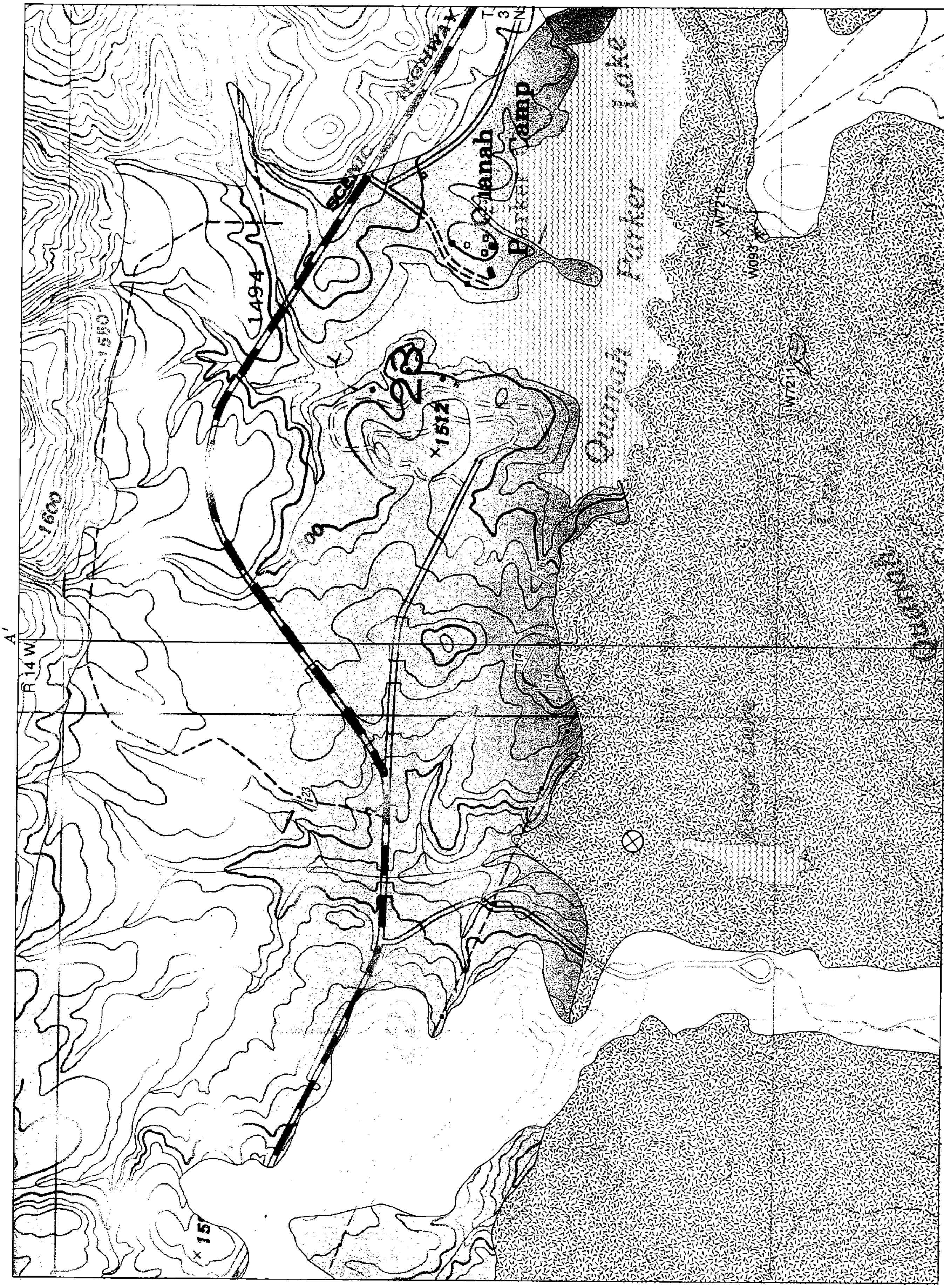

Figure 130. Geologic map for Stop 5. Map scale, 1:12,000.

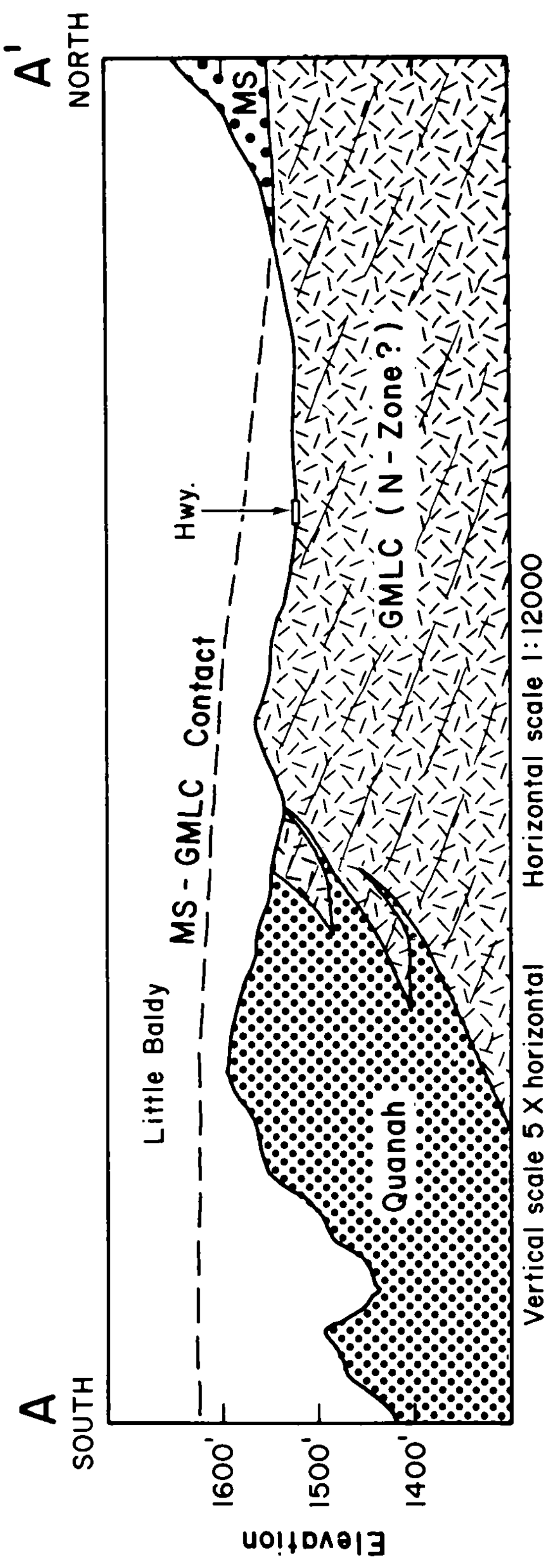

Figure 131. Cross section from south to north across map.

can be seen (fig. 132). Prominent fracture patterns of various origins abound in the vicinity. Some of those thought to be due to magma flowage (Cambrian in age) are shown in figure 133, a site which lies just south of the parking area but viewed more advantageously from the west side of the dam. In other parts of the surrounding area, other fractures of tectonic origin complicate the geology.

Three areas to the south and east are worth noting. An extra overflow for the lake crosses the road about 250 to 300 m east of the parking area. In the drainage exposures south of the road, abundant quench features in the granite are impressive (fig. 134). Somewhat southeast of this is an outcrop of Meers Quartzite and Carlton Rhyolite (W–093) (fig. 135) that weathers to tightly fractured ridges.

Farther down the overflow drainage, a zone occurs where angular inclusions (W–7211) are common. Most of these seem to be fragments of Carlton Rhyolite, but some may be dirty quartzite or Mount Scott granite. They have some fractures that do not extend out into the host Quanah (fig. 136), implying a pre-Quanah origin. Modal analyses of some of these rocks are given in table 33.

The walk from the dam northwestward across to Camp Doris crosses several additional rock types: aplite dikes and Hale Spring–type pegmatites. An aplite farther west, north of Osage Lake, was identified as a uranium prospect by Al-Shaieb and others (1980). Table 34 presents some of their trace-element data for that occurrence. Some of the aplites are contorted, suggesting continued movement of the magma at even late stages of crystallization. Near the top of Little Baldy, a pegmatoid dike 6 cm wide is full of riebeckitic or arfvedsonitic amphiboles that are 2 cm long. This dike is exactly like those in the Hale Spring area.

The granite–gabbro contact in this area can be closely located from the granite side, where the Quanah stands up as a small wall or bluff. This contact was interpreted as a fault by Chase and Miser on the State geologic map (Miser, 1954) and by Havens (1977). However, abundant evidence can now be cited for an intrusive origin. Apophyses of granite extend out into the gabbro. In detail, the contact makes corners and sharp turns, as do other intrusive contacts in the Wichitas. The gabbro here is probably the N Zone(?) of the Glen Mountains Layered Complex. Primary dips are to the east generally, suggesting tilting *before* granite emplacement. Although chemical determinations of whole rocks from a layered sequence are difficult to interpret, an average of seven determinations given by Alipouraghtapeh (1979) is shown for reference in table 35.

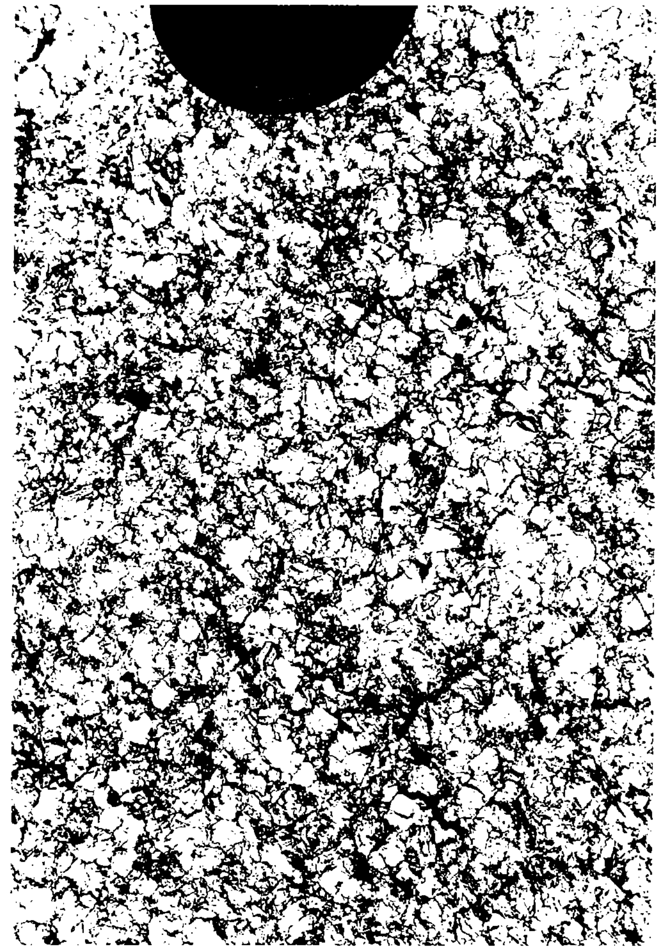

Figure 132. Photograph of typical weathered surface on normal coarse-grained Quanah granite at dam parking area. Feldspar grains are about 1 cm across.

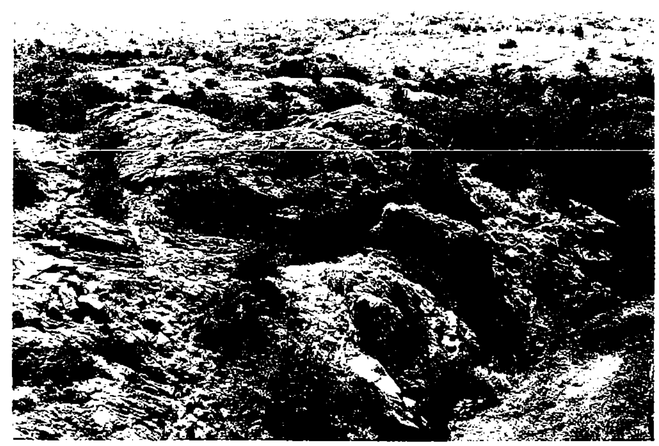

Figure 133. View of Quanah Granite looking southeastward across Quanah Creek from west side of Quanah Parker Lake Dam. Fracture pattern in outcrop dipping to south here is interpreted as delineating flowage motions in crystallizing magma.

TABLE 33.—MODAL ANALYSES OF IGNEOUS ROCKS FROM QUANAH PARKER LAKE AREA (STOP 5)

	Mt. Scott Inclusion in Quanah W7211A	CR Inclusion in Quanah W7211C	Quanah: Normal W7211B	Quanah: Quenched W7212	Quanah: Fine W753A
	NW NW NW NE 26-3N-14W			NE SE SW SE 23-3N-14W	NW NW SE NE 21-3N-14W
Qtz-P		3.5		4	21.75
Alk-F-P	25.0	7.0		17	21.50
Qtz-G	16.5	34.75	43.75	33.25	21.75
Alk-F-G	47.0	48.5	51.5	41	30.75
Plag	1.5	2.0	tr	tr	-
Hornbl	1.75	-	-	-	-
Biotite	tr	tr	2.25	1.25	1.75
Opaques	3.75	2.0	2.25	1.25	2.
Apatite	tr	-	-	-	-
Sphene	-	-	.25	-	-
Zircon	tr	tr	tr	tr	.25
Fluorite	-	tr	tr	-	.25
Alteration	4.5	2.25	tr	2.25	-
Hematite					tr

TABLE 34.—ANALYSES OF APLITE DIKE AT OSAGE LAKE (STOP 5)

(Uranium prospect 23 of Al-Shaieb and others, 1980)

Sample #/ppm	U_3O_8	Ti	V	Mn	Cu	Zn	Li	Ba	Sr	Y	Zr	Nb
124	52	156	45	160	11	162	14	620	65	40	284	43
125	54	309	25	150	1	545	44	260	50	95	7369	163
126	15	100	5	80	5	53	200	80	25	51	692	50
127	39	500	5	480	6	577	602	80	20	66	5885	123

Figure 134. Photograph of quenched Quanah granite with interfingering of coarse and fine facies.

Figure 135. Photograph of Carlton Rhyolite and Meers Quartzite, graywacke facies (W–093).

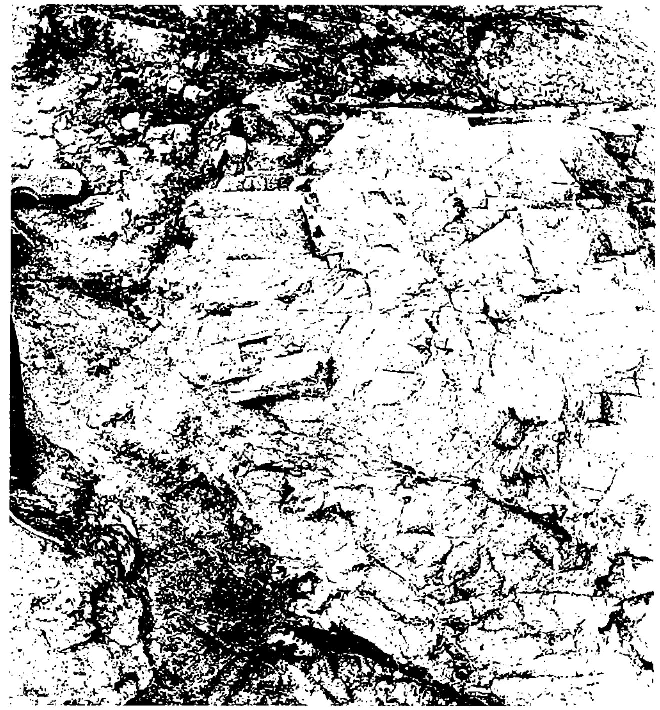

Figure 136. Photograph of xenolith 1 to 1 ½ – m long, showing fracture pattern terminating against Quanah granite host.

TABLE 35.—AVERAGED CHEMICAL COMPOSITION GLEN MOUNTAINS LAYERED COMPLEX (STOP 5)

(From Alipouraghtapeh, 1979)

	Wt %
SiO_2	49.1
TiO_2	.39
Al_2O_3	31.0
FeO	2.45
MgO	1.44
MnO	.03
CaO	10.5
Na_2O	3.5
K_2O	.43
P_2O_5	.24
	ppm
Cu	32
Cr	9
Zn	30
Pb	20
Ni	15
Ba	120
Sr	521
Rb	9
V	80

STOP 6—FRENCH LAKE DAM

Transitional Quanah Granite intrusive into Glen Mountains Layered Complex, French Lake Dam. NW¼ sec. 20, T. 3 N., R. 14 W., Comanche County, Oklahoma. **M. C. Gilbert.**

Introduction

This stop is best approached by starting from the parking area for French Lake and taking the footpath around the southeastern side of the lake to the dam (fig. 137). Location W–917 is on the north side of West Cache Creek, which requires crossing the dam. At this location, clear evidence can be seen for intrusion of the Quanah Granite into the Glen Mountains Layered Complex (N Zone?) (fig. 138). The importance of these relations is to correct the interpretation of faulting previously held for these two units, as displayed on the State geologic map (Miser, 1954) and carried forward by Havens (1977). Gilbert (1978a, 1981a, 1982) recently discussed this revision.

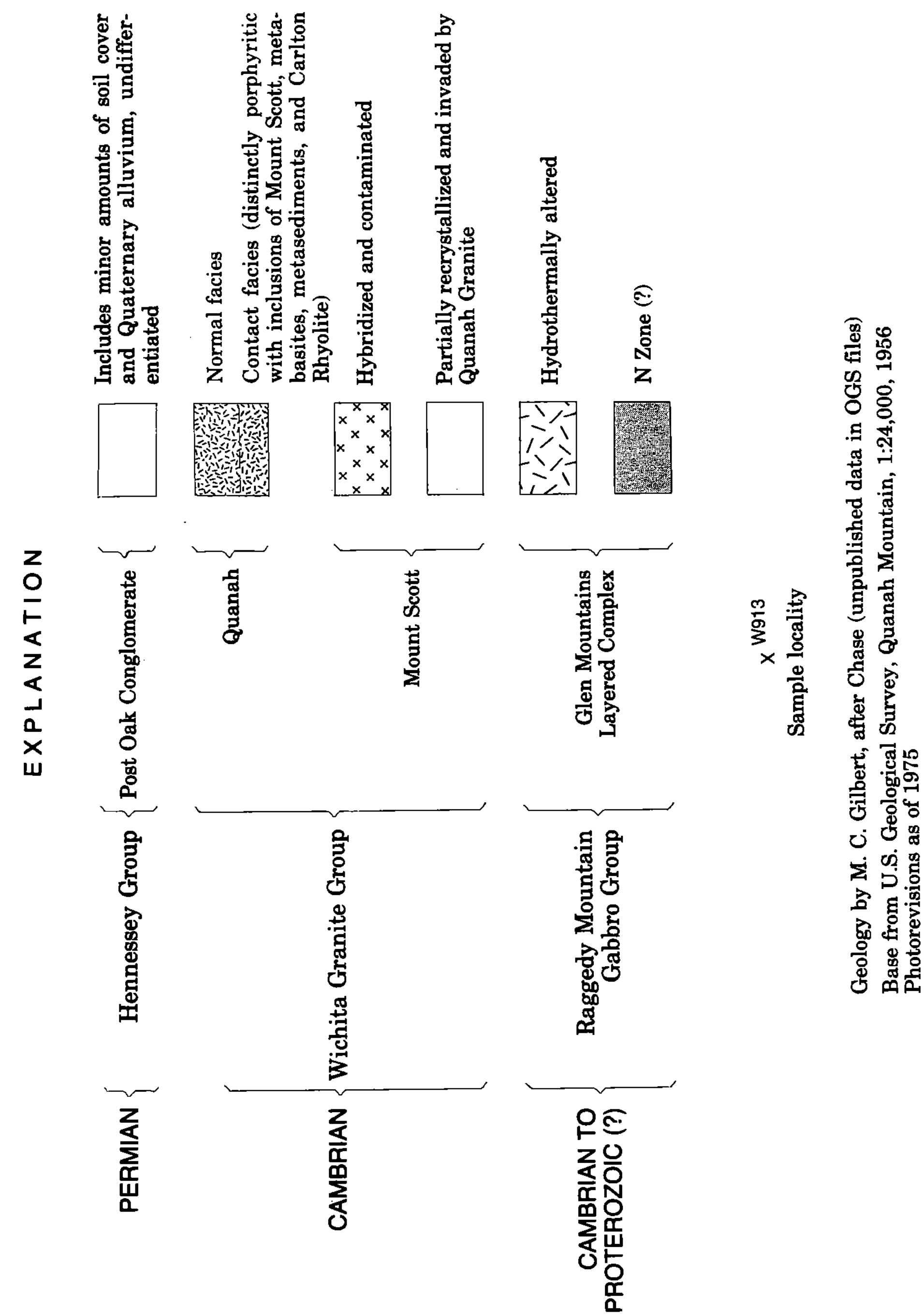

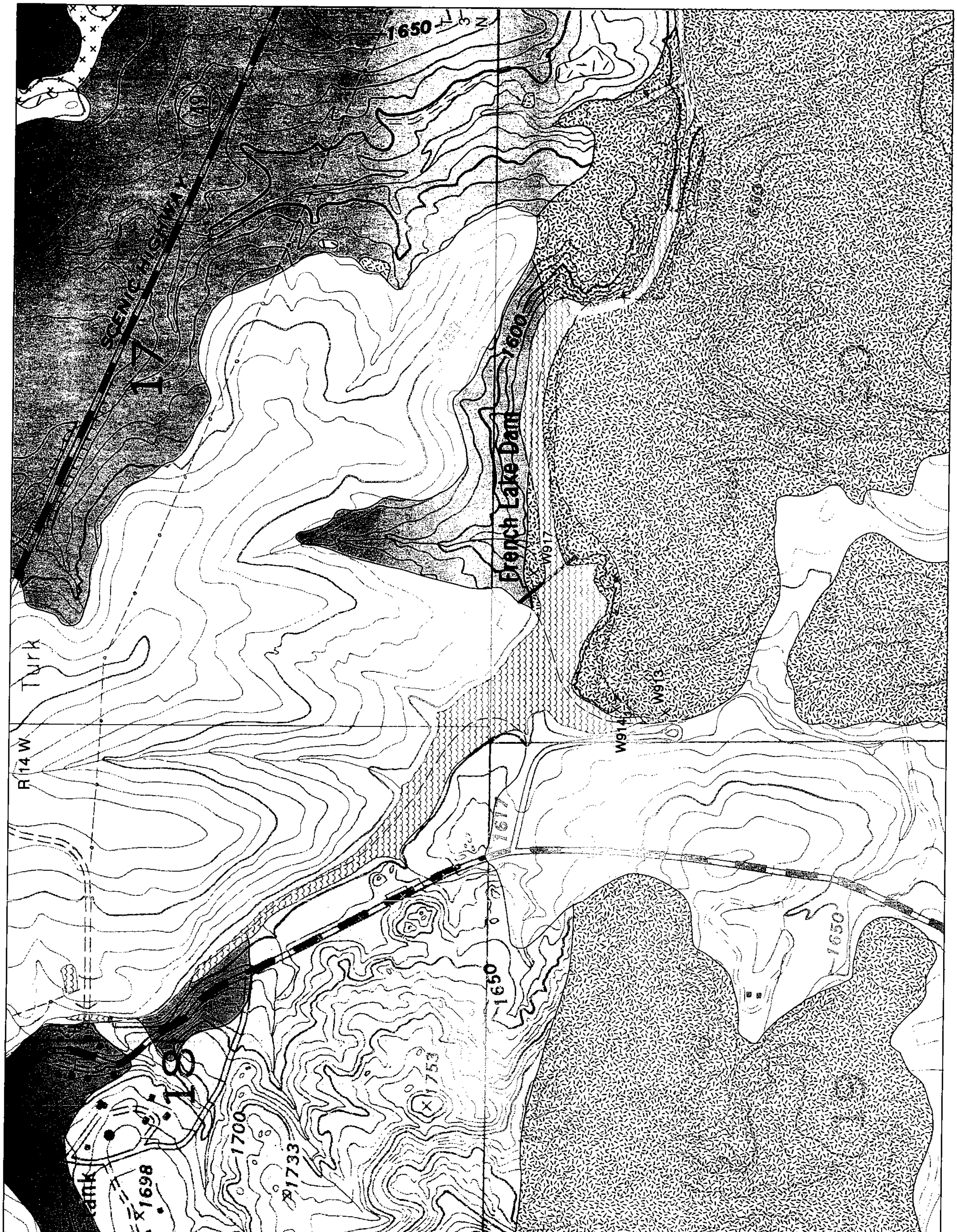

Figure 137. Geologic map for Stop 6. Map scale, 1:12,000.

Geology

A brief listing of features encountered along the footpath or in the vicinity is given. Table 36 gives modal determinations for some of the rock units.

1. Quanah Granite is somewhat finer here than at Quanah Parker Lake (Stop 5), even though both seem equally close to the contact. The appreciable width of the contact or marginal facies implies that the Quanah quenched against more than the Glen Mountains Layered Complex. It is probable that the Mount Scott Granite sill overlay this immediate vicinity. Consequently, the Quanah Granite quenched laterally and vertically in this area. The Mount Scott has since been eroded back, and our evidence for its former position lies in the number of inclusions of Mount Scott here, the variable porphyritic character of the Quanah, and regional topographic shelves that may represent the former floor of the Mount Scott Granite sill.
2. Just across the bridge from the parking area, a horizontal aplitic dike (about 30 cm thick) occurs that represents late-stage Quanah crystallization. Along the upper contact is a vuggy quartz zone, implying vapor saturation. Departing eastward from the path, a number of Mount Scott inclusions can be found in the Quanah.
3. At a distance of approximately 180 m along the trail, particularly at a small bend in the path around a boulder, a number of angular xenoliths are found (fig. 139). Rhyolite fragments, and particularly other fragments interpreted as metasedimentary, are more fractured than the porphyritic host Quanah. This fracturing appears to have formed before inclusion into the magma. The abundance of xenoliths other than Mount Scott suggests that the Quanah did not displace the Mount Scott significantly, at least regionally. Instead, the Quanah has intruded into the volcanic matrix that was the original host for the Mount Scott. By intruding into that matrix and finally against the Mount Scott, it trapped fragments of the preexisting rock.

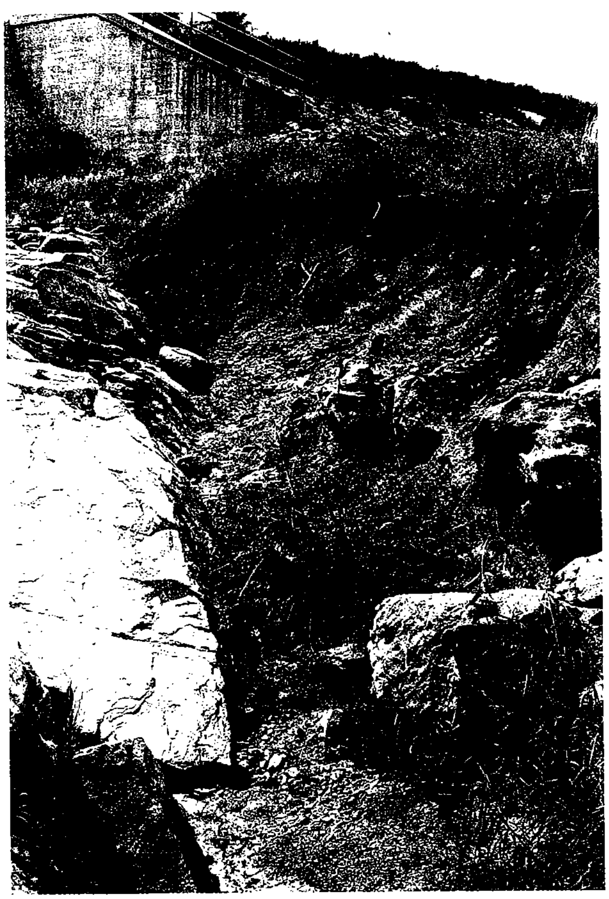

Figure 138. Photograph looking westward along contact where Quanah Granite on left (south) has intruded Glen Mountains Layered Complex on right (north). Boulders protruding from altered and weathered matrix in places are pieces of layered complex. Rock surface dipping steeply northward is contact of granite against gabbro.

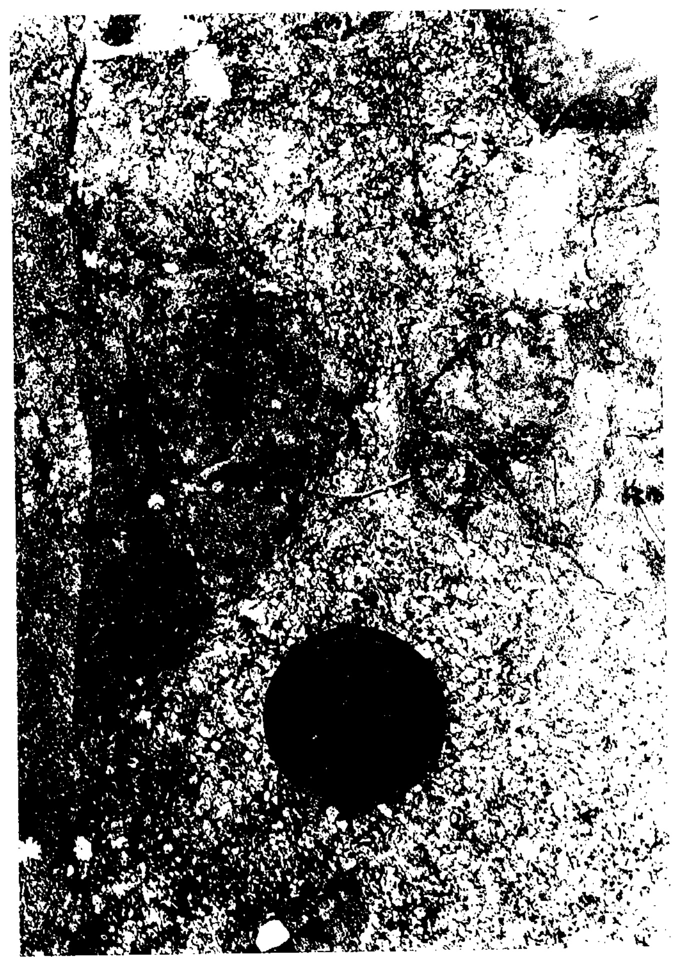

Figure 139. Photograph of outcrop along trail where angular fragments of Mount Scott Granite, Carlton Rhyolite, and metasediments(?) are found.

4. At French Lake Dam, the following features should be viewed:
   a. Gabbro–granite contact. Note the granitoid dikes in the Glen Mountains Layered Complex, which generally parallel the contact.
   b. Some of the granitoid dikes several tens of meters inside the gabbro seem to have Mount Scott affinities and provide additional argument that the Mount Scott overlay this area.
   c. The Glen Mountains Layered Complex unit here is provisionally interpreted as the N Zone.
   d. Aplites are abundant in the marginal Quanah (fig. 140). The Quanah is variably textured from coarse to porphyritic.
   e. Xenoliths are abundant with some units, which themselves carry earlier xenoliths or dikes (fig. 141).
   f. Mafic inclusions are not so common, but one that appears to have a distorted pancake shape is present (figs. 142, 143). The precursor rock for this inclusion is problematic, but for the present it is taken to be basaltic volcanic.

Figure 140. Photograph of typical aplite dikes in Quanah at W–917 (French Lake Dam). Note pen for scale.

TABLE 36.—MODAL ANALYSES OF IGNEOUS ROCKS FROM FRENCH LAKE AREA (STOP 6)

	Aplite in Quanah W913	Quenched Quanah W914B	Quanah W914C	CR in Quanah W915C	Granitoid Dike in GMLC W916A	Mafic Inclusion in Quanah W917B	Quanah W917C
	SW SW NW NW 20-3N-14W	NE SE NW NW 20-3N-14W		C SW NW NW 20-3N-14W	NE NE NW NW 20-3N-14W	SE NE NW NW 20-3N-14W	
Qtz-P		13		2.75	4		
Alk-F-P		39.75		.5	9.5		
Qtz-G	38.25	21	35.5	31.75	38		27.75
Alk-F-G	58.75	21.5	55.75	33.75	44		65.25
Plag	tr	.5		26.0		22.5	3.0
Amphibole		3.75	5.75	2.5		35	2.75
Biotite		.25	.25	tr	tr	30.83	tr
Opaques	1.75	.25	2.25	2.25	3.25		1.
Apatite			tr				tr
Sphene			.5	tr			
Zircon	.25	tr	tr				tr
Fluorite	.25	tr	tr	.25			
Alteration	.75	tr	tr	.25	.75	11.67	.25
Epidote	tr	tr	tr	tr			
Hematite		tr			.5		
Other							

Figure 141. Photograph of xenoliths in Quanah, which themselves carry other fragments or earlier dikes.

Figure 143. Photomicrograph of mafic inclusion in figure 142. View 2.6 × 1.75 mm, with crossed nicols.

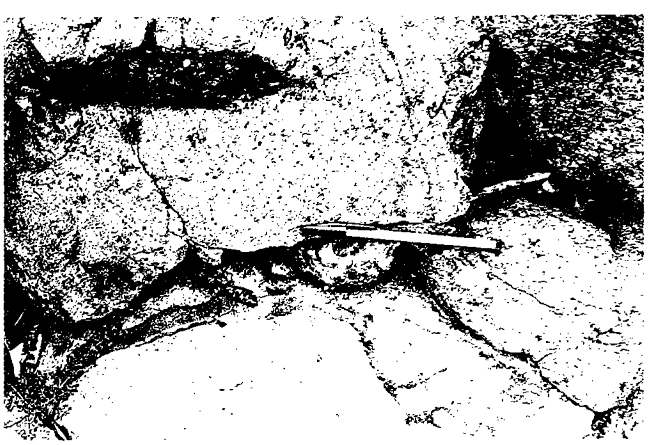

Figure 142. Photograph of small mafic enclave.

STOP 7—EAGLE (CRATERVILLE) PARK AREA

Cache granite–Quanah Granite contact, Eagle Park (Craterville Park)–Hill 1545 area, Fort Sill Military Reservation. Secs. 6, 7, 18, T. 2 N., R. 13 W., and secs. 1, 12, 13, T. 2 N., R. 14 W., Comanche County, Oklahoma. **M. C. Gilbert**.

Introduction

Schoonover (1948) and Green (1952) mapped this area originally. The contacts shown on the present map do not differ significantly from theirs except that ours are placed on a topographic base (fig. 144). Hamilton (1959) reported chemical data from Hill 1545, apparently from what is here being called the Cache granite. Al-Shaieb (1978) used the north side of Hill 1545 as a stop for a field trip emphasizing radioactive anomalies, apparently in the Quanah Granite.

The area beautifully illustrates intrusive contact relations of regional scale between two granites: one relatively coarse grained, one fine grained (fig. 145). These relations are clearly visible from U.S. Highway 62 and State Highway 115. Both Schoonover and Green saw these differences. Schoonover considered the fine-grained granite as Mount Scott (then called "Lugert") but also recognized another fine-grained granite called "aplite." Status of the latter unit is not yet resolved. Green called the fine-grained granite "Cache," a designation found useful by Myers and others (1981) in their study of the chemistry of the Wichita Granite Group. All workers recognize the relatively coarse-grained granite as Quanah.

The topography in this area is controlled by rock type and fracture patterns. It has long been noted that core–stones and tors are larger and more prominent in areas of Quanah Granite (fig. 146). This is confirmed by comparison of surfaces underlain by the two rock types here (fig. 145), and the rough surface of the Quanah Granite (fig. 146). Taylor (1915) pointed out in the Wichitas that wider spaced fractures correlate with coarser grain size. The reason for this does not seem to have been explained. It does not appear to be some differing mechanical response of different rock textures to the same applied stress (in the Pennsylvanian). Most of the finer grained rocks, that is, the Cache, quenched rapidly, possibly even to a partially glassy state. Thus, the change in volume from the liquid state to the crystalline state, with a contraction of 5 to 10 percent in these rocks, could not be taken up gradually. Apparently, many fractures and incipient fractures formed immediately on cooling (in the Cambrian), just as columnar jointing forms in basalts. Later tectonic stresses could have propagated and extended these, but their distribution and pattern would need to have been partly set early. The coarser grain size of the Quanah indicates that it cooled more slowly. In this case, the contraction on crystallization was taken up more gradually by liquid–crystal movement in response to the ambient load. Consequently, fewer and more widely spaced fractures of this type formed. In general, Quanah tors are larger farther west, and smallest in the east as in this area. Granophyric texture is common in the Quanah only in the east. These two observations indicate that the crystallizing Quanah had a lower overburden pressure here and a higher pressure to the west.

EXPLANATION

PERMIAN { Hennessey Group { Post Oak Conglomerate { **Includes minor amounts of soil cover and Quaternary alluvium, undifferentiated**

CAMBRIAN { Wichita Granite Group { **Quanah** / **Cache**

x W743
Sample locality

Geology by M. C. Gilbert, after Schoonover (1948) and Green (1952)
Base from U.S. Geological Survey, Mount Scott, 1:24,000, 1956
Photorevisions as of 1970

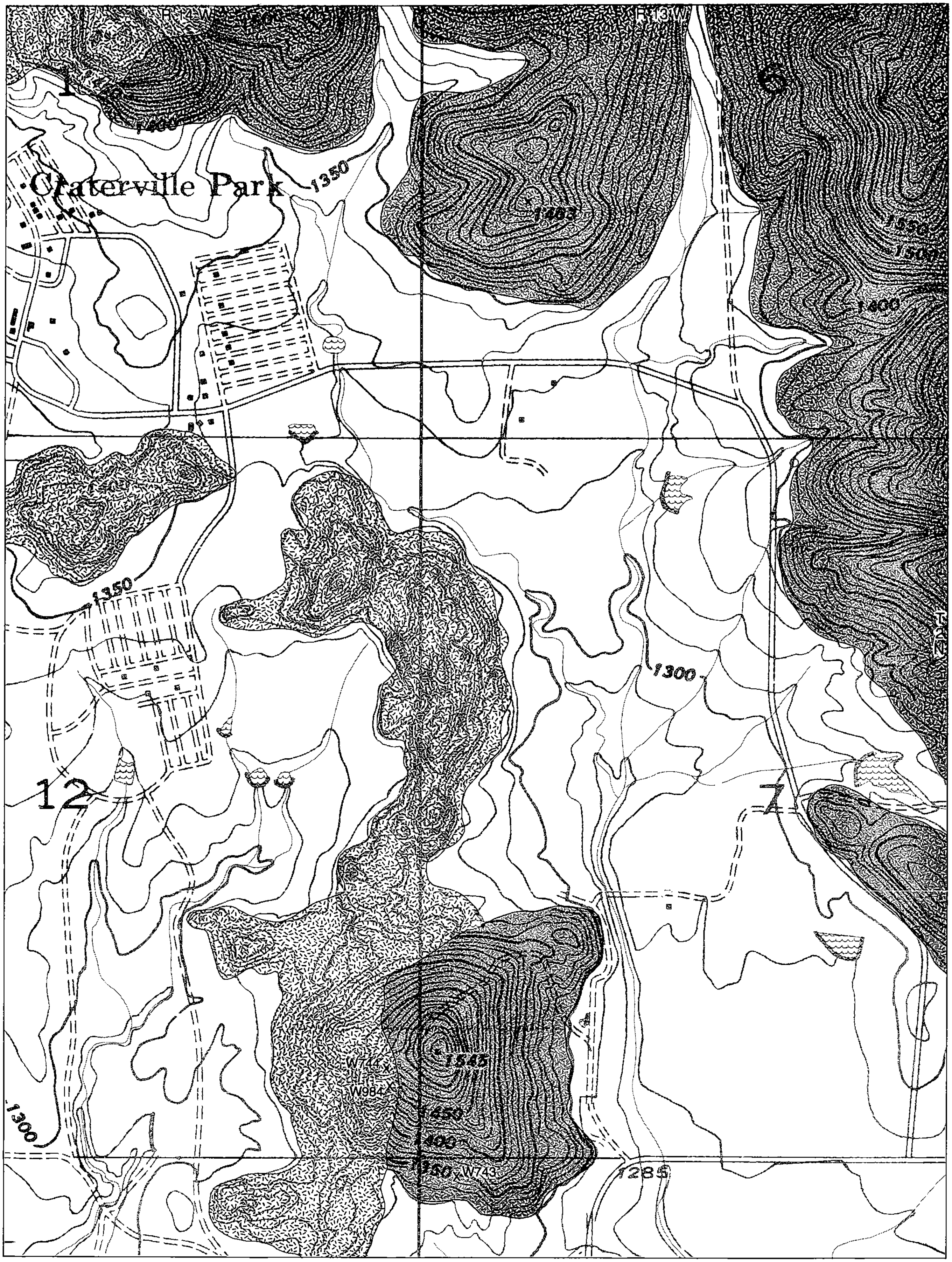

Figure 144. Geologic map for Stop 7. Map scale, 1:12,000.

Cache–Quanah Contact

Table 37 lists modal determinations for the Cache granite, one of its aplites, and the Quanah Granite. The Cache is a fine-grained, granophyric granite with a low color index (see table 6 for chemical data). Ferromagnesian minerals are oxides and biotite. In places, it has abundant miarolitic cavities, many of which are lined with coarser alkali feldspar and well-terminated quartz crystals. The Cache is highly fractured and normally does not support many trees.

The Quanah is a relatively coarse-textured rock (crystal sizes to about 1 cm) for the Wichita Mountains. It is noted for the presence of riebeckite (sodic amphibole) or biotite. In some other areas, these facies seem to be distinct, but at this stop both have been reported. Evidence for Quanah intruding Cache can be summarized as (1) quenching of Quanah near the contact (fig. 147), and (2) apophyses of Quanah protruding into Cache, although these are harder to find. This order of intrusion is consistent throughout the Wichitas, where fine-grained granites are older than coarse-grained granites. Presumably this is due to the continued build-up of the rhyolitic cover with time. Although the structural horizon where the granites intrude seems to be fixed, the overburden pressure increased with time as a function of the increasing stratigraphic thickness.

Table 38 presents trace-element data collected by Al-Shaieb and others (1980). The Cache is distinctly poorer in U, Zn, Li, Ba, Zr, and Nb. This might be expected if the Cache had lost its vapor phase quickly and had lost these elements with it. In contrast, the Quanah had a more effective cover and the vapor was contained; more hydrous phases formed on cooling to capture these elements.

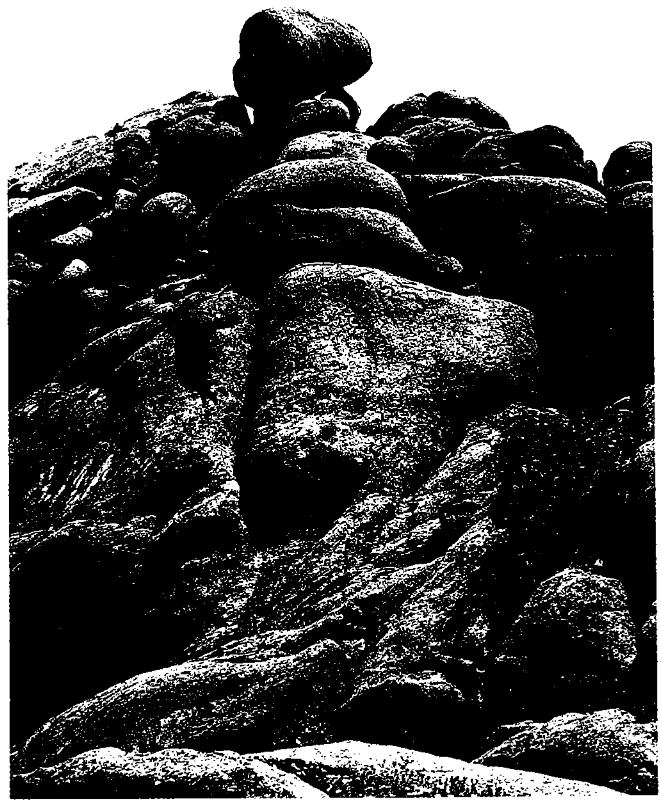

Figure 146. Photograph of a well-known feature of tor topography, known as a tor or inselberg or castle koppie (Twidale, 1976). Such turret features are a function of fracture spacing and original (Permian) *subsurface* weathering. This one in NE¼NW¼NE¼ sec. 12, T. 2 N., R. 14 W., is typical of those developed on Quanah Granite bedrock (see Gilbert, this guidebook, for discussion of tectonic significance).

Figure 145. Photograph looking northward across Eagle Park area. Coarse topography on left (west) side of hill in middle ground is younger Quanah Granite; smooth slope on east side is older Cache granite. This distinctive contact is visible from nearby roads and can be traced locally. Contact interdigitates farther north and east, becoming more complex and less easy to follow.

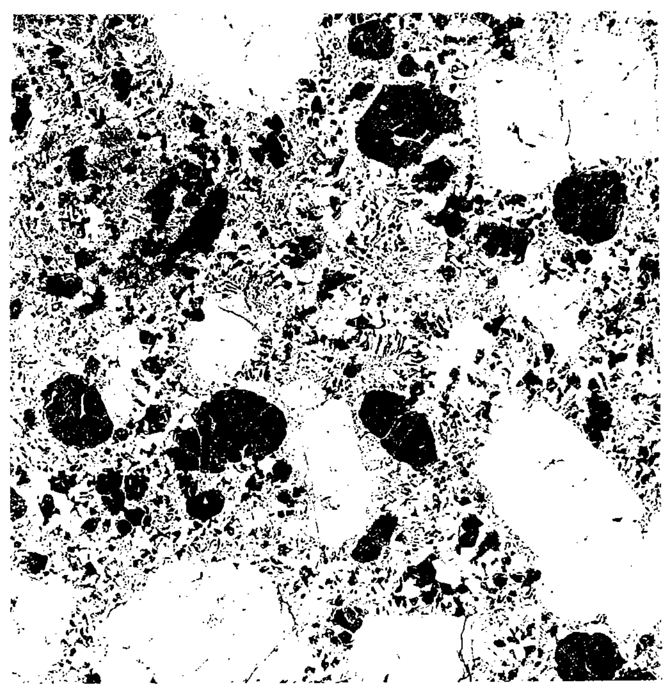

Figure 147. Photograph of a 1-inch-wide thin section of Quanah Granite (W–984) quenched upon intrusion against Cache. Early alkali feldspars and quartz (dark gray) are phenocrysts in micrographic matrix of quartz and alkali feldspar.

TABLE 37.—MODAL ANALYSES OF IGNEOUS ROCKS FROM CRATERVILLE PARK AREA (STOP 7)

	Cache		(Aplite)	Quanah			
	W742	W743	W743B	W744	W744	S-Coarse	S-Porphyritic
	SE NE NE 13-2N-14W	NW NW NW 18-2N-13W		NW SE SE SE 12-2N-14W		12-2N-14W	13-2N-14W
Qtz-P	10.75	8.5	.25	18.75	12.5		
Alk-F-P	13.75	12.25	tr	22.25	25.75		
Qtz-G	27.75	29.75	33	23.75	28.75	25	28
Alk-F-G	48	47.25	63.25	32	30.75	70	70.5
Plag	-	-					
Amphibole	-	-		tr	tr	1.0 (R)	.05 (R)
Biotite	tr	.25		1.75	.75		
Opaques	tr	1.75	3.5	2	1.25	.5	.1
Sphene	-	-		tr		tr	tr
Zircon	tr	tr	tr	tr	.25	tr	tr
Fluorite	tr	.25	tr	tr	tr	tr	tr
Alteration	-	-				3.4	1.2
Hematite	tr	tr	tr	tr			
Other	-	-	tr			tr(apatite)	tr(apatite)

TABLE 38.—TRACE-ELEMENT CONTENTS FROM HILL 1545 AND VICINITY (STOP 7)

(From Al Shaieb and others, 1980)

Sample #/ppm	U_3O_8	Ti	V	Mn	Cu	Zn	Li	Ba	Sr	Y	Zr	Nb
142-Q	47	900	0	60	3	94	12	60	15	79	4695	144
143-Q	13	600	0	120	4	165	46	200	35	61	1314	73
144-Q	11	600	5	120	44	63	46	150	10	61	893	65
117-C	7	600	5	30	6	29	2?	20	20	45	349	42

Q = Quanah; C = Cache

STOP 8—HIDE-A-WAY AREA

Relations among Carlton Rhyolite–Meers Quartzite? (Pratt Hill quartzite)–Mount Scott Granite–late diabase, Hide-A-Way (SW Lake Elmer Thomas), Fort Sill Military Reservation, about 10 miles northwest of Lawton. SE¼NE¼ sec. 23, T. 3 N., R. 13 W., Comanche County, Oklahoma. **J. R. Miller, M. C. Gilbert,** and **J. R. Sides**.

Outcrops of granite, microgranite, rhyolite, diabase, and quartzite occur within the immediate vicinity of Hide-A-Way Cove (fig. 126). Just west of Hide-A-Way Cove, recent sediments have originated from erosion of the granite and rhyolite. Tables 39, 40, and 41 give relevant chemical and modal data for the rocks.

The hills to the north of Hide-A-Way Cove are composed of Mount Scott Granite (fig. 127). The Mount Scott is a leucogranite that is porphyritic to phaneritic and generally fine grained. Major constituents are micropegmatite, microperthite, and quartz, with minor hornblende, magnetite, and sphene. Chemical determination of the unit is given in table 6. Outcrops of Mount Scott Granite commonly are covered with exfoliation-derived boulders, yielding classic tor topography (Gilbert, 1979; and this guidebook). The granite is pink to red on fresh surfaces and weathers to dark brick red. Exposures of diabase occur in the immediate vicinity of Hide-A-Way parking area. This is known as late diabase, because such bodies cut all other igneous units in the Wichitas. A new XRF determination is presented in table 41, which is quartz-normative owing to the unusually high Fe content. Petrographically, abundant blebs and stringers of secondary oxides are seen. Other analyzed late diabases (Gilbert and Myers, in preparation) appear to be olivine-normative.

Hills underlain by the Carlton Rhyolite Group occur south of Hide-A-Way Cove, on Fort Sill Military Reservation. This is the largest outcrop of Carlton Rhyolite in southern Oklahoma (see table 4). In this region, Carlton Rhyolite is highly silicified and contains phenocrysts of perthite and quartz. The groundmass is felsiphyric and consistently contains microscopic grains of rounded magnetite. The fresh rhyolite is pinkish red, and weathers to reddish brown. Outcrops of the rhyolite break into polygonal blocks owing to intense jointing in the rock (fig. 148). These polygonal blocks are easily weathered and transported, and outcrops of rhyolite commonly have smooth surfaces. The rhyolite is highly brecciated at fault contacts. At Hide-A-Way Cove, some of the rhyolite is an ash-flow tuff with preserved fiamme that indicate a dip of about 35° to the south. Elsewhere in southern Oklahoma, the rhyolite contains lava flows and agglomerates.

Pratt Hill quartzite (informal field term) occurs at the parking area and extends eastward along the southern shore of Lake Elmer Thomas (fig. 149). The quartzite is best exposed on the steep northern slope of Pratt Hill, where it is in sharp contact with overlying Carlton rhyolite. The quartzite is composed mainly of fine-grained quartz and white micas, with

Figure 148. Photograph of columnar block of Carlton Rhyolite in which alkali feldspar phenocrysts are aligned.

Figure 149. Photograph of lightly banded quartzite.

TABLE 39.—MODAL ANALYSES OF SILICIC IGNEOUS ROCKS FROM HIDE-A-WAY AREA (STOP 8)

	Carlton Rhyolite						Mt. Scott	
	W034C NE SW NW 24-3N-13W	W775 NW SW NW 24-3N-13W	W796 SE SE NW 23-3N-13W	Schoonover	W-121 NW NW SE 23-3N-13W	Sides & Miller Average of 2	W795 SW NE SW NE 23-3N-13W	W793 NW NE SE NE 23-3N-13W
Qtz-P	3.0	4.25	4.75	11.0	7.0	5.2	4.25	4.75
Alk-F-P	6.0	7.0	7.25	6.0	11.0	9.9	23.75	22
Qtz-G	} 79.0	} 77.75	} 85.75	30.0	} 81.6	} 81.2	27.75	30
Alk-FG				30.0			37.25	40
Plag			tr	–				
Hornbl				–			3.5	.5
Biotite	5.0		tr	–				1.0
Opaques	3.5	1.5	1.75	1.1	.4	.2	1.75	1.75
Sphene	tr		tr	–			tr	tr
Zircon	tr		tr	.1	tr		tr	tr
Fluorite	tr	1.25	tr	tr			tr	tr
Apatite				tr			tr	
Alteration	3.5	5.75	.5	17.2		.7	1.25	tr
Hematite	tr			4.5			.5	tr
Other	ep	2.5 (veins)			tr	2.8 (vein)		

TABLE 40.—MODAL ANALYSES OF MEERS QUARTZITE FROM HIDE-A-WAY AREA (STOP 8)

	W033 C SW SW NW 24-3N-13W	W776 SE SE NE 23-3N-13W	PH-2	PH-10	ET-11	ET-13	PH-29
				From Sides and Miller			
Quartz	71.75	45.5	52.4	47.3	37.4	45.7	99
White mica	8.25	25.25	45.1	–	–	52.8	tr
Matrix micas	18.50	26.25	–	49.6	54.1	–	–
Andalusite	1.0	–	–	–	–	–	–
Opaques	.25	2.75	1.3	1.5	4.7	1.2	–
Other	.25	.25	1.3	1.5	2.3	0.3	–

TABLE 41.—BULK-ROCK ANALYSES FROM AREA OF STOPS 4 AND 8

	Carlton Rhyolite		Meers Quartzite		Late diabase
	W-121 NW NW SE 23-3N-13W	GWC199 NE NE SE 15-3N-13W	WEH1584 SW NE NW 24-3N-13W	W776 SE SE NE 23-3N-13W	W983 SE NW SE NE 23-3N-13W
Wt%					
SiO_2	76.61	76.54	73.19	69.25	47.59
TiO_2	nd	.25	.20	0.39	3.91
Al_2O_3	12.10	11.72	13.87	16.72	12.96
Fe_2O_3	2.20	2.37	5.07	3.39	
FeO		.32			15.42
MnO	.01	.02	.13	0.11	0.25
MgO	.07	.04	.20	0.64	5.43
CaO	1.14	.13	1.22	0.03	8.66
Na_2O	3.37	3.55	1.34	0.41	1.67
K_2O	4.55	4.60	5.02	4.71	0.44
P_2O_5	.01	.03	.09	0.03	0.73
Original Total	104.34	100.00	not given	98.20	97.39
Norms					
qtz	36.7	37.9	43.5		4.1
or	26.9	27.2	29.6		2.7
ab	28.4	30.0	11.3		14.5
an	4.4	0.8	5.5		27.3
cor			4.2		
Trace Elements ppm					
Ba	4653	1600	4494		
Rb		100		229	18
Sr	105		204	14	373
Zn	98		185		
Th	26		18		
U	4		<2		

feldspar absent everywhere but the Hide-A-Way Cove parking area. Andalusite has been identified in one sample, its first reported occurrence in Oklahoma. The quartzite is white to light gray, dark gray green where chlorite occurs (to 20 percent), and is not well bedded. The unit is described more fully elsewhere in this guidebook (Sides and Miller).

During Middle Cambrian time, the rhyolite was pyroclastically erupted onto an eroded gabbro surface; the rhyolite pile was at least 1.4 km (4,500 ft) thick. The gabbro, Proterozoic(?) to Cambrian in age (see Bowring and Hoppe, this guidebook), crops out 2.5 miles north of Hide-A-Way Cove. The Mount Scott Granite was injected as a sill, 152 to 274 m (500 to 900 ft) thick, along the rhyolite–gabbro contact. The Mount Scott Granite (Wichita Granite Group) and the Carlton Rhyolite Group are comagmatic, and formed 525 million years ago (Ham and others, 1964). The Pratt Hill quartzite appears to have been a sedimentary unit that was deposited on the eroded gabbro surface. The possibility does exist that the quartzite is a xenolith of sediment into which the gabbro intruded. However, the Pratt Hill may not correlate well with the Meers Quartzite (see Sides and Miller, and Gilbert, for discussions). The rhyolite and granite of the southeastern Wichita Mountains (Hide-A-Way Cove area) locally appear to be folded into a southeast-plunging syncline (Schoonover, 1948). The Carlton Rhyolite outcrop south of Hide-A-Way Cove is diamond shaped (map view) and trends northwestward. The Mount Scott Granite outcrop wraps around the rhyolite on the north, northeast, and west sides. Gilbert has argued (Stop 4) that the Mount Scott overlies Carlton here; figure 127 shows that interpretation. The axis of this syncline is about 2 miles south of Hide-A-Way Cove, and trends northwestward. Its relation to the broader anticlinal structure of the region is not well understood.

STOP 9—WELSH HILL

Mount Scott and Medicine Park(?) Granites. S½ sec. 13, N½ sec. 24, T. 3 N., R. 12 W., Comanche County, Oklahoma. **M. C. Gilbert.**

Introduction

This stop is on private land, and permission must be secured to enter. Here, Mount Scott Granite lies in contact with distinctly porphyritic rock that has a finely crystalline, granophyric groundmass (fig. 150). Schoonover (1948) mapped it as rhyolite, but we show it as belonging to the Medicine Park granite (table 5; fig. 150). This is not a certain correlation, because Permian plains cover possible outcrops between here and the type area farther west. Nevertheless, the granite has interesting textural features, warranting its inclusion in this guidebook.

Mount Scott Granite

The outcrops on Welsh Hill are the most easterly exposures of the Mount Scott Granite and the Wichita Granite Group. The road cut made by State Highway 49 provided granite sample W–738, the bulk chemistry of which has been determined (tables 42, 43). The rock is similar in most respects, petrographi-

EXPLANATION

PERMIAN
Hennessey Group
Post Oak Conglomerate — Includes minor amounts of soil cover and Quaternary alluvium, undifferentiated

CAMBRIAN
Wichita Granite Group
Medicine Park
Mount Scott

x W738 Sample locality

Strike and dip of layering in granites defined by alignment of alkali feldspar phenocrysts (and a subparallel fracture system), generalized

Geology by M. C. Gilbert, after Schoonover (1948) and R. E. Denison (unpublished written communication, 1977)

Base from U.S. Geological Survey, Fort Sill, 1:24,000, 1956
Photorevisions as of 1970 and 1975

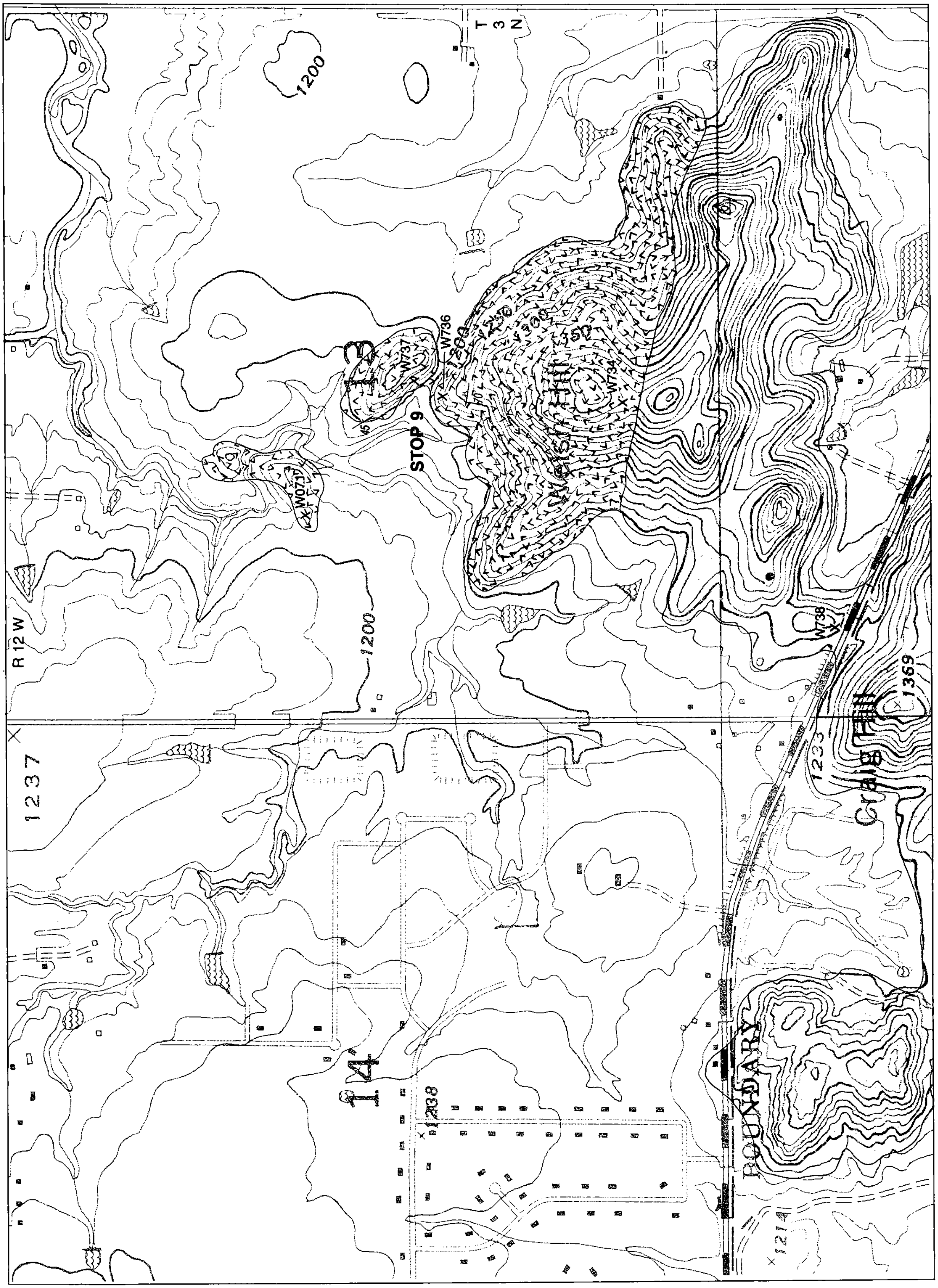

Figure 150. Geologic map of Welsh Hill area, Stop 9. Map scale, 1:12,000.

cally and chemically, to Mount Scott that is 55 km to the west, near Lake Tom Steed (fig. 151). This is an incredible lateral extent for a granite sheet estimated to be 250 to 500 m thick. Small mafic inclusions, ovoid feldspars, and porphyritic and granophyric texture characterize the granite in this road cut. No significant variations appear in the granite in this area.

Mount Scott–Medicine Park Contact

This contact was shown as a fault by Havens (1977). Although the contact can be traced across Welsh Hill, and located within a few meters, no clear exposure of the detailed relations has been found. The rocks on either side do not appear granulated or brecciated. Mount Scott Granite dips to the south; Medicine Park granite dips steeply to the north. At the map scale, the contact is straight, but locally its trace along the topography does not shift in the way a simple planar surface would. It appears to be an intrusive contact, with the Medicine Park being younger.

Medicine Park Granite

This unit is strongly fractured, which complicates determination of dip direction. Dips reported on the map (fig. 150) are based on layering defined by alignment of alkali feldspar phenocrysts. One of this granite's most striking features is the development of abundant miarolitic cavities. In a small, northwest-trending valley crossing the northern end of Welsh Hill, such cavities dominate the rock's appearance. Entrance to this valley is through the Foxfire Housing Development (with permission). The rocks cropping out here are highly oxidized and redder than usual. Some of the cavities are flattened in the layering, suggesting flow or compaction after gas (H_2O + CO_2?) exsolution. Most of the cavities are 1 by 1 cm to 1 by 2 cm, with approximately 30 cavities intersected on a grid of 20 by 20 cm.

The rock is better described as a granite than an extrusive flow rock (figs. 152, 153). It may be related to rhyolitic dikes that cut Mount Scott Granite farther west. Those dikes and the Medicine Park granite may be from the same magmatic event.

TABLE 42.—MODAL ANALYSES OF IGNEOUS ROCKS FROM WELSH HILL (STOP 9)

	Mt. Scott	Medicine Park			
	W738 NE SW NW NW 24-3N-12W	W734 NE SE SW 13-3N-12W	W736 NE NE SW 13-3N-12W	W737 NE NE SW 13-3N-12W	W071 NW SW SE NW 13-3N-12W
Qtz-P	6.5	3.75	1	5.75	3.75
Alk-F-P	21.25	20	19.75	7.5	7.5
Qtz-G	27.5	31	33.5	42	37
Alk-FG	40.0	38	42.25	42	47
Plagioclase	-	tr	-	-	-
Hornbl	2.0	-	-	-	-
Biotite	-	-	.5	.75	.25
Opaques	2.5	2	2	1.75	.75
Sphene	-	.25	-	-	-
Zircon	-	-	.25	tr	-
Fluorite	tr	tr	-	.25	tr
Alteration	tr	2.5	.75	tr	tr
Epidote	.25	tr	-	-	-
Hematite	-	2.5	tr	tr	-
Other	-	-	-	-	3.75 (Qtz vein)

Figure 151. Photograph of thin section (1 inch wide) of Mount Scott Granite (W–938). Ovoid feldspars and granophyric texture are prominent.

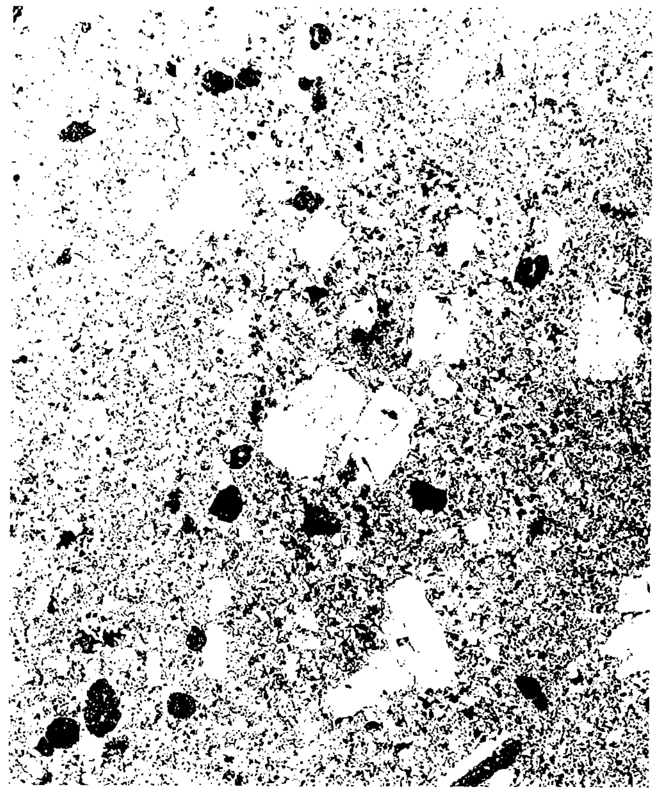

Figure 152. Photograph of thin section (1 inch wide) of Medicine Park(?) granite (W–735). Most of dark-gray to black areas are quartz. Alkali feldspar and quartz phenocrysts appear partially corroded and broken.

TABLE 43.—BULK-ROCK ANALYSIS OF MOUNT SCOTT GRANITE

Wt%	W738
SiO_2	72.18
TiO_2	.46
Al_2O_3	12.28
Fe_2O_3	3.74
MnO	.09
MgO	.27
CaO	1.23
Na_2O	3.83
K_2O	4.20
P_2O_5	.07
LOI	.64
	98.99
ppm	
Rb	128
Sr	95

Figure 153. Photomicrograph of Medicine Park(?) granite (W–074), showing pronounced granophyric texture in graphic pattern. View 1.75 × 2.15 mm, with crossed nicols.

STOP 10—BLUE CREEK CANYON

Geology of Paleozoic sedimentary rocks, including Cambrian Reagan Sandstone and Honey Creek, Fort Sill, and Signal Mountain Formations; Ordovician McKenzie Hill and Cool Creek Formations; and Permian Post Oak Conglomerate. Secs. 2, 3, 10, 11, T. 4 N., R. 13 W., Comanche County, Oklahoma. **R. N. Donovan, A. Babaei,** and **D. J. Sanderson.**

Introduction

The land on both sides of Blue Creek Canyon belongs to Mr. and Mrs. Charlie B. Oliver of the Kimbell Ranch. We are very grateful to them for allowing us constant access to their land. Visitors are requested to obtain permission to examine the rocks from the ranch and to respect the area.

Recently, one of us (Donovan), in conjunction with Dr. Dave Sanderson, of Queen's University, Belfast, and several graduate students from the Department of Geology at Oklahoma State University (Babaei, 1980), has been engaged in a long-term study of the Slick (or Limestone) Hills north of the Wichita Mountains. The purpose of the present excursion is to examine some of the more accessible geologic elements of these hills. In particular, we will examine outcrops of high quality on both sides of the road running through Blue Creek Canyon. These outcrops present features of interest to sedimentologists, stratigraphers, structural geologists, and volcanologists. The exposures will be examined on two walks of about a mile each. In addition, if time permits, there will be two short roadside stops to examine features associated with the Post Oak Conglomerate. Figure 154 is a

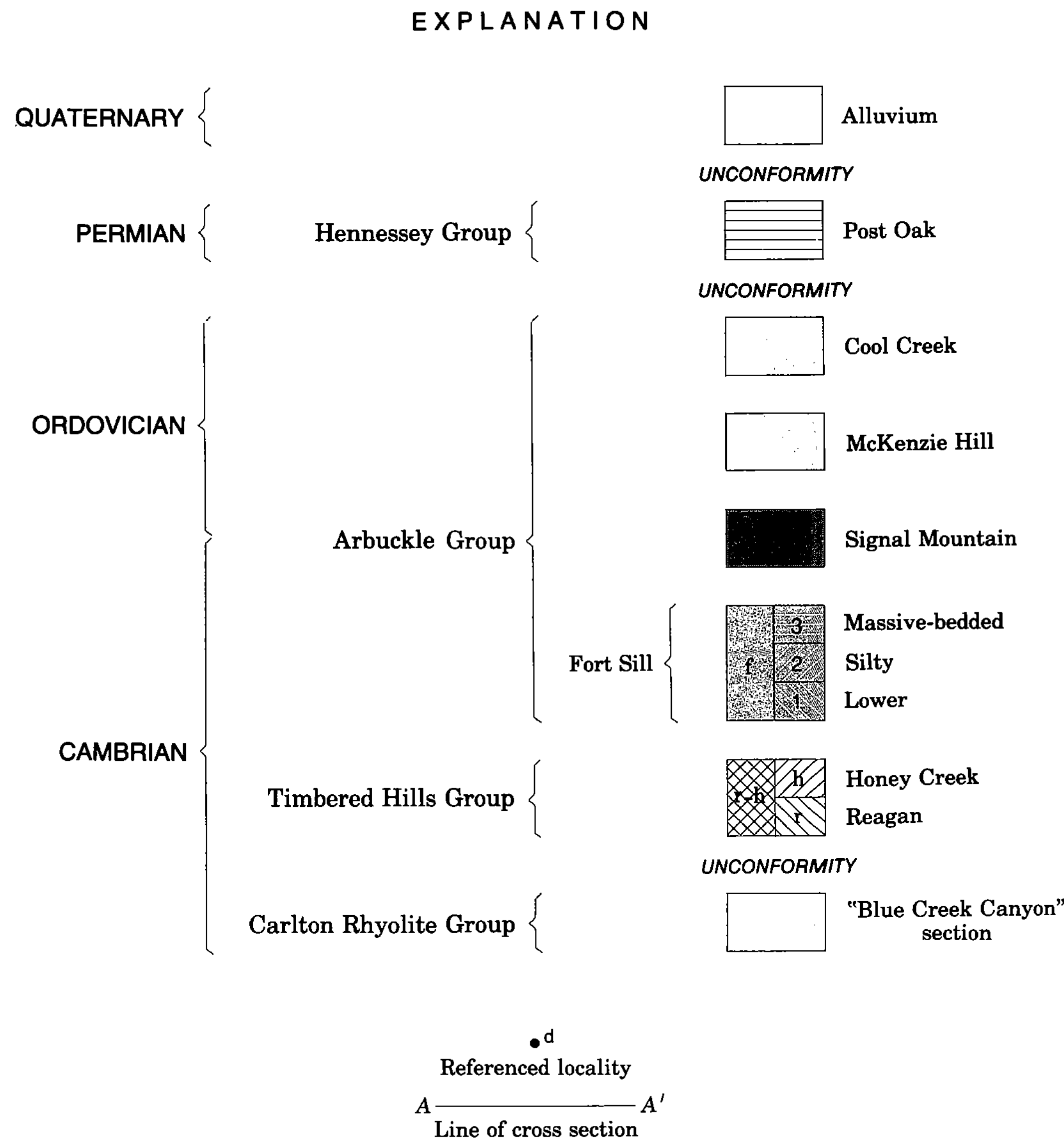

Geology by R. N. Donovan and A. Babaei

Base from U.S. Geological Survey, Meers, 1:24,000, 1956
Photorevisions as of 1975

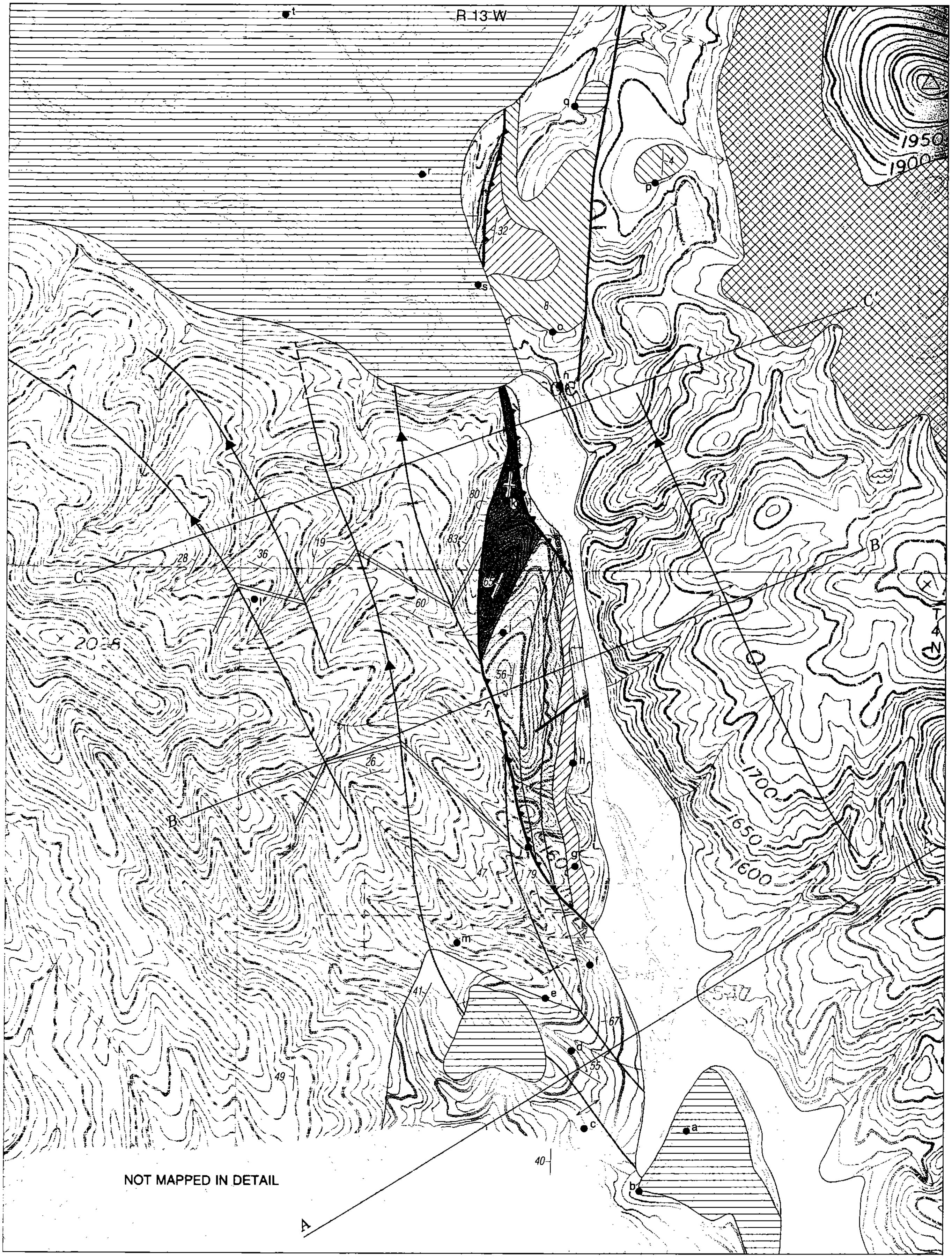

Figure 154. Geologic map of Blue Creek Canyon area. Map scale, 1:12,000.

geologic map of the Blue Creek Canyon area and highlights some of the principal features examined during the course of the day. Figure 155 is a series of cross sections from this map. Reference should also be made to several diagrams in the article by Donovan in this guidebook.

Outline of Geology

Rocks exposed in the area of Blue Creek Canyon are as follows:

9. Recent alluvium.
8. Post Oak Conglomerate.
7. Cool Creek Formation.
6. McKenzie Hill Formation (6 and 7 are of Ordovician age).
5. Signal Mountain Formation.
4. Fort Sill Formation (4 and 5 are of Cambrian age; 4 through 7 are assigned to the Arbuckle Group).
3. Honey Creek Formation.
2. Reagan Sandstone (2 and 3 are of Cambrian age and are assigned to the Timbered Hills Group).
1. Carlton Rhyolite Group (Cambrian).

Profound unconformities separate the Carlton Rhyolite Group from the Timbered Hills Group, and the Cool Creek Formation from the Post Oak Conglomerate.

The Blue Creek Canyon Fault is a north-trending, high-angle reverse fault that has thrust Cambrian rocks westward over Ordovician rocks (fig. 155). This major fault separates the Blue Creek Horst (to the east) from the Lawtonka Graben. The Ordovician rocks, within the graben, are intensely folded.

Itinerary

First walk, *a–m*; second walk, *n–q*; additional localities, *r–t*. Localities shown in figure 154.

a. The Post Oak Conglomerate at Red Hill is a breccio-conglomerate consisting of pebble-sized clasts of Ordovician limestone. At the eastern edge of the hill (close to the road), the conglomerate unconformably overlies greatly fractured Carlton Rhyolite. The unconformity is irregular and shows some evidence of penecontemporaneous slippage down the rhyolite slope. Fracturing is probably due to the Blue Creek Canyon Fault, which can be projected to pass close to the exposure beneath the conglomerate. A small copper deposit, consisting of chalcocite and secondary malachite in a gangue of sparry calcite, is located at the unconformity. The hill is a good vantage point for viewing folds in the Ordovician limestones.

b. At the western end of Red Hill, the Post Oak Conglomerate rests with angular unconformity on the Ordovician McKenzie Hill Formation. The principal branch of the Blue Creek Canyon Fault passes beneath the Post Oak at Red Hill.

c. A slightly disharmonic first-order anticline can be traced for more than a mile northward from Red Hill. It is one of five first-order folds in the area (one of which is the hanging-wall anticline east of the Blue Creek Canyon Fault).

d. At several localities, disharmony in first-order folds is resolved into second-order folds that show features such as asymmetry, overturn, cleavage, and faulted-out limbs (fig. 156). Orientation of these minor folds deviates markedly from first-order folds. Cleavage and overturn are generally more common in the southern part of the area, where displacement in the Blue Creek Canyon Fault is greatest (about 2,400 ft).

e. The base of the Cool Creek Formation is a calcarenite rich in quartz sand, which has weathered to form a conspicuous gully, and is a reasonable lithostratigraphic marker zone. The basal Cool Creek sediment shows much small-scale cross-bedding (fig. 157).

f. A highly asymmetric first-order syncline within the graben parallels the Blue Creek Canyon Fault. The eastern limb is highly fractured and in places is cut out by the fault. In addition, the limb shows overturned beds that dip as much as 60°.

g. At the southern end of the outcrop of the Carlton Rhyolite–Timbered Hills unconformity, the Honey Creek Formation directly above the unconformity contains several beds of biomicrite; the most common fossils are orthid brachiopods that formed shell banks of some stability.

h. The unconformity is well exposed in a small prospect pit. In detail, the surface is extremely irregular and is overlain by a basal breccia and cross-bedded, very coarse-grained calcarenites rich in pelmatozoan fragments (figs. 158, 159).

i. The Blue Creek Canyon Fault is well exposed where the upper massive member of the Fort Sill Formation is faulted against the Cool Creek Formation, as the former is a ridge-forming element. The fault plane clearly can be seen to dip to the east at a steep angle.

j. The uppermost massive member of the Fort Sill Formation is a conspicuous feature of the hanging-wall anticline (a "first-order" fold east of the fault). Bedding in this member has been obscured in places by numerous low-angle joints that dip generally to the southeast at about 45°. The contact between the Fort Sill and Signal Mountain Formations is easily determined, because the latter formation does not form significant relief.

k. At the northern end of Blue Creek Canyon, the Signal Mountain Formation, exposed in a quarry, shows the effects of compression between two branches of the Blue Creek Canyon Fault. Considerable minor fault movement has occurred along weak mudstone layers in the formation. A few yards north of the quarry, the two branches of the fault converge and the Signal Mountain Formation is faulted out completely (fig. 160).

l. A walk of a few hundred yards west from the quarry crosses several first-order fold axes. The geometry of *en-echelon* relationships is clearly displayed (fig. 161). Many features of the sedimentology of the Cool Creek Formation (stromatolites, oolitic calcarenites, intraformational conglomerates) are well exposed.

m. The walk back from locality *l* to Red Hill illustrates additional aspects of fold geometry and sedimentology in beautifully exposed ground.

n. The road (State Highway 58) follows the line of Blue Creek Canyon. The canyon floor consists of recent alluvium. At the northern end of the canyon, a fault branch is indicated by the spatial relationships of the rhyolite and overlying formations. This fault has been inferred along the entire length of the canyon trench, although it is not exposed (fig. 158).

Although the Carlton Rhyolite weathers to a rather uniform surface, individual flows of pyroclastic units can be distinguished, particular-

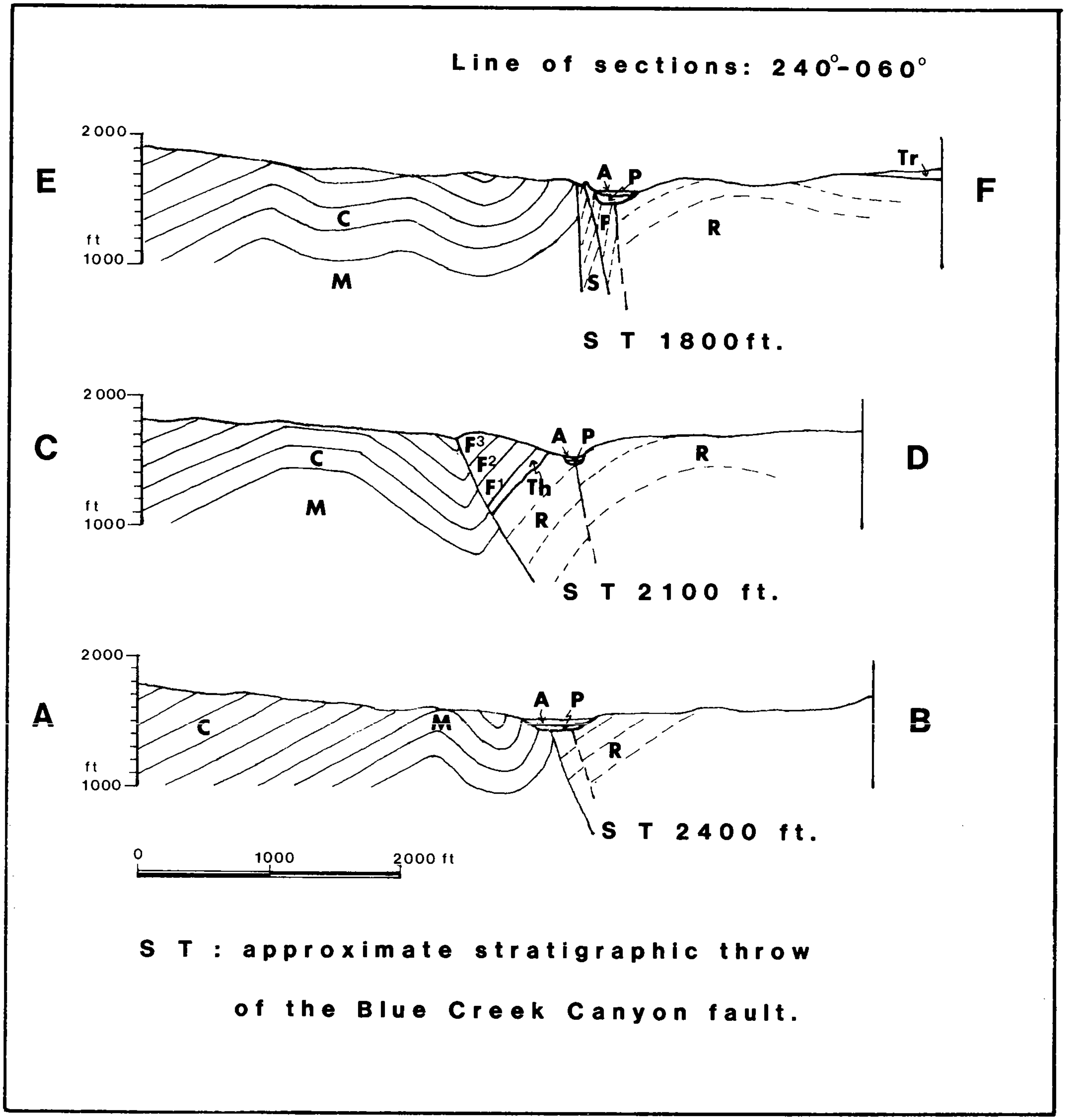

Figure 155. Cross sections in Blue Creek Canyon area.

Figure 156. Axial-plane cleavage in hinge of a north-plunging anticline in Cool Creek Formation close to Blue Creek Canyon Fault. Cleavage has obscured bedding (latter has been highlighted).

Figure 157. Base of Cool Creek Formation, which is a quartz-rich calcarenite showing discontinuous intraformational conglomerates and small-scale trough cross-bedding.

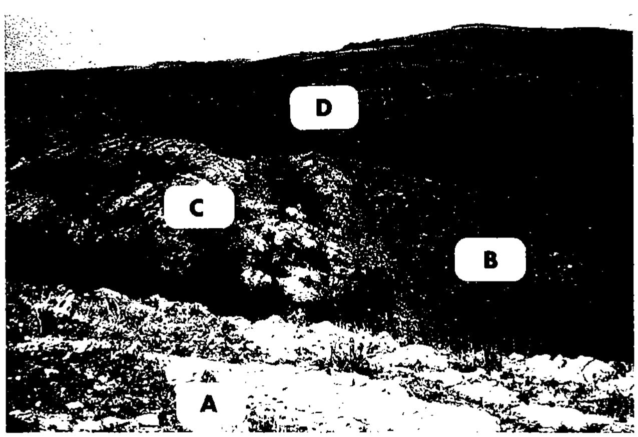

Figure 158. View of Blue Creek Canyon from south. In foreground are limestones of Cool Creek Formation *(A)*; Blue Creek Canyon Fault runs through gully beyond. Middle ground consists of western limb of hanging-wall anticline and shows Carlton Rhyolite (*B*) overlain unconformably by Cambrian carbonates (*C*). On far side of Blue Creek Canyon, features in Carlton Rhyolite dip into the canyon (near *D*).

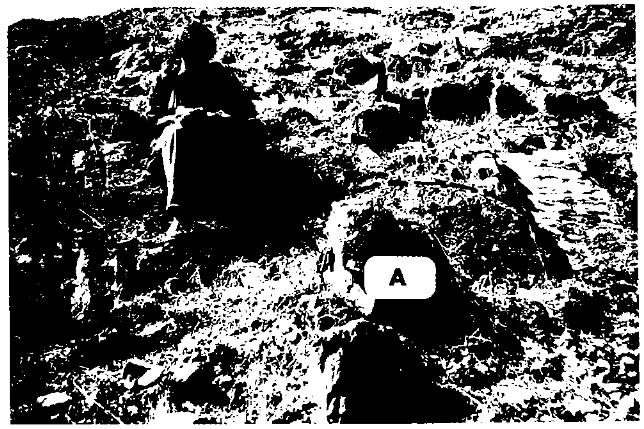

Figure 159. Detail of irregular unconformity between Carlton Rhyolite (*A*) and Honey Creek Formation.

Figure 160. View, to north, of northern part of Blue Creek Canyon. Upper member of Fort Sill Limestone in foreground. A fault branch separates this formation from featureless hillside formed by Signal Mountain Formation; main fault branch separates latter formation from Cool Creek Formation which forms rugged relief in left distance. Two faults converge in center distance, beyond quarry; Signal Mountain Formation is faulted out.

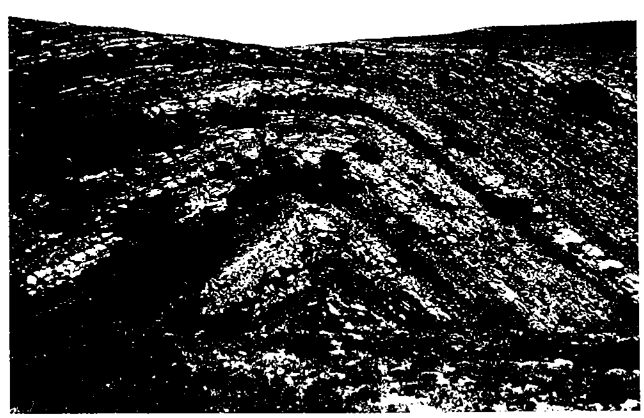

Figure 161. View northwestward from locality *I* showing first-order anticline.

ly where they occur in the hanging-wall anticline east of the road. At one locality in Blue Creek itself, a pebble conglomerate with clasts of variable composition and roundness is developed. The rock texture is mictitic and presumably records a mudflow.

o. At the northern end of Blue Creek Canyon, the Reagan Sandstone lies unconformably on the Carlton Rhyolite. The basal Reagan is a 9-in. bed of medium-grained, well-rounded, quartz-rich sandstone with a richly hematitic matrix. Overlying this is a pebble conglomerate, about 1–2 ft thick, consisting of small (1 in. diameter) pebbles of rhyolite set in a matrix of quartz/glauconite sand. The conglomerate is overlain by richly glauconitic, fine-grained sandstones with small- and medium-scale cross-bedding. In a deep prospect pit, the gradational transition from the Reagan Sandstone to the Honey Creek Formation is marked by the appearance of lenticular bodies of coarse sparite.

p. Farther to the northeast, across a fault (downthrown to the west) that has eroded to form a gully, a second section of Reagan is exposed as a thin layer of sediment resting unconformably on poorly seen Carlton Rhyolite. The basal Reagan is a very poorly sorted breccia containing numerous clasts of rhyolite, which is overlain by coarse-grained, well-sorted, rounded-quartz sandstone characterized by medium- to large-scale (sets 2 ft thick) cross-bedding.

q. At a bearing of N. 40° W. from *p* is an enigmatic exposure of Post Oak Conglomerate. From a distance, this exposure appears to consist of lower Paleozoic limestone; on close examination, it is a boulder breccia composed of huge (to 20 ft in diameter), angular blocks of diverse limestone types. Most clasts appear to have been derived from the Fort Sill Formation. The deposit, which rests on the Carlton Rhyolite, is interpreted as a remnant of a fault-scarp talus.

r, s, t. The Post Oak Conglomerate can be conveniently examined at several localities on State Highway 58. The unconformity between the conglomerate and the underlying lower Paleozoic limestones is highly irregular. At locality *s*, the basal Post Oak is a coarse breccio-conglomerate (clasts as much as 18 in. diameter) situated within Blue Creek Canyon, indicating that, at least at the northern end, this valley is an exhumed Permian feature. At higher levels (locality *r*), the Post Oak is a finer grained, open-framework breccio-conglomerate exhibiting spectacular cements. Most of the cement is drusy sparite (to ½ in.); coarse, euhedral pyrite and barite are later.

At locality *t*, a caliche (calcrete) zone is intercalated within breccio-conglomerates (fig. 162). This caliche can be traced in surrounding areas, and records a period of nondeposition on a Post Oak alluvial fan. The caliche is a micritic deposit that firmly binds lower Paleozoic limestone pebbles. Overlying and underlying breccias are cemented by drusy sparite; the overlying breccia contains a few fragments of reworked caliche.

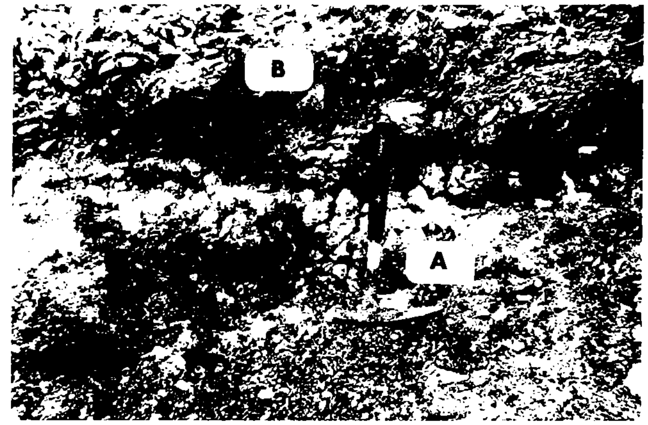

Figure 162. Calcrete zone (*A*) developed at a disconformity in Post Oak Conglomerate. Sparite-cemented breccio-conglomerate (*B*) occurs above disconformity.

STOP 11—HIGHWAY 19 AREA

Sedimentology of lower Paleozoic limestones beneath Permian Post Oak Conglomerate, exhibiting karst features below the unconformity. Along State Highway 19, about 5 miles northeast of Blue Creek Canyon, in Caddo County, Oklahoma. **R. N. Donovan.**

On State Highway 19, about 5 miles northeast of Blue Creek Canyon, the road has been excavated through a hill of lower Paleozoic limestone. This hill has been exhumed from beneath Permian Post Oak Conglomerate cover (fig. 163); the top of the road cut is very close to the original Permian land surface. Features of interest (in addition to the sedimentology of the lower Paleozoic limestones) include karst fissures developed beneath the unconformity. Essentially two types of fissures occur, both developed preferentially along north-trending joints in the limestone. Detritus-filled fissures that presumably were in direct contact with the Permian land surface are found at the eastern end of the exposure (fig. 164). The detritus consists of limestone fragments firmly cemented by reddened micrite. The second type was not in direct contact with the surface and consists of small, open vadose cave systems (fig. 165). Various types of flowstone line these fissures.

Arguments for a Permian age for these small cave systems are strong but not definitive. Two sets of major joints cut the lower Paleozoic limestones, along azimuths of about 100° and 170° (fig. 163). The 170° set has been greatly widened by cave development, and the 100° set, less so. This indicates a major vadose drainage with a northerly trend. Existing exhumed relief indicates a vector to the north. This vector is in accord with surface drainage directions as indicated by cross-bedding in the Post Oak Conglomerate. Although modern drainage is also in the same general direction, this drainage is incised within the Post Oak Conglomerate; it is difficult to account for the development of recent karst fissures in a recently exhumed lower Paleozoic hill.

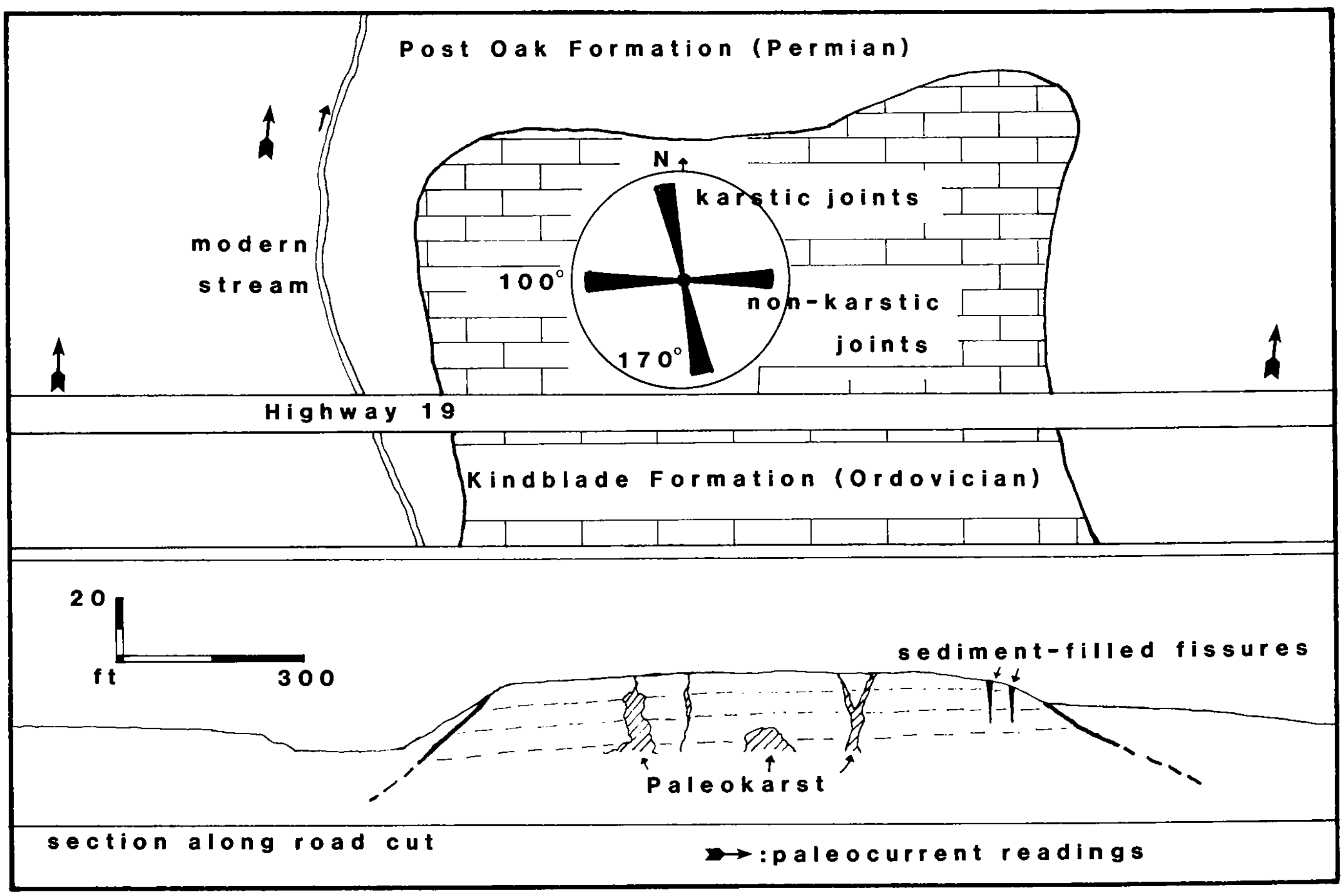

Figure 163. Sketch map and section through road cut on State Highway 19, showing exhumation of Permian topography and karst. Rose diagram shows joint maxima (based on 43 readings).

Figure 164. Sediment-filled karstic fissure in limestones of the Kindblade Formation exposed at eastern end of road cut.

Figure 165. Open cave in Kindblade limestone on southern face of road cut.

REFERENCES CITED

Adams, S. R., 1977, Geochemistry of the Wichita Granite Group in the Wichita Mountains, Oklahoma: Oklahoma State University unpublished M.S. thesis, 74 p.

Aleinikoff, J. N., **Dusel-Bacon, C.**, **Foster, H. L.**, and **Futa, K.**, 1981, Proterozoic zircon from augen gneiss, Yukon–Tanana Upland, east-central Alaska: Geology, v. 9, p. 469–473.

Alipouraghtapeh, Samad, 1979, Geochemistry of major and trace elements of the "Raggedy Mountain Gabbro Group," Wichita Mountains, southwestern Oklahoma: Oklahoma State University unpublished M.S. thesis, 116 p.

Al-Shaieb, Z. F., 1978, Guidebook to uranium mineralization in sedimentary and igneous rocks of Wichita Mountains region, southwestern Oklahoma: Oklahoma City Geological Society, 73 p.

Al-Shaieb, Z. F., **Hanson, R. E.**, **Donovan, R. N.**, and **Shelton, J. W.**, 1980, Petrology and diagenesis of sandstones in the Post Oak Formation (Permian), southwestern Oklahoma: Journal of Sedimentary Petrology: v. 50, p. 43–50.

Al-Shaieb, Z. F., **Shelton, J. W.**, **Donovan, R. N.**, **Hanson, R. E.**, **May, R. T.**, **Hansen, C. A.**, **Morrison, C. M.**, **White, S. J.**, and **Adams, S. R.**, 1977, Evaluation of uranium potential in selected Pennsylvanian and Permian units and igneous rocks in southwestern and southern Oklahoma: U.S. Departemnt of Energy Open-File Report GJBX–35(78), 248 p.

Al-Shaieb, Z. F., **Thomas, R. G.**, and **Stewart, G. F.**, 1980, Uranium resource evaluation, Lawton Quadrangle, Oklahoma and Texas: Contract report to Bendix Field Engineering Corporation, Subcontract 78–131–E and Contract DE–AC13–76GO1664.

Amsden, T. W., 1975 [1976], Hunton Group (Late Ordovician, Silurian, and Early Devonian) in the Anadarko Basin of Oklahoma: Oklahoma Geological Survey Bulletin 121, 214 p.

Anderson, J. E., Jr., 1969, Development and time distribution of texturally altered tuff, Davis Mountains, Texas: Geological Society of America Bulletin, v. 80, p. 2075–2080.

——— 1970, Recognition and time distribution of texturally altered welded tuff: Geological Society of America Bulletin, v. 81, p. 287–292.

Anderson, J. L., and **Cullers, R. L.**, 1978, Geochemistry and evolution of the Wolf River Batholith, a late Precambrian rapakivi massif in north Wisconsin, U.S.A.: Precambrian Research, v. 7, p. 287–324.

Anderson, K. C., 1946, The occurrence and origin of pegmatites and miarolitic cavities in the Wichita Mountain system, Oklahoma: University of Oklahoma unpublished M.S. thesis, 65 p.

Arth, J. G., 1979, Some trace elements in trondhjemites—their implications to magma genesis and paleotectonic setting, *in* Barker, F., editor, Trondhjemites, dacites, and related rocks: Elsevier, New York, p. 123–132.

Babaei, A., 1980, The structural geology of part of the Limestone Hills in the Wichita Mountains, Caddo and Comanche Counties, Oklahoma: Oklahoma State University unpublished M.S. thesis, 63 p.

Bain, H. F., 1900, Geology of the Wichita Mountains: Geological Society of America Bulletin, v. 11, p. 127–144.

——— 1904, Reported ore deposits of the Wichita Mountains, Appendix, *in* Taff, J. A., Preliminary report on the geology of the Arbuckle and Wichita Mountains in Indian Territory and Oklahoma: U.S. Geological Survey Professional Paper 31, p. 82–83.

Barker, F., **Wones, D. R.**, **Sharp, W. N.**, and **Desborough, G. A.**, 1975, The Pikes Peak Batholith, Colorado Front Range, and a model for the origin of the gabbro–anorthosite–syenite–potassic granite suite: Precambrian Research, v. 2, p. 97–160.

Barthelman, W. B., 1968, Upper Arbuckle (Ordovician) outcrops in the Unap Mountain–Saddle Mountain area, northeastern Wichita Mountains, Oklahoma: University of Oklahoma unpublished M.S. thesis, 65 p.

Bickford, M. E., **Chase, R. B.**, **Nelson, B. K.**, **Shuster, R. D.**, and **Arruda, E. C.**, 1981, U–Pb studies of zircon cores and overgrowths, and monozite: implications for age and petrogenesis of the northeastern Idaho Batholith: Journal of Geology, v. 89, p. 433–457.

Bickford, M. E., **Harrower, K. L.**, **Hoppe, W. J.**, **Nelson, B. K.**, **Nusbaum, R. L.**, and **Thomas, J. J.**, 1981, Rb–Sr and U–Pb geochronology and distribution of rock types in the Precambrian basement of Missouri and Kansas: Geological Society of America Bulletin, pt. 1, v. 92, p. 323–341.

Bickford, M. E., and **Lewis, R. D.**, 1979, U–Pb geochronology of exposed basement rocks in Oklahoma: Geological Society of America Bulletin, pt. 1, v. 90, p. 540–544.

Bonin, B., **Grelou-Orsini, C.**, and **Vialette, Y.**, 1978, Age, origin, and evolution of the anorogenic complex of Evisa (Corsica): a K–Li–Rb–Sr study: Contributions to Mineralogy and Petrology, v. 65, p. 425–432.

Booth, S. L., 1981, Structural analysis of portions of the Washita Valley Fault Zone, Arbuckle Mountains, Oklahoma: Shale Shaker, v. 31, p. 107–120.

Brewer, J. A., **Brown, L. D.**, **Steiner, D.**, **Oliver, J. E.**, **Kaufman, S.**, and **Denison, R. E.**, 1981, A Proterozoic basin in the southern Mid-Continent of the United States revealed by COCORP deep seismic reflection profiles: Geology [in press].

Brewer, J. A., **Good, R.**, **Oliver, J. E.**, **Brown, L. D.**, and **Kaufman, S.**, 1982, COCORP profiling across the Southern Oklahoma Aulacogen: overthrusting of the Wichita Mountains and compression within the Anadarko Basin: Geology [in review].

Brookby, H. E., 1969, Upper Arbuckle (Ordovician) outcrops in Richards Spur–Kindblade Ranch area, northeastern Wichita Mountains, Oklahoma: University of Oklahoma unpublished M.S. thesis, 73 p.

Brown, R. W., 1977, A sample fusion technique for whole-rock analysis with the electron microprobe: Geochimica et Cosmochimica Acta, v. 41, p. 435–438.

Brown, W. G., 1982, Washita Valley Fault system—a new look at an old fault, *in* Borger, J. G., editor, Technical proceedings of American Association of Petroleum Geologists Mid-Continent Section 1981 Meeting, Oklahoma City: Oklahoma City Geological Society [in press].

Burke, K., and **Dewey, J. F.**, 1973, Plume-generated triple junctions: key indicators in applying plate tectonics to old rocks: Journal of Geology, v. 81, p. 406–433.

Burke, W. H., **Otto, J. B.**, and **Denison, R. E.**, 1969, Potassium–argon dating of basaltic rocks: Journal of Geophysical Research, v. 74, p. 1082–1086.

Burnham, C. W., and **Jahns, R. H.**, 1962, A method for determining the solubility of water in silicate melts: American Journal of Science, v. 260, p. 721–745.

Burwell, A. L., 1956, Potash agstone from Oklahoma: Oklahoma Geology Notes, v. 16, p. 12–23.

Chappell, B. W., and **White, A. J. R.**, 1974, Two contrasting granite types: Pacific Geology, v. 8, p. 173–174.

Chase, G. W., 1950a, The igneous rocks of the Roosevelt area, Oklahoma: University of Oklahoma unpublished M.S. thesis, 108 p.

——— 1950b, Geologic map of basic igneous rocks in the Raggedy Mountains, Wichita Mountains system, Oklahoma: Oklahoma Geological Survey Preliminary Map.

——— 1951, Titaniferous magnetite in basic rocks of the Wichita Mountains, Oklahoma: The Hopper, Oklahoma Geological Survey, v. 11, no. 2, p. 11–20.

——— 1954, Permian conglomerate around Wichita Mountains, Oklahoma: American Association of Petroleum Geologists Bulletin, v. 38, p. 2028–2035.

Chase, G. W., **Frederickson, E. A.**, and **Ham, W. E.**, 1956, Résumé of the geology of the Wichita Mountains, Oklahoma, *in* Petroleum geology of southern Oklahoma: American Association of Petroleum Geologists, v. 1, p. 35–55.

Dalrymple, G. B., 1979, Critical tables for conversion of K–Ar ages from old to new constants: Geology, v. 7, p. 558–560.

Decker, C. E., 1939, Progress report on the classification of the

Timbered Hills and Arbuckle groups of rocks, Arbuckle and Wichita Mountains, Oklahoma: Oklahoma Geological Survey Circular 22, 62 p.

Denison, R. E., 1966, Basement rocks in adjoining parts of Oklahoma, Kansas, Missouri, and Arkansas: University of Texas unpublished Ph.D. dissertation, 292 p.

——— 1978, Basement rocks in the Arbuckle Mountains, *in* Wickham, J. S., and Denison, R. E., editors, Structural style of the Arbuckle region: University of Oklahoma Guidebook for Geological Society of America, South-Central Section, Annual Meeting, Field Trip 3, p. 42–46.

Denison, R. E., Lidiak, E. G., Bickford, M. E., and **Kisvarsanyi, E. B.**, 1981, Geology and geochronology of Precambrian rocks in the central interior region of the United States.

Ernst, W. G., 1962, Synthesis, stability relations, and occurrence of riebeckite and riebeckite–arfvedsonite solid solutions: Journal of Geology, v. 70, p. 689–736.

Estes, L. D., 1980, Geology of the Saddle Mountain Quadrangle and petrology of the Layered Series, eastern Wichita Mountains, Oklahoma: University of Texas, Arlington, unpublished M.S. thesis, 172 p.

Estes, L. D., Fischer, J. F., and **Taylor, R. J.**, 1978, Stratigraphy of layered anorthosites in the eastern Wichita Mountains, Oklahoma [abstract]: Geological Society of America Abstracts with Programs, v. 10, p. 5.

Evans, O. F., 1929, Old beach markings in the western Wichita Mountains: Journal of Geology, v. 37, p. 76–82.

Ewart, A., 1979, A review of the mineralogy and chemistry of Tertiary–Recent dacitic, latitic, rhyolitic, and related salic volcanic rocks, *in* Barker, F., editor, Trondhjemites, dacites, and related rocks: Elsevier, New York, p. 13–121.

Feinstein, S., 1979, Subsidence and thermal history of the Southern Oklahoma Aulacogen: University of Oklahoma unpublished M.S. thesis, 84 p.

——— 1981, Subsidence and thermal history of Southern Oklahoma Aulacogen: implications for petroleum exploration: American Association of Petroleum Geologists Bulletin, v. 65, p. 2521–2533.

Flawn, P.T., 1956, Basement rocks of Texas and southeast New Mexico: University of Texas Publication 5605, 261 p.

Gibson, R. G., III, 1981, Petrography and geochemistry of mafic enclaves in the Reformatory Granite, western Wichita Mountains, Oklahoma: Allegheny College, Meadville, Pennsylvania, unpublished B.S. thesis, 41 p.

Gilbert, M. C., 1960, The geology of the western Glen Mountains, Oklahoma: University of Oklahoma unpublished M.S. thesis, 48 p.

——— 1978a, Quanah Granite–Gabbro relations, Wichita Mountains [abstract]: Geological Society of America Abstracts with Programs, v. 10, p. 6.

——— 1978b, Wichita Mountains mapping project [abstract]: Geological Society of America Abstracts with Programs, v. 10, p. 6.

——— 1978c, Lake Burford area, Wichita Mountains Wildlife Refuge: Oklahoma Geology Notes, v. 38, cover and p. 42.

——— 1978d, Anorogenic Cambrian granite/rhyolite of the southern Mid-Continent [abstract]: Geological Society of America Abstracts with Programs, v. 10, p. 407–408.

——— 1979, Wichita Mountains geomorphology and implications for tectonic history [abstract]: Geological Society of America Abstracts with Programs, v. 11, p. 147.

——— 1981a, Comments on structure within Wichita Mountains crustal block: American Association of Petroleum Geologists Bulletin, v. 65, p. 1498.

——— 1981b, Timing and chemistry of igneous events associated with the Southern Oklahoma Aulacogen [extended abstract]: Conference on Planetary Rifting, LPSI Sponsor, December.

——— 1982, Comments on structure within the igneous core, Wichita Mountains crustal block, *in* Borger, John G., editor, Technical Proceedings of American Association of Petroleum Geologists Mid-Continent Section 1981 Meeting, Oklahoma City: Oklahoma City Geological Society [in press].

Gilbert, M. C., and **Myers, J. D.**, 1980, Further characterization of Cambrian Wichita granites: E⊕S, American Geophysical Union Transactions, v. 61, p. 411–412.

——— 1981, Aspects of the trace element geochemistry of Wichita granites [abstract]: Geological Society of America Abstracts with Programs, v. 13, p. 237.

Green, J. H., 1952, Igneous rocks of the Craterville area, Wichita Mountains, Oklahoma: University of Oklahoma unpublished M.S. thesis, 63 p.

Groshong, R. H., and **Rodgers, D. A.**, 1978, Left-lateral strike-slip fault model, *in* Wickham, J. S., and Denison, R. E., editors, Structural style of the Arbuckle region: University of Oklahoma Guidebook for Geological Society of America South-Central Section Annual Meeting, Field Trip 3, p. 1–7.

Haggerty, S. E., 1976, Opaque minerals in terrestrial igneous rocks, *in* Rumble, Douglas, III, editor, Oxide minerals: Mineralogical Society of America Short-Course Notes, v. 3, p. Hg-101–Hg-300.

Hahn, K. R., 1978, Relations of the mafic rocks exposed in the Meers area, Wichita Mountains, Oklahoma [abstract]: Geological Society of America Abstracts with Programs, v. 10, p. 6.

Ham, W. E., 1969, Regional geology of the Arbuckle Mountains, Oklahoma: Oklahoma Geological Survey Guidebook 17, 52 p.

Ham, W. E., Denison, R. E., and **Merritt, C. A.**, 1964, Basement rocks and structural evolution of southern Oklahoma: Oklahoma Geological Survey Bulletin 95, 302 p.

Ham, W. E., Merritt, C. A., and **Frederickson, E. A.**, 1957, Field conference on geology of the Wichita Mountain region: Oklahoma Geological Survey Guidebook 5, 58 p.

Ham, W. E., and **Wilson, J. L.**, 1967, Paleozoic epeirogeny and orogeny in the central United States: American Journal of Science, v. 265, p. 332–407.

Hamilton, W. B., 1956, Precambrian rocks of Wichita and Arbuckle Mountains, Oklahoma: Geological Society of America Bulletin, v. 67, p. 1319–1330.

——— 1959, Chemistry of granophyres from Wichita lopolith, Oklahoma: Geological Society of America Bulletin, v. 70, p. 1119–1125.

——— 1960, Silicic differentiates of lopoliths: International Geological Congress, 21st, Copenhagen, Norden, 1960, pt. 13, Petrographic provinces, igneous and metamorphic rocks, p. 59–67.

Hanks, C. L., 1978, Petrology and occurrence of a magnetite–ilmenite–olivine rock in the Wichita Mountains [abstract]: Geological Society of America Abstracts with Programs, v. 10, p. 7.

Hanson, G. N., 1980, Rare-earth elements in petrogenetic studies of igneous systems: Annual Reviews of Earth and Planetary Sciences, v. 8, p. 371–406.

Hanson, R. E., 1977, Petrology and geochemistry of the Carlton Rhyolite, southern Oklahoma: Oklahoma State University unpublished M.S. thesis, 161 p.

Hanson, R. E., and **Al-Shaieb, Z. F.**, 1980, Voluminous subalkaline silicic magmas related to intracontinental rifting in the Southern Oklahoma Aulacogen: Geology, v. 8, p. 180–184.

Harlton, B. H., 1951, Faults in sedimentary part of Wichita Mountains of Oklahoma: American Association of Petroleum Geologists Bulletin, v. 35, p. 988–999.

——— 1963, Frontal Wichita Fault system of southwestern Oklahoma: American Association of Petroleum Geologists Bulletin, v. 47, p. 1552–1580.

——— 1972, Faulted fold belts of southern Anadarko basin adjacent to frontal Wichitas: American Association of Petroleum Geologists Bulletin, v. 56, p. 1544–1551.

Havens, J. S., 1977, Reconnaissance of the water resources of the Lawton Quadrangle, southwestern Oklahoma: Oklahoma Geological Survey Hydrologic Atlas 6, sheet 1 of 4, fig. 2, geologic map, scale 1:250,000.

Hiss, W. L., 1960, Ferromagnesian minerals in basic igneous rocks, Raggedy Mountains area, Wichita Mountains, Oklahoma: University of Oklahoma unpublished M.S. thesis, 104 p.

Hoffman, M. G., 1930, Geology and petrology of the Wichita Mountains: Oklahoma Geological Survey Bulletin 52, 83 p.

Hoffman, Paul, Dewey, J. F., and **Burke, Kevin**, 1974, Aulacogens and their genetic relation to geosynclines, with a Proterozoic example from Great Slave Lake, Canada, *in* Dott, R. J., Jr., and Shaver, R. H., editors, Modern and ancient geosynclinal sedimentation: Society of Economic Paleontologists and Mineralogists Special Publication 19, p. 38–55.

Huang, W. T., 1955, Occurrences of leucogranogabbro and associated igneous rocks in the Wichita Mountains, Oklahoma: American Journal of Science, v. 253, p. 341–357.

——— 1958, Riebeckite granite in the Wichita Mountains, Oklahoma: Geological Society of America Bulletin, v. 69, p. 1191–1192.

Huang, W. T., and **Merritt, C. A.**, 1952, Preferred orientation of olivine crystals in troctolite of the Wichita Mountains, Oklahoma: American Mineralogist, v. 37, p. 865–868.

——— 1954, Petrography of the troctolite of the Wichita Mountains, Oklahoma: American Mineralogist, v. 39, p. 549–565.

Hunter, H. E., 1960, Topographic control by primary igneous structures in the Raggedy Mountains, southwestern Oklahoma: Oklahoma Geology Notes, v. 20, p. 112–115.

——— 1967, Raggedy Mountain Gabbro Group, *in* Stone, G. T., editor, The structure and igneous rocks of the Wichita Mountains, Oklahoma: University of Oklahoma Guidebook for Geological Society of America South-Central Section Annual Meeting, Field Trip, p. 34–41.

——— 1970, Raggedy Mountain Gabbro Group: Compass of Sigma Gamma Epsilon, v. 48, p. 27–31.

Johnson, E. L., 1955, Geology of the pegmatites in the Hale Spring area, Wichita Mountains, Oklahoma: University of Oklahoma unpublished M.S. thesis, 87 p.

Johnson, H. D., 1960, Mineralogical study of altered basic intrusive rocks, Wichita Mountains, Oklahoma: University of Oklahoma unpublished M.S. thesis, 62 p.

Johnson, K. S., and **Denison, R. E.**, 1973, Igneous geology of the Wichita Mountains and economic geology of Permian rocks in southwest Oklahoma: Oklahoma Geological Survey Guidebook for Geological Society of America Annual Meeting, Dallas, Field Trip 6, 33 p.

Jones, V. L., and **Lyons, P. L.**, 1964, Vertical-intensity magnetic map of Oklahoma: Oklahoma Geological Survey Map GM–6, scale 1:750,000.

Jones, W. R., **Peoples, J. W.**, and **Howland, A. L.**, 1960, Igneous and tectonic structures of the Stillwater complex, Montana: U.S. Geological Survey Bulletin 1071-H, p. 281–340.

Karns, A. W., 1961, Ophitic pyroxene from the Raggedy Mountains area, Wichita Mountains, Oklahoma: University of Oklahoma unpublished M.S. thesis, 68 p.

Krogh, T. E., 1973, A low-contamination method for hydrothermal decomposition of zircon and extraction of U and Pb for isotopic age determinations: Geochimica et Cosmochimica Acta, v. 37, p. 485–494.

Leeder, M. R., 1975, Pedogenic carbonates and flood-sediment accretion rates: a quantitative model for alluvial-zone lithofacies: Geological Magazine, v. 112, p. 257–270.

Loiselle, M. C., and **Wones, D. R.**, 1979, Characteristics and origin of anorogenic granites [abstract]: Geological Society of America Abstracts with Programs, v. 11, p. 468.

Luza, K. V., 1978, Seismicity and tectonic relationships of the Nemaha Uplift in Oklahoma: U.S. Nuclear Regulatory Commission, NUREG./CR-0050, R6A, 61p.

Lynn, H. B., 1980, Migration and interpretation of deep crustal seismic reflection data: Stanford University unpublished Ph.D. dissertation, 159 p.

Lyons, P. L., 1964, Bouguer gravity anomaly map of Oklahoma: Oklahoma Geological Survey Map GM–7, scale 1:750,000.

Mayes, J. W., 1947, A further study of the Tepee Creek Formation, Wichita Mountains, Oklahoma: University of Oklahoma unpublished M.S. thesis, 45 p.

Merritt, C. A., 1948, Meers quartzite: Oklahoma Academy of Science Proceedings, v. 28, p. 76–77.

——— 1958, Igneous geology of the Lake Altus area, Oklahoma: Oklahoma Geological Survey Bulletin 76, 70 p.

——— 1965, Mt. Scott Granite, Wichita Mountains, Oklahoma: Oklahoma Geology Notes, v. 25, p. 263–272.

——— 1966, Rim albite in coarse-grained Quanah Granite, Wichita Mountains, Oklahoma: Oklahoma Geology Notes, v. 26, p. 211–213.

——— 1967, Names and relative ages of granites and rhyolites in the Wichita Mountains, Oklahoma: Oklahoma Geology Notes, v. 27, p. 45–53.

Merritt, C. A., and **Ham, W. E.**, 1941, Pre-Cambrian zeolite–opal sediments in the Wichita Mountains, Oklahoma: American Association of Petroleum Geologists Bulletin, v. 25, p. 287–299.

Milanovsky, E. E., 1981, Aulacogens of ancient platforms: problems of their origin and tectonic development: Tectonophysics, v. 73, p. 213–248.

Miller, J. A., 1981, Uranium potential of Lower Permian arkosic facies, northern Kiowa County, Oklahoma: Oklahoma State University unpublished M.S. thesis, 65 p.

Miser, H. D., 1954, Geologic map of Oklahoma: U.S. Geological Survey and Oklahoma Geological Survey, scale 1:500,000.

Muehlberger, W. R., **Denison, R. E.**, and **Lidiak, E. G.**, 1967, Basement rocks in continental interior of United States: American Association of Petroleum Geologists Bulletin, v. 51, p. 2351–2380.

Myers, J. D., and **Gilbert, M. C.**, 1980, Chemistry of Wichita granites: E⊕S, American Geophysical Union Transactions, v. 61, p. 1155–1156.

Myers, J. D., **Gilbert, M. C.**, and **Loiselle, M. C.**, 1981, Geochemistry of the Cambrian Wichita Granite Group and revisions of its lithostratigraphy: Oklahoma Geology Notes, v. 41, p. 172–195.

Nelms, J. L., 1958, The Fort Sill formation of the Wichita Mountains, Oklahoma: University of Oklahoma unpublished M.S. thesis, 91 p.

Nichols, C. R., 1968, Alteration of igneous rocks in the Lugert area, Kiowa County, Oklahoma: University of Oklahoma unpublished M.S. thesis, 140 p.

Oliver, J., **Dobrin, M.**, **Kaufman, S.**, **Meyer, R.**, and **Phinney, R.**, 1976, Continuous reflection profiling of the deep basement, Hardeman County, Texas: Geological Society of America Bulletin, v. 87, p. 1537–1546.

Petzel, G. J., 1974, Evaluation of data from the first Earth Resources Technology Satellite for the purpose of structural analysis in the Anadarko basin, Oklahoma and Texas: University of Oklahoma unpublished M.S. thesis, 107 p.

Phelps, D. W., 1975, Phase chemistry of the Layered Series, Raggedy Mountain Gabbro Group, Oklahoma: Rice University unpublished M.A. thesis, 122 p.

Powell, B. N., 1976, Relation of the layered series to other rocks of the Wichita complex, Oklahoma, and resulting Precambrian structural implications [abstract]: Geological Society of America Abstracts with Programs, v. 8, p. 59.

——— 1978, Bimodal gabbroic magmatism in the Wichita Province, Oklahoma [abstract]: Geological Society of America Abstracts with Programs, v. 10, p. 24.

——— 1981, Basic magmatism of the Southern Oklahoma Aulacogen: Lunar and Planetary Institute Workshop on Magmatic Processes of Early Planetary Crusts, p. 82–84.

Powell, B. N., and **Fischer, J. F.**, 1976, Plutonic igneous geology of the Wichita Magmatic Province, Oklahoma: Oklahoma Geological Survey Special Publication 76–1, 35 p.

Powell, B. N., **Gilbert, M. C.**, and **Fischer, J. F.**, 1980, Lithostratigraphic classification of basement rocks of the Wichita province, Oklahoma: Geological Society of America Bulletin, pt. 1, v. 91, p. 509–514, and pt. 2, v. 91, p. 1875–1994.

Powell, B. N., and **Phelps, D. W.**, 1977, Igneous cumulates of the Wichita province and their tectonic implications: Geology, v. 5, p. 52–56.

Pruatt, M. A., 1975, The Southern Oklahoma Aulacogen: a geophysical and geological investigation: University of Oklahoma unpublished M.S. thesis, 59 p.

——— 1976, Geophysical interpretations, *in* Powell, B. N., and Fischer, J. F., Plutonic igneous geology of the Wichita Magmatic Province, Oklahoma: Oklahoma Geological Survey Special Publication 76–1, 35 p.

Pruatt, M. A., and **Reiter, Leon**, 1976, Geologic and petrologic interpretations of geophysical anomalies over the Southern Oklahoma Aulacogen [abstract]: Geological Society of America Abstracts with Programs, v. 8, p. 60.

Richardson, S. W., **Gilbert, M. C.**, and **Bell, P. M.**, 1969, Experimental determination of kyanite–andalusite and andalusite–sillimanite equilibria: the aluminum silicate triple point: American Journal of Science, v. 267, p. 259–272.

Roggenthen, W. M., **Fischer, J. F.**, **Napoleone, G.**, and

Fischer, A. G., 1981, Paleomagnetism and age of mafic plutons, Wichita Mountains, Oklahoma: Geophysical Research Letters, v. 8, p. 133–136.

Rotan, P. M., 1960, Preferred orientation of plagioclase in basic rocks, Raggedy Mountains, southwestern Oklahoma: University of Oklahoma unpublished M.S. thesis, 62 p.

Rowland, T. L., 1974, Lone Star 1 Rogers Unit captures world depth record: Oklahoma Geology Notes, v. 34, p. 185–189.

Salop, J. L., 1977, Precambrian of the Northern Hemisphere and general features of geological evolution: Elsevier, New York, 378 p.

Schoonover, F. E., 1948, The igneous rocks of the Fort Sill Reservation, Oklahoma: University of Oklahoma unpublished M.S. thesis, 123 p.

Scofield, Nancy, 1968, Vertical variation in the layered series, Raggedy Mountain Gabbro Group, Kiowa County, Oklahoma: University of Oklahoma unpublished M.S. thesis, 155 p.

Scofield, Nancy, and **Gilbert, M. C.,** 1980, Geochemistry of late alkali amphiboles from Wichita granites [abstract]: Geological Society of America Abstracts with Programs, v. 12, p. 16.

Sides, J. R., and **Stockton, M. L.,** 1981, Common lead analysis of Glen Mountains Layered Complex and Mt. Scott Granite, Wichita Mountains, Oklahoma [abstract]: Geological Society of America Abstracts with Programs, v. 13, p. 262.

Soule, K. D., 1951, The igneous geology of Bear Mountain and vicinity, Wichita Mountains, Oklahoma: University of Oklahoma unpublished M.S. thesis, 51 p.

Spencer, A. B., 1961, Geology of the basic rocks of the eastern portion of the Raggedy Mountains, southwestern Oklahoma: University of Oklahoma unpublished M.S. thesis, 46 p.

Steel, R. J., 1974, Corn-stone (fossil caliche)—its origin, stratigraphic and sedimentological importance in the New Red Sandstone, western Scotland: Journal of Geology, v. 82, p. 351–369.

Steiger, R. H., and **Jager, E.,** 1977, Subcommission on geochronology: convention on the use of decay constants in geochronology and cosmochronology: Earth and Planetary Science Letters, v. 36, p. 359–362.

Steiner, J. C., Jahns, R. H., and **Luth, W. C.,** 1975, Crystallization of alkali feldspar and quartz in the haplogranite system $NaAlSi_3O_8$–$KAlSi_3O_8$–SiO_2–H_2O at 4 kb: Geological Society of America Bulletin, v. 86, p. 83–98.

Sri-Israporn, S., 1977, Deep structure of the Southern Oklahoma Aulacogen: University of Oklahoma unpublished M.S. thesis, 68 p.

Stith, D. A., 1968, Petrology of the Hennessey Shale (Permian), Wichita Mountain area, Oklahoma: University of Oklahoma unpublished M.S. thesis, 113 p.

Stitt, J. H., 1978, Biostratigraphy and depositional history of the Timbered Hills and Lower Arbuckle Groups, Western Arbuckle Mountains, Oklahoma, *in* Ham, W. E., editor, Regional geology of the Arbuckle Mountains, Oklahoma: Oklahoma Geological Survey Guidebook for American Association of Petroleum Geologists and Society of Economic Paleontologists and Mineralogists Annual Meeting, Oklahoma City, Field Trip 1, p. 19–23.

Stockton, M. L., and **Giddens, J. D.,** 1982, Expanded stratigraphy of the Glen Mountains Layered Complex [abstract]: Geological Society of America Abstracts with Programs, v. 14, p. 137.

Taff, J. A., 1904, Preliminary report on the geology of the Arbuckle and Wichita Mountains in Indian Territory of Oklahoma: U.S. Geological Survey Professional Paper 31, 97 p. [Reprinted 1928 as Oklahoma Geological Survey Bulletin 12.]

Takken, Suzanne, 1968, Subsurface geology of north Gotebo area, Kiowa and Washita Counties, Oklahoma, *in* Beebe, B. W., editor, Natural gases of North America: American Association of Petroleum Geologists Memoir 9, v. 2, p. 1492–1508.

Tanner, W. F., 1954, Wave-cut erosion surface in the Wichita Mountains: Shale Shaker, v. 5, no. 4, p. 5–11.

Taylor, C. H., 1911, Granites of Oklahoma, *in* Gould, C. N., and others, Preliminary report on the structural material of Oklahoma: Oklahoma Geological Survey Bulletin 5, p. 40–59.

——— 1915, Granites of Oklahoma: Oklahoma Geological Survey Bulletin 20, 108 p.

Taylor, R. J., 1978, Petrography of the Layered Series, Saddle Mountain Quadrangle, eastern Wichita Mountains, Oklahoma: University of Texas, Arlington, unpublished M.S. thesis, 66 p.

Thornton, E. C., 1975, Anorthosite–gabbro–granophyre relationships, Mount Sheridan area, Oklahoma: Rice University unpublished M.A. thesis, 65 p.

Tilton, G. R., Davis, G. L., Wetherill, G. W., and **Aldrich, L. T.,** 1957, Isotopic ages of zircon from granites and pegmatites: American Geophysical Union Transactions, v. 38, p. 360–371.

Tilton, G. R., Wetherill, G. W., and **Davis, G. L.,** 1962, Mineral ages from the Wichita and Arbuckle Mountains, Oklahoma, and the St. Francois Mountains, Missouri: Journal of Geophysical Research, v. 67, p. 4011–4019.

Tomlinson, C. W., and **McBee, William, Jr.,** 1962, Pennsylvanian sediments and orogenies of Ardmore district, Oklahoma, *in* Branson, C. C., editor, Pennsylvanian System in the United States—a symposium: American Association of Petroleum Geologists, p. 461–500.

Tuttle, O. F., and **Bowen, N. L.,** 1958, Origin of granite in the light of experimental studies in the system $NaAlSi_3O_8$–$KAlSi_3O_8$–SiO_2–H_2O: Geological Society of America Memoir 74, 153 p.

Twidale, C. R., 1976, Analysis of landforms: John Wiley & Sons Australasia Pty. Ltd., 572 p.

Walper, J. L., 1949, Igneous rocks of the Cold Springs area, Wichita Mountains, Oklahoma: University of Oklahoma unpublished M.S. thesis, 71 p.

——— 1951, Assimilation in the Cold Springs area of the Wichita Mountains igneous complex, Oklahoma: American Journal of Science, v. 249, p. 47–65.

Webster, R. E., 1977, Evolution of a major petroleum province: the Southern Oklahoma Aulacogen: Compass of Sigma Gamma Epsilon, v. 54, p. 59–71.

Weiblen, P. W., and **Morey, G. B.,** 1980, A summary of the stratigraphy, petrology, and structure of the Duluth Complex: American Journal of Science, v. 280-A, p. 88–133.

Wetherill, G. W., 1956, Discordant uranium–lead ages, I: American Geophysical Union Transactions, v. 37, p. 320–326.

Wickham, J. S., 1978, The Southern Oklahoma Aulacogen, *in* Wickham, J. S., and Denison, R. E., editors, Structural style of the Arbuckle region: University of Oklahoma Guidebook for Geological Society of America South-Central Section Annual Meeting, Field Trip 3, p. 9–41.

Widess, M. B., and **Taylor, G. C.,** 1959, Seismic reflections from layering within the Precambrian basement complex, Oklahoma: Geophysics, v. 24, p. 417–452.

Wilband, J. T., and **Wasuwanich, P.,** 1980, Models of basalt petrogenesis: lower Keweenawan diabase dikes and middle Keweenawan Portage Lake Lavas, upper Michigan: Contributions to Mineralogy and Petrology, v. 75, p. 395–406.

Wones, D. R., 1981, Mafic silicates as indicators of intensive variables in granitic magmas: Mining Geology, v. 31, p. 191–212.

York, D., 1966, Least-squares fitting of a straight line: Canadian Journal of Physics, v. 44, p. 1079–1086.